



Politecnico di Torino

Politecnico di Torino

MASTER OF SCIENCE IN CIVIL ENGINEERING

Master's Thesis

Analysis of the intersection between tunnel, shafts, and cross passages in a metro project

Candidate:

MOHAMED MAGDI OMER

Supervisors:

Prof. MONICA BARBERO

ENG. GIOVANNI QUAGLIO

ENG. DOMENICO PARISI

Academic Year 2021-2022

Acknowledgement

First and foremost, I am extremely grateful to my supervisor, Prof. Monica Barbero, for her continuous support and advice. She has encouraged me all the time during my thesis period.

I would like to extend my sincere thanks to Eng. Giovanni Quaglio for the opportunity to work on such an interesting topic; his invaluable supervision, immense knowledge and plentiful experience have pushed me to sharpen my thinking and brought my work to a higher level. Also, I would like to offer my special thanks to Eng. Domenico Parisi for his guidance, observations and giving me very important suggestions during my study.

I'm proud of and grateful for my time working in Geodata and my gratitude for all the staff in the company.

Dedication

To my parents, no amount of words will be enough to tell how grateful I am to you. Thank you for everything you've done for me. May Allah's love, blessing, and mercy be with you every day.

My forever love and appreciation to my brothers Omer and Amin, my sisters Ola and Maab, and all my big family and friends.

To the soul of my grandmom, thank you for your infinite love and kindness; I would not be the person I am today without your help. May Allah bless your soul and grant you the highest state in heaven.

Abstract

The high-stress concentration, accompanied by the significant disturbance of the surrounding strata are the effects that characterise the construction of the transition areas that connect a vertical shaft with the subway tunnel by a cross passage due to the complex and irregular geometries at these intersection areas.

Considering a case study of a project that includes eight ventilation\emergency shafts connected to a metro tunnel by different lengths of cross passages, this thesis studies the behaviour and the stability of the construction at the transition areas. Moreover, the good and worst scenario has been studied based on the geological conditions in the intersection areas among the eight regions. Furthermore, a suggested preliminary design for the primary support for the two geological conditions was introduced. A system of bolts and shotcrete has been chosen for stabilising the tunnel and the cross passages in the good scenario conditions, while for the stability of the shaft excavation, struts as temporary support and shotcrete as primary support until the installation of the final lining has been assumed.

Whereas, for the worst scenario, a composite liner of steel sets and shotcrete for the stability of the tunnel and the cross passage, and micro piles to stabilise the excavation of the shafts in addition to the shotcrete until the installation of the final lining, turned out to be the best choice.

The problem of the stress states and the displacements around the intersection areas is a clear three-dimensional problem. Therefore, the Finite-Element-Method (FEM) software RS3 (Rocscience,2022) was used to analyse the surface subsidence, the plastic zones of the surrounding rock, and the stress and displacement distribution induced by the construction at the intersection areas. Then, the suggested support systems were introduced.

The considered project uses rectangular shafts and horseshoe-shaped cross passages with a slight curvature at the crown. Eventually, this thesis presented the possibility of using a recommended models for the shafts and the cross passages by using elliptical shafts and a more curved horseshoe shape for the cross passages, which helped to reduce the stress concentration and the total displacement for the excavation boundaries as well as decreases the disturbance in the surrounding strata. These recommended models are much more robust by utilising the arch effect; consequently, the need for stabilising systems is considerably minimised compared

to the original model; therefore, the recommended models are anticipated to behave better, leading to a more economical solution for the project.

List of contents

Acknowledgement	i
Dedication	i
Abstract	ii
List of contents.....	iv
List of figures	vii
List of Tables	xii
Chapter 1: Introduction.....	1
1.1 Research description and objectives.....	1
1.2 Thesis Overview	3
Chapter 2: Literature review	4
2.1 Tunnelling in urban environment	4
2.2 Vertical shafts, cross passages, and the problem of the intersection with tunnel.....	10
2.2.1 shafts	10
2.2.2 cross passages & the intersection problem:.....	10
2.4 FEM & (RS3, RS2).....	16
2.4.1 FEM method	16
2.4.2 RS3 & RS2	18
2.5 Modelling of the material properties	18
Chapter 3: The Case study	23
3.1 Geometry and geological representation of the considered sections	25
3.1.1 The favourable scenario “section 1”	26
3.1.2 The worst scenario “section 2”	29
Chapter 4: Methodology	32
4.1 Geometry in Rhino 7.....	32
4.2 Modelling in RS3 & RS2.....	33
4.3 Modelling in Revit & Navisworks.....	34
Chapter 5: Analysis and outputs (favourable scenario).....	35

5.1 Analysis of the section related to the favourable scenario	36
5.2 3D FEM numerical model by RS3	36
5.2.1 Geometry	37
5.2.2 Geological model.....	40
5.2.3 Material properties.....	40
5.2.4 Boundary conditions, mesh setup & initial in-situ stresses.....	42
5.2.5 Construction sequencing (staging)	44
5.3 Results from 3D analysis	49
5.3.1 The initial state of stresses.....	49
5.3.2 The stress state.....	50
5.3.3 Plastic Zones.....	51
5.3.4 Transverse surface settlement.....	53
5.3.5 Longitudinal surface settlement.....	56
5.3.6 Total displacements	59
5.4 Design of the support for the structures in the good scenario	61
5.4.1 Support for the cross passages & Metro Tunnel (section at the intersection region)	61
5.4.2 support for the shafts	64
5.4.3 Stresses induced on the support systems	65
5.4.4 shotcrete on the shaft, cross passage & the tunnel	66
5.5 Detailing related to the good scenario	67
5.5.1 Intersection area overview (section for the intersection area).....	68
5.5.2 Section A-A (Cross passage cross-section).....	69
5.5.3 Section B-B (Shaft cross-section)	69
5.6 2D FEM numerical model by RS2	70
5.6.1 Numerical Model in 2D.....	70
5.6.2 Results of the 2D analysis	72
Chapter 6: Analysis and outputs (worst scenario conditions)	76
6.1 Geology and geo-mechanical parameters for materials	77
6.1.1 Geology.....	77
6.1.2 Material properties & constitutive models	77

6.2 Numerical modelling	79
6.2.1 Numerical model in 2D	80
6.2.2 results of the 2D analysis.....	88
6.2.3 Numerical model in 3D	98
6.2.4 Results of 3D analyses using RS3	107
6.2.5 Detailing related to the worst scenario	119
Chapter 7: Suggested models for the shafts & cross-passages.....	122
7.1 Suggested model for the vertical shafts.....	122
7.2 Suggested model for the cross passages	126
7.3 Analysis of the recommended model	128
7.3.1 Staging (construction sequencing):	130
7.4 Results.....	132
7.4.1 Initial state of stresses.....	132
7.4.2 state of stresses	132
7.4.3 Plastic zones.....	134
7.4.4 Transverse surface settlement trough	135
7.4.5 Total displacement.....	137
7.5 Design of the support for the structures for the recommended model	141
7.5.1 Results.....	142
Chapter 8: Conclusion and recommendations	148
References.....	153
Appendix	154

List of figures

Figure 1 Stability ratio, Cesarin & Mair (1981)	5
Figure 2 Centrifuge testing (Vardoulakis et al. 2009)	6
Figure 3 Ground movement towards the face (Vardoulakis et al. 2009)	6
Figure 4 Gaussian curve for representing the transverse settlements above a tunnel in soft ground. (After Dimmock and Mair 2007a, used with permission from ICE Publishing and Professor Lord R.J. Mair.)	7
Figure 5 Longitudinal settlement profile above tunnels in soft ground, showing the difference in distribution for open-face tunnelling and where there is significant face support. (After Mair and Taylor 1997.)	9
Figure 6 3D representation of the surface settlement as a tunnel is constructed in soft ground. (Attewell 1995, after Yeates 1985.)	9
Figure 7 Example of a ventilation\emergency shaft excavation.....	10
Figure 8 Example of the intersection area of a cross passage and main tunnel	11
Figure 9 Relationship between additional roof settlement at main tunnel and distance from intersection centre.	15
Figure 10 Continuum vs discontinuum.....	16
Figure 11 Types of the boundary conditions	18
Figure 12 The yield surfaces of the Hardening Soil model; deviatoric yield surface (red) and elliptical cap (blue) (roscience documentation)	19
Figure 13 Hyperbolic stress-strain curve in a drained compression triaxial test.....	20
Figure 14 Variation of axial stress versus axial strain in an oedometer, and definition of Eoedref	21
Figure 15 Orthophoto with the metro tunnel line	23
Figure 16 Natural tunnel vs the artificial one	24
Figure 17 Sections demonstrated the intersection region	24
Figure 18 Shaft\ cross passage intersection (section c-c)	25
Figure 19 Plan demonstrates the shaft type (a) & shaft type (b)	25
Figure 20 Geology related to the good scenario	26
Figure 21 Tunnel cross-section (section 1).....	27
Figure 22 Cross passage section	27
Figure 23 Cross passage type (a)	27
Figure 24 Cross passage type (b).....	28
Figure 25 Shaft types (a), (b)	28
Figure 26 Geology related to the worst scenario	29
Figure 27 Metro tunnel section 2	30
Figure 28 cross passage type (a) for section 2	30
Figure 29 cross passage type (b) cross section	31

Figure 30 Shafts (a & b) cross sections	31
Figure 31	32
Figure 32 example of the importing geometry process	33
Figure 33 The 3D model in Rhino 7	38
Figure 34 The Model in RS3	38
Figure 35 Longitudinal view of the intersection area	39
Figure 36 Transversal view of the intersection area	39
Figure 37 Equivalent continuum model external boundary dimensions	40
Figure 38 Model restraints	43
Figure 39 Model mesh	43
Figure 40 Mucking process for the shaft's excavated materials	45
Figure 41 Example of the top heading & bench excavation for the metro tunnel...	46
Figure 42 Example of the top heading & bench excavation for the cross-passage type (a) at stage 221	47
Figure 43 Example of the top-down full-face excavation for the vertical shaft type (a) at stage 240	47
Figure 44 Example of the top heading & bench excavation for the cross-passage type (b) at stage 257	48
Figure 45 Example of the top-down full-face excavation for the vertical shaft type (b) at stage 269	48
Figure 46 Initial in-situ state of stresses (σ_1 total)	49
Figure 47 stress state at the end of the excavation (σ_1 total)	50
Figure 48 Developments of the plastic zones due to the excavation at the intersection	51
Figure 49 Plastic zones for cross-passage (a)/metro tunnel intersection & cross passage (a)/shafts(a) intersection	52
Figure 50 Plastic zones for cross-passage (b)/metro tunnel intersection & cross passage (b)/shafts(b) intersection	52
Figure 51 plastic zones extension	53
Figure 52 Transverse surface settlement trough at the end of the metro tunnel excavation	54
Figure 53 Displacement in Z direction vs query distance at the surface at stage 212	54
Figure 54 Surface settlement trough at the end of the excavation process at the intersection	55
Figure 55 Displacement in Z direction vs query distance at the surface at stage 273	55
Figure 56 Scheme for the longitudinal surface settlement trough	56
Figure 57 Longitudinal surface settlement trough	56
Figure 58 Displacement in Z direction vs query distance at the surface in the	

longitudinal direction of the tunnel.....	57
Figure 59 Longitudinal surface settlement trough at the end of the excavation.....	58
Figure 60 Displacement in Z direction vs the longitudinal query distance at the surface	58
Figure 61 Total displacement for tunnel excavated cantor (at stage 212).....	59
Figure 62 Total displacement at the end of the excavation (stage 273)	60
Figure 63 Total displacement at the end of the excavation (stage 273 considering 212 as reference stage).....	60
Figure 64 Rock support chart (NGI, 2015).....	62
Figure 65 Axial Force FA (bolts)	65
Figure 66 Axial stress (bolts).....	66
Figure 67 Displacement on X-direction for the shotcrete	67
Figure 68 Intersection area overview with detailing	68
Figure 69 Section A-A (Cross passage cross-section).....	69
Figure 70 Section B-B (Shaft cross-section)	69
Figure 71 2D external boundaries.....	71
Figure 72 2D model mesh.....	71
Figure 73 Initial in-situ state of stresses (2D).....	72
Figure 74 sigma 1 vs query distance at the right boundaries of the models.....	73
Figure 75 sigma 1 vs query distance at the end of the tunnel excavation	73
Figure 76 Yielded elements at the end of the tunnel excavation	74
Figure 77 Total displacement at the end of the excavation (2D).....	74
Figure 78 Total displacement at the end of the tunnel excavation (stage 212)	75
Figure 79 Surface settlement trough from the 2D & 3D results.....	75
Figure 80 Stratigraphy for section 2	76
Figure 81 The simplification of the stratigraphy	77
Figure 82 The Failure mechanism consists of a wedge and a prismatic body	80
Figure 83 Geometrical parameters.....	81
Figure 84 Forces acting on the system.....	81
Figure 85 Face stability analysis.....	83
Figure 86 Tunnel geometry & the external boundaries	84
Figure 87 Model mesh & the restraints	85
Figure 88 The primary lining input data.....	87
Figure 89 Initial in-situ state of stress.....	88
Figure 90 State of stress at the end of the excavation (stage 3).....	88
Figure 91 Plastic zones at the end of the excavation (stage 3)	89
Figure 92 Total displacement at the end of the excavation (stage 3)	89
Figure 93 Total displacement vs the excavation boundary query distance (at stage 3).	89
Figure 94 Vertical displacement Vs query distance at the surface.....	90

Figure 95 Total displacement at the end of the excavation	92
Figure 96 Total displacement vs the excavation boundary query distance (at stage 3)	93
Figure 97 Vertical displacement Vs query distance at the surface.....	93
Figure 98 Axial force on the lining.....	94
Figure 99 Axial force vs the lining boundary distance.....	94
Figure 100 Bending moment on the lining	95
Figure 101 Bending moment vs the lining boundary distance	95
Figure 102 Shear force on the lining	96
Figure 103 Support capacity plot.....	97
Figure 104 Creating of the 3D model in Rhino7 software	98
Figure 105 Imported geometry into the RS3	99
Figure 106 Longitudinal view of the intersection area.....	99
Figure 107 Transversal view of the intersection area	100
Figure 108 3D model external boundaries.....	100
Figure 109 Micro piles overview	101
Figure 110 The primary lining input data	102
Figure 111 Example of the tunnel excavation	103
Figure 112 Example of the excavation of the cross passage type (a).....	104
Figure 113 Example of the shaft (a) excavation	105
Figure 114 Example of the cross passage type (b) excavation.....	105
Figure 115 Example of the shafts (b) construction.....	106
Figure 116 Initial state of stresses.....	107
Figure 117 stress state RS3 results (stage 108).....	108
Figure 118 stress state RS2 (stage 3)	108
Figure 119 Plastic zones RS3 results (stage 108).....	109
Figure 120 Plastic zones RS2 results (stage 3).....	109
Figure 121 Total displacement RS3 results (stage 108)	110
Figure 122 Total displacement RS2 results (stage 3)	110
Figure 123 surface settlement trough at stage (108).....	111
Figure 124 Z displacement VS query distance at the surface.....	112
Figure 125 Surface settlement trough curve	112
Figure 126 Yielded elements (stage 168)	113
Figure 127 Surface settlement trough.....	114
Figure 128 Query at the ground surface	114
Figure 129 Z displacement vs query distance at the surface	115
Figure 130 Total displacement (stage 168).....	115
Figure 131 Axial forces (X & Y directions).....	116
Figure 132 Axial force (Z- direction)	117
Figure 133 Bending moment (about X & Y axis)	117

Figure 134	Bending moment about (Z-direction).....	118
Figure 135	Intersection area overview with detailing	120
Figure 136	Section A-A (Cross passage cross-section).....	121
Figure 137	Section B-B (Shaft cross-section)	121
Figure 138	Orthophoto for the shafts in section 1	123
Figure 139	Original and recommended shaft cross-section type (a)	124
Figure 140	Original vs recommended shaft (a) model	124
Figure 141	Original and recommended shaft cross-section type (b).....	125
Figure 142	Original vs recommended shaft (b) model.....	125
Figure 143	Original and recommended cross passage cross-section type (a)	127
Figure 144	Original vs recommended cross passage (a) model	127
Figure 145	Original and recommended cross passage cross-section type (b).....	128
Figure 146	Original vs recommended cross passage (b) model	128
Figure 147	3D models in Rhino 7 & RS3.....	129
Figure 148	Transversal & longitudinal views for the intersection area	129
Figure 149	Model stages	131
Figure 150	Initial in situ state of stress	132
Figure 151	state of stress at the end of excavation (stage 283)	133
Figure 152	Plastic Zones overview.....	134
Figure 153	The extension of the yielded elements	134
Figure 154	Transverse surface settlement trough	135
Figure 155	Displacement in Z-direction vs Query distance at the surface.....	136
Figure 156	surface settlement at the end of excavation.....	137
Figure 157	Total displacement 8stage (212).....	138
Figure 158	Total displacement stage 283	139
Figure 159	Total displacement (only the effect of the shafts & cross passages excavation)	140
Figure 160	Axial Force FA(bolts)	142
Figure 161	Axial stress (bolts).....	143
Figure 162	161 Displacement on (X, Y & Z)-directions for the shotcrete.....	143
Figure 163	model in Revit	145
Figure 164	project phases in Revit.....	146
Figure 165	Model in Navisworks	146
Figure 166	Navisworks Simulation Video.....	147
Figure 167	Example of the stability of wedges on a vertical shaft using UnWedge code (SF from LEM).....	151
Figure 168	Example of the stability of wedges on a vertical shaft using RS3 software (SF from SSR method).....	151

List of Tables

Table 1 Typical K-values	8
Table 2 Guidelines for support design in tunnel intersection area Hsiao et al. (2008)	14
Table 3 Suggestions for area with additional support Hsiao et al. (2008).....	15
Table 4 Material properties of Basalt	42
Table 5 Excavation & support suggestions by Bieniawski	46
Table 6 Bolts fully bonded properties for the tunnel & cross passages	63
Table 7 Fibre-reinforced shotcrete properties for the tunnel & cross passages	63
Table 8 Shotcrete Properties for the vertical shafts	64
Table 9 Material properties of the Lava.....	78
Table 10 Material properties of the fractured Lava	78
Table 11 Material properties of the sandy soil	78
Table 12 Material Properties of the fragment Pyroclastic rock.....	79
Table 13 Material Properties of the silty sand	79
Table 14 input data for the Anagnostou Kovari method for calculating the required stabilizing force at the face (S)	83
Table 15 Primary lining parameters.....	87
Table 16 Hardening soil model parameters for the sandy soil	91
Table 17 Hardening soil model parameters for the fragment pyroclastic rock	91
Table 18 Hardening soil model parameters for the silty sand	92
Table 19 Micro piles properties	102
Table 20 Primary lining input data	103
Table 21 Bolts fully bonded properties for the tunnel & cross passages	141
Table 22 Fibre-reinforced shotcrete properties for the tunnel & cross passages...	141
Table 23 Shotcrete Properties for the vertical shafts	141

Chapter 1: Introduction

1.1 Research description and objectives

With the development of underground transportation networks, the use of vertical shafts and cross passages is inevitable. They are important elements to be constructed for a variety of reasons, including emergency exits, ventilation, and maintenance access. The transition section connecting the shaft and the cross-passage, as well as the section connecting the cross passage with a subway underground tunnel, has a priority concern during the subway underground excavation because these transit sections are characterized by irregular and complex geometries, therefore during the construction of these intersection regions, the development of high-stress concentrations and large ground deformations at these regions can be introduced. Therefore, a conservative design and construction of these intersection areas are considered fundamental to a successful overall underground construction.

The objective of this thesis is to study the behaviour and the stability of the intersection area between a metro tunnel and a cross-passage, as well as the intersection between the vertical shaft and the cross-passage. Furthermore, a suggested preliminary design is presented for the cross-passage, the vertical shaft, and the section of the metro tunnel in contact with the cross passage.

The case study considered for this dissertation involves 8 compensation shafts that are sized to comply with both fire brigade and ventilation requirements for a metro tunnel, therefore these shafts will be connected to the metro tunnel considering different lengths of the cross-passage tunnels which have the same functionality to comprise a ventilation chamber and an emergency exit. This project is in the preliminary design phase, therefore most of the information and the data are sensitive and company protected. For this reason, the data and the information in this dissertation will be addressed in a way that fulfils the scope and the objective of this thesis.

The problem of the stress states and the displacements around the intersection region between the shaft and cross passage, and the intersection region between the metro tunnel and the cross-passage, is a three-dimensional problem. Therefore, modelling the intersections in three dimensions is the best way to represent the ground deformations and the induced stresses. The Finite-Element-Method (FEM) software

RS3 (Rocscience,2022) is used to analyse the resulting surface subsidence, the plastic zone of the surrounding rock, and the stress and displacement distribution induced by the construction at the intersection regions, besides the design of the desired components: (the cross-passages, the vertical shafts, and the metro tunnel at the contact area). In the considered project, the length of the cross-passages that connects the ventilation shafts to the metro tunnel is characterized by small length, therefore these cross passages are between two regions characterized by high-stress concentration due to the intersection problem, consequently, the problem of the intersections between the shaft, cross-passage and the metro tunnel must be studied together in one model to examine the effect on the short cross-passages during the construction.

Since this study is dealing with a design in the preliminary phase, the 3D FEM analysis is supported by a simple 2D FEM analysis using RS2 (Rocscience,2022) software. This approach is implemented to have a sort of model validation.

The analysis was carried out on two sections, representing the favourable and the worst scenarios considering the stratigraphy of the intersection areas. The favourable scenario is related to the intersection positioned in a region where only a layer of shallow basalt is apparent, whereas, For the worst scenario the intersection of the tunnel with the cross passage and the shaft is positioned in a region where a presence of a challenging geological formation characterised by the intersection of a thick lava layer with different thin layers of loose soil with poor mechanical properties.

Consequently, a detailed design of the three structures will be represented as the thesis outcome. For each structure, two sections will be signified with the support type and construction sequence.

The considered project uses rectangular shafts and horseshoe-shaped cross passages with a slight curvature at the crown. Eventually, this thesis presented the possibility of using a recommended models for the shafts and the cross passages by using elliptical shafts and a more curved horseshoe shape for the cross passages, which helped to reduce the stress concentration and the total displacement for the excavation boundaries as well as decreases the disturbance in the surrounding strata. These recommended models are much more robust by utilising the arch effect; consequently, the need for stabilising systems is considerably minimised compared to the original model; therefore, the recommended models are anticipated to behave better, leading to a more economical solution for the project.

1.2 Thesis Overview

Chapter 2:

It gives the reader the basic concepts about the introduced topic by addressing a general discussion about the problem, therefore general information will be reported such as shallow tunnels, cross-passages, vertical shafts, and other related topics.

Chapter 3:

This chapter describes the case study by giving general information about the project (for instance, the geometry of the structures and the stratigraphy in the two considered sections where the analysis is performed).

Chapter 4:

This chapter describes the methodology that is followed in this thesis. A flow chart is presented showing the sequence, accompanied by a description of the procedure in each phase and each software.

Chapter 5 & 6:

These chapters are the core of this dissertation, where the models and the analysis are introduced. The outputs and the detailing are presented.

Chapter 7:

This chapter introduces a recommended model for the shafts & cross-passages. The behaviour and the response of this model applying the same initial conditions are compared to the original model. In addition to that, a simplified Building information modelling (BIM) procedure is illustrated for the recommended model in order to simulate the construction sequence.

Chapter 8:

In this chapter, a summary of this study is introduced, followed by suggestions and recommendations for further work.

Chapter 2: Literature review

In this chapter, four sub-sections are presented to cover the topic of the problem of the intersection between the metro tunnel, cross passages & vertical shafts. In the first sub-section, it is fundamental to introduce brief information about shallow tunnels in the urban environment and the related concerns that must be taken into account during shallow tunnels construction. Then in the second sub-section general information about vertical shafts & cross passages is introduced, then highlighting the main consideration of this thesis which the problem of their intersection to the metro tunnel. While, in the third subsection, general information about the method used for the analysis, which is the Finite-Element-Method (FEM) and the considered used software RS2 & RS3 are presented. Furthermore, the fourth subsection includes detailed information about the constitutive models that considered to define the different materials involved in the analysis.

2.1 Tunnelling in urban environment

The response of the ground and nearby structures to tunnelling constitutes a complex soil-structure interaction problem. The conditions around tunnels depend on the stress state in the ground, soil type, tunnel geometry, construction technique and permeability of the tunnel lining. When taking into consideration a typical urban environment, where buildings are above where the tunnels are to be constructed, the complexity of tunnelling conditions increases even more.[1]

With urban tunnel construction growing worldwide, accurately predicting the ground and structural response to tunnelling and the associated risks is crucial. This is fundamental to safeguarding the urban fabric, such as existing infrastructure for transport and services and historic and sensitive structures. Therefore, two aspects must be addressed: the tunnel stability analysis & the induced ground movement.[1]

The aim of the stability analysis is to ensure safety against soil collapse in front of the tunnel face. On the other hand, the deformation analysis deals with the determination of the pattern of ground deformation that will result from the construction works. These ground deformations should be within a tolerable threshold to prevent damage to surface or subsurface structures.[2]

For instance, many authors introduced analytical procedures to calculate the stability at the tunnel face and the crown by connecting them with the displacement at the

surface. For example, considering undrained conditions, based on the stability ratio N , Cesarin & Mair (1981) gave a set of curves to compute the displacement at the surface, crown, and face; these curves are based on (Broms & Bennemark, 1967; Peck, 1969) suggested equation for the stability ratio N :

$$N = \frac{\sigma_s + \gamma Z - \sigma_t}{c_u} < \text{or} = 6-7$$

Where:

γ = unit weight of the soil (KN/m^3)

Z = depth to the tunnel axis ($C + \frac{D}{2}$) (m)

C = the overburden (m)

D = tunnel diameter (m).

σ_s = Surface surcharge pressure (KPa)

σ_t = tunnel support pressure (KPa)

In the diagram in figure (1) by Cesarin & Mair (1981) the displacements are given for different N values, given by $\frac{\sigma_s - \sigma_t}{c_u}$:

δ_s = Surface displacement.

δ_c = Crown displacement.

δ_f = Face displacement.

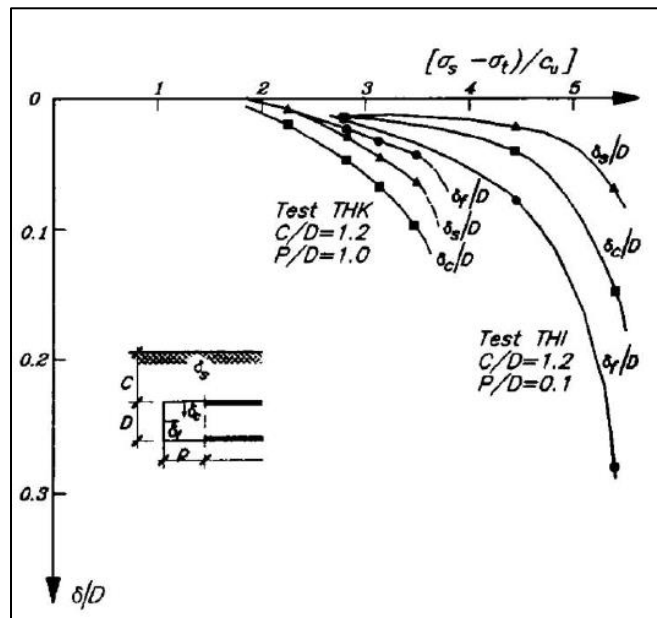


Figure 1 Stability ratio, Cesarin & Mair (1981)

Moreover, under drained conditions, many authors introduce analytical equations to evaluate the stability of the face based on the centrifuge test, such as (Vardoulakis et al. 2009):

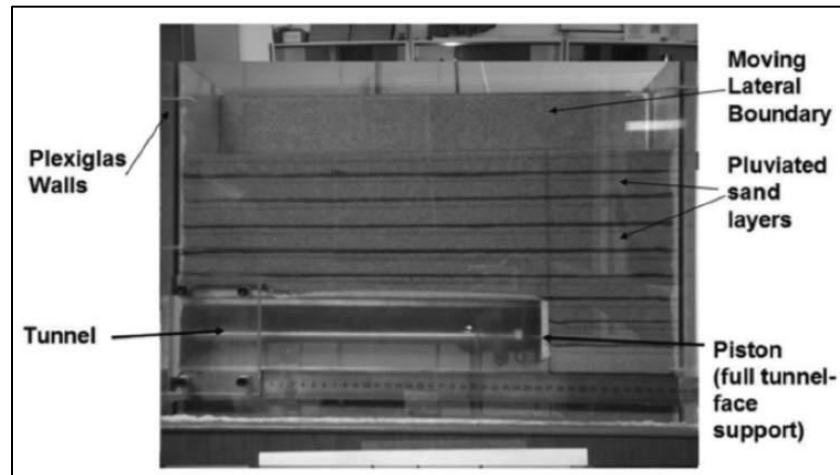


Figure 2 Centrifuge testing (Vardoulakis et al. 2009)

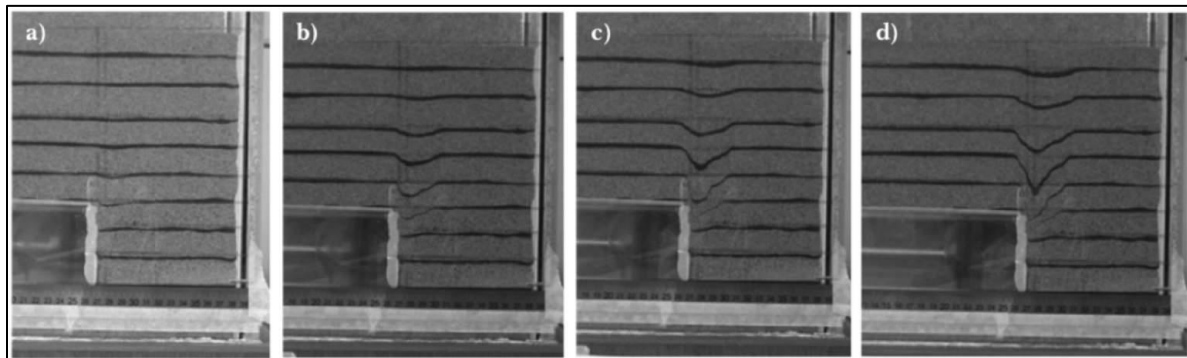


Figure 3 Ground movement towards the face (Vardoulakis et al. 2009)

The stability of the tunnel during the construction is connected to the induced ground movements caused by the construction. These ground movements concerning their effects on the adjacent structures and how these movements are monitored during the construction process.[3]

When tunnelling in the hard ground (rock), ground movements are generally not a problem, except in squeezing ground conditions. In soft ground, however, displacements can occur for several reasons, such as deformation of the ground towards the face due to stress relief and the distortion of the tunnel lining as it starts to take the ground loading. These aspects can result in displacements reaching the ground surface, which can be particularly significant in urban areas, where they can

influence overlying or adjacent structures such as buildings, other tunnels, and services. In contrast, if there are no ground–structure interaction effects, these ground movements are termed ‘greenfield’ movements. It is essential to estimate these ground movements so that tunnelling techniques can be optimised to control the movements of overlying or adjacent structures.[3]

Indeed, these days enormous advances in computer-based numerical methods for calculating ground displacements are being made, such as the FEM software “this dissertation considers the numerical methods based on FEM software RS2 and RS3 to evaluate the surface settlement due to the construction at the intersection regions”. However, there are empirical-based methods in the literature to evaluate the surface settlement in soft ground.

Schmidt (1969) and Peck (1969b) established, via case history data, that the ground surface settlement ‘trough’ above tunnels, that is, normal (or ‘transverse’) to the direction of the tunnel, can be described by an inverted normal probability (or ‘Gaussian’) curve:

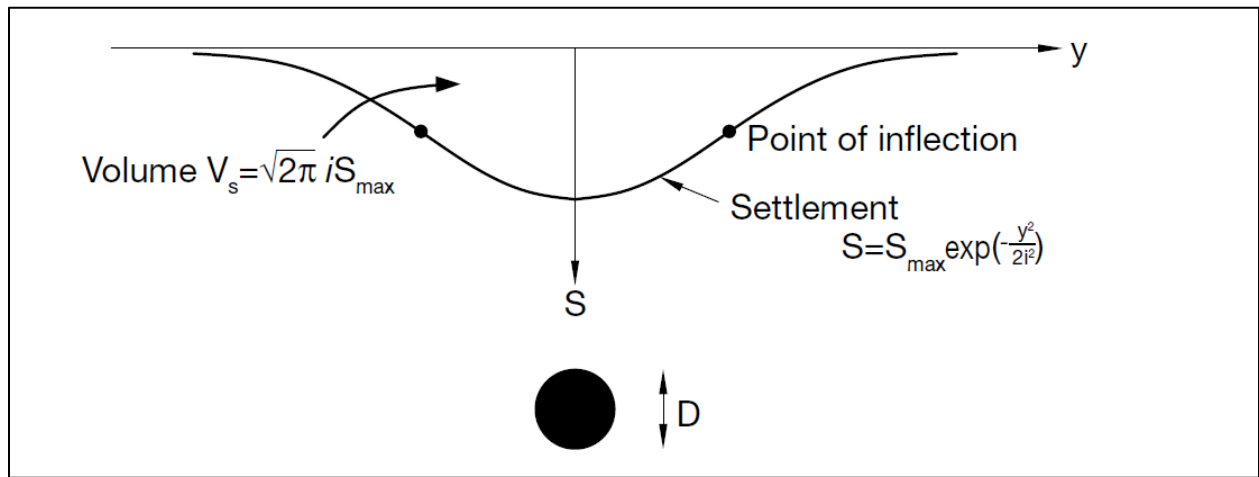


Figure 4 Gaussian curve for representing the transverse settlements above a tunnel in soft ground. (After Dimmock and Mair 2007a, used with permission from ICE Publishing and Professor Lord R.J. Mair.)

From the equations in the above (figure 4), $S(y)$ is the vertical settlement at point y , S_{max} is the maximum settlement directly above the tunnel centreline, y is the transverse horizontal distance from the tunnel centreline of the trough, and i is the trough width parameter, which represents the point of inflection on the transverse profile, equivalent to one standard deviation in a normal probability distribution. This has subsequently been confirmed by numerous authors from other case history data, for example, O’Reilly and New (1982) and Attewell et al. (1986).[3]

The geometry of the settlement trough is uniquely defined by selecting values for the volume, V_s , and the trough width parameter, i .

There are several empirically derived methods for estimating the trough width parameter i . It has been shown by various researchers based on case history data, for example, O'Reilly and New (1982), that the trough width parameter at the ground surface is an approximately linear function of the depth of the tunnel, H , and is mainly independent of the tunnel construction method and tunnel diameter, the relationship as follows:

$$i = KH$$

where H is the depth from the ground surface to the tunnel axis level and K is representing the ground conditions and it can be estimated as shown in table (!):

Soil type	K
Stiff fissured clay	0.4-0.5
Glacial deposits	0.5-0.6
Soft silty clay	0.6-0.7
Granular soils above the water table	0.2-0.3

Table 1 Typical K-values

In the longitudinal direction to the tunnel construction, it has been found that the vertical displacements can be estimated, following examination of several tunnel construction case histories in clays (Attewell and Woodman 1982, Attewell et al. 1986), by a 'cumulative probability curve' as illustrated in Figure (5):

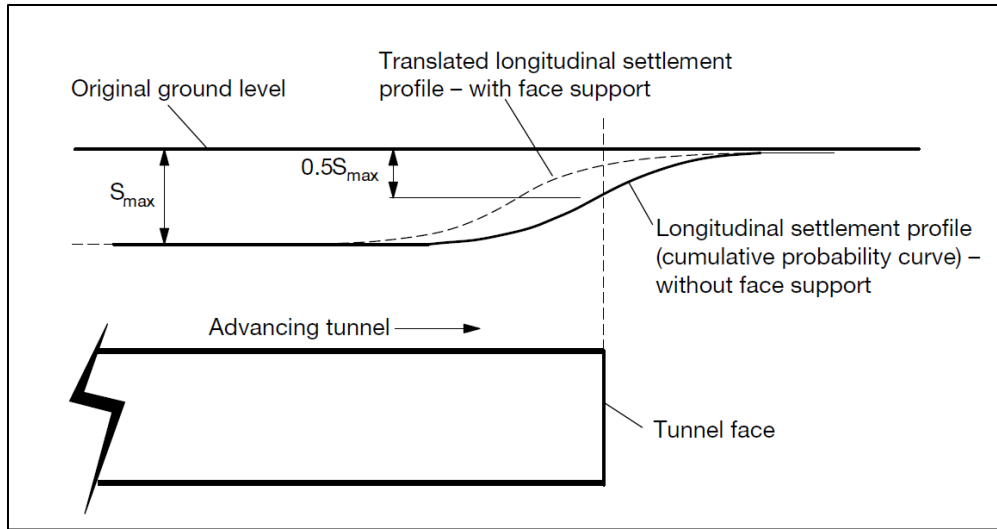


Figure 5 Longitudinal settlement profile above tunnels in soft ground, showing the difference in distribution for open-face tunnelling and where there is significant face support. (After Mair and Taylor 1997.)

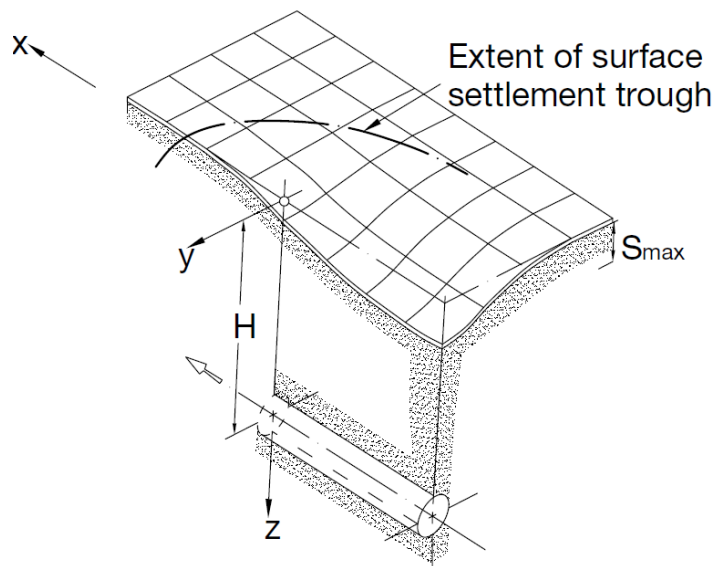


Figure 6 3D representation of the surface settlement as a tunnel is constructed in soft ground. (Attewell 1995, after Yeates 1985.)

Therefore, in this thesis, it is fundamental to address the problem of the surface settlement due to the tunnel construction, in addition to showing the effect of the construction of the cross passages and the shafts on the surface settlement in the considered case study. These mentioned aspects are presented in the analysis section in chapters 5 and 6 using the numerical methods.

2.2 Vertical shafts, cross passages, and the problem of the intersection with tunnel

2.2.1 shafts

shafts are vertical or inclined openings that connect the ground surface to the tunnel. Many shafts, although used for construction, have uses as permanent shafts. They can be used for deep foundations such as for structures that must be set on competent rock. This would require the sinking of the shaft through the overburden.

Shafts have been used as wet wells for the storage of wastewater and pump stations. They can function as ventilation shafts for underground subway tunnels. Also, once the tunnel is driven, the shaft can be used as a station at the tunnel level and for access to the station by using the shaft for elevators, stairways, or both. In the mining industry, shafts have a multitude of uses, they can be used or the hoisting of muck or transporting of materials, ventilation, hoisting of men, and emergency exits.[4]

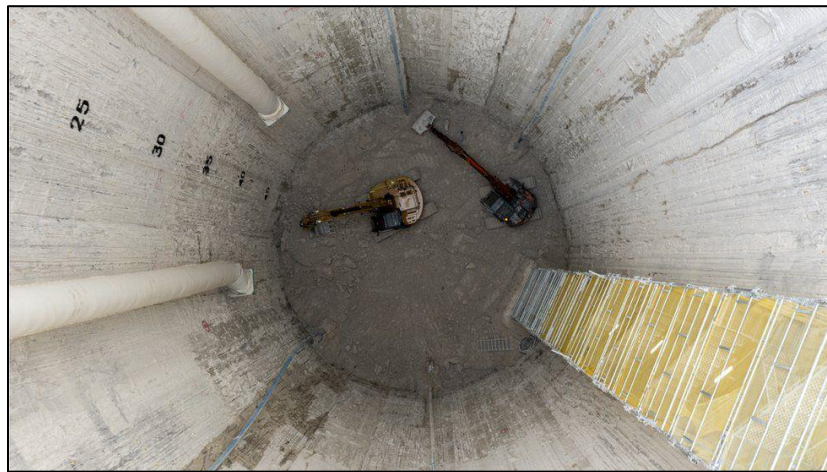


Figure 7 Example of a ventilation/emergency shaft excavation

2.2.2 cross passages & the intersection problem:

Cross passages are required to be constructed for a certain length of underground metro tunnels to provide for emergency and maintenance access. In general, a cross passage is either built between two tunnels, or can be connected between the tunnel and surface level through the vertical shaft [5]. As the current case study, the cross passages and shafts are constructed for emergency access and ventilation in a long metro tunnel.



Figure 8 Example of the intersection area of a cross passage and main tunnel

Rock behaviour at the intersection area of the main tunnel and the cross passage, as well as cross-passage\shaft intersection is a complicated, three-dimensional problem. Additional tunnel deformation and increasing support load were often observed during construction due to further disturbance of rock masses surrounding the intersection area. Conventionally, a support system heavier than the normal tunnel section was adopted to counter the adverse effects of complicated stress conditions (Guo, 2010; Hsiao, 2009). Tunnelling underground Construction projects may experience significant issues like lining cracking and working face collapsing due to the ignorance of the behaviour of the rock mass at the intersection areas. Such problems are even more critical in urban areas with buildings affected by the induced progressive ground movements. [6], [7]

Therefore, particular considerations have to be taken into account for such projects such as the considered case study of this thesis.

Most of the previous studies on tunnel behaviour in the intersection area were conducted by studying stress concentration factors using elastoplastic theory. Photoelasticity experiments were conducted by Riely (1964) and Pant (1971) to study stress surrounding tunnel intersection areas as the effectiveness of the theory is proved in structural engineering and geotechnical engineering.

Due to rapid development of modelling techniques, 3D analysis was used more widely by researchers, such as Thareja et al. (1980, 1985) and Takino et al. (1985), on the displacements and liner stresses in the intersection area by considering various rock properties and intersection angles. As for the design of the support system,

Tsuchiyama et al. (1988) examined the excavation of an access tunnel with an oblique angle of 45 degree to the existing main tunnel through a 3D numerical analysis. It was found that the affected area along the main tunnel, which requires additional support work, is about one tunnel diameter on the obtuse angle side and about three tunnel diameters on the acute angle side from the point of intersection.

Moreover, the practice adopted by JNC (Japan Nuclear Development Institute, 1999) requires that additional reinforcement be installed at the intersection area extending four tunnel diameters on the acute angle side and around the same distance on the obtuse angle side. More recently, the area with additional reinforcement was suggested by Nonomura et al. (2004) for the rough estimate of support requirement. Chen et al. (2002) and Hsiao et al. (2004) conducted 3D elasto-plastic analysis of tunnel behaviour in the intersection area. [6]

As well as simulations of the intersection area were also conducted by engineers around the world, and some suggestions on the design of the tunnel intersection were proposed. However, these studies were only aimed at the specified case since it is impossible to provide design suggestions for tunnel intersections under various geological and geometrical conditions.

❖ Support design for tunnel intersection

A critical issue for tunnel intersection is the design of primary support, including the increase of supporting strength and range with additional reinforcement. According to Hsiao et al. (2008) a proposed guideline for the support design at the intersection areas based on the 3D numerical analyses under various tunnelling conditions, including rock strength, rock mass rating, rock covering, and intersection angle can be introduced. The guideline introduced three categories of design philosophy used in the tunnel intersection depend on strength/stress ratio of rock mass (σ_{cm}/P_0) where σ_{cm} is the uniaxial compressive strength of rock mass and P_0 is the field stress, where it has been founded that this ratio plays an important role in tunnel intersection behaviour [7]. The three categories of design philosophy are described briefly as follows:

1. Only local strengthening of the support system is designed in the intersection area, such as increasing the thickness of shotcrete, and the density or length of rock bolt. This first design philosophy is due to the fact that the location of a tunnel intersection is commonly chosen in the so-called “good geological area”. At such an area, severe tunnel deformation is not expected.

Strengthening of support system is mainly aimed at avoiding local potential wedge failure. Therefore, the first design philosophy is reasonable for the ground of slightly or non-squeezing condition ($\sigma_{cm}/P_0 > \text{or} = 0.5$).

2. There is no difference in support design between the intersection and normal tunnel area. But the measure of degrading rock mass rating is used to install a heavier support system in the intersection area. For instance, one third of the Q-value is suggested for the tunnel intersection.
3. Heavier support system is directly designed in the intersection area.

The second and the third design philosophies adopt the heavy support system to strengthen the ground around the intersection. Basically, the designs are generally too conservative for slightly or non-squeezing rock. The design philosophy is more suited for moderately squeezing ground by reducing tunnel deformation. For highly squeezing conditions, Adoption of heavy support design alone may not overcome extremely poor rock conditions. Auxiliary measures, such as special excavation arrangement and/or ground improvement by grouting, should be used to improve tunnel stability. Based on prior discussions, three categories of support design suggestions for different geological condition are proposed, are shown in table (2).

Geological condition	Support design suggestions
Slightly or non-squeezing rock ($\sigma_{cm}/P_0 \geq 0.5$)	<ul style="list-style-type: none"> • Only strengthening support system to prevent potential wedge failure in the intersection area, such as increasing the thickness of shotcrete, and the density or length of rock bolt • Monitoring instruments should be installed to examine tunnel stability
Moderately squeezing rock $0.25 \leq \sigma_{cm}/P_0 \leq 0.5$)	<ul style="list-style-type: none"> • Reducing rock mass rating in order to install heavier support work or design a more conservative support system in the intersection area. • Monitoring instruments should be installed to examine tunnel stability. Carry out detailed visual inspection on tunnel conditions and increase monitoring frequency during construction
Severely squeezing rock ($\sigma_{cm}/P_0 \leq 0.25$)	<ul style="list-style-type: none"> • Conservative excavation processes and support system should be used in the intersection area. Auxiliary measures, such as ground improvement, should be made if necessary. 3D numerical analysis is suggested to assess the appropriateness of tunnel design. • Monitoring instruments should be installed to examine tunnel stability. Carry out detailed inspection on tunnel conditions and increase monitoring frequency during construction

Table 2 Guidelines for support design in tunnel intersection area Hsiao et al. (2008)

❖ Range of additional support

The range requires additional support in the tunnel intersection area is another important topic. Suggestions for area with additional reinforcement based on the relationship between additional roof settlement and the distance from the intersection as shown in figure (9). And the Suggestions for area with additional support are shown in table (3).

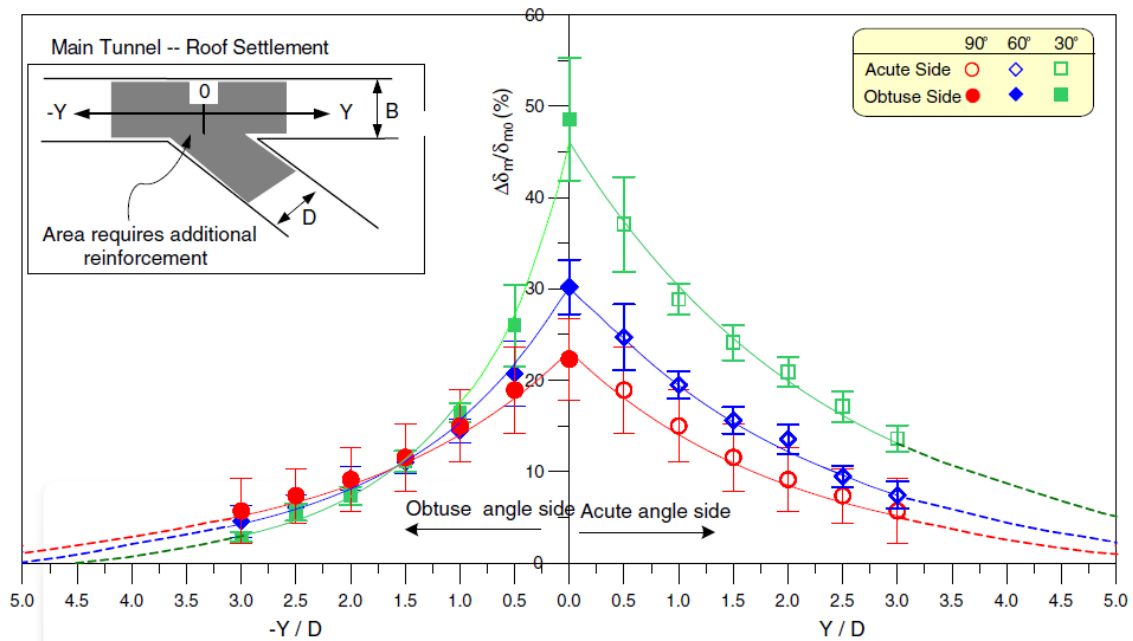


Figure 9 Relationship between additional roof settlement at main tunnel and distance from intersection centre.

Geological condition	Extent suggestions for additional system support		
Slightly or non-squeezing rock ($\sigma_{cm}/P_0 \geq 0.5$)	No additional system support need in intersection area, only support in preventing potential wedge failure		
Moderately squeezing rock ($0.25 \leq \sigma_{cm}/P_0 \leq 0.5$)		Acute angle side	Obtuse angle side
	90°	1.0D*	1.0D
	60°	1.5D	1.0D
	30°	2.5D	1.0D
Severely squeezing rock ($\sigma_{cm}/P_0 \leq 0.25$)		Acute angle side	Obtuse angle side
	90°	1.5D	1.5D
	60°	2.5D	1.5D
	30°	3.5D	1.5D

*D: span of access tunnel.

Table 3 Suggestions for area with additional support Hsiao et al. (2008)

This proposed suggestions by Hsiao et al. (2008) are intended as preliminary design guid for the analysis of the intersection at the considered case study for this thesis.

2.4 FEM & (RS3, RS2)

2.4.1 FEM method

The geotechnical model is a schematic representation of reality that able to describe the fundamental aspects of the behaviour of the ground. To build the model it is fundamental to decide if to adopt a continuum model, equivalent continuum model or a discontinuum model, to represent the specific geotechnical problem. The continuum model is representing the soils and the massive rock masses, while the equivalent continuum is for the heavily fractured rock masses, and the discontinuum model is to represent the moderately jointed rock masses.

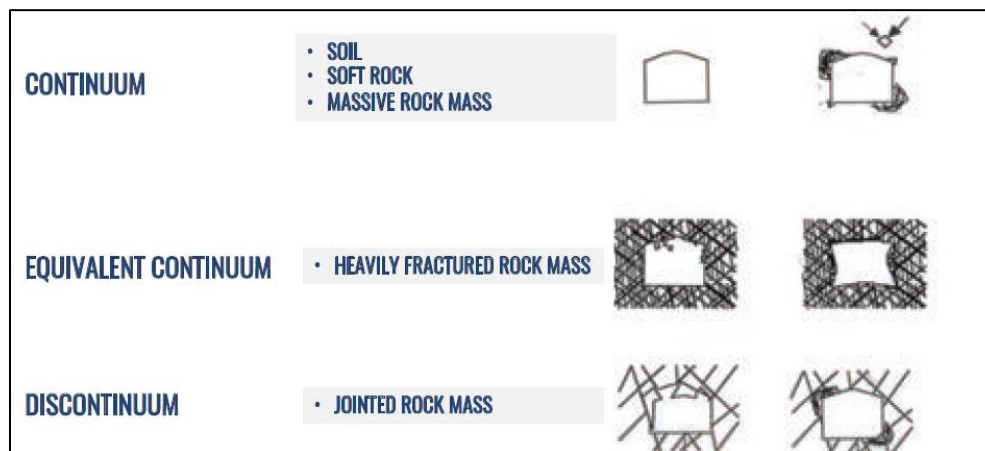


Figure 10 Continuum vs discontinuum

The computer-based numerical methods are techniques usually used to represent the geotechnical problems due to the most cases of the non-linear constitutive behaviour of the ground materials and yet a few cases that can be solved analytically and restrictive hypotheses accompany them.

Generally, numerical methods can be divided into differential methods and integral methods. The differential methods are commonly used to solve problems in elasticity and plasticity. This introduces the finite difference method and finite element method, which are similar in practice and different in mathematics, and they both require an approximation made with a specific domain. They are more robust to represent a continuum or equivalent continuum models than representing a discontinuum model.

In the finite element method, the general concept is that the geotechnical problem is

approximated in a region, which in turn, is divided into several discrete elements, which provides a physical approximation to the continuity of the displacement and stresses within the considered region.

When a finite element method is used, the following steps are respected:

1- Definition of the domain

Since it is not possible to model something which infinite “the ground”, it is essential to set finite boundaries, for example in the considered shallow tunnel excavation project, usually in the practice a rectangular shape is considered to define the domain.

2- Element discretization

The selected domain should be discretised in a number of smaller regions, called finite elements. It is a geometrical problem of sampling a region, and a correct discretization can optimise the process, reducing the computation time.

3- Definition of the primary variable and how it should vary over a finite element

In geotechnical engineering, the displacement is usually considered as the primary variable.

4- Writing of the element equations for the single element adopting an appropriate variational principal for the primary variable.

To write the element equations, it is fundamental to define the material properties and the constitutive equations.

5- Combination of the element equations in order to form the global equations

6- Application of the boundary conditions in order to modify the global equations

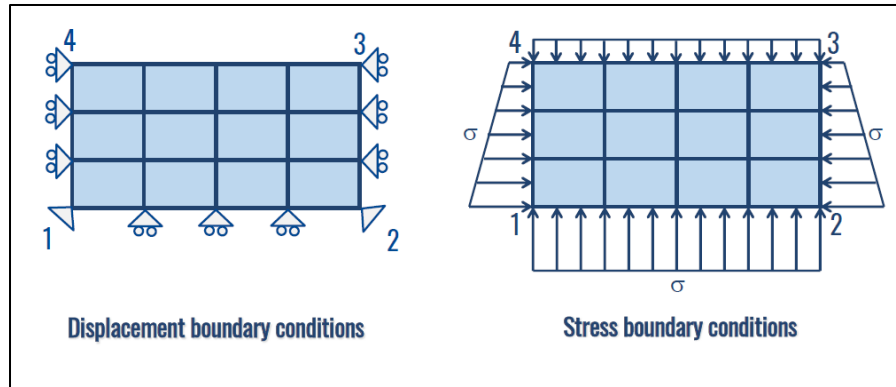


Figure 11 Types of the boundary conditions

7- Solution of the global equations

The displacement is obtained at all the nodes and the stresses and strains are derived as secondary quantities

8- Interpretation of the results

2.4.2 RS3 & RS2

They are FEM software developed by Rocscience. RS3 is a 3D program for the analysis of geotechnical structures for civil and mining applications. Applicable for both rock and soil. RS3 is a general-purpose finite element analysis program for underground excavations, tunnel and support design, surface excavation, foundation design, embankments, consolidation, groundwater seepage and more. While the same description is applied to the RS2, but it is a 2-dimensional analysis program.

2.5 Modelling of the material properties

As mentioned in the first chapter, the analysis involved the presence of rock masses and loose soils. Indeed, several yield criterions could be used in geotechnical engineering to represent the strength behaviour of rock & soils. In the analysis, the well-known Hoek and Brown criterion is to be used for defining the rock masses' behaviour, while for loose soil, the Mohr Coulomb criterion is considered, however, under some conditions, using different constitutive model to represent in a better way the behaviour of the loose soils instead of the typical elastio-plastic model is preferred, for example using of the hardening soil model which indicates that the plastic deformation in soils starts from the early stages of loading. In the following brief, information about the hardening soil model is presented.

❖ Hardening soil model

Experimental evidence indicates that plastic deformation in soils starts from the early stages of loading. To capture such behaviour in a constitutive model, the typical elastic perfect plastic models are inadequate. To simulate such behaviour, constitutive models that utilise a hardening law after initial yielding is required. The main feature of the hardening soil model (Schanz and Vermeer 1999) is its ability to simulate hardening behaviour. The hardening in this model is divided to deviatoric and volumetric hardenings by utilizing a shear and a cap yield surface. The model also uses nonlinear elastic behaviour that relates the elastic modulus to the stress level. [8], [9]

The model utilizes three yield surfaces that includes deviatoric (shear), volumetric (cap) and tension cut off. The yield surfaces and hardening characteristics of this Model are illustrated in figure (12).

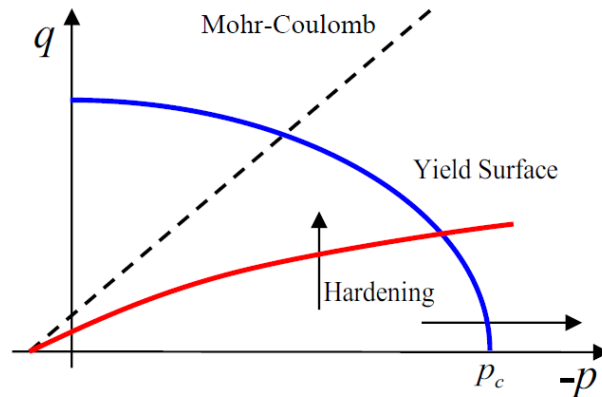


Figure 12 The yield surfaces of the Hardening Soil model; deviatoric yield surface (red) and elliptical cap (blue) (rocscience documentation)

The formulations of these three mechanisms, definition of yield surfaces and their corresponding plastic potential and hardening law are presented below.

1- Deviatoric Hardening Mechanism

The deviatoric mechanism is the core of this model and at it uses the Mohr Coulomb material properties in its definition and at its ultimate state reaches to the failure defined by corresponding Mohr-Coulomb yield surface. The yield surface of the deviatoric mechanism is defined as:

$$F_s = \frac{q}{E_i(1 - \frac{q}{q_a})} - \frac{q}{E_{ur}} - \varepsilon_q^{p-shear}$$

Where q is the deviatoric stress and $\varepsilon_q^{p-shear}$ is the deviatoric plastic strain generated only by the deviatoric mechanism. The E_{ur} is the elastic modulus in unloading and reloading:

$$E_{ur} = E_{ue}^{ref} \left(\frac{c \cos \varphi + \sigma_1 \sin \varphi}{c \cot \varphi + p_{ref} \sin \varphi} \right)^m$$

where E_{ue}^{ref} is the reference elastic modulus for unloading/reloading at stress level equal to the reference pressure, p_{ref} . Power m , controls the stress dependency of the elastic modulus and it is within the range of $0.5 < m < 1.0$.

The Mohr-Coulomb function, with ultimate friction angle (φ) and cohesion (c), is used in the definition of q_a .

$$q_a = \frac{q_f}{R_f}, q_f = (c \cot \varphi + \sigma_1) \frac{2 \sin \varphi}{1 - \sin \varphi}$$

R_f is the failure ratio and one of the material parameters (less than 1.0 with a default value 0.9).

The other parameter in the definition of yield surface, that controls the slope of hyperbolic curve, is E_i

$$E_i = \frac{2E_{50}}{2 - R_f}, E_{50} = E_{50}^{ref} \left(\frac{c \cos \varphi + \sigma_1 \sin \varphi}{c \cot \varphi + p_{ref} \sin \varphi} \right)^m$$

E_{50}^{ref} is a reference stiffness modulus at the reference pressure.

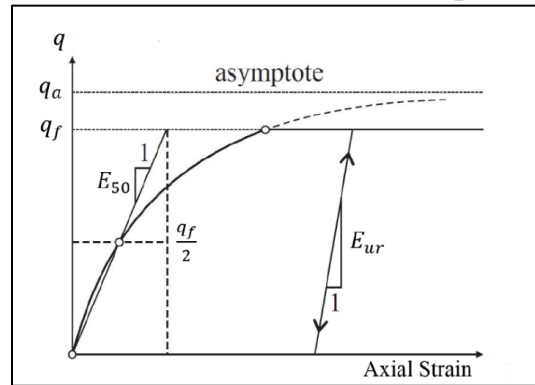


Figure 13 Hyperbolic stress-strain curve in a drained compression triaxial test

2- Volumetric Hardening Mechanism

The main role of the volumetric mechanism (cap) is to close the elastic domain in space (p - q) on the hydrostatic (p) axis and simulate the densification/compaction of the material. The cap in the Hardening Soil model is has an elliptical shape with its apex on the q axis:

$$F_c = \left(\frac{q^*}{\alpha}\right) + p^2 - p_c^2 = 0$$

where p_c is the location of the intersection of this yield surface with the p axis, and α is the shape factor for the elliptical shape of the cap. The stress invariant q^* is defined as:

$$q^* = \frac{a}{f(\theta)}, f(\theta) = \frac{3 - \sin \varphi}{2 (\sqrt{3} \cos \theta - \sin \theta \sin \varphi)}$$

The hardening for these yield surfaces is considered for p_c and it is attributed to volumetric plastic strain generated only by the cap yield surface.

$$\varepsilon_v^{p-cap} = \frac{\beta}{1-m} \left(\frac{p_c}{p_{ref}}\right)^{1-m} \quad or \quad \dot{p}_c = \frac{p_{ref}}{\beta} \left(\frac{p_c}{p_{ref}}\right)^m$$

where β is another parameter for this model that controls the hardening of the cap. The cap parameters α and β are not direct parameters of the model. They are evaluated from the combination of other parameters especially E_{oed} and K_0^{nc} . These last two parameters are material parameters for the hardening Soil model and can be evaluated from an oedometer test. K_0^{nc} is the coefficient of lateral pressure for normal consolidation, and E_{oed} in an oedometer test is the slope of the variation of axial stress versus axial strain. E_{oed}^{ref} is the slope of the aforementioned curve at axial stress equal to the reference pressure.

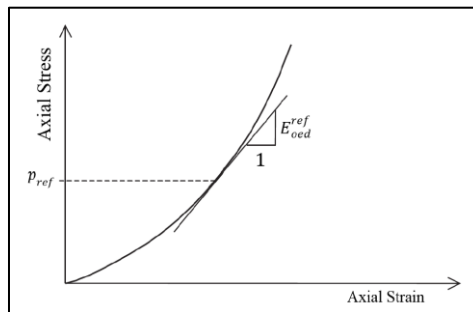


Figure 14 Variation of axial stress versus axial strain in an oedometer, and definition of E_{oed}^{ref}

3- Tension Cut off

This mechanism is to incorporate the tensile strength of the material to this model. In this mechanism the minor principal stress is limited to the tensile strength of the material. The flow rule is associated, and the mechanism has no hardening.

$$F_T = \sigma_1 - T = 0$$

T is the tensile strength of the material.

Chapter 3: The Case study

The case study is a shallow underground metro tunnel. The system is characterised by three functional components: tunnel, stations and ventilation\emergency shafts. The tunnel, hosting two railway tracks, was designed to provide a mix of conventional and mechanised excavation techniques. The stations were conceived referring, case by case, to both cavern and cut & cover layout. Finally, several compensation shafts were sized to comply with the fire brigade and ventilation requirements. The geotechnical and structural analysis of these civil works is characterised by the interaction between the shallow lava stone layer with different sedimentary loose soil.

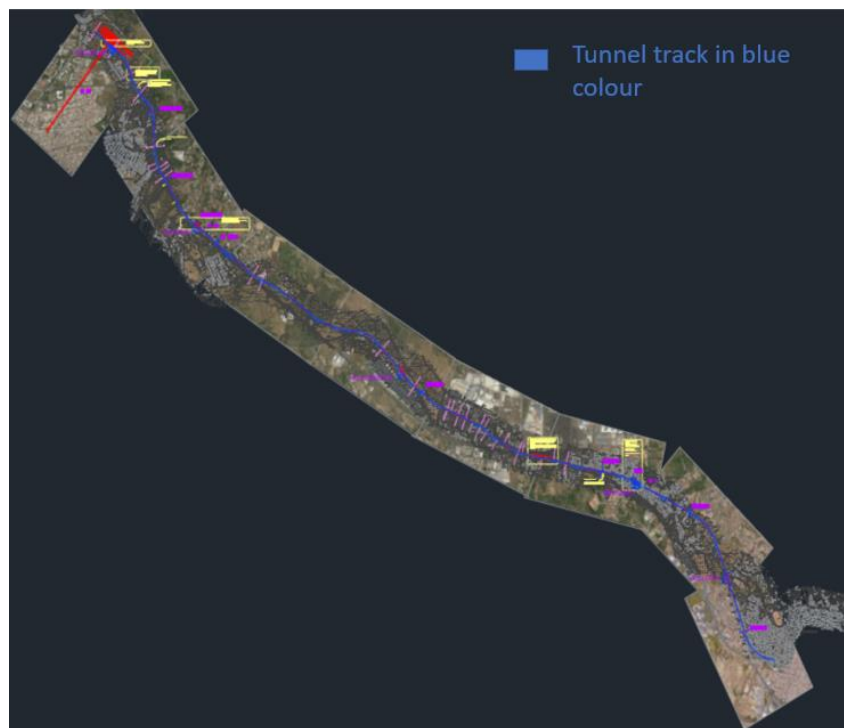


Figure 15 Orthophoto with the metro tunnel line

The tunnel's elevation varies; when the tunnel is close to the surface, it is referred to as an artificial tunnel and the excavation method is by cut and cover method, whereas, if the tunnel has a considerable overburden, it is referred to as a natural tunnel and will be excavated using conventional methods.

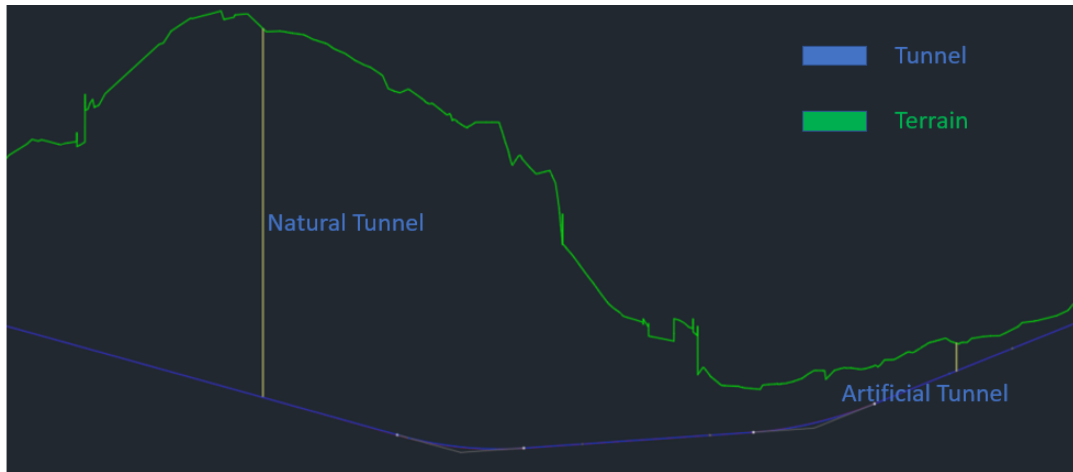


Figure 16 Natural tunnel vs the artificial one

The intersection of the natural tunnel with the cross-passage and the shafts will be considered in this dissertation to meet the scope mentioned in the introduction.

The reason for constructing the shafts and the cross passages in this project is for ventilation and emergency purposes. Figures (17) & (18) demonstrate the shafts, cross passage, and the intersection area.

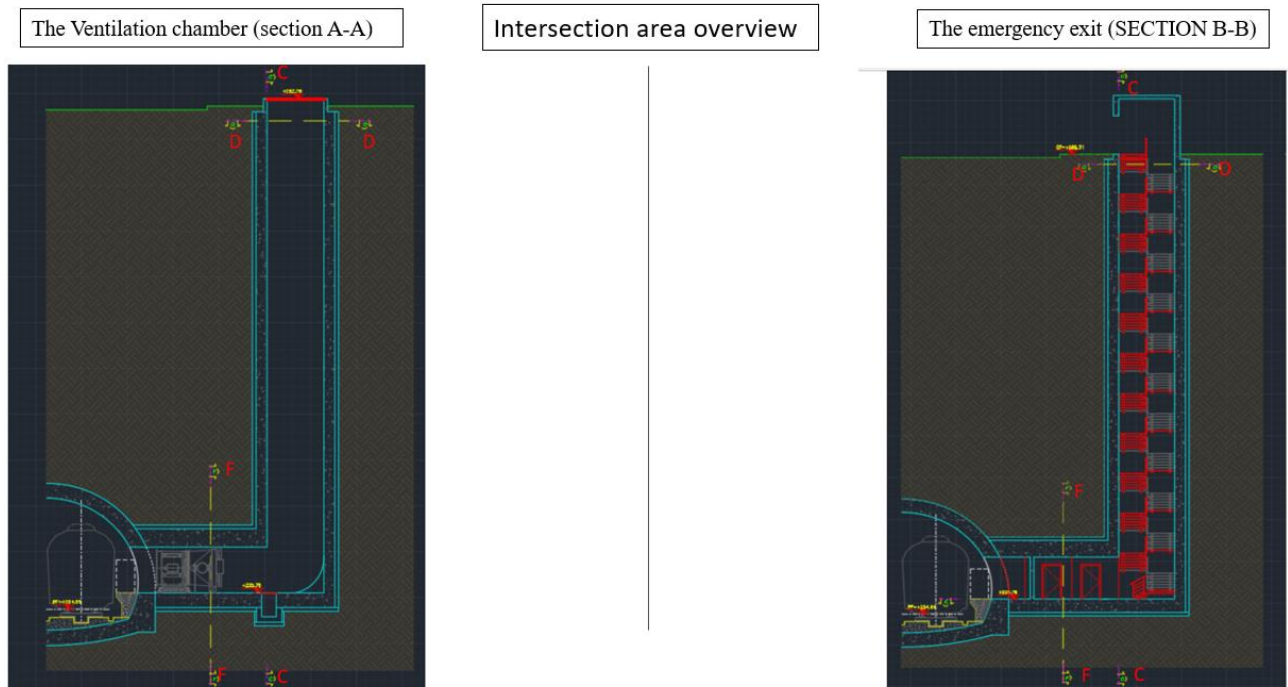


Figure 17 Sections demonstrated the intersection region

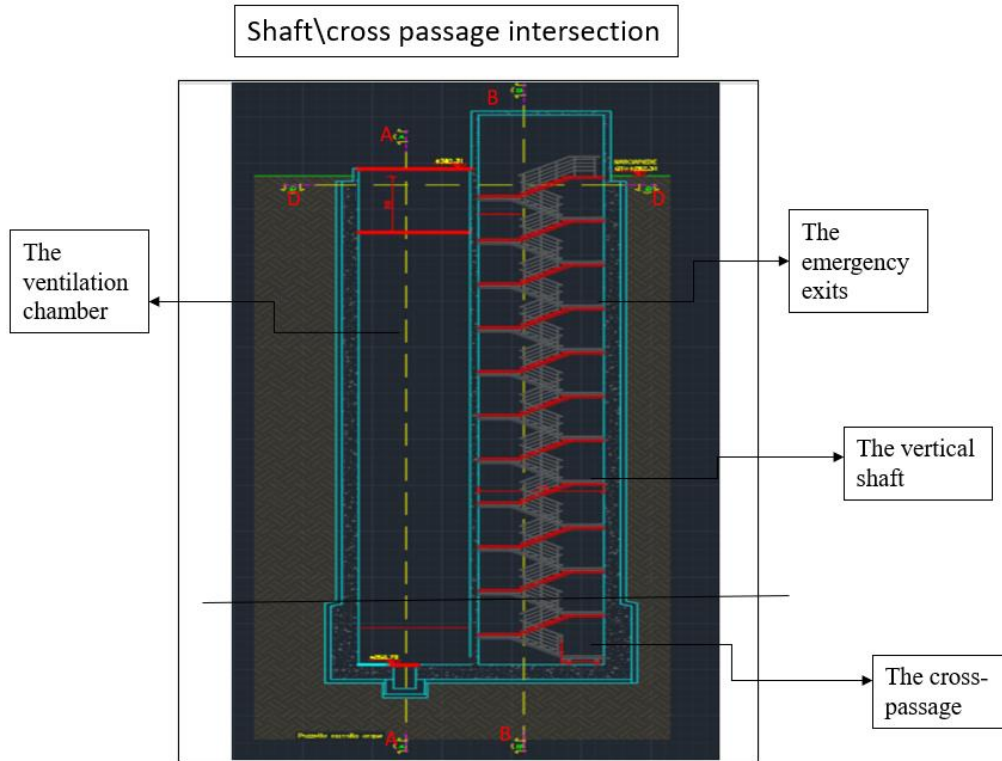


Figure 18 Shaft\ cross passage intersection (section c-c)

3.1 Geometry and geological representation of the considered sections

In this project, the natural tunnel is intersected by eight ventilation shafts. The shafts are divided into four sections, each section containing two ventilation shafts (shaft (a) & shafts (b)).

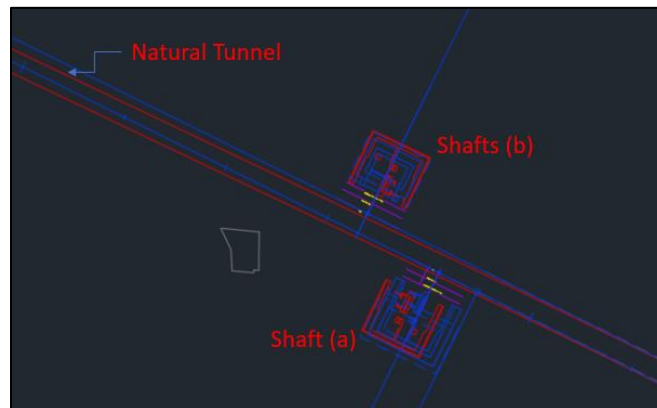


Figure 19 Plan demonstrates the shaft type (a) & shaft type (b)

For the analysis and design of the intersection area, it was decided to examine the favourable and worst stratigraphic scenarios among the eight ventilation shafts.

3.1.1 The favourable scenario “section 1”

The favourable scenario “section1” is related to the intersection positioned in a region where only a layer of shallow basalt is present, as illustrated in figure (20).

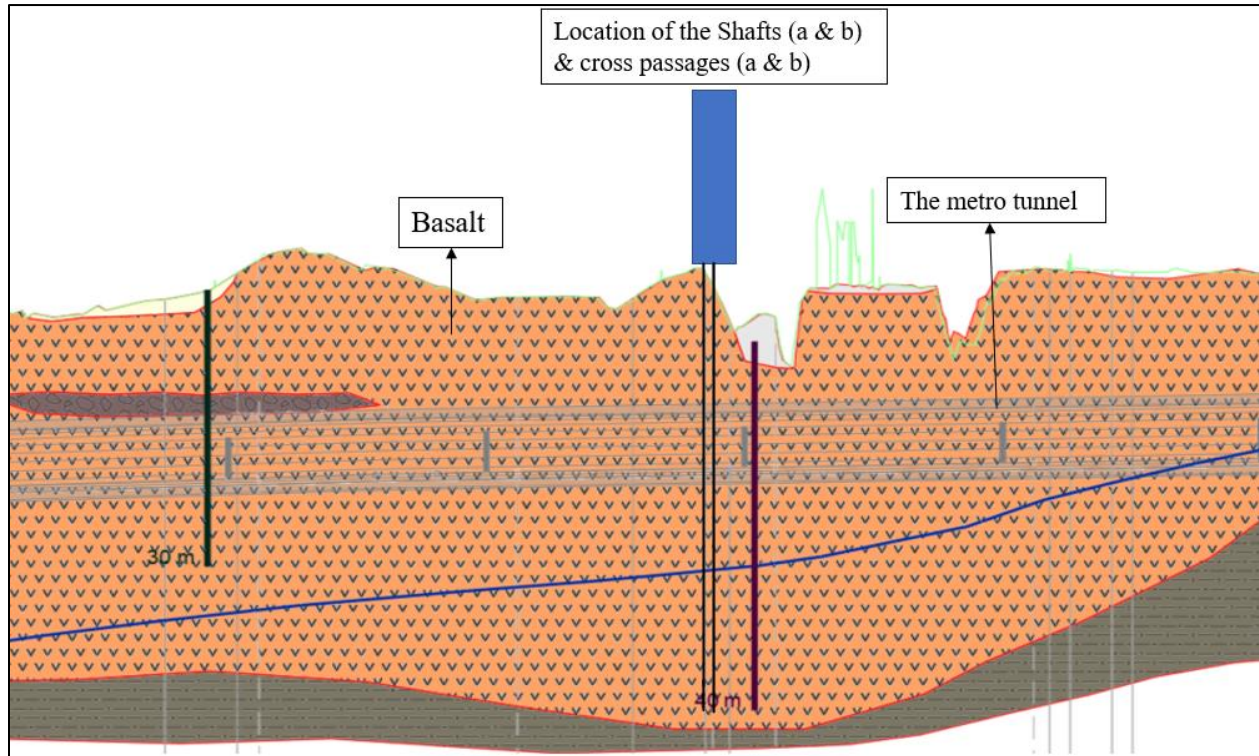


Figure 20 Geology related to the good scenario

This section is called section 1; therefore, the geometry of the three components of the intersection will be named section 1.

❖ Metro Tunnel “section 1”

The metro tunnel “section 1” has a horseshoe shape, and since we are in a good rock mass, the tunnel will be designed without an invert as shown in figure (21).

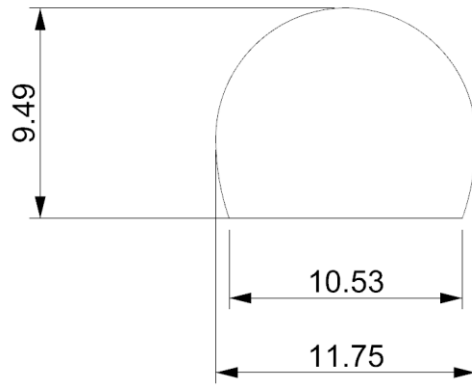


Figure 21 Tunnel cross-section (section 1)

❖ Cross-passage “section1”

As shown before in the figure (17), the cross passage involves two parts. One part is for the ventilation chamber, and the other part is for the emergency exits, and it has the cross section reported in figure (22).

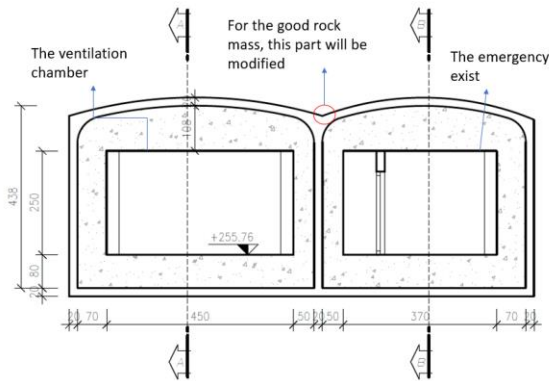


Figure 22 Cross passage section

It has been decided that, in the good rock mass, the cross section of the cross passage should have the shape that shown in figure (23).

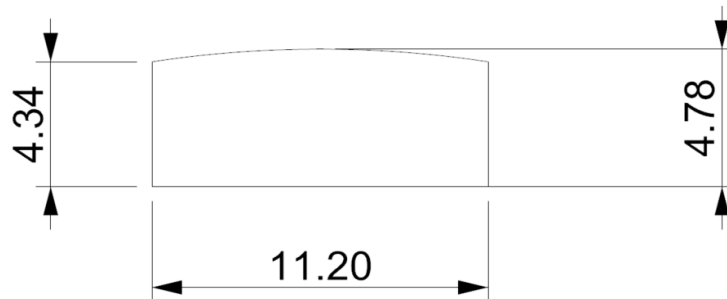


Figure 23 Cross passage type (a)

But the above description is referred to the cross-passage type (a). Only an emergency exist is instead included for the cross passage type (b). The cross-section for the cross-passage type (b) is illustrated in figure (24).

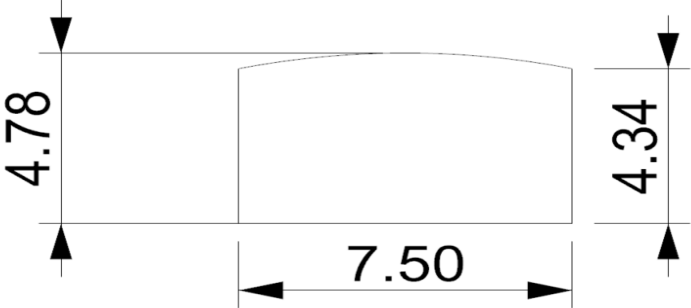


Figure 24 Cross passage type (b)

❖ **Vertical shaft “section 1”**

The cross-section of the vertical shaft has a rectangular shape. As mentioned before, in the shaft type (a), both an emergency exist and a ventilation chamber are included, while in the shaft type (b), only an emergency exist is included. The cross-sections for the shafts type (a) and (b) are illustrated in figure (25).

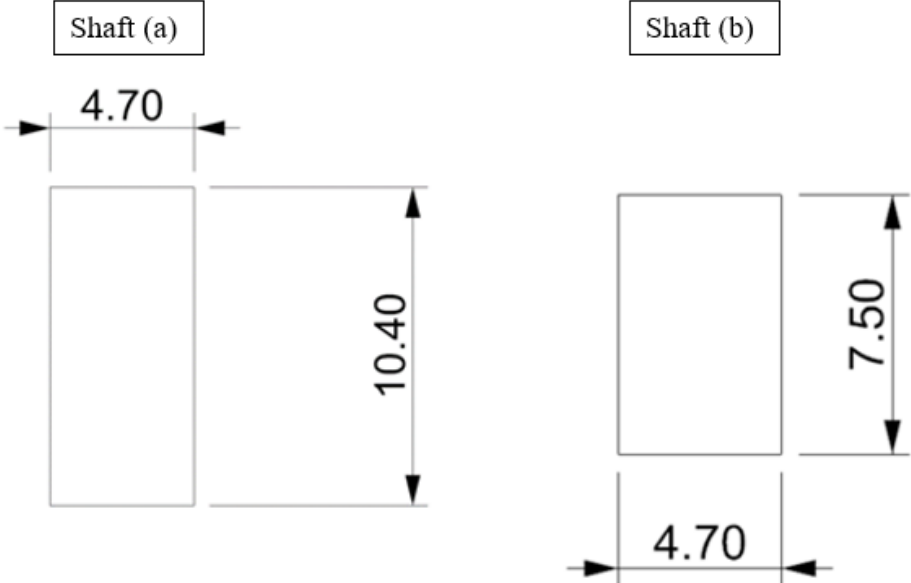


Figure 25 Shaft types (a), (b)

3.1.2 The worst scenario “section 2”

For the worst scenario “section 2”, the intersection of the tunnel with the cross passage and the shaft is positioned in a region where a presence of a challenging geological formation characterised by the intersection of a thick lava layer with different thin layers of loose soil with poor mechanical properties, as presented in figure (26).

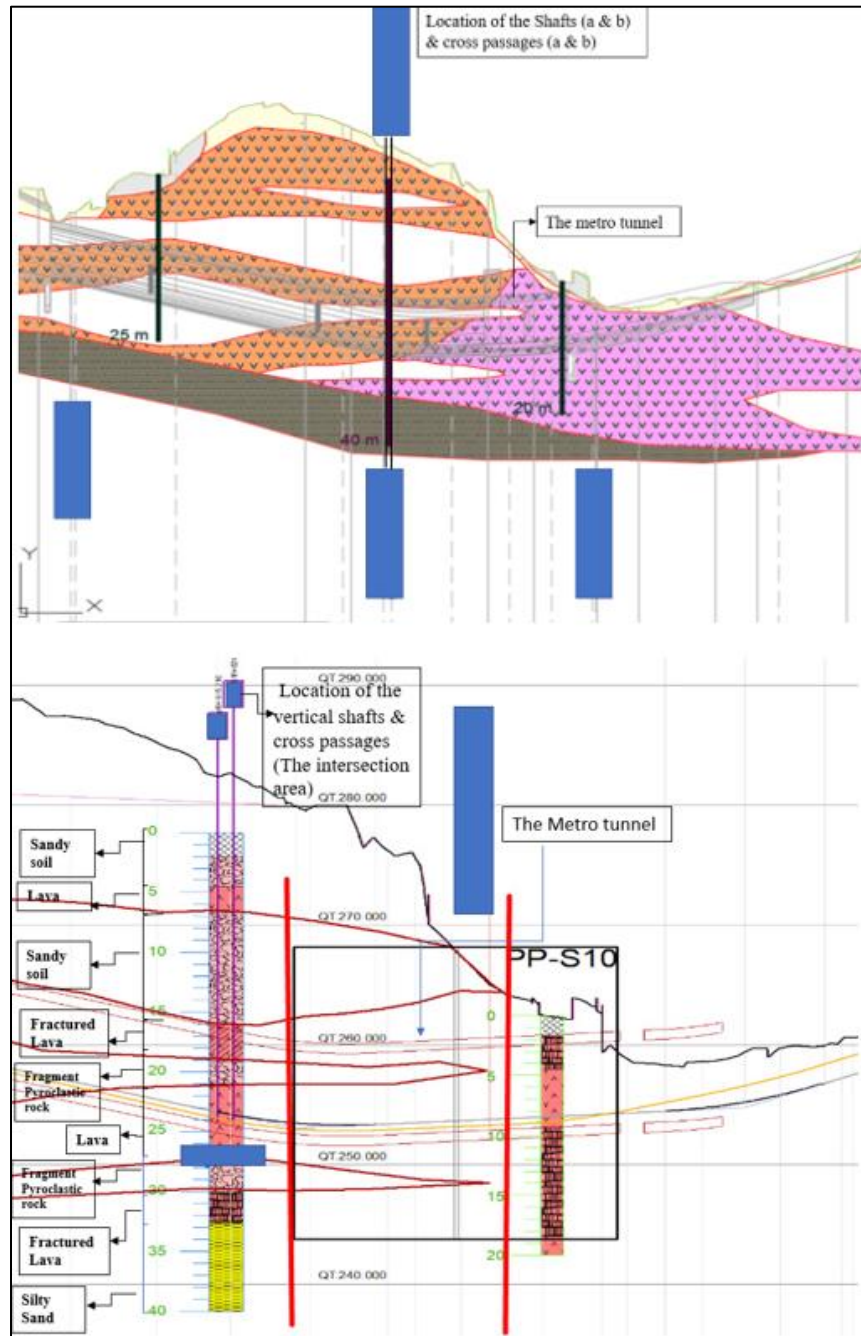


Figure 26 Geology related to the worst scenario

This section is called section 2 therefore the geometry of the three components of the intersection will be named section 2.

❖ **Metro Tunnel “section 2”**

The metro tunnel has a more circular shape. Because this part of the metro tunnel crosses a loose soil and fractured rock mass characterised by poor mechanical properties, it will be designed with an invert, as illustrated in figure (27).

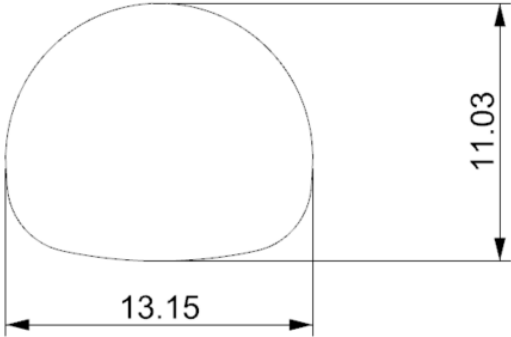


Figure 27 Metro tunnel section 2

❖ **Cross-passage “section 2”**

The cross passage in the worst scenario respects the shape shown in figure (28):

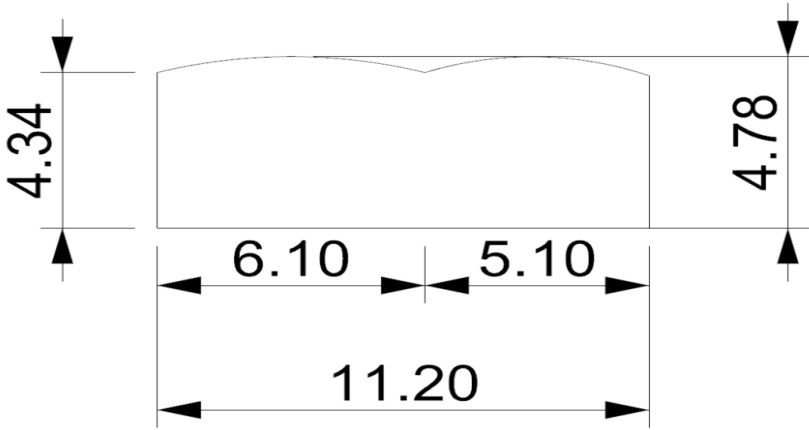


Figure 28 cross passage type (a) for section 2

The cross passage type (b) is with the same dimensions as in the case of the favourable scenario. The cross-section for the cross passage type (b) is illustrated below in figure (29).

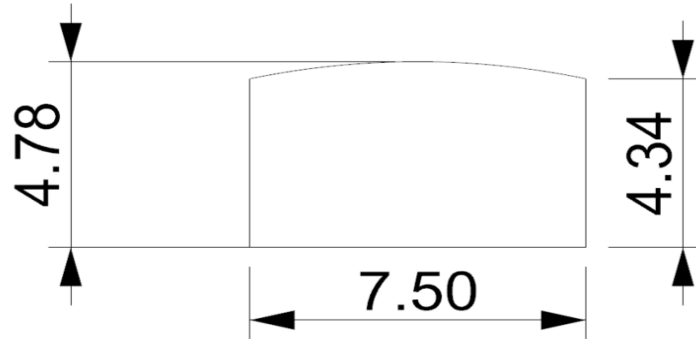


Figure 29 cross passage type (b) cross section

❖ Vertical shaft “section 2”

The cross section of the vertical shafts is always rectangle and has the same dimensions of the case of the favourable scenario. The cross sections for the shafts type (a) and (b) are illustrated in figure (30).

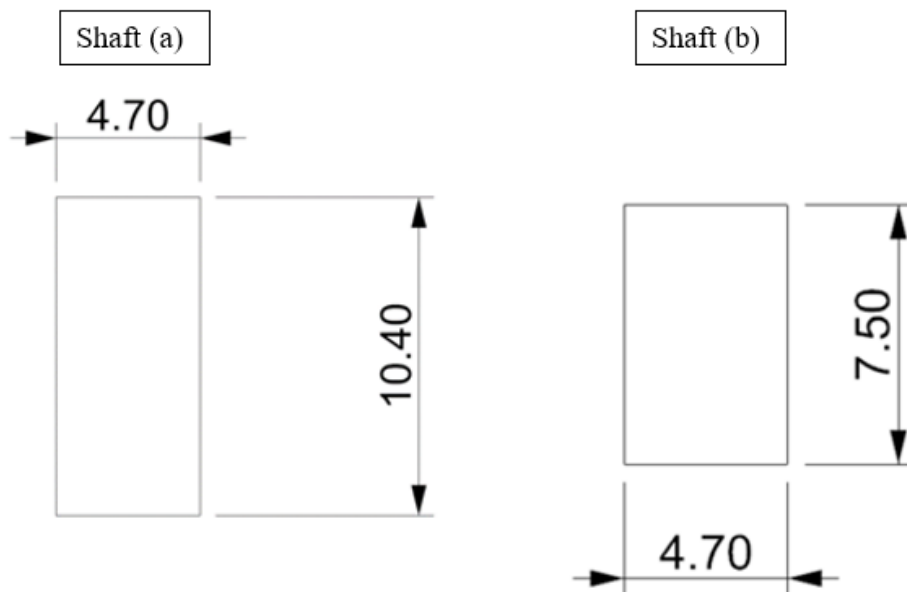


Figure 30 Shafts (a & b) cross sections

Chapter 4: Methodology

This chapter describes the methodology that is followed in this thesis. A flow chart is presented in figure (31) showing the sequence, accompanied by a description of the procedure in each phase and the used softwares.

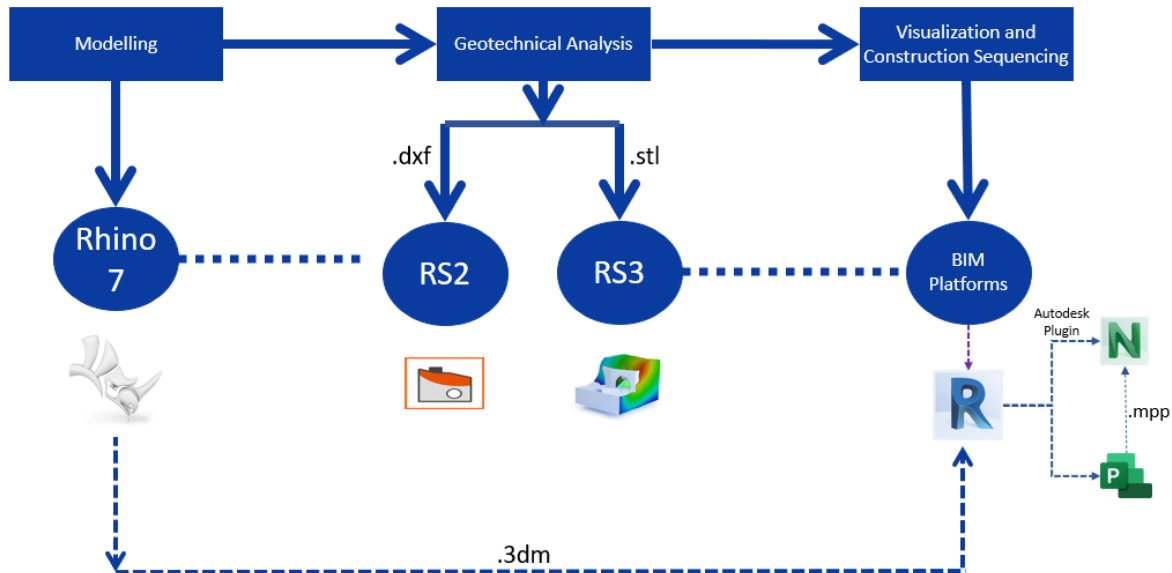


Figure 31

4.1 Geometry in Rhino 7

The first phase is to create the geometry of the intersection areas. The geometry especially at the intersection regions, is complicated due to the irregular and complex geometries involved. However, the ability to import external files in various formats is a powerful and valuable feature of RS3; these details prompted the choice to build the model in Rhino 7, which is an effective tool for modelling complex geometries.

Knowing the geometry of the cross-sections and other structural elements, it was possible to create the model in Rhino 7 by the “closed extrusion” command, which generates a closed volume respecting the initial input geometry. After completing the creation of all the elements, each element is saved in “. stl” format, therefore, they can be imported into the RS3 software.

4.2 Modelling in RS3 & RS2

The second phase is to perform the geotechnical analysis. Therefore, starting from the 3D model in RS3, the first step after importing the geometry into RS3 from Rhino7, is using the repair geometry tool, which is the last step of the import geometry process. The geometry repair tool has been added to RS3 to fix the defects in imported geometry within RS3 instead of using external third-party software. After using this tool, it has been found that there are no defects in all imported geometry.

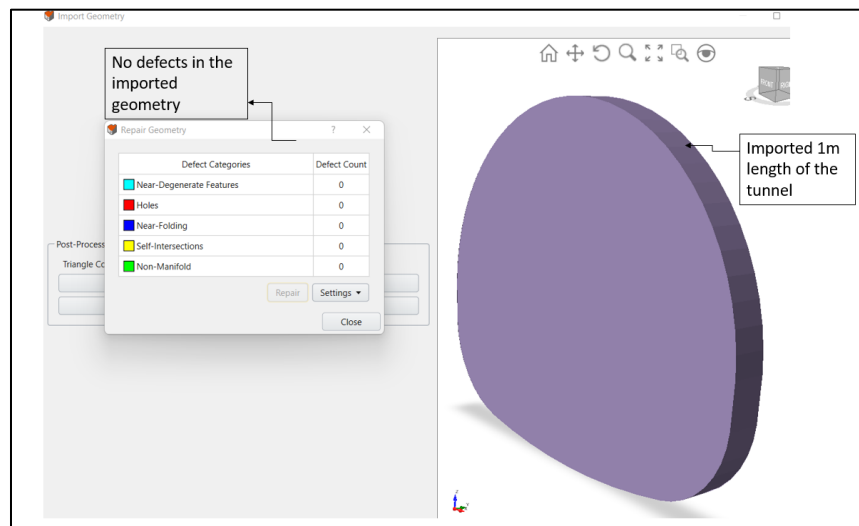


Figure 32 example of the importing geometry process

The next step was to use the important tool in the software, which is the “Divide All geometries”, an essential function for model creation. Analogously subdividing external boundaries creating material regions in enclosed polylines in the RS2 two-dimensional software, “Divide All geometries” in RS3 splits three-dimensional external volume into smaller pieces for materials, supports or loading assignments. Furthermore, after subdividing the geometries, assigning the material properties to each element was possible. The procedure to create the model restrains, mesh and the project stages, are introduced in detail in the 3D analysis part in chapters 5,6 and 7.

For modelling in RS2, the geometry of the tunnel section is a bit complex, and it is impossible to create this complex section by the “excavation boundary” command in the RS2 software. Therefore, it was preferred to import the 2D section of the tunnel from Rhino7 using the dxf format to simulate the correct tunnel section. The detail of the model restrains, mesh and the project stages are reported in the 2D analysis part in chapters 5 and 6.

4.3 Modelling in Revit & Navisworks

In this phase, a visualisation of the final recommended 3D model has been performed. First, the 3D model was imported from Rhino7 to Revit using the “3dm” format. In Revit, the tool of project phases has been used; phases are a great tool to filter elements by stages in a project. Each element or geometry was updated with the phase number associated and previously defined with it, this assigned number respects the construction sequencing used in the geotechnical 3D analysis for each element. Then the model is transferred to Navisworks using the Autodesk plugin in Revit.

Navisworks is a software responsible for creating a simulation of construction by allowing the users to open and combine 3D models, navigate around them in real-time and review the model using a set of tools including comments, redlining, viewpoint, and measurements. With the advantage of Autodesk integration, the project phases that were done in Revit were synchronised with the Navisworks; then, phases were connected to the imported Microsoft project file, which includes the same phases with assumed project scheduling. Eventually, by integrating the three components “Revit, Navisworks & MS project”, it was possible to visualise the construction sequencing of the project in Navisworks.

Chapter 5: Analysis and outputs **(favourable scenario)**

As mentioned in chapter one, this project is in the preliminary design phase, in this phase, the only way to reduce the uncertainties “which is the main concern in all geotechnical problems” is to perform an initial design based on the most feasible conditions (geology, geotechnical parameters, and construction methods). This is aided by behavioural prediction, contingency plans, and trigger values for the monitoring system.

The adopted procedure for the initial analysis & design of the problem “the intersection between a metro tunnel with a cross passage and a shaft” is as follows:

- 1- Analyse a section of the tunnel near the intersection region in 2D using RS2 FEM software. The reason for performing such analysis is to have a reference for the behavioural limits, which could be expected due to the excavation of the tunnel, cross passage, and the shaft (for example the surface settlement trough, plastic zones, stresses state, radial or total displacement distribution). The results from the 2D analysis are to be compared with the 3D model results “before the excavation takes place at the intersection region”. Therefore, a simple model for the tunnel section near the intersection area was realised in RS2. The 2D model analysis and results are introduced in section (5.6).
- 2- The main analysis related to the intersection problem is developed using the 3D RS3 FEM software to check the behaviour due to the construction at the intersection areas. The 3D model analysis procedure is introduced in section (5.1), and the results of the 3D model are reported in sections (5.3) & (5.4).

So, in this chapter, the geotechnical models and the analyses are introduced, followed by the outputs and the detailing. The analysis and the outputs of the models are divided into two parts (analysis and the outputs of the section related to the favourable scenario in terms of stratigraphy “this part is introduced in this chapter” & the analysis and the outputs of the section pertaining to the worst scenario in term of stratigraphy “this part is introduced in chapter 6”).

5.1 Analysis of the section related to the favourable scenario

As shown in the 3rd chapter, the favourable scenario is characterised by a rock mass composed of only basalt, with a GSI (Geological Strength Index) ranging between 40 to 50. This part introduces the analyses of section (1), “that is related to the favourable scenario condition”. The numerical models and the analysis procedure are presented in the following sections.

5.2 3D FEM numerical model by RS3

Since the analysis of the intersection area is the core of this thesis, the numerical modelling procedure is introduced first for the 3D model using RS3, defining all the information required to perform the analysis. Then the part of the 2D model is presented to support some results of the 3D model and to allow the comparison of the 2D model & the 3D model.

Numerical modelling is a powerful tool to deal with complicated problems such as the intersections between structures, as in this current case study. Before starting the analysis, there are some missing data in this project that must be dealt with conservatively for successful preliminary numerical modelling.

It is mentioned in the geological report that the surrounding rock mass has some degree of fracturing. However, there is no data regarding this, on the structure of the rock mass (number of sets of discontinuities, their orientation, and characteristics). Consequently, it is impossible to know if any discontinuity intersects the structures. To deal with this problem, it has been decided that the discontinuities could be implicitly considered by modifying the overall material properties, i.e., implementing an equivalent continuum model. Therefore, the quality of the rock mass in section (1) related to the good scenario was reduced in a way to perform a conservative analysis at the intersection areas. The related material properties of the rock mass are introduced in the section (5.2.3). The second reason to reduce the quality of the rock mass is to follow the suggestion by Hsiao et al. (2008) which indicates that: the measure of degrading rock mass rating is used to install a heavier support system in the intersection area. For instance, one third of the Q-value is suggested for the tunnel intersection.

The other missing data is the (k_0), i.e., the ratio between the horizontal and the vertical geostatic stresses (σ_h / σ_v). In the numerical modelling, it has been decided to consider $k_0 = 1$, since no related tests were performed to evaluate it.

In section (1), because of the presence of fair rock mass, the selected primary support for the stability of the metro tunnel and the cross passages are constituted by rock bolts with sprayed reinforced shotcrete. For the vertical shafts, the struts should be used as temporary support to stabilise the excavation with the sprayed reinforced shotcrete.

Moreover, the excavation was first simulated in intrinsic conditions (without support) to examine the excavation stability in this rock mass and the extension of the plastic zones. From the extension of the plastic zones, the required length of the rock bolts could be known. Then, after designing the support system, the model was run again considering the mentioned support system, and the results such as the axial forces on the bolts are introduced.

The results of the excavation without\with the support are presented in sections (5.3) and (5.4) respectively.

In the following part, the full procedure for the numerical modelling in RS3 is presented.

5.2.1 Geometry

Geometry creation, especially at the intersection regions, is complicated due to the irregular and complex geometries at these intersections. Rs3 has a powerful and practical feature which is the possibility to import external files in several formats. Due to these facts, it has been decided to create the model in Rhino 7 figure (33), which is a powerful tool for modelling complex geometries; therefore, after completing the geometries of all elements, each element is saved as a closed volume in “.stl” format, then each element is imported to RS3, which allows the possibility to assign the required materials properties to each element.

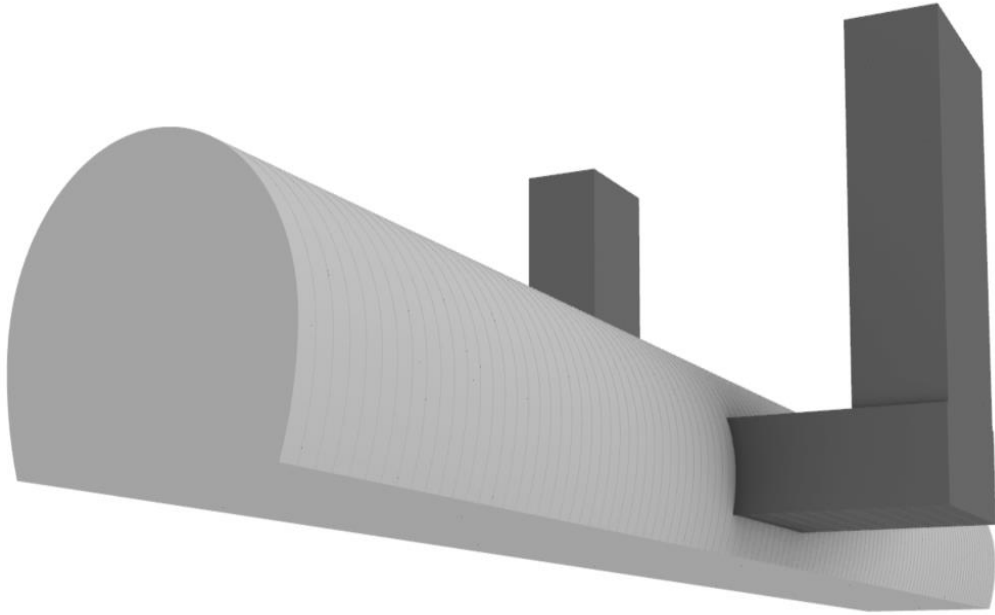


Figure 33 The 3D model in Rhino 7

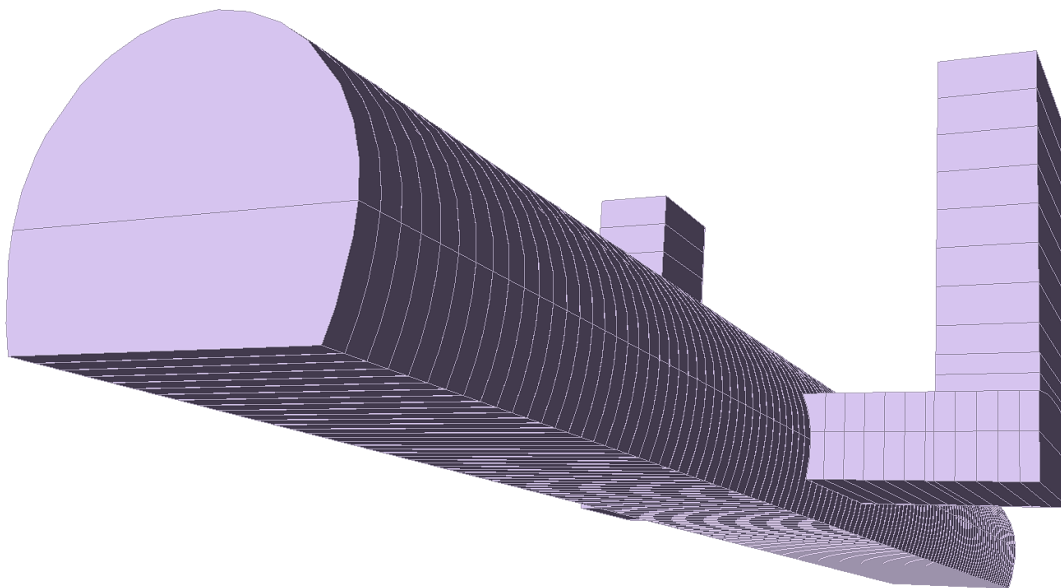


Figure 34 The Model in RS3

It's important to state that, the length of the shafts and the cross passages are taken from the original documents of the project. The considered length for the metro tunnel is the length in contact with the cross-passage. Still, to consider the extension of the effect on the longitudinal distance of the tunnel “due to the demolishing activity from the metro tunnel for opening to the cross-passage”, it has been decided to consider a tunnel length of 40 m more than 3 x the span of the tunnel “as suggested

in the literature (Hsiao et al. (2008)) ” from each end of the cross passages (a) and (b) as shown in figure (35). This will increase in a significant amount the number of staging and the computational time, but it was a conservative way to evaluate the length of the tunnel that could be affected by the excavation of the cross-passage, therefore, to indicate the required range of the additional support at the intersection for the main tunnel.

The total length considered for the metro tunnel equals 106 m as shown in figure (35).

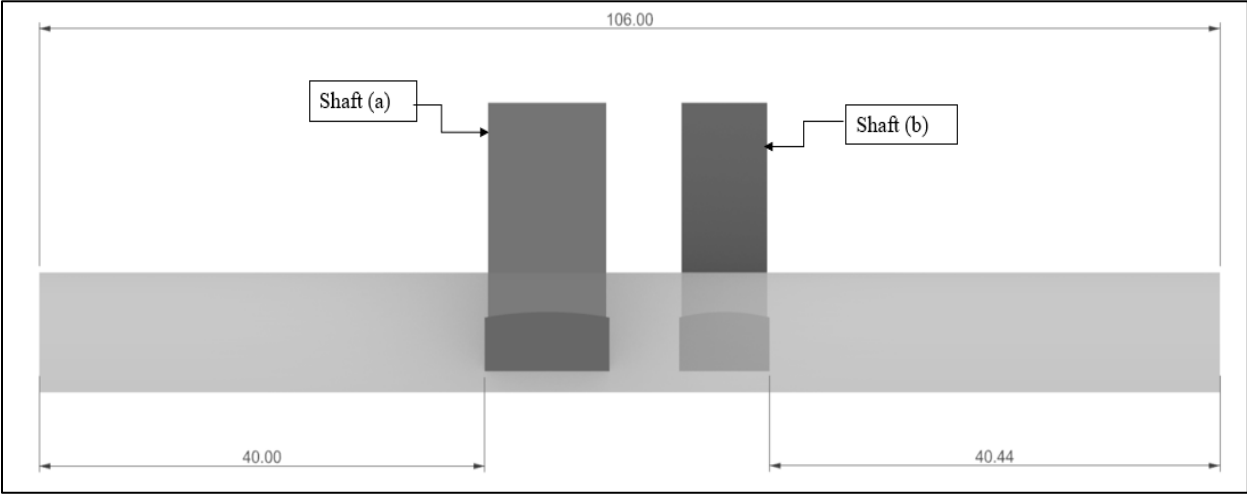


Figure 35 Longitudinal view of the intersection area

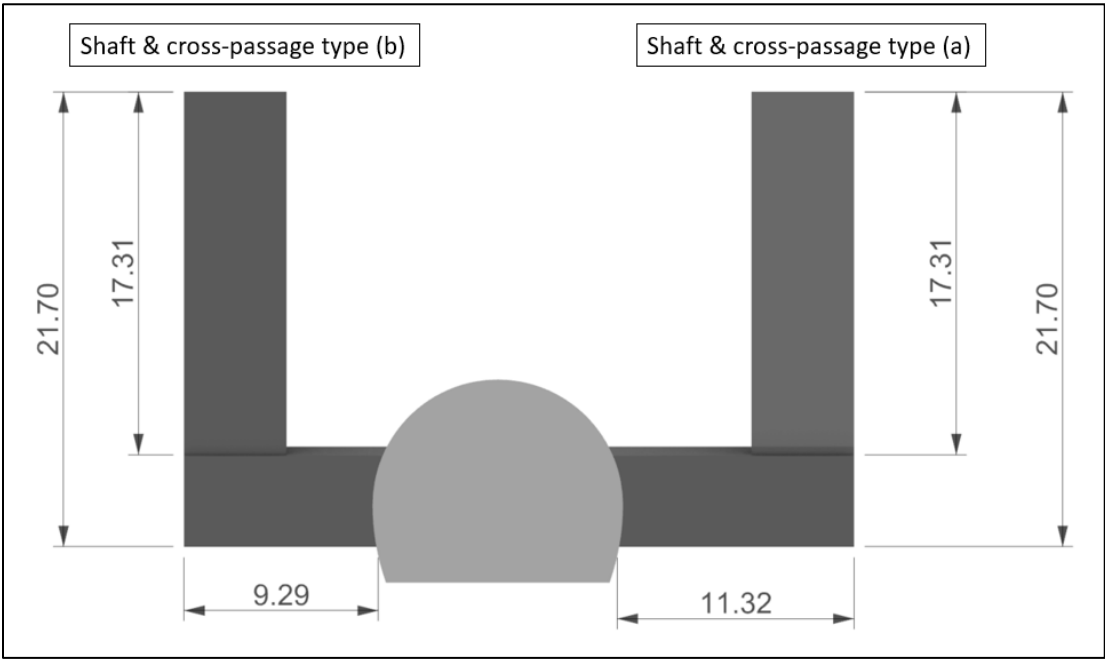


Figure 36 Transversal view of the intersection area

5.2.2 Geological model

Concerning the site & geological conditions, the stratum medium was modelled as a homogeneous single layer. Moreover, based on the geological survey report, for the area of the intersection at the favourable scenario conditions (section 1), the surrounding rocks are only composed of basalt with a GSI (Geological Strength Index) (Geological Strength Index) ranging from 40 to 50, intersected by a certain degree of fracturing.

Since the data and the orientations are missing, it was decided to only consider one layer of basalt by decreasing the rock mass quality, as well as to have a conservative design at the intersection which could lead to install heavier support at these critical areas. The considered GSI for the surrounded rock mass is equal to 30 “this value is less than one third of the Q-value”

Taking into account the size of the finite element model, it was decided to use an external box of (A = 236m, B = 236m, C = 71.7m) figure (37).

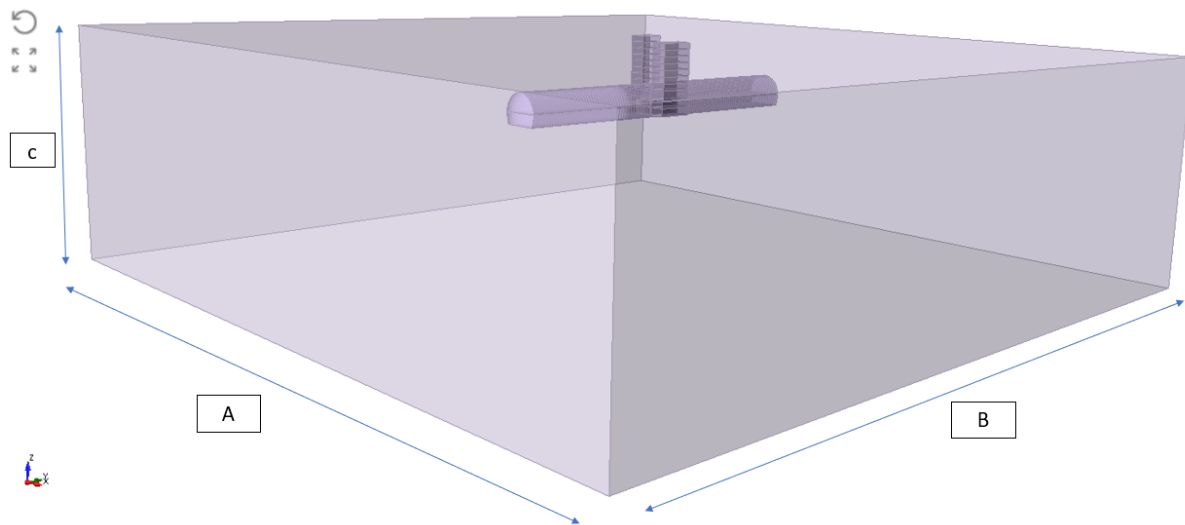


Figure 37 Equivalent continuum model external boundary dimensions

5.2.3 Material properties

Several yield criteria could be used in geotechnical engineering to represent the conditions of the rock mass. It has been decided to use the nonlinear generalised

Hoek & Brown criterion which has the advantage of being used with the same formulation for both intact rock and rock mass [10]

$$\sigma'_1 = \sigma'_3 + (m_b \sigma_{ci} \sigma'_3 + s_b \sigma_{ci}^2)^\alpha$$

Where:

σ'_1 & σ'_3 : The major and minor effective principal stresses respectively.

σ_{ci} : The uniaxial compressive strength (UCS) of the intact rock

m_b , s_b & α are calculated as:

$$m_b = m_i * e^{\frac{GSI-100}{RSF_m}}$$

$$s_b = e^{\frac{GSI-100}{RSF_s}}$$

$$\alpha = \alpha = \frac{1}{2} + \frac{1}{6} (e^{\frac{GSI}{15}} - e^{-\frac{20}{3}})$$

Where:

GSI: (Geological Strength Index) relates the failure criterion to geological observations in the field.

m & s : parameters representing the lithotype and the fracturing degree of the rock mass, respectively.

m_b and s_b : Rock mass parameters

m_i : the intact rock parameter

$$RSF_s = 9 \text{ \& } RSF_m = 28$$

The physical and mechanical parameters assumed for the basalt are shown in Table (4)

Basalt			
Unit Weight	γ	26	KN/m ³
Deformability modulus	E	2563.6	MPa
Poisson ratio	ν	0.3	-
Uniaxial compressive strength of the intact rock (UCS)	σ_{ci}	90	MPa
Intact rock parameter	m_i	17	-
Rock mass parameter	m_b	1.39544	-
Rock mass parameter	s_b	0.000418942	-
Rock mass parameter	α	0.522344	-

Table 4 Material properties of Basalt

5.2.4 Boundary conditions, mesh setup & initial in-situ stresses

❖ Boundary conditions

Concerning the restraints, the model is set as a shallow model (close to the surface), so the “auto restrain surface” option in RS3 was used. This option is a convenient shortcut for automatically applying default restraint boundary conditions on the external boundary for surface models. When the “auto restrain surface” option is selected, XYZ restraints are assigned to the bottom of the external boundary, XY restraints are set for the sides of the external boundaries, while no restraints are assigned to the top surface (ground surface) (i.e., free). When using this option, RS3 automatically determines the top surface (ground surface) of the model. The model constraints are shown in figure (38) below:

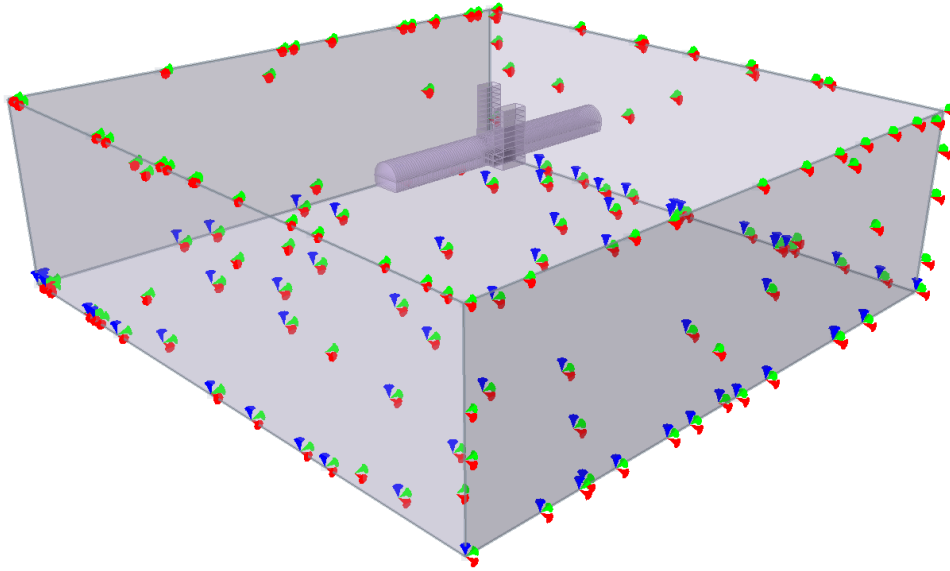


Figure 38 Model restraints

❖ The Mesh

For the realization of the mesh, 4 noded tetrahedral graded elements mesh has been adopted. The meshed model is showed in figure (39).

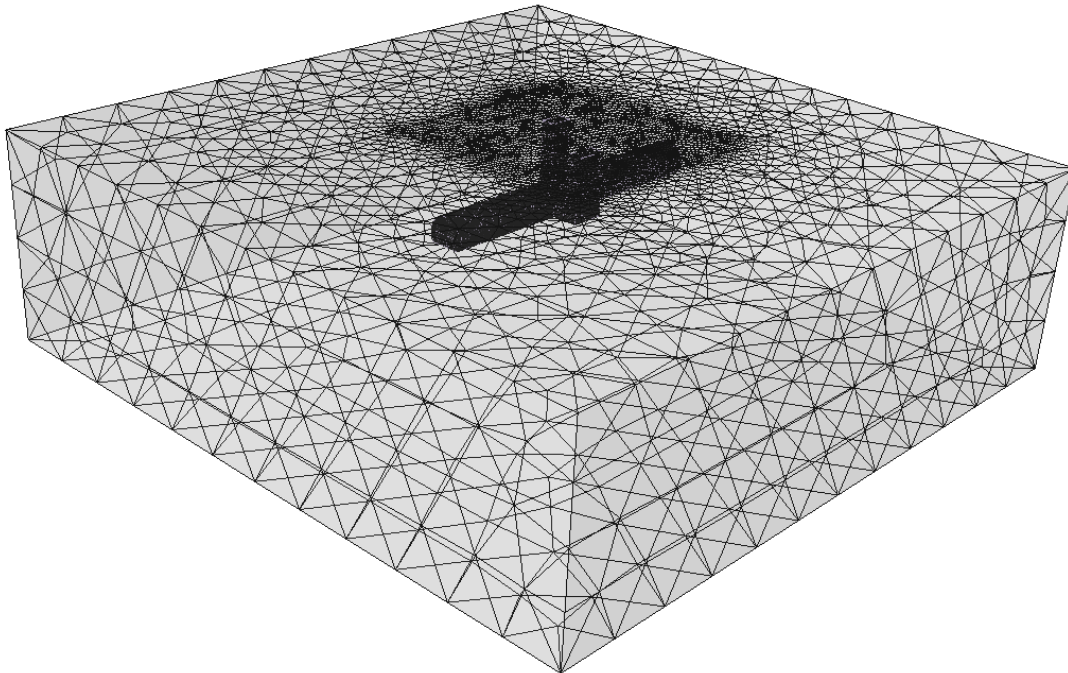


Figure 39 Model mesh

❖ Initial in situ state of stresses

Since we are facing a shallow underground excavation problem, the initial state of stress is not constant. The RS3 software includes the “field stress” option, which allows defining the in-situ stress conditions prior to excavation.

There are two options for defining the field stress in RS3: the Constant or the Gravity field stress. The Gravity field stress option is used to determine an in-situ stress field which varies with depth. Gravity field stress is typically used for surface or near-surface excavations. The overlying material's depth and unit weight determine the vertical stress distribution throughout the model. The horizontal stresses are then calculated by multiplying the vertical stress by the Horizontal/Vertical Stress Ratio (k_0); this implies hydrostatic conditions in the horizontal plane. In this current model, the gravity field stress option is selected and as mentioned before, k_0 was assumed to be equal to 1.

5.2.5 Construction sequencing (staging)

By referring to the project documents, it has been informed that the mucking of the excavated materials from the vertical shafts will be through the metro tunnel, not from the surface, and the construction sequencing will be as follows:

- 1- Excavation of the metro tunnel.
- 2- Excavation of the cross passage from the metro tunnel (mucking of the excavated materials will be through the tunnel).
- 3- Excavation of the vertical shafts from the surface and the mucking will be through pipes to the cross passage and then mucking will be from the tunnel.

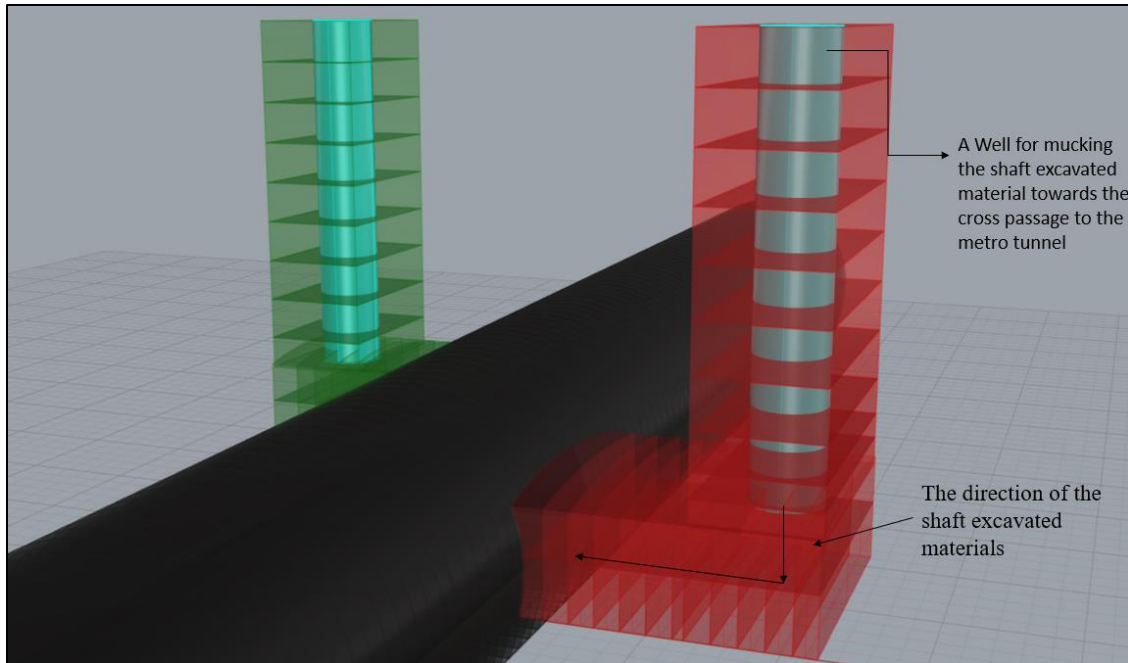


Figure 40 Mucking process for the shaft's excavated materials

Therefore, this construction sequencing was respected for the stage's simulation in all numerical models.

The construction process was simulated using step by step approach. A total of (273) stages were used for the simulation. As mentioned before in section (5.2) the excavation was first simulated in intrinsic conditions (without support) to examine its stability and to obtain the extension of the plastic zones. From the extension of the plastic zones, the required length of the rock bolts could be known. Then after designing the support system, the model was run again considering the mentioned support. The results of the excavation without\with the support are presented in sections (5.3) and (5.4) respectively.

In the staging process, the excavation was simulated by removing the selected materials, and the supporting structures were simulated by activating the structural elements. Moreover, in the model with a support system, the supporting structures were installed on a stage after the excavation.

The construction process respects the suggestion by Bieniawski that based on the RMR classification (for the considered Basalt the $RMR = 35$).

Rock mass class	Excavation	Rock bolts (20 mm diameter, fully grouted)	Shotcrete	Steel sets
I – Very good rock RMR: 81-100	Full face, 3 m advance	Generally no support required except spot bolting		
II – Good rock RMR: 61-80	Full face , 1-1.5 m advance. Complete support 20 m from face	Locally, bolts in crown 3 m long, spaced 2.5 m with occasional wire mesh	50 mm in crown where required	None
III – Fair rock RMR: 41-60	Top heading and bench 1.5-3 m advance in top heading. Commence support after each blast. Complete support 10 m from face	Systematic bolts 4 m long, spaced 1.5-2 m in crown and walls with wire mesh in crown	50-100 mm in crown and 30 mm in sides	None
IV – Poor rock RMR: 21-40	Top heading and bench 1.0-1.5 m advance in top heading. Install support concurrently with excavation, 10 m from face	Systematic bolts 4-5 m long, spaced 1-1.5 m in crown and walls with wire mesh	100-150 mm in crown and 100 mm in sides	Light to medium ribs spaced 1.5 m where required
V – Very poor rock RMR: < 20	Multiple drifts 0.5-1.5 m advance in top heading. Install support concurrently with excavation. Shotcrete as soon as possible after blasting	Systematic bolts 5-6 m long, spaced 1-1.5 m in crown and walls with wire mesh. Bolt invert	150-200 mm in crown, 150 mm in sides, and 50 mm on face	Medium to heavy ribs spaced 0.75 m with steel lagging and forepoling if required. Close in- vert

Table 5 Excavation & support suggestions by Bieniawski

Therefore, the following model stages have been adopted:

- 1- The first stage represents the original geostatic or the initial condition. So, in this stage, the information about the initial in situ state of stress will be introduced.
- 2- Starting from the second stage, the start of the top heading & bench excavation for the metro tunnel. The excavation length at each step in the construction was 1 m.
Before excavating the cross-passage type (a), the entire considered length of the metro tunnel (106 m) was excavated following the modelling stages (2-212).

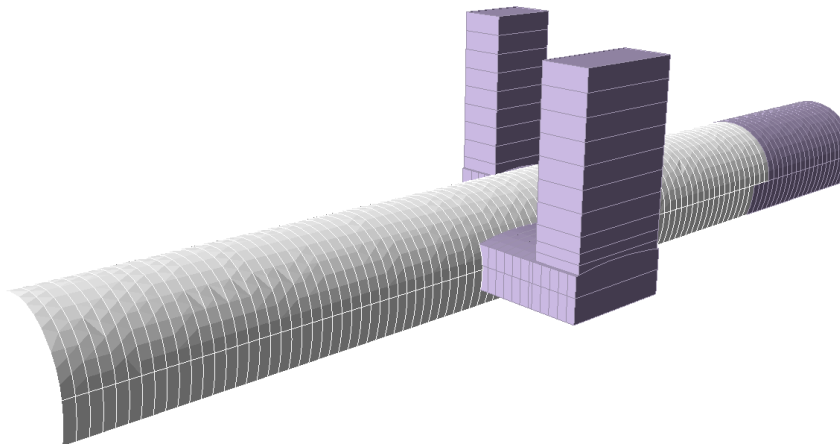


Figure 41 Example of the top heading & bench excavation for the metro tunnel

- 3- From stage 213, the excavation of the cross-passage type (a) from the tunnel was started. The excavation length at each step in the construction was 1 m. Before beginning to excavate the vertical shaft type (a), the entire considered length of the cross passage (a) was excavated following the modelling stages (213-236).

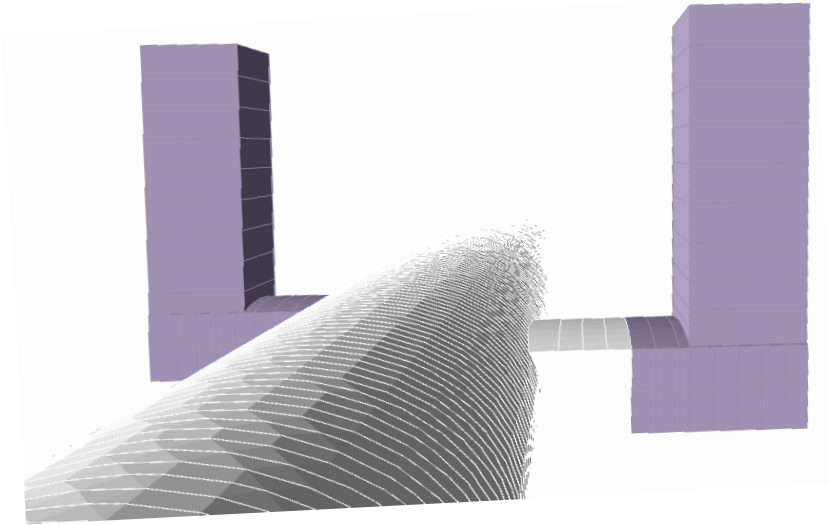


Figure 42 Example of the top heading & bench excavation for the cross-passage type (a) at stage 221

- 4- From the ground surface, starting from stage 237, the vertical shaft type (a) was excavated using the top-down full-face excavation method. The length of the excavation step was 2 m. Before starting to excavate the cross passage type (b), the entire considered length of the shaft type (a) was excavated following the modelling stages (237-246).

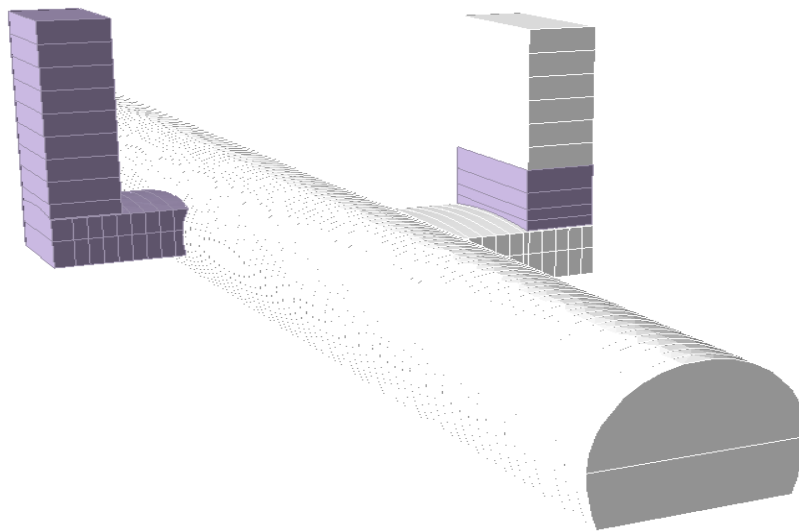


Figure 43 Example of the top-down full-face excavation for the vertical shaft type (a) at stage 240

- 5- From stage 246, the excavation of the cross-passage type (b) from the tunnel was started. The excavation length at each step in the construction was 1 m. Before beginning to excavate the vertical shaft type (b), the entire considered length of the cross passage (b) was excavated following the modelling stages (246-264)

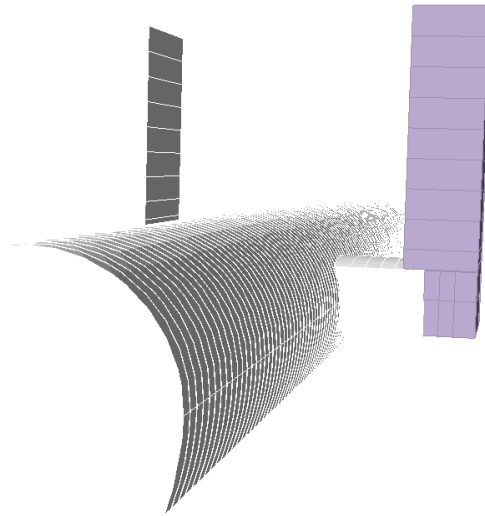


Figure 44 Example of the top heading & bench excavation for the cross-passage type (b) at stage 257

- 6- From stage 265, the vertical shaft type (b) was excavated starting from the ground surface using the top-down full-face excavation method. The length of the excavation step was 2 m. The considered shaft type (b) length was excavated following the modelling stages (265-273).

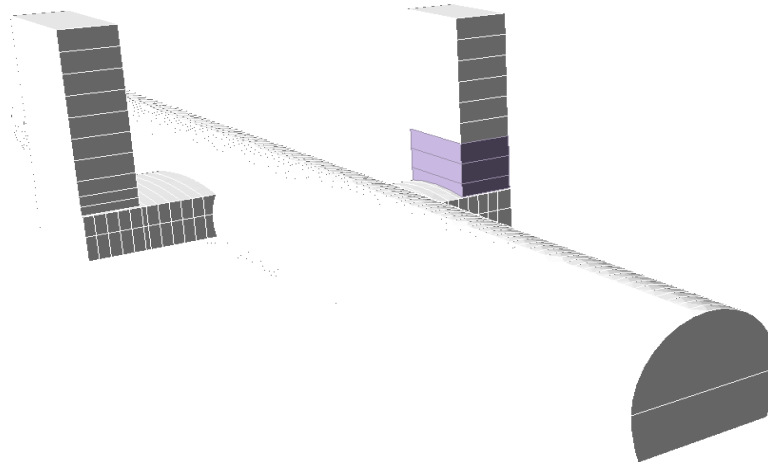


Figure 45 Example of the top-down full-face excavation for the vertical shaft type (b) at stage 269

5.3 Results from 3D analysis

5.3.1 The initial state of stresses

As mentioned previously, the state of stress is not constant but changes with depth. The result of the state of stress, which is at stage 1, is demonstrated in figure (46)

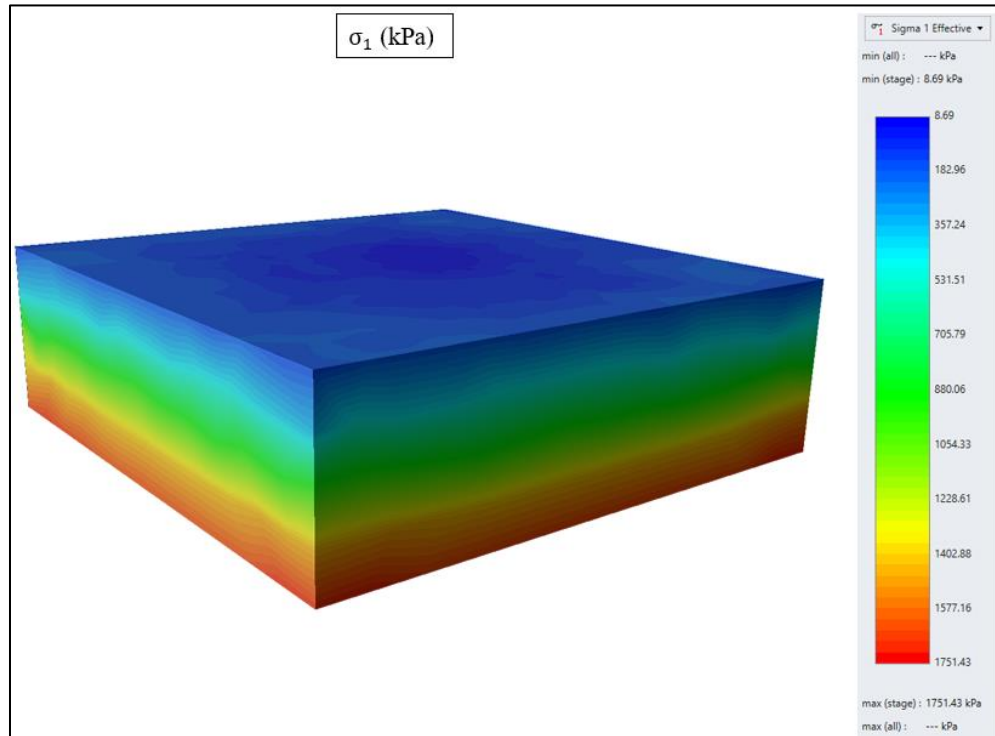


Figure 46 Initial in-situ state of stresses (σ_1 total)

Since k_0 was set to 1, the other initial state of stresses σ_2 and σ_3 follows the same trend. The remaining initial in-situ state of stress results are introduced in the (Appendix) section.

5.3.2 The stress state

Stress concentration is a significant concern during the construction of tunnel intersections. The stress state obtained at the end of the excavation (stage 273) is illustrated.

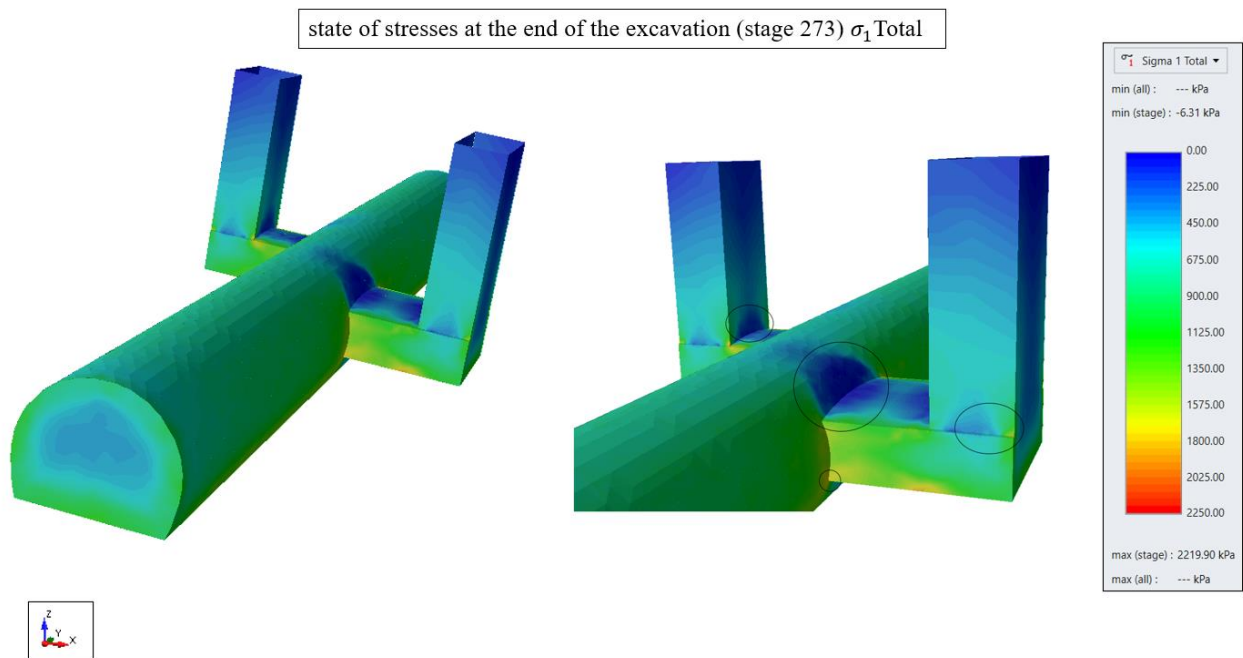


Figure 47 stress state at the end of the excavation (σ_1 total)

From figure (47), it can be clearly seen that the concentration of the stresses occurs at the intersections, with the maximum values at the corners of the contact between the cross-passage and the tunnel, and also at the shafts/cross passages contact.

In addition, it is noticeable that the concentration of the stresses at the length of the cross-passage, especially at the crown. This is due to the cross-passage's small length and the crown's slight curvature.

The results of the other stress state σ_2 and σ_3 are attached to this thesis in the (Appendix) section.

5.3.3 Plastic Zones

This part illustrates the developments of the yielded elements due to the construction of the intersection regions. The following results refer to the end of the excavation (stage 273).

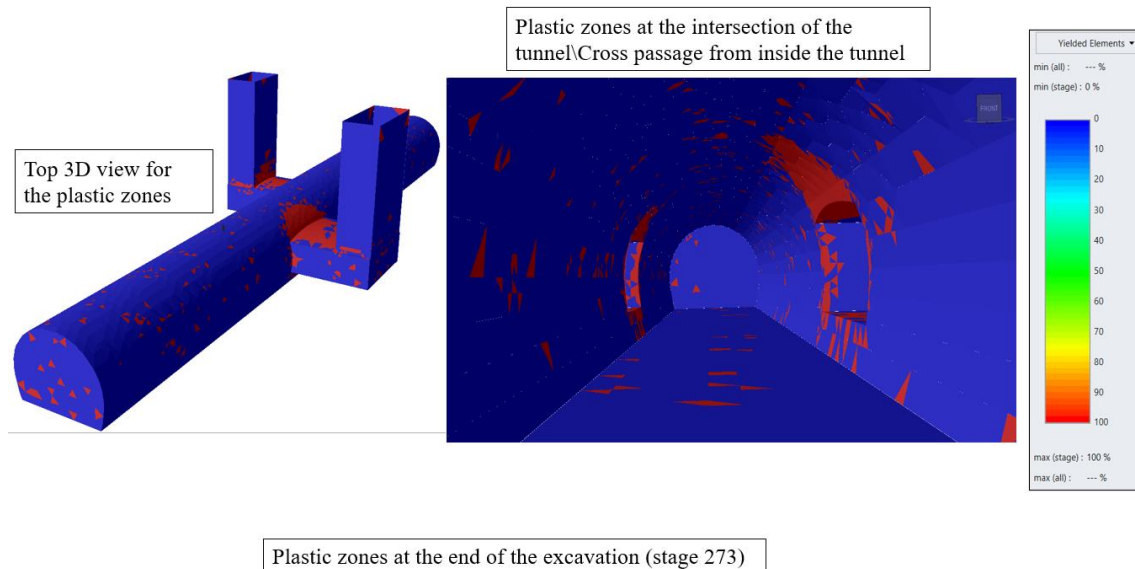


Figure 48 Developments of the plastic zones due to the excavation at the intersection

Figure (48) shows that the plastic zones are concentrated at the intersection regions. Furthermore, the plastic zones are significantly concentrated along the cross-passages length. This is due to the small distance between the two areas that are characterised by significant stress concentration and the crown's slight curvature of the cross passage.

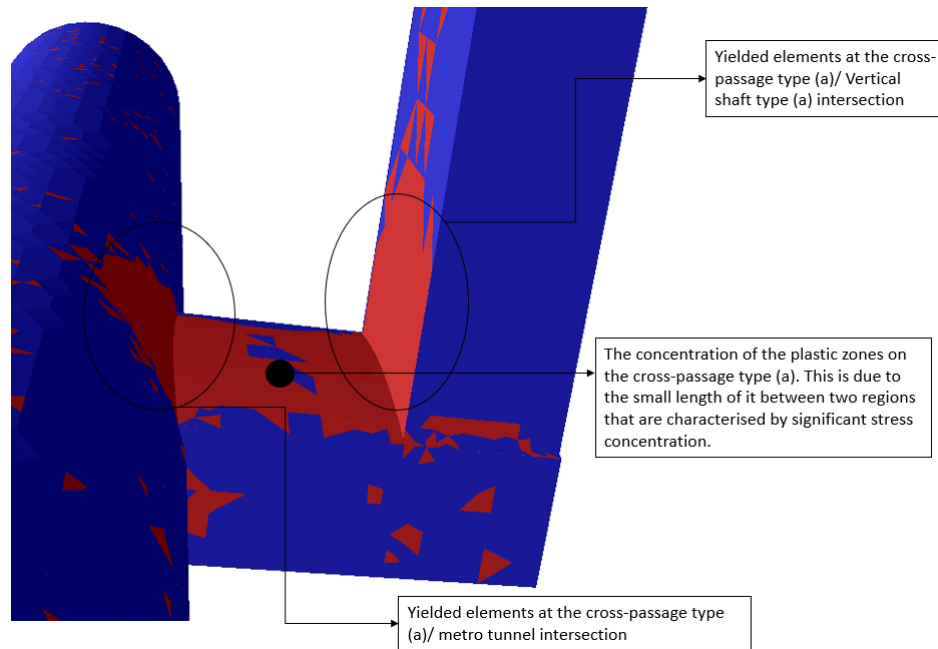


Figure 49 Plastic zones for cross-passage (a)/metro tunnel intersection & cross passage (a)/shafts(a) intersection

Figure (49) refer to the cross passage type (a), but the trend is the same for the intersection of the tunnel & the cross-passage type (b) with the vertical shaft type (b). However lower plastic zones extension is observed as shown figure (50). This is due to the fact that the span of the cross-passage type (b) (7.5m) is lower than the cross-passage type (a) (11.2m).

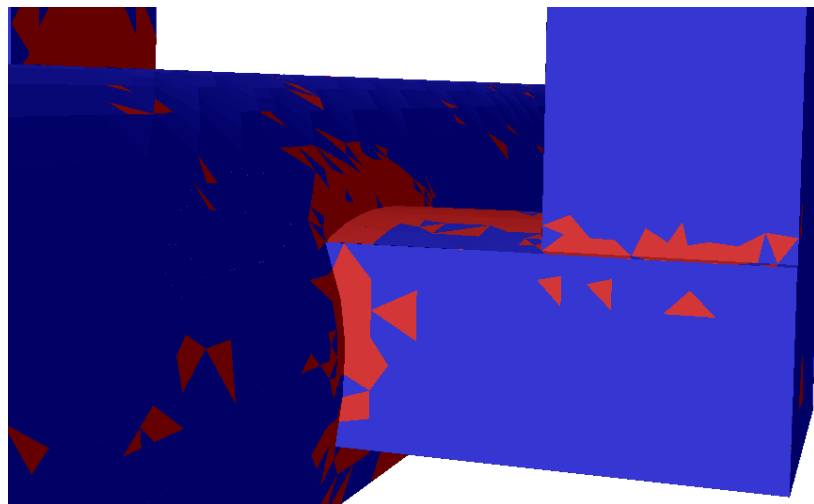


Figure 50 Plastic zones for cross-passage (b)/metro tunnel intersection & cross passage (b)/shafts(b) intersection

Moreover, it is fundamental to estimate the length of the extension of the plastic zones to indicate the length of the bolts that must be adopted and the required range for the additional support along the longitudinal section of the tunnel at the intersections.

Regarding this analysis, the area with the higher extension of the plastic zone is considered, which is related to the shaft (a), and cross-passage (a).

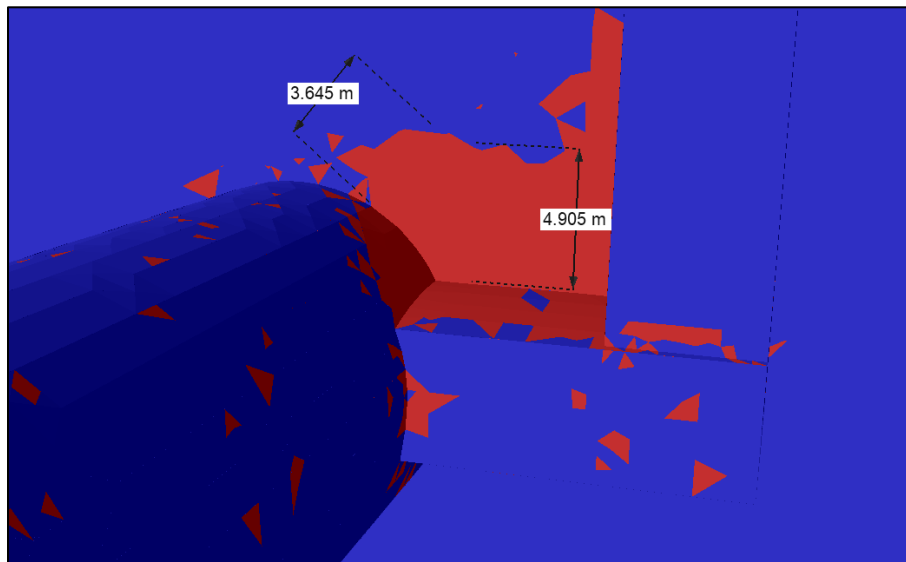


Figure 51 plastic zones extension

5.3.4 Transverse surface settlement

Tunnel excavation inevitably induces deformation in the soil and rock masses around the tunnel and changes the stress distribution. As a result, in shallow excavation these stress redistribution and deformations propagate up to the ground surface and form a settlement trough. The transverse settlement trough immediately following tunnel construction is well described by a Gaussian distribution curve.

To introduce the effect of the excavation of the cross passages and the shafts on the surface settlement trough, the results are shown at different stages.

1- At the end of the metro tunnel excavation (stage 212) (before the cross passage and shaft excavation).

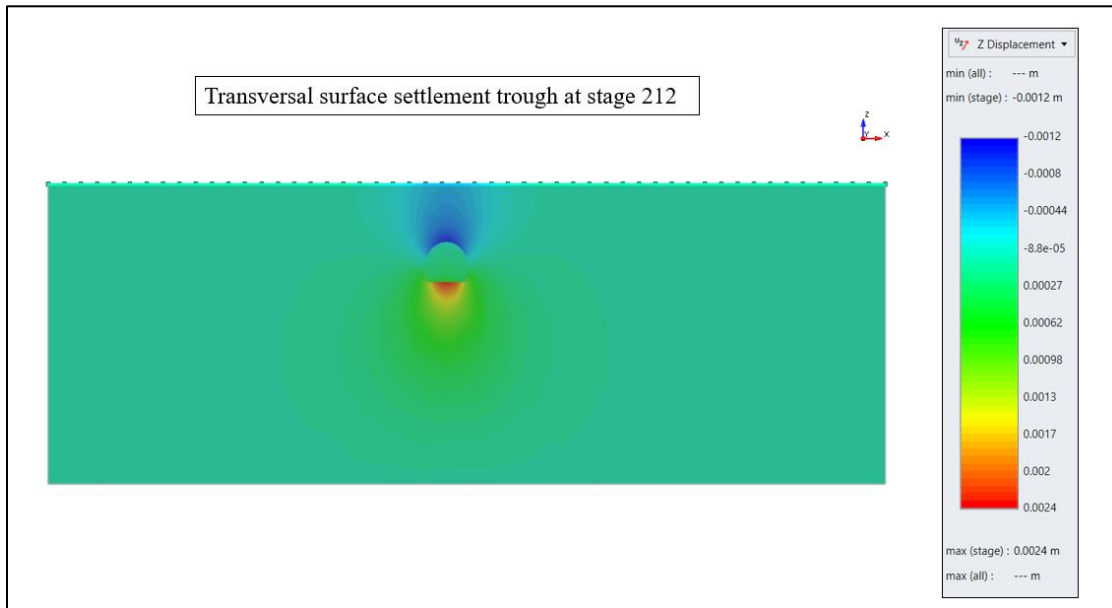


Figure 52 Transverse surface settlement trough at the end of the metro tunnel excavation

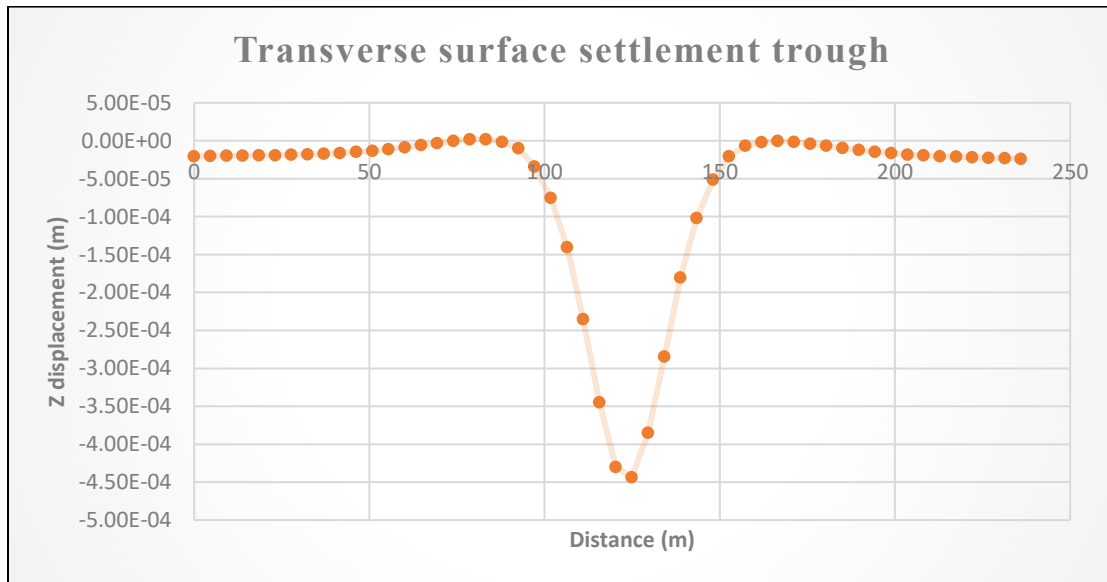


Figure 53 Displacement in Z direction vs query distance at the surface at stage 212

Considering the stratigraphy, it was expected to have a negligible effect on the surface settlement, and this is what was obtained by the numerical simulations: the surface displacement due to the metro tunnel excavation is close to zero (0.4 mm) in the good scenario conditions.

- 2- At the end of the excavation of the shafts & the cross passages “considering the intersection between the cross passage (a) / shaft (a) & cross passage (b) /shafts (b)”.

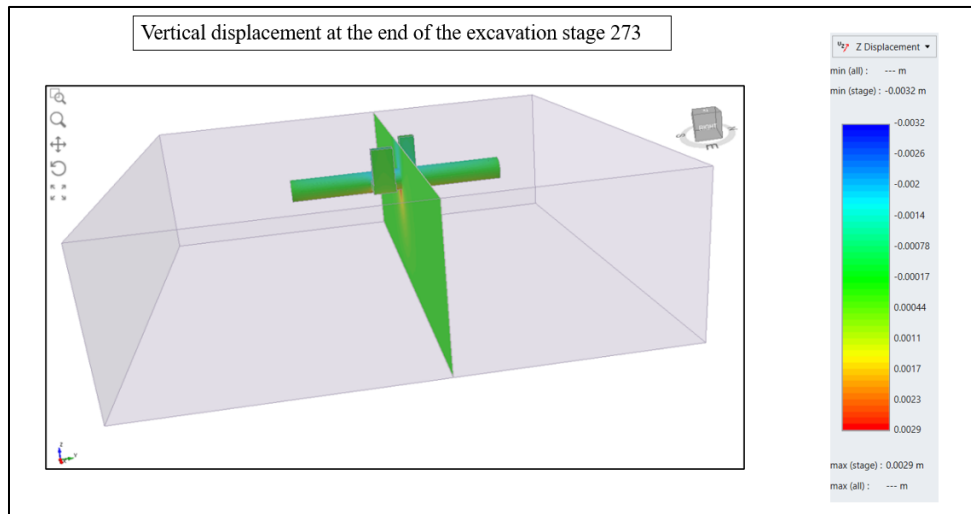


Figure 54 Surface settlement trough at the end of the excavation process at the intersection

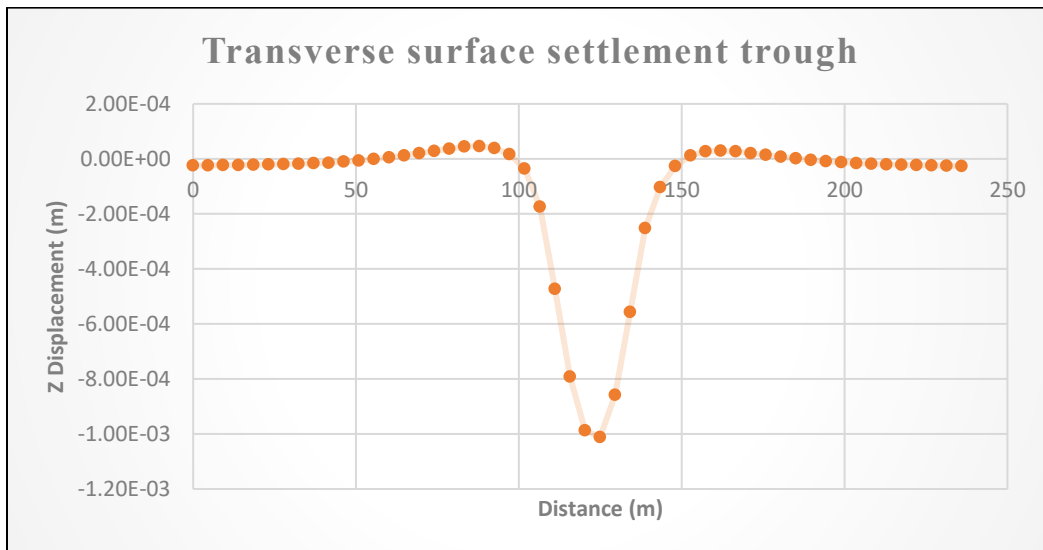


Figure 55 Displacement in Z direction vs query distance at the surface at stage 273

It can be observed that, the effect of the excavation of the cross passages a&b and shafts a&b is not significant (from 0 to 1 mm). Therefore, in the favourable scenario there are no concerns about the settlement at the surface due to the excavation of the cross passage and the shafts.

5.3.5 Longitudinal surface settlement

The longitudinal surface settlement trough could be evaluated, taking into account the scheme of figure (56).

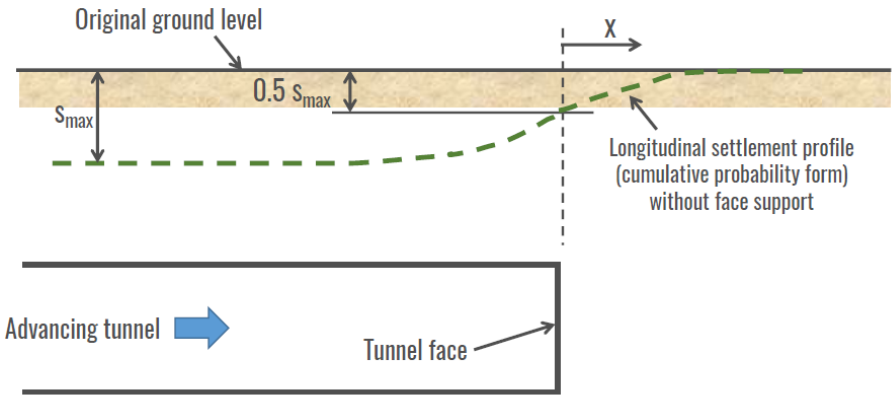


Figure 56 Scheme for the longitudinal surface settlement trough

- Longitudinal surface settlement evaluation at stage 151 during metro tunnel excavation:

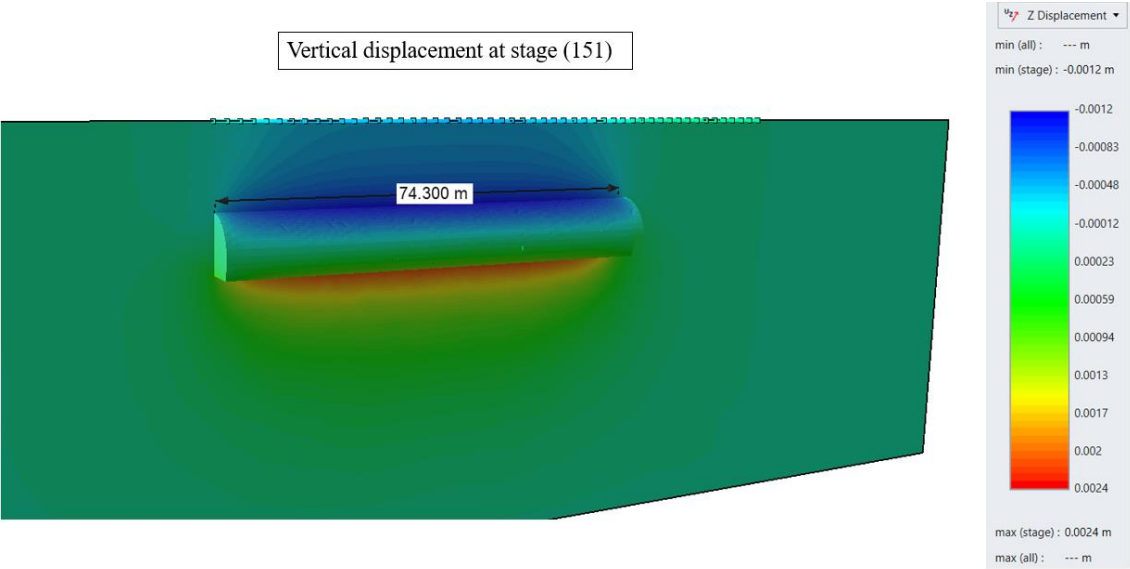


Figure 57 Longitudinal surface settlement trough

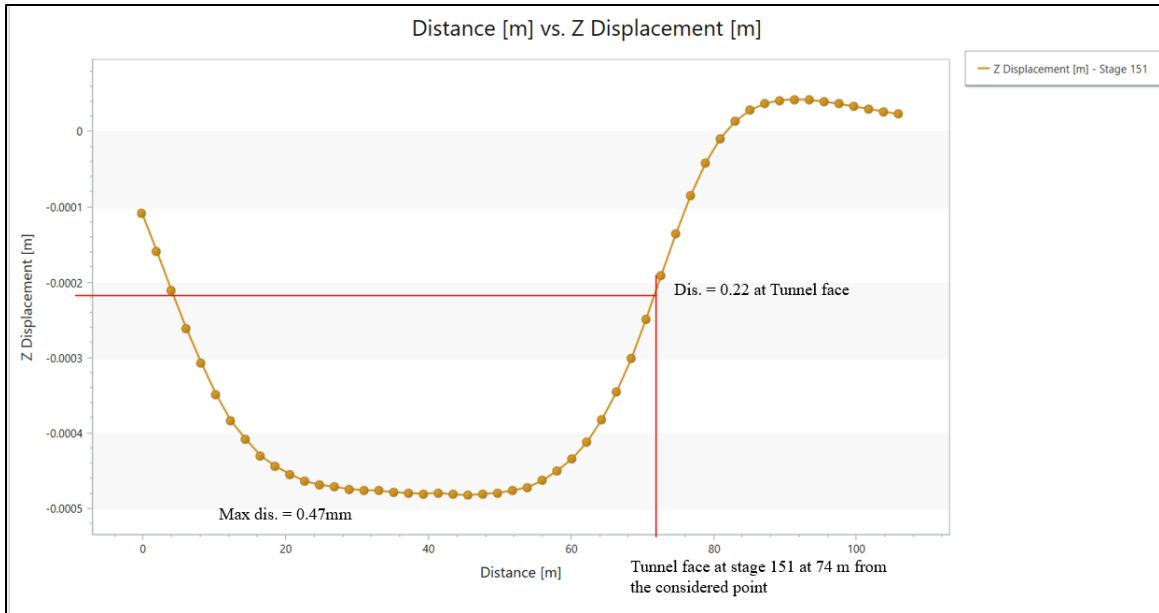


Figure 58 Displacement in Z direction vs query distance at the surface in the longitudinal direction of the tunnel

It can be clearly seen that from figures (57) & (58), the maximum displacement is equal to 0.47mm due to the excavation of the metro tunnel only, as observed for transverse section, and the trend is succeeded to represent the cumulative probability form at the tunnel face as expected (50% of the maximum displacement).

- The effect of excavation of the cross passages and the shafts (stage 273) is presented in the figures (59) & (60).

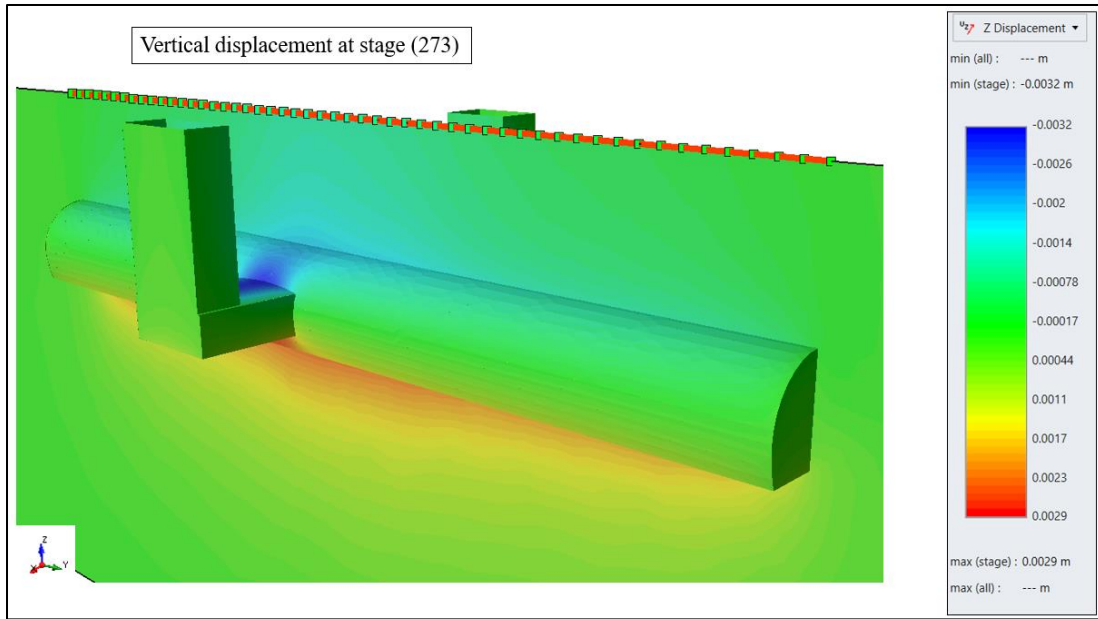


Figure 59 Longitudinal surface settlement trough at the end of the excavation

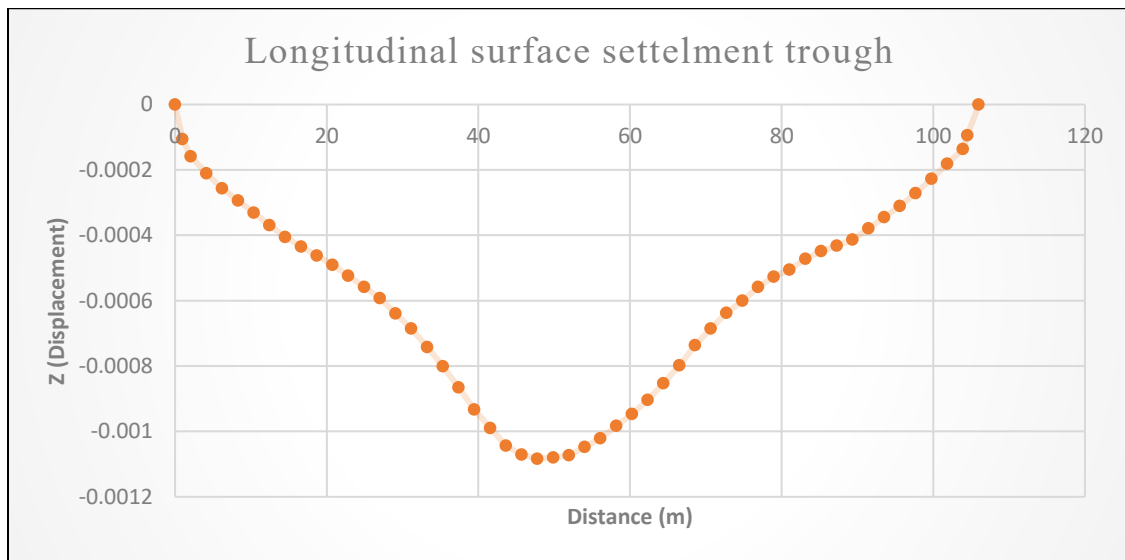


Figure 60 Displacement in Z direction vs the longitudinal query distance at the surface

Figures (59) & (60) describe the shape of the longitudinal surface settlement curve after the excavation of the shafts & the cross passages, which, as mentioned before, reached a maximum value equal to 1mm.

5.3.6 Total displacements

The total displacement at a certain point is the resultant of the displacements in the 3 directions:

$$\text{Total displacement} = \sqrt{X^2 + Y^2 + Z^2}$$

It is always positive, and it is helpful to represent the convergence of the excavated volumes. The total displacement due to the metro tunnel excavation is presented firstly at (stage 212), then the effect of the cross-passage and the shafts are shown (stage 273).

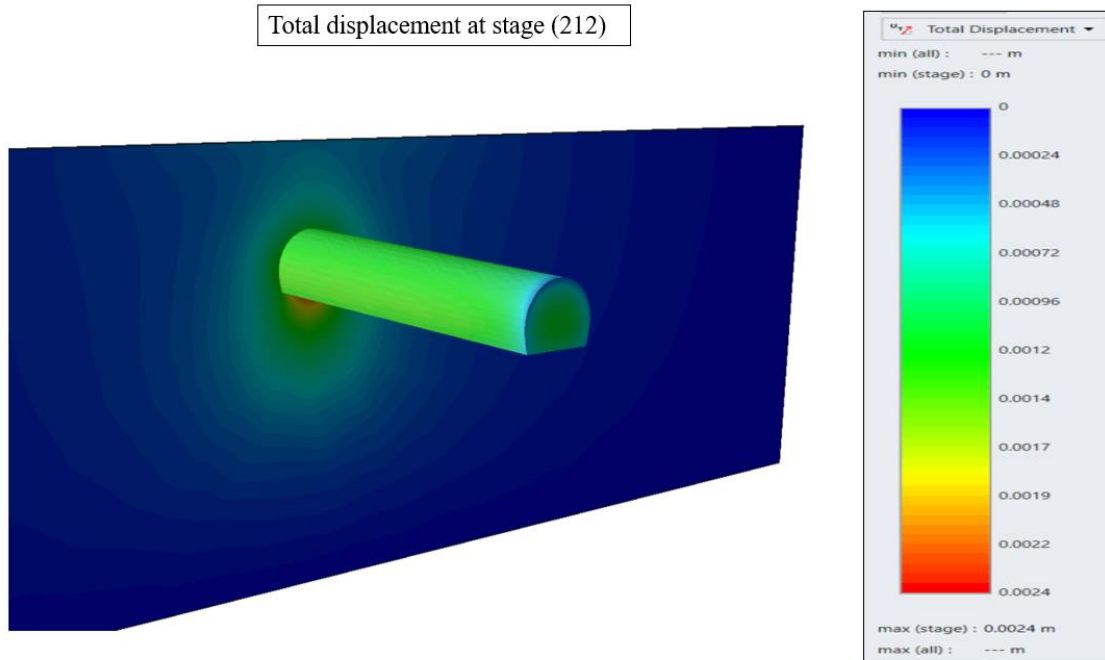


Figure 61 Total displacement for tunnel excavated cantor (at stage 212)

The maximum total displacement is concentrated at the invert of the tunnel with a maximum value equal to 2.4 mm.

- The total displacement due to the excavation at the interaction's regions (stage 273) is represented in the figure below:

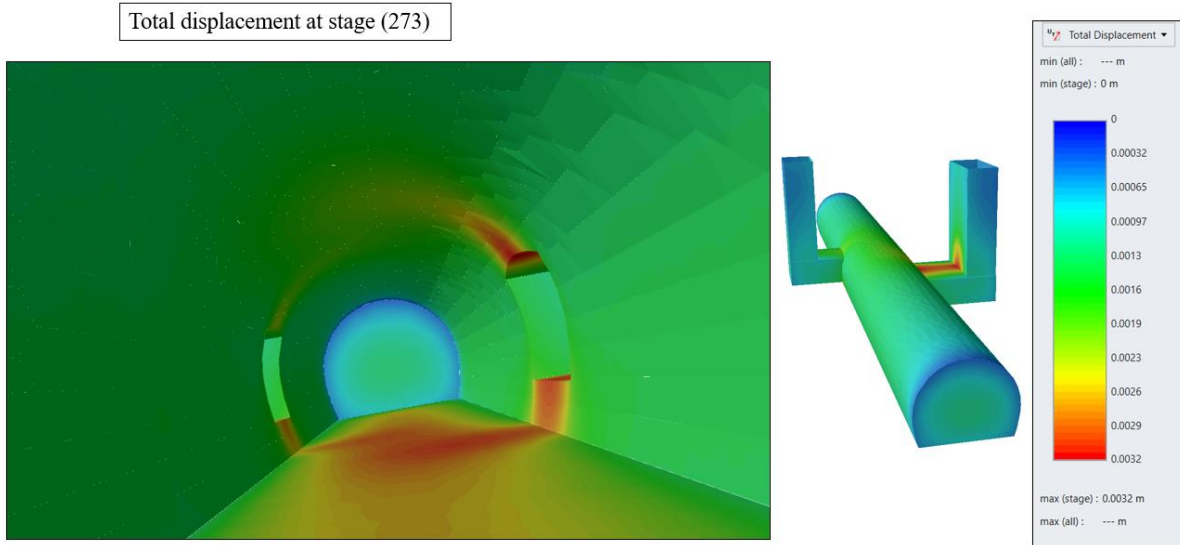


Figure 62 Total displacement at the end of the excavation (stage 273)

It can be clearly seen that the maximum total displacement is localised at the intersections regions, especially the intersection between the metro tunnel and the cross passage (a), since it is required to open 11.2m (span of the cross-passage) from the tunnel. Maximum total displacement can reach a value of 3.2 mm.

- By considering a reference stage at the end of the excavation of the metro tunnel (stage 212) to demonstrate exactly the effect of the shaft and the cross passage the results are demonstrated below:

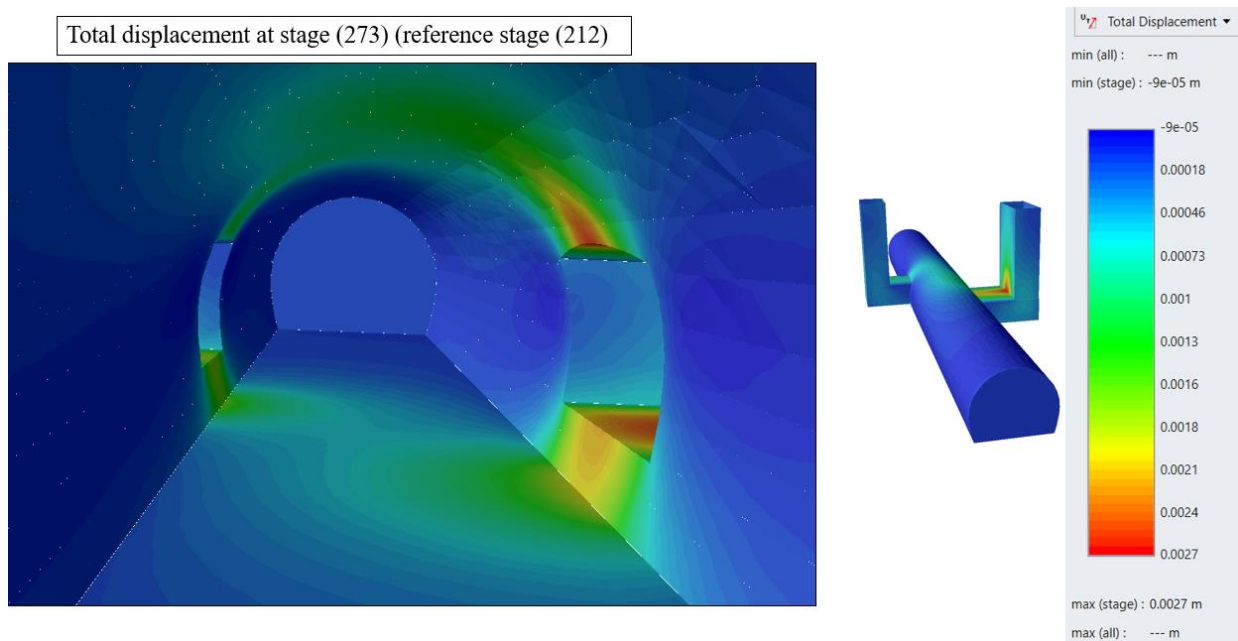


Figure 63 Total displacement at the end of the excavation (stage 273 considering 212 as reference stage)

After considering the reference stage (212) to show the total displacement, the effect due to excavation of the cross passages and the shafts was presented in figure (63), with a maximum total displacement equal to 2.7mm localised at the intersection of the cross-passage (a) with the metro tunnel and also with the shaft type (a).

5.4 Design of the support for the structures in the good scenario

5.4.1 Support for the cross passages & Metro Tunnel (section at the intersection region)

Besides the results from the model in intrinsic conditions by considering the extension of the plastic zones, a preliminary design approach of the support based on the Rock Mass Quality system (Barton, 1974) is used to assess the reinforcement suggested for the case. The Q-value can be obtained through the following formula, which correlates the GSI and the Q:

$$GSI = 9\ln Q + 39$$

The geological report states that the quality of the rock mass GSI ranges between 40 and 50. Still, as mentioned before, the GSI was considered equal to 30 to assess the degree of fracturing in the rock mass by reducing the quality of the overall rock mass, moreover, the other reason is to have a conservative support to be installed at the intersection area.

The Q-value can be calculated using the above equation, and the value obtained is 0.368.

This Q-value can be used for a preliminary selection of the type of reinforcement expected to be considered for the underground excavation. In the support chart provided by Barton and Grimstad shown in figure (64), the Q-values are plotted along the horizontal axis and the equivalent dimension along the vertical axis on the left side. For a given combination of Q-value and span or height in m, a given type of support is suggested, and the support chart is divided into areas according to the type of reinforcement. The support chart is based on empirical data; it can be a guideline for the design of support for underground excavation. In the case of bolts,

their length can also be derived and depends on the span or wall height of the underground opening and the degree of the rock mass quality.

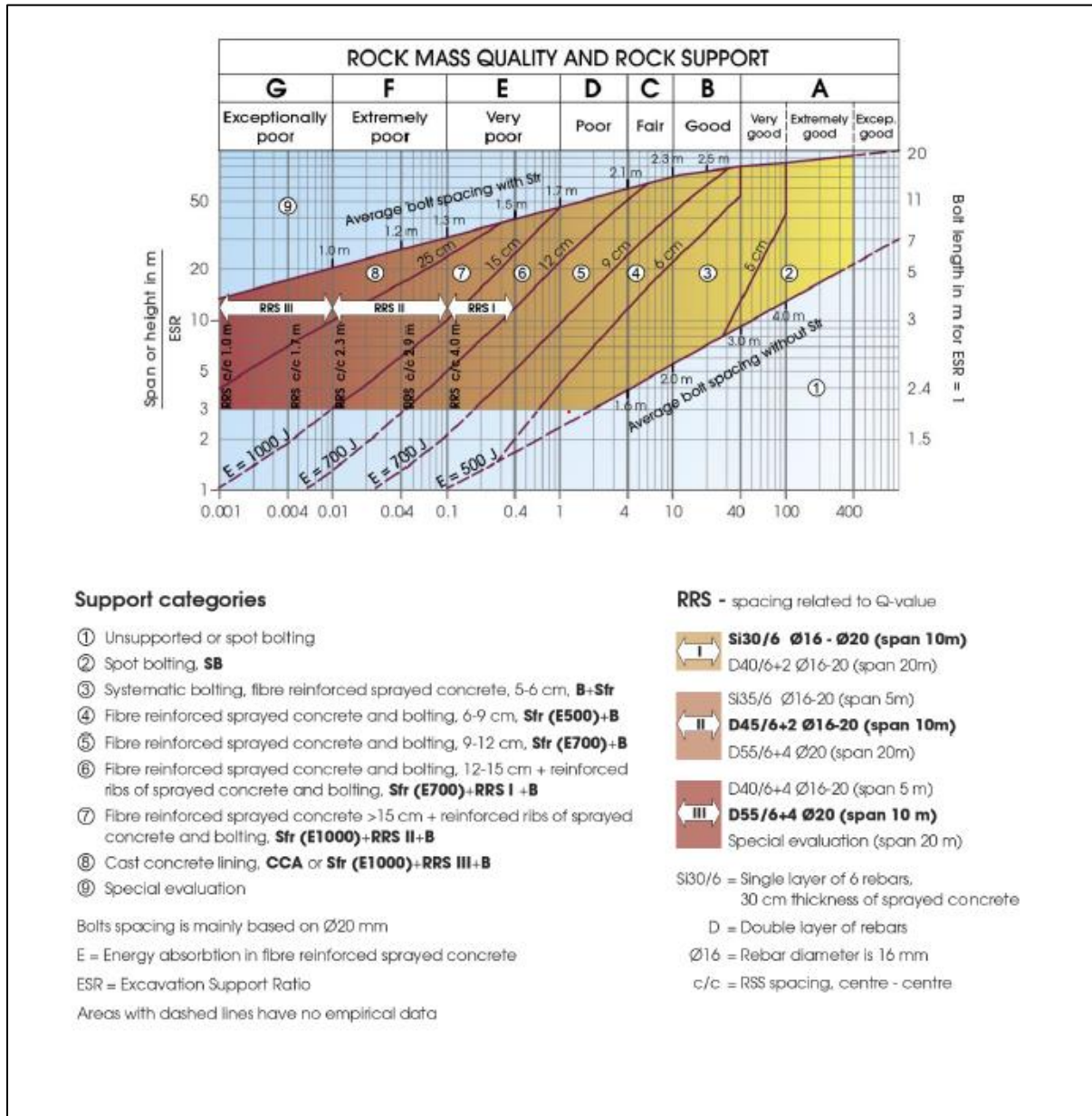


Figure 64 Rock support chart (NGI, 2015)

Therefore, knowing the Q-value and the span of the cross-passage (a) (11.2 m) and the tunnel (11.75 m), the support systems for the cross passage and the section of the

metro tunnel at the intersection regions were selected, in addition to taking into account the results of the extension of the plastic zones from the 3D FEM analysis.

❖ Support for the tunnel & Cross Passages

The results from the above chart are to use fibre reinforced sprayed concrete (12-15cm) and bolting with a length equal to 4m and spacing of 1.5. However, considering the 3D FEM analysis, it has been decided to consider for the intersection area the support for the tunnel and cross passages.

Bolts Fully Bonded	
Bolts diameter (mm)	25
Bolts modulus E (MPa)	3.50E+05
Tensile capacity (KN)	265
Residual tensile capacity (KN)	265
Length of the bolts pattern (m)	5
Spacing between the bolts (m)	1

Table 6 Bolts fully bonded properties for the tunnel & cross passages

Fibre-reinforced shotcrete	
Elastic modulus E (KPa)	1.50E+07
Poisson ratio (-)	0.2
Thickness (cm)	20

Table 7 Fibre-reinforced shotcrete properties for the tunnel & cross passages

Fully bonded bolts in RS3 are divided into bolt elements according to where the bolts cross the finite element mesh. These bolt elements act independently of each other. Neighbouring fully bonded bolt elements do not influence each other directly, but only indirectly through their effect on the rock mass.

In the fully bonded bolt model, the stiffness of the grout, and the strength and stiffness of the bolt/grout interface are considered. The failure mechanism of the bolt

is by tensile rupture of the bolt. The amount of relative slip at this interface, and the stiffness of the interface, determine how much shear force is generated at the bolts.

5.4.2 support for the shafts

For the stability of the shaft excavation, it has been decided to use struts and shotcrete as primary support. Regarding the simulation of the struts and the shotcrete, in the numerical model, only the shotcrete is considered. Therefore, for simplification, considering RS3 command “standard liner” to model a liner with flexural rigidity (i.e., resistance to bending), such as a shotcrete or concrete liner. It requires defining the thickness and the elastic properties of the liner. To be more conservative, as mentioned before, only the properties of shotcrete were used, and they are the same as the reinforced shotcrete that is used for the tunnel and cross-passages, as well as they are modelled by the same RS3 command, which is the standard liner.

Struts & shotcrete	
Young's Modulus (KPa)	15 E+07
Poisson's Ratio (-)	0.2
Thickness (m)	0.2

Table 8 Shotcrete Properties for the vertical shafts

Therefore, the described support system for the shaft, cross-passage and tunnel is added to the same model introduced in intrinsic conditions, but regarding the metro tunnel, from the analysis in intrinsic conditions, it has been decided to add the selected support system at the range of the intersection since it is the interest of this thesis. Moreover, considering the stages, the supporting structures were installed in a stage after each 1m excavation by activating the structural elements; due to this, the overall stages at the end increased by one stage. Therefore, the stages of the support model are 274.

5.4.3 Stresses induced on the support systems

In this part, the results of the analyses with the installation of the support, at the last stage are introduced.

❖ Bolts

1- Axial Force F_A :

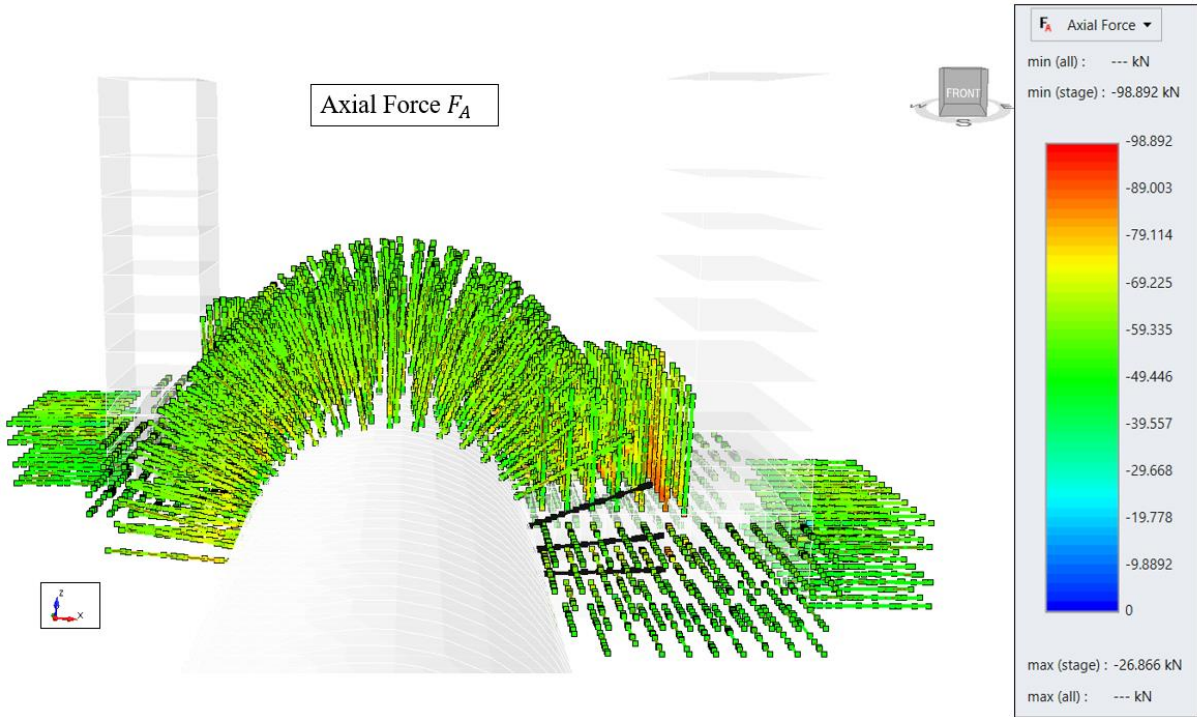


Figure 65 Axial Force F_A (bolts)

It can be clearly seen that the bolts are loaded in a range from 27 kN to 99 kN with the maximum values localised in the bolts near the intersections. As mentioned before about the fully bonded bolts model, the stiffness of the grout and the strength and stiffness of the bolt/grout interface are considered. So, the failure mechanism of the bolt is by tensile rupture of the bolt, which is 265 kN. Therefore, the bolt pattern to support the cross-passage & the tunnel at the intersection areas in the good scenario conditions is accepted.

The results of axial stresses are given below:

2- Axial stress σ_A :

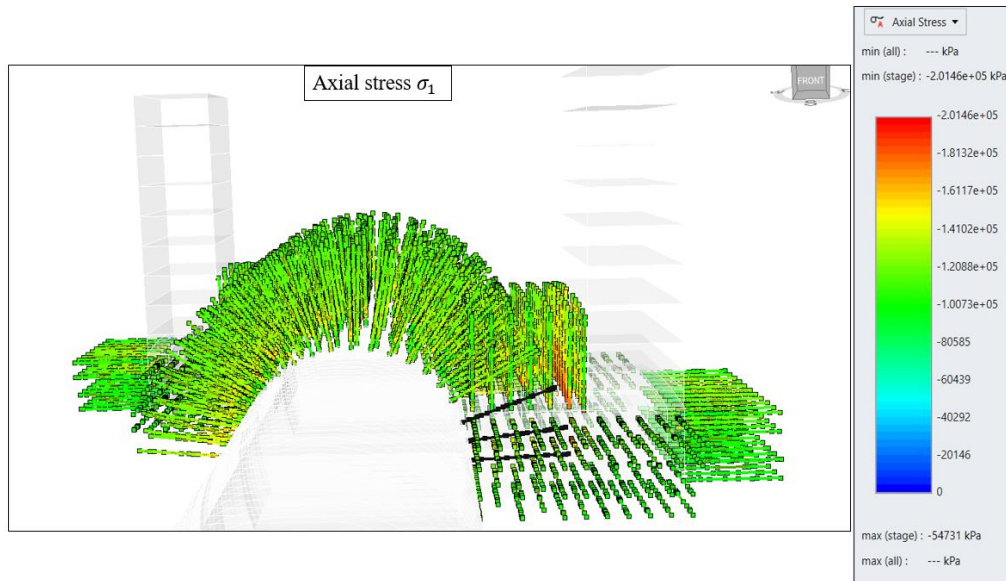


Figure 66 Axial stress (bolts)

5.4.4 shotcrete on the shaft, cross passage & the tunnel

- Displacement in X direction:

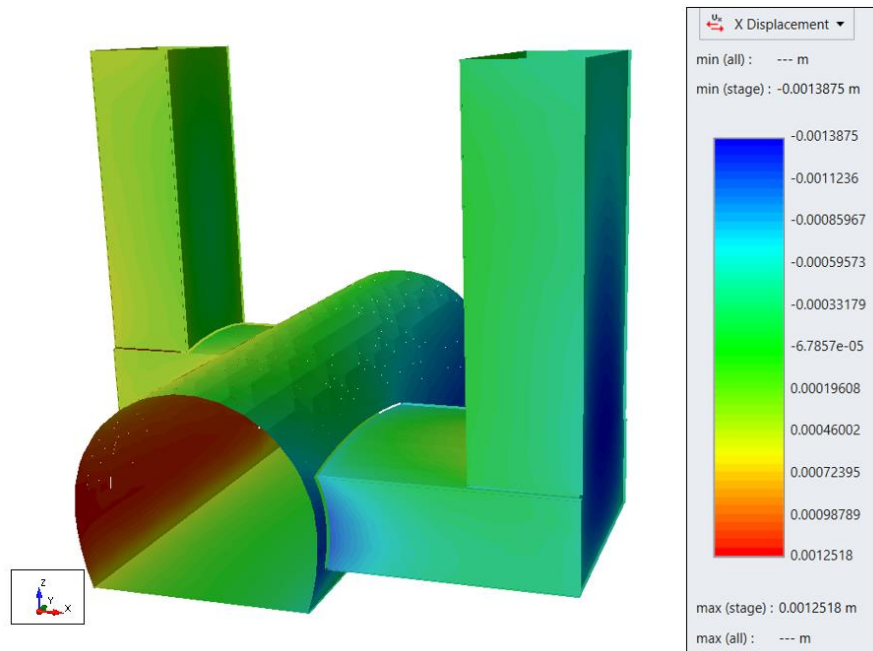


Figure 67 Displacement on X-direction for the shotcrete

The maximum displacement in X direction is about 1.4 mm on the shaft (a) and the tunnel, as shown in the figure (66). The results for the displacement in the Y direction are maximum 0.7mm on the shaft (a) & (b). In the Z direction: 1.9 mm at the crown of the tunnel and the cross passages & 2.8mm at the invert of the tunnel and the cross passages. These results are acceptable, and the support system in good conditions is approved. All of the results are attached to this thesis in the appendixes.

5.5 Detailing related to the good scenario

This chapter introduces a representation of the detailing for the elements at the intersection region related to the good scenario conditions. The detailing is presented only for the shaft (a) and cross passage (a) since the trend is the same for the shaft (b) & cross passage (b).

5.5.1 Intersection area overview (section for the intersection area)

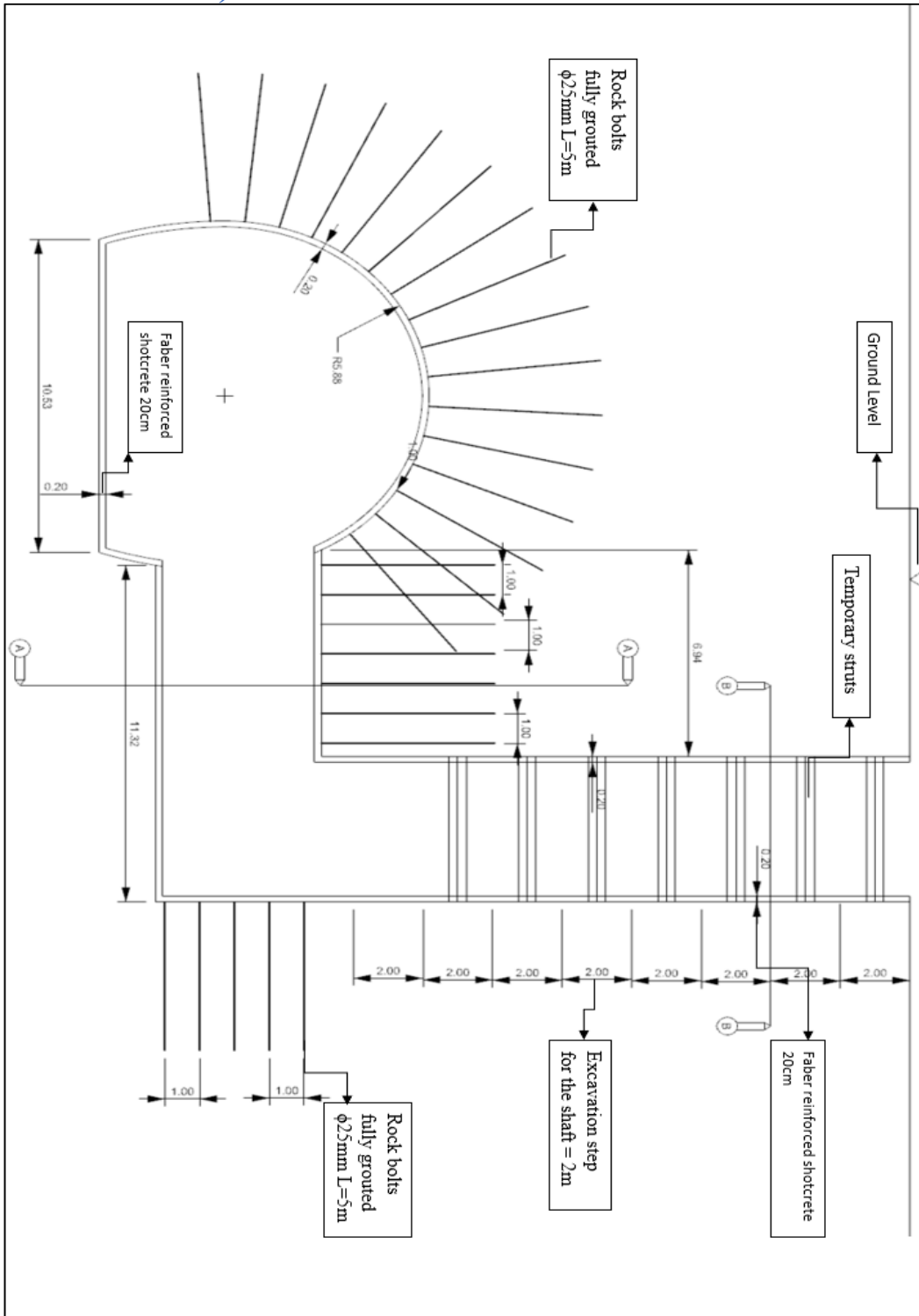


Figure 68 Intersection area overview with detailing

5.5.2 Section A-A (Cross passage cross-section)

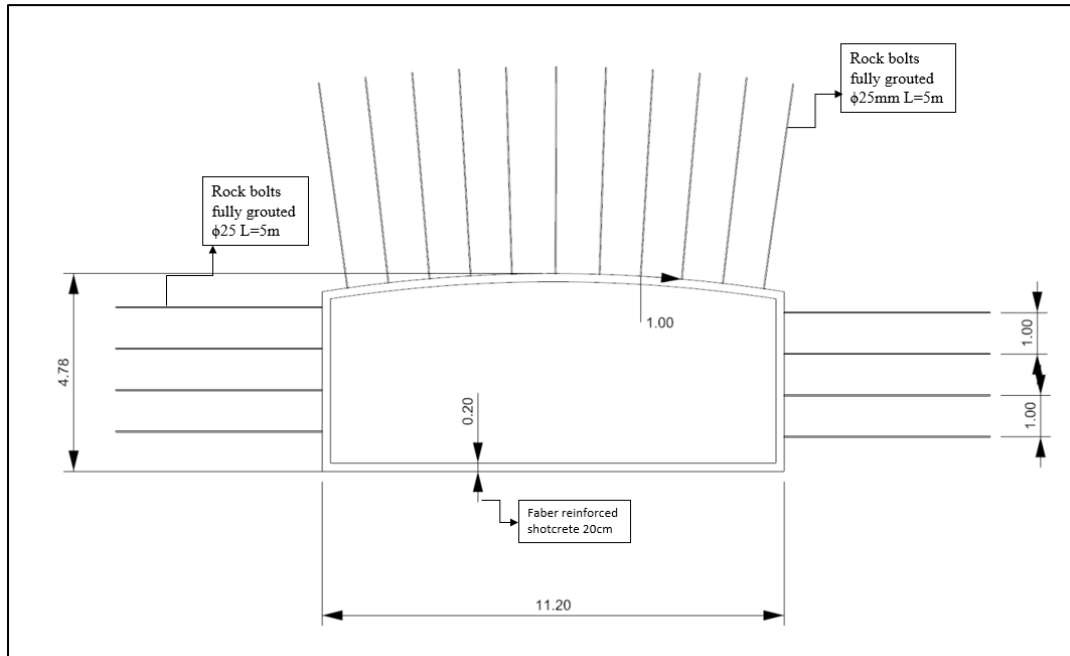


Figure 69 Section A-A (Cross passage cross-section)

5.5.3 Section B-B (Shaft cross-section)

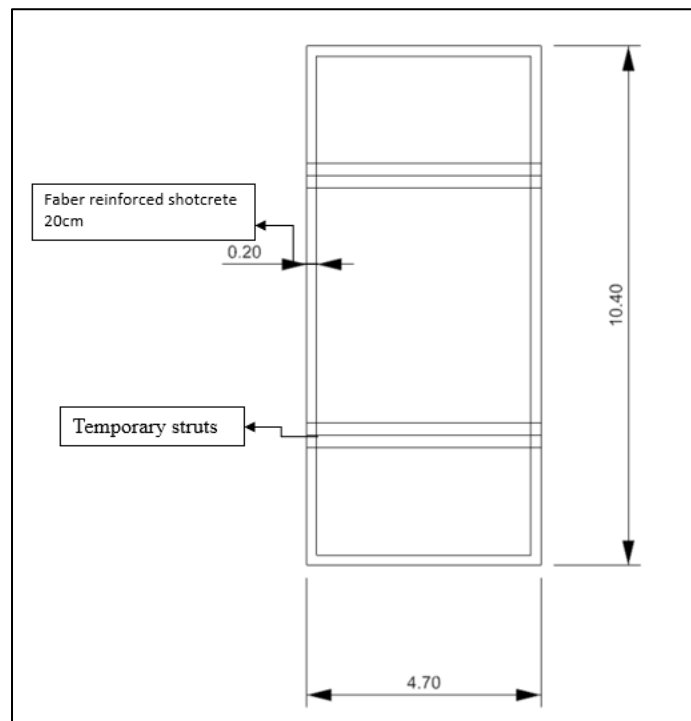


Figure 70 Section B-B (Shaft cross-section)

5.6 2D FEM numerical model by RS2

The case study analysed in this thesis is in a preliminary design phase. Therefore, there is an absence of monitoring data and field measurements because the construction has not yet begun. Due to this reason, it has been decided to run the analysis for a section of the metro tunnel near the intersection region in 2D prior to starting the 3D analysis to get a reference for the behaviour limitation that could be generated by the excavation of the cross passages and the excavation of the shafts. The results of the 2D analysis (stress state, plastic zones, total displacement & the surface settlement trough) are compared to the 3D results at stage 212 (the end of the excavation of the metro tunnel and before the excavation of the cross passages and the shafts) to provide some validity and confidence for the 3D results. The following is the procedure for the numerical modelling in 2D using RS2 software.

5.6.1 Numerical Model in 2D

The exact equivalent continuum model presented in the 3D was used for the 2D model. Therefore, the geological model & materials' properties are the same.

❖ Geometry

Knowing the geometry of the tunnel, it was possible to draw the 2D section of the tunnel. Moreover, regarding the external boundaries, the considered section of the tunnel is located near the intersection. Therefore, the considered overburden (19.7m) is the same one presented in the 3D model. Furthermore, the external boundaries dimensions are 236m in the horizontal axis (10 * the tunnel diameter) with a total depth in vertical axis of 71.7m from the surface. Figure (71) shows the geometry of the tunnel and the external boundaries dimension.

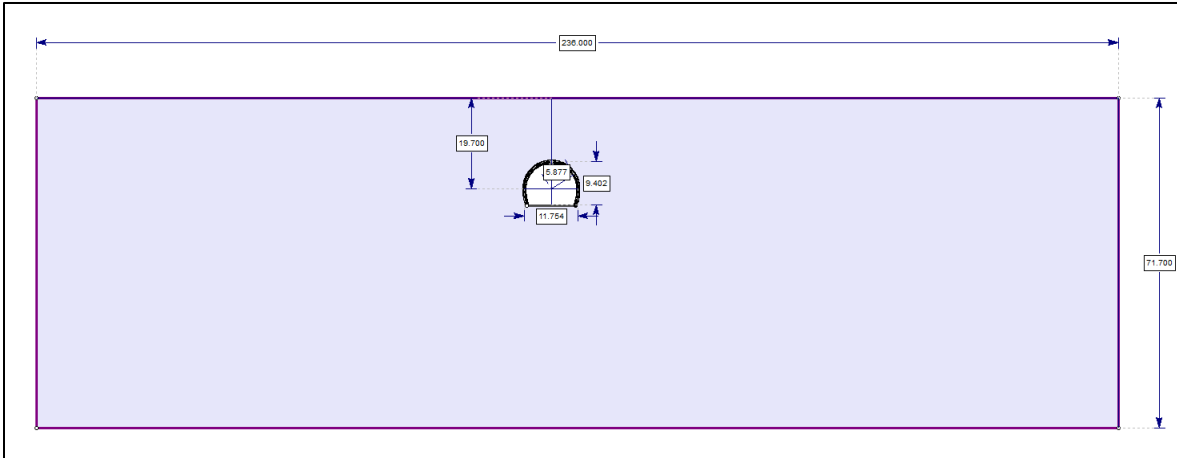


Figure 71 2D external boundaries

❖ Mesh setup and restraints

For the realisation of the mesh, three noded triangular elements mesh were used. Moreover, in the zone of the excavation, the density of the mesh was increased to obtain better results.

Whereas, for the restraints, since it is a shallow tunnel, the upper boundaries are set as free, where the appropriate displacement for the sides and the down boundaries are set using rollers and hinges as in the figure (72):

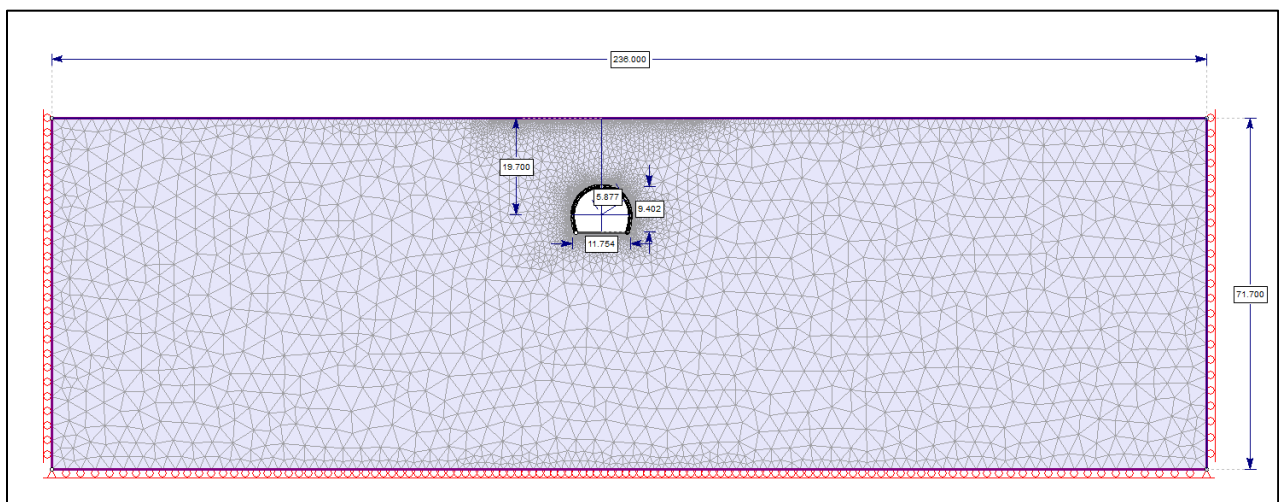


Figure 72 2D model mesh

❖ Stages

Having the advantage of the good rock mass, it was decided to run the analysis in the intrinsic conditions (without support) to indicate the extension of the plastic zones due to the tunnel excavation. Therefore, regarding the stages for the excavation simulation, it is not necessary to simulate gradual excavation by applying the stress release to the model since it was seeking the results after full excavation conditions. Consequently, the model stages are two, where stage one represents the original geological model, moving to the second one for the tunnel excavation.

5.6.2 Results of the 2D analysis

1- Initial state of stress

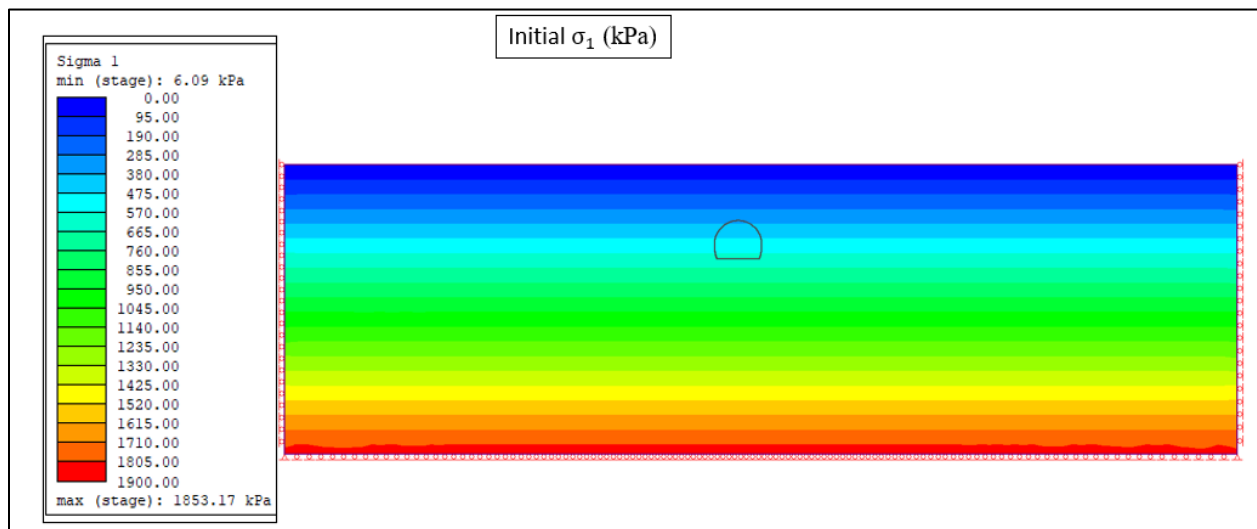


Figure 73 Initial in-situ state of stresses (2D)

It can be clearly noticed that the trend is quite the same between the 2D & 3D results. The chart (figure 73) below represents the vertical query distance at the right boundary of the two and three-dimensional models for stage one.

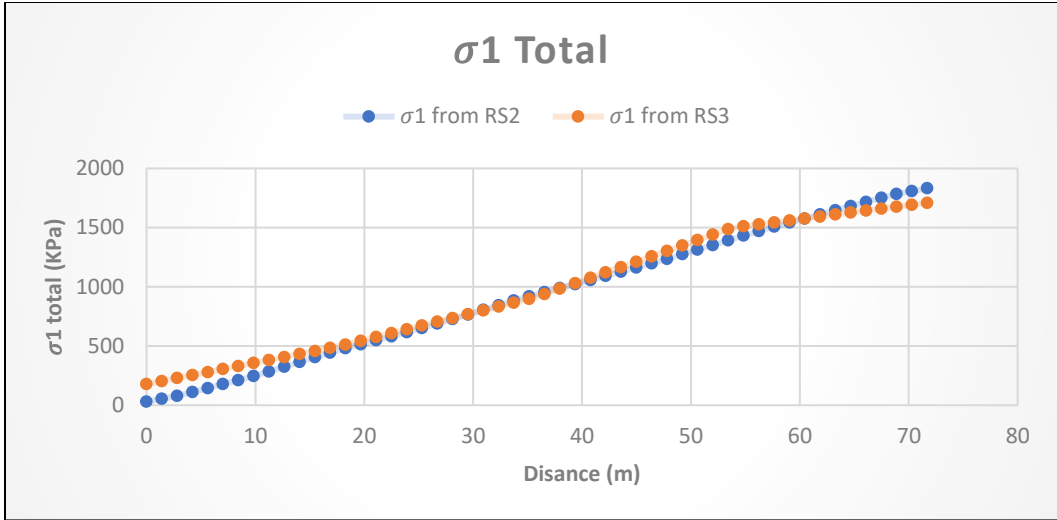


Figure 74 sigma 1 vs query distance at the right boundaries of the models

2- Stress state at the end of the excavation

The results are compared between stage 2 of the 2D numerical model and stage 212 of the 3D model (the end of the excavation of the tunnel); the vertical query distance starts from 8.7 m in the x-direction from the centre of the tunnel of the 2D & 3D model (Y=0).

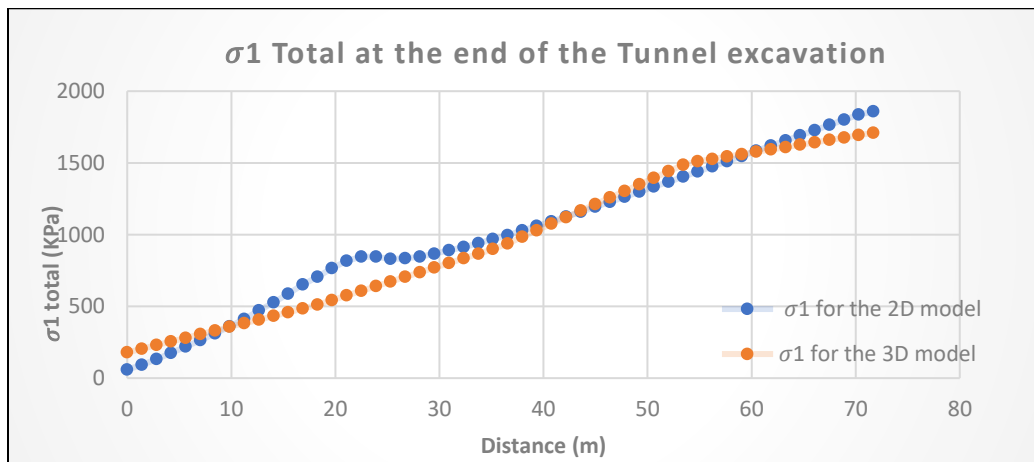


Figure 75 sigma 1 vs query distance at the end of the tunnel excavation

3- Plastic zones

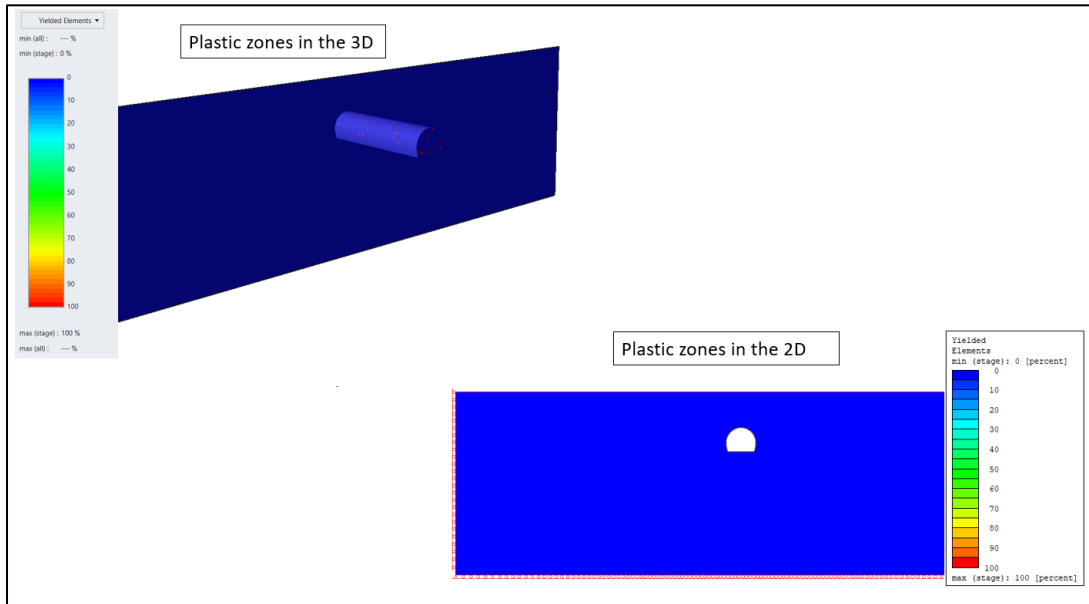


Figure 76 Yielded elements at the end of the tunnel excavation

It can be clearly seen that, the development of the yielded elements due to the excavation of the tunnel is negligible; this is because of the good surrounding rock mass. The results in the 2D & 3D are very close.

4- Total displacement

The results of the 2D model at stage 2 are compared to the results from the 3D model at stage 212 (the end of the tunnel excavation).

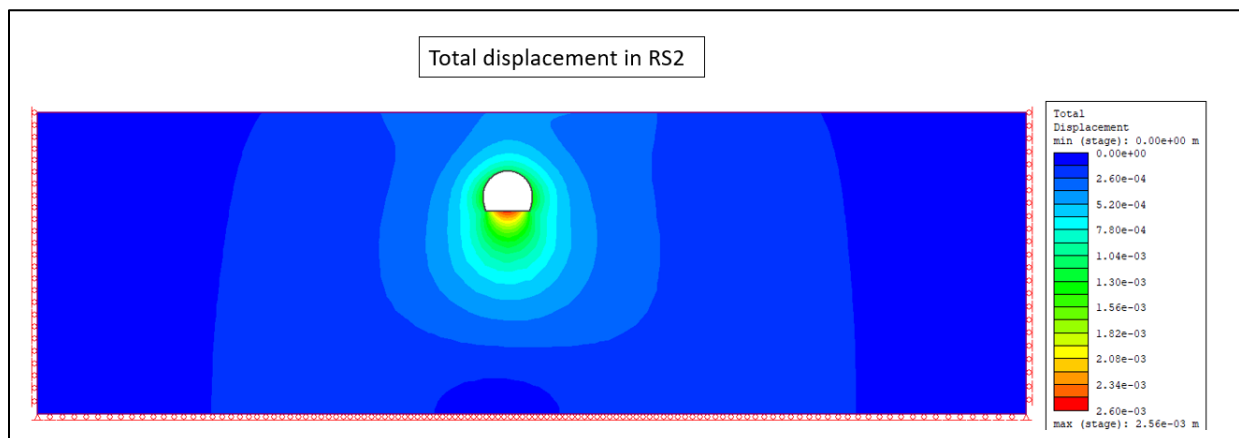


Figure 77 Total displacement at the end of the excavation (2D)

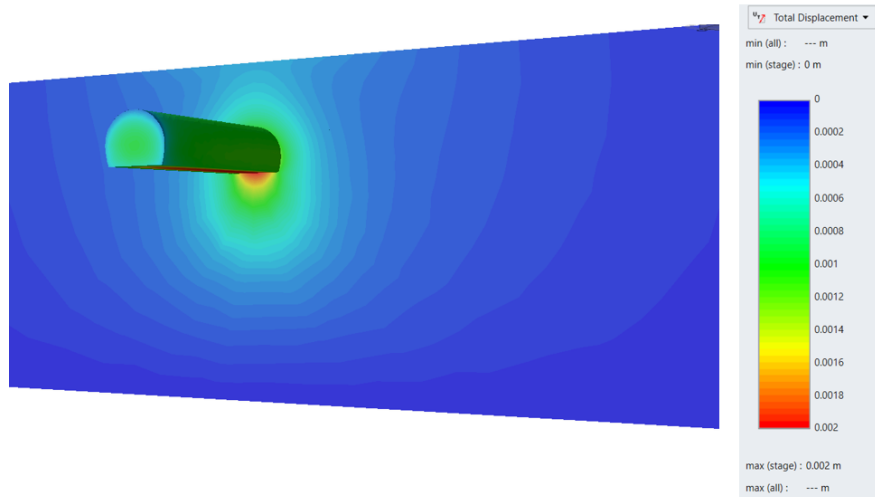


Figure 78 Total displacement at the end of the tunnel excavation (stage 212)

It is noticeable that, both results in 2D & 3D illustrate the same trend, with a maximum value of the total displacement at the invert of the tunnel (2.6mm).

5- Surface settlement trough

The results of the 2D model at stage 2 are compared to the results from the 3D model at stage 212 (the end of the tunnel excavation).

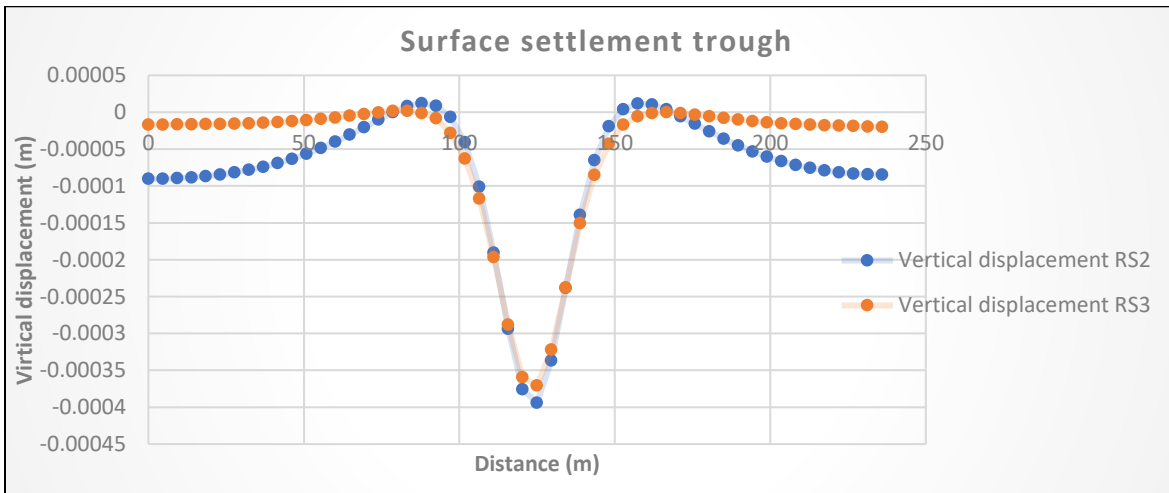


Figure 79 Surface settlement trough from the 2D & 3D results

It can be clearly seen that, both results in 2D & 3D illustrate the same trend, with a maximum value of the surface settlement 0.4mm.

Chapter 6: Analysis and outputs (worst scenario conditions)

As shown in the 3rd chapter, the worst scenario conditions for the intersection area (section 2) are characterised by different layers of soil and rock, as illustrated in the following figure (80).

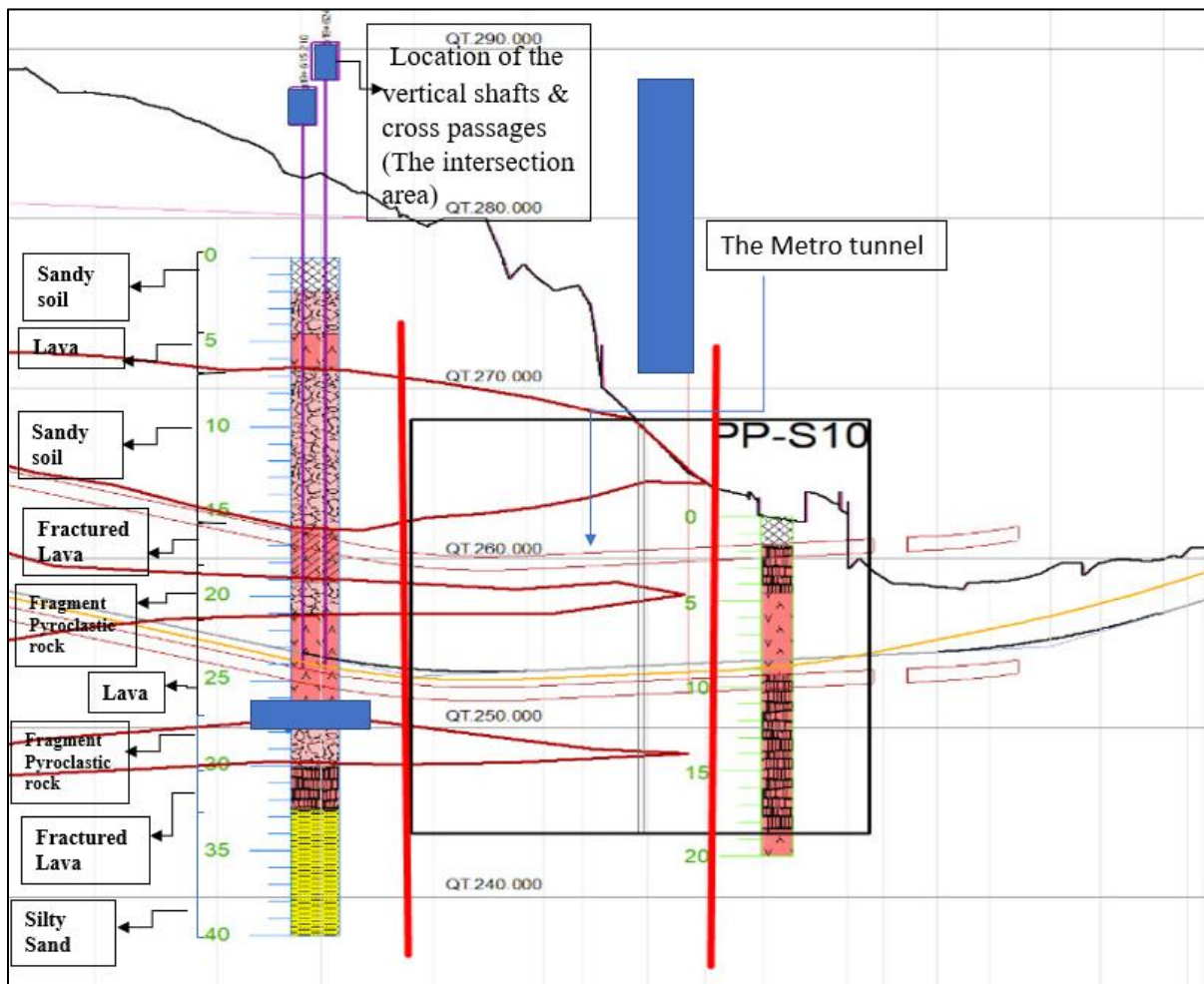


Figure 80 Stratigraphy for section 2

Before introducing the numerical models, the representation of the stratigraphy and the geo-mechanical characterisation of the materials are presented.

6.1 Geology and geo-mechanical parameters for materials

6.1.1 Geology

Concerning the site & geological conditions, the stratum was simplified to a horizontally homogeneous layered distribution. Moreover, it has been decided to simplify the stratigraphy but consider conservative simplifications. The stratigraphy simplifies by neglecting the thin layer (1.6m) of stiff lava at a depth of 11.5m from ground level by considering a continuous (17.61m) of the sandy soil layer from the ground level. It has been found that the effect of this layer on the surface settlement is negligible; therefore, to reduce the number of mesh elements in the numerical model, it has been decided to consider only a sandy soil layer 17.61m thick. The same was done for the fractured lava layer (2.8m) at depth (32.5m) by considering a continuous layer (total of 6m) of the weak fragment pyroclastic rock below the tunnel. The following figure (81) illustrates the considered layers and the location of the tunnel, cross-passages & the shafts.

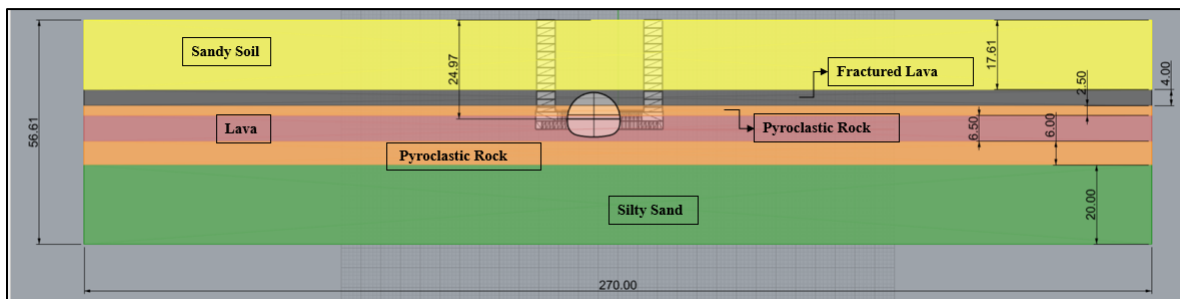


Figure 81 The simplification of the stratigraphy

6.1.2 Material properties & constitutive models

It has been decided to use the nonlinear generalised Hoek & Brown criterion to represent the rock masses (lava & fractured lava), whereas, for the loose soil (sandy soil, silty sand & the fragment pyroclastic layer), the Mohr Coulomb criterion was used. The material properties are collected in the tables below:

1- Lava:

Lava			
Unit Weight	γ	26	kN/m ³
Deformability modulus	E	3.59E+03	MPa
Poisson ratio	ν	0.3	-
Uniaxial compressive strength of the intact rock (UCS)	σ_{ci}	90	MPa
Intact rock parameter	m_i	17	-
Rock mass parameter	m_b	1.994	-
Rock mass parameter	s_b	0.001	-
Rock mass parameter	a	0.511	-
Cohesion	C	0.372	MPa
Friction angle	ϕ	62.5	°

Table 9 Material properties of the Lava

2- Fractured Lava:

Fractured Lava			
Unit Weight	γ	26	kN/m ³
Deformability modulus	E	523.737	MPa
Poisson ratio	ν	0.3	-
Uniaxial compressive strength of the intact rock (UCS)	σ_{ci}	25	MPa
Intact rock parameter	m_i	17	-
Rock mass parameter	m_b	1.167	-
Rock mass parameter	s_b	2.404E-4	-
Rock mass parameter	a	0.531	-
Cohesion	C	00.127	MPa
Friction angle	ϕ	50.326	°

Table 10 Material properties of the fractured Lava

3- Sandy Soil

Sandy soil			
Deformability modulus	E	70	MPa
Poisson ratio	ν	0.3	-
Unit Weight	γ	21	kN/m ³
Cohesion	c	5	kPa
Friction angle	ϕ	33	°

Table 11 Material properties of the sandy soil

4- Fragment Pyroclastic rock

Fragment Pyroclastic rock			
Deformability modulus	E	120	KPa
Poisson ratio	ν	0.3	-
Unit Weight	γ	21	kN/m ³
Cohesion	c	10	kPa
Friction angle	ϕ	35	°

Table 12 Material Properties of the fragment Pyroclastic rock

5- Silty sand

Silty sand			
Deformability modulus	E	100	KPa
Poisson ratio	ν	0.3	-
Unit Weight	γ	18	kN/m ³
Cohesion	c	20	kPa
Friction angle	ϕ	27	°

Table 13 Material Properties of the silty sand

6.2 Numerical modelling

The same procedure presented in the 5th chapter for analysis of (section 1) is respected. Therefore, the first thing is to analyse a section of the tunnel near the intersection region in 2D using RS2 FEM software. The reason for performing such analysis is to have a reference for the behavioural limits, which could be most probably due to the excavation of the tunnel, cross-passage and the shaft. The results from the 2D analysis are to be compared with some of the 3D model results before the excavation takes place at the intersection region. Therefore, a simple model for the tunnel section near the intersection area was realised in RS2. The analysis and results will be introduced in section (6.2.2). Then, the analysis related to the intersection problem was carried out using RS3 FEM software to check the behaviour due to the construction at the intersection area; this part is introduced in the section (6.2.3).

6.2.1 Numerical model in 2D

The results of the 2D analysis (stress state, plastic zones, total displacement & the surface settlement trough) are to be compared to 3D results at a stage related to the end of the excavation of the metro tunnel and before the excavation of the cross passages and the shafts) to provide some validity and confidence for the 3D results.

Concerning the stratigraphy, the overburden and the face of the metro tunnel in section 2 are characterised by the presence of weak soil. Therefore, it was essential to check the stability of the face analytically.

❖ 6.2.1.1 Face stability of the tunnel in section 2

The stability of the tunnel face is to be assessed analytically first. To do so, the Anagnostou Kovari (1996) method is considered.

Based on the method proposed by Anagnostou & Kovari (1996) [11], and according to this model, the failure mechanism is characterised by a wedge and a prismatic body which is extended up to the surface, as shown in figure (82)

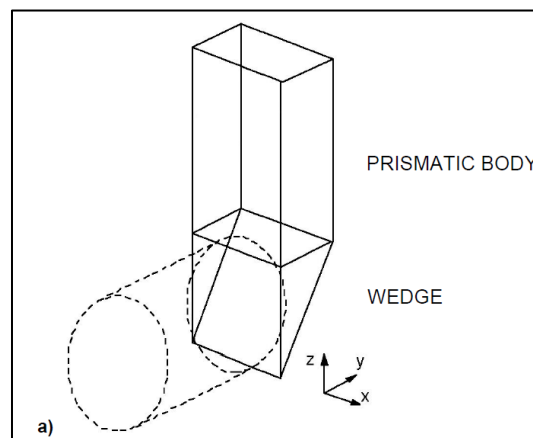


Figure 82 The Failure mechanism consists of a wedge and a prismatic body

The method is based on a limit equilibrium analysis of the forces acting on the system as shown in the following figures (83) & (84).

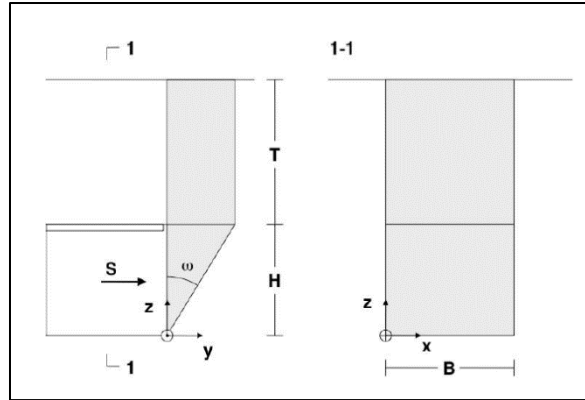


Figure 83 Geometrical parameters

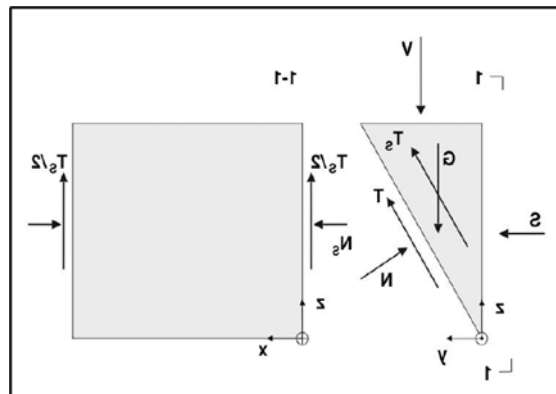


Figure 84 Forces acting on the system

Since the tunnel at the considered section is above the water table, the long-term stability of the tunnel face will be assessed. The formulas to evaluate the needed stabilising force applied to the face is given below for different angle of the wedge (ω):

$$S = \frac{F \sigma_v + G}{\tan(\omega + \phi)} - \frac{T_s + c \frac{B H}{\cos \omega}}{\cos \omega (\tan \omega + \tan \phi)}$$

Where:

- $V = F \cdot \sigma_v$ is the load acting on the wedge [KN].
- G is the wedge weight [KN].
- ω is the angle of the wedge [$^\circ$].

- φ is the soil friction angle [$^{\circ}$].
- T_s is the shear force acting on the wedge [KN].
- c is the soil cohesion [KPa].
- B is the wedge width [m].
- H is the wedge height [m].
- The value of the force S is obtained by geometrical considerations: the base area of the prismatic body F , the perimeter U , and their ratio R :

$$R = \frac{F}{U}, \quad F = B H \tan \omega, \quad U = 2(B + H \tan \omega).$$

- The weight of the wedge G is obtained from the relation:

$$G = \gamma \frac{1}{2} B H^2 \tan \omega.$$

- The value of the vertical load is calculated from the equation:

$$\sigma_v = \frac{R\gamma - c}{\lambda \tan \phi} \left(1 - e^{-\lambda \tan \phi \frac{T}{R}} \right)$$

Where:

λ is the coefficient of lateral stress for the vertical loading equal to 0.8 (it is a factor ranges from 0.8 to 1 according to Anagnostou & Kovari (1996)).

T is the depth of the cover [m].

- And at the end the value of the shear force T_s , acting on the sliding surface of the wedge, is evaluated as follows:

$$T_s = H^2 \tan \omega \left(c + \lambda_k \tan \phi \frac{2\sigma_v + H\gamma}{3} \right)$$

Where:

λk is the coefficient of lateral stress for the shear force at the lateral surface equal to 0.4 (it is a factor ranges from 0.4 to 0.5 according to Anagnostou & Kovari (1996)).

The input data:

The considered materials for this analysis are the fractured Lava, sandy soil & the fragment pyroclastic rock; the material properties were introduced in section (6.1.2) in tables 7,8 & 9, respectively. The other input data is shown in table (14).

B	13.35	m
H	11.23	m
TY	18.33	m

Table 14 input data for the Anagnostou Kovari method for calculating the required stabilizing force at the face (S)

The factor of safety that was applied to reduce geotechnical parameters ($c, \tan\phi$) is equal to 2 “it is a conservative safety factor used in practice since there is no indication in a particular reference to rely on such as NTC2018 or the Eurocode”.

- After applying the average values of the parameters on the equations, the results of the needed stabilising force are represented in the table & graph below:

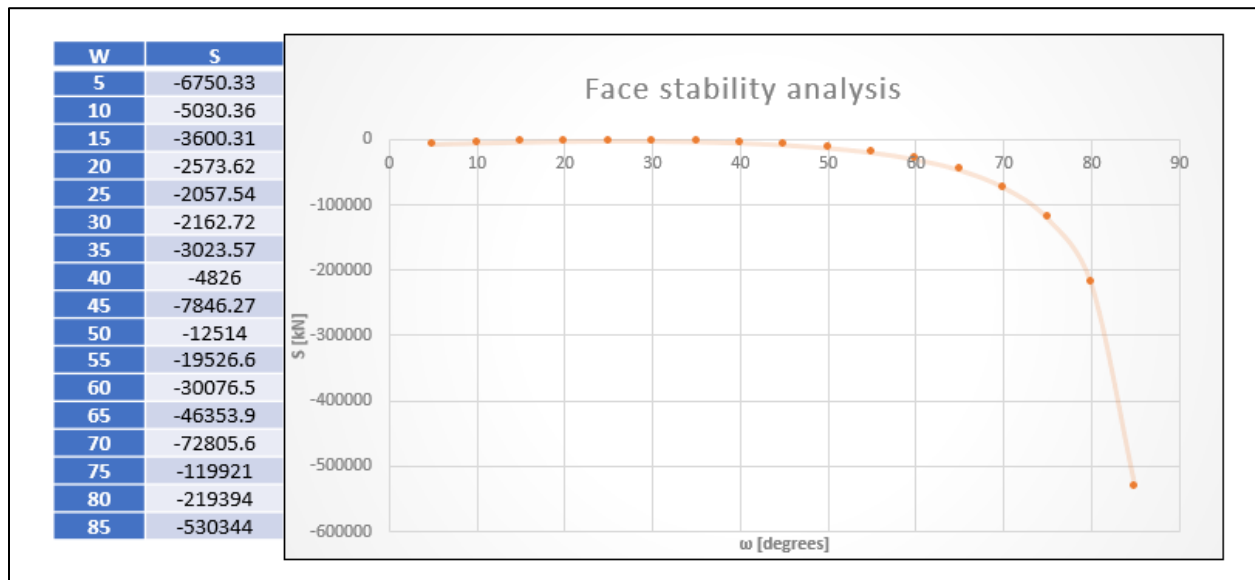


Figure 85 Face stability analysis

From the result in figure (85), all values for the support forces are negative. This means that the tunnel face should be self-supported. However, a minimum amount of fibre glass elements fully grouted inside the tunnel face is recommended in practice, but in the numerical models this was not considered.

❖ 6.2.1.2 Geometry

The geometry of the section of the tunnel is a bit complex. Therefore, it was preferred to import the 2D section of the tunnel from Rhino7 using the “.dxf” format. Moreover, regarding the external boundaries, the considered tunnel section is located near the intersection. Therefore, the considered overburden (24.97m) is the same one presented in the 3D model. Moreover, the dimensions of the external boundaries are set as 270m in the horizontal direction (10 * the tunnel diameter) with a total depth of the boundaries in the vertical direction 56.61m from the surface. Figure (86) demonstrates the geometry of the tunnel and the external boundaries dimensions.

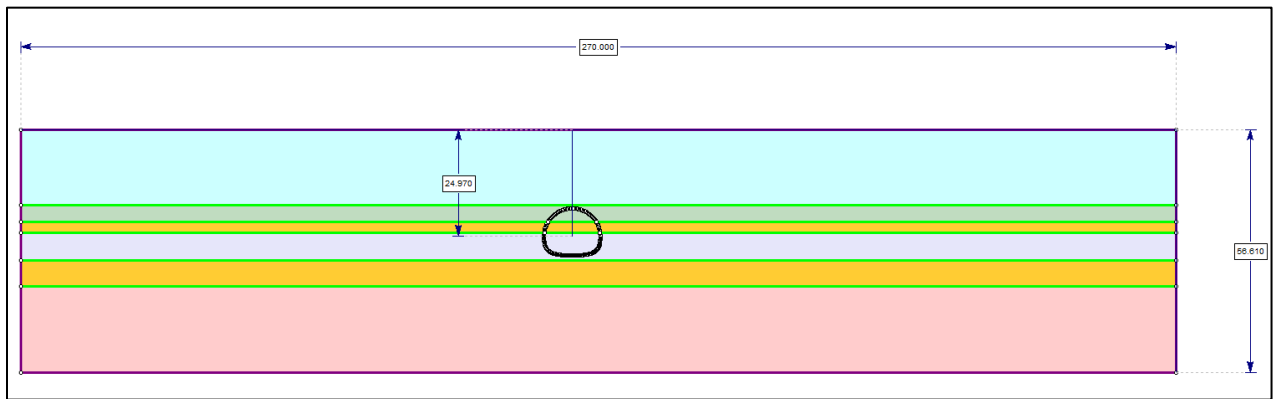


Figure 86 Tunnel geometry & the external boundaries

❖ 6.2.1.3 Mesh setup and restraints:

For the realisation of the mesh, three noded triangular elements mesh were assumed. Moreover, in the zone of the excavation, the density of the mesh was increased to obtain better results.

Whereas, for the restrains, since it is a shallow tunnel, the upper boundaries are set as free, where the appropriate displacement for the sides and the down boundaries are set using roller and hinges as shown in figure (87).

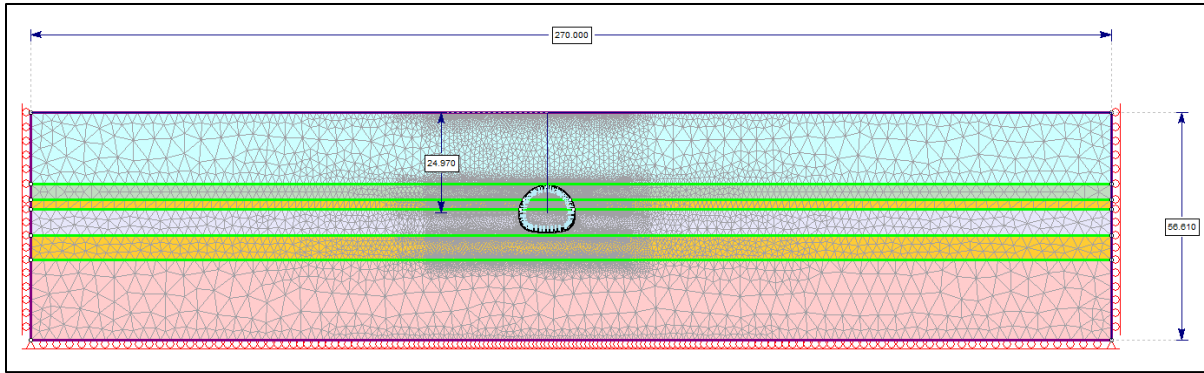


Figure 87 Model mesh & the restraints

❖ 6.2.1.4 stages

Concerning the stages, it was necessary to consider three stages. The **first stage** represents the original geological conditions. The **second stage** is set for the tunnel excavation; here, in this stage, it is essential to simulate the gradual excavation process. Therefore, stress relaxation must be applied by using the command “induced stress load” in RS2. Considering the convergence confinement method, it has been found that from 1m of the face “where the installation of the primary support takes place” it could consider a 50% of the stress release.

Moving to the **third stage**, which is related to the installation of the primary support, concerning the geological conditions, the considered primary support for this section is the composite lining which is constituted of steel sets and shotcrete.

- **The parameters of the primary support**

Concerning the parameters used for the primary lining, the ‘equivalent section’ approach " proposed by Carranza-Torres C, Diederichs M (2009)[12] was considered. The analysis included an equivalent model based on the parameters of a

steel arch & the shotcrete; the method considers the lining composed of two different materials, material 1 or the rib, and material 2, or concrete. Each of these materials must be assigned the respective deformability parameters; in particular, the compressibility coefficient D and the flexibility coefficient K . the parameter D which for an arch of cross-sectional area A and Young's modulus E , in plane-stress conditions, is

$$D = EA$$

and for the same section, in plane-strain conditions, is

$$D = \frac{EA}{1 - \nu^2}$$

where ν is the Poisson's ratio of the material

the parameter K which for the section in plane-stress conditions results:

$$K = EI$$

and for plane-strain conditions:

$$K = \frac{EI}{1 - \nu^2}$$

Knowing these parameters, the equivalent thickness t_{eq} & the equivalent elastic modulus E_{eq} can be calculated:

$$t_{eq} = \sqrt{12 * \frac{K_1 + K_2}{D_1 + D_2}}$$

$$E_{eq} = \frac{n * (D_1 + D_2)}{b * t_{eq}}$$

The selected model for the (section 2) scenario is IPN200 + shotcrete 30cm, the parameters are shown in figure (88)

INPUT PRIMARY LINING				
Element 1				
RIBS (c) <input checked="" type="checkbox"/>	h_1	200	mm	Height of the ribs
	b_1	90	mm	Width of flange
	a_1	7.5	mm	Width of web
	e_1	11.3	mm	Thickness of flange
	r	7.5	mm	
	A_1	0.00334	m ²	Area of rib
	I_1	0.0000214	m ⁴	Moment of inertia
	E_1	210	GPa	Young modulus for steel
Geometrical characteristics of rib				
	s	1	m	Distance between ribs
	n	2.00	N/m	Elements per meter

Element 2				
SPRITZ (s) <input checked="" type="checkbox"/>	h_2	300	mm	Thickness of spritz
	b_2	1000	mm	Width
	A_2	0.14666000	m ²	Area of spritz between 2 ribs
	I_2	0.001104	m ⁴	Moment of inertia
	E_2	15	GPa	Young modulus of spritz

Figure 88 The primary lining input data

Therefore, the selected equivalent thickness t_{eq} & the equivalent elastic modulus E_{eq} that was applied to the standard liner in RS2 are reported in table (15).

E_{eq}	19.7	GPa
t_{eq}	0.3	m

Table 15 Primary lining parameters

6.2.2 results of the 2D analysis

1- Initial state of stress:

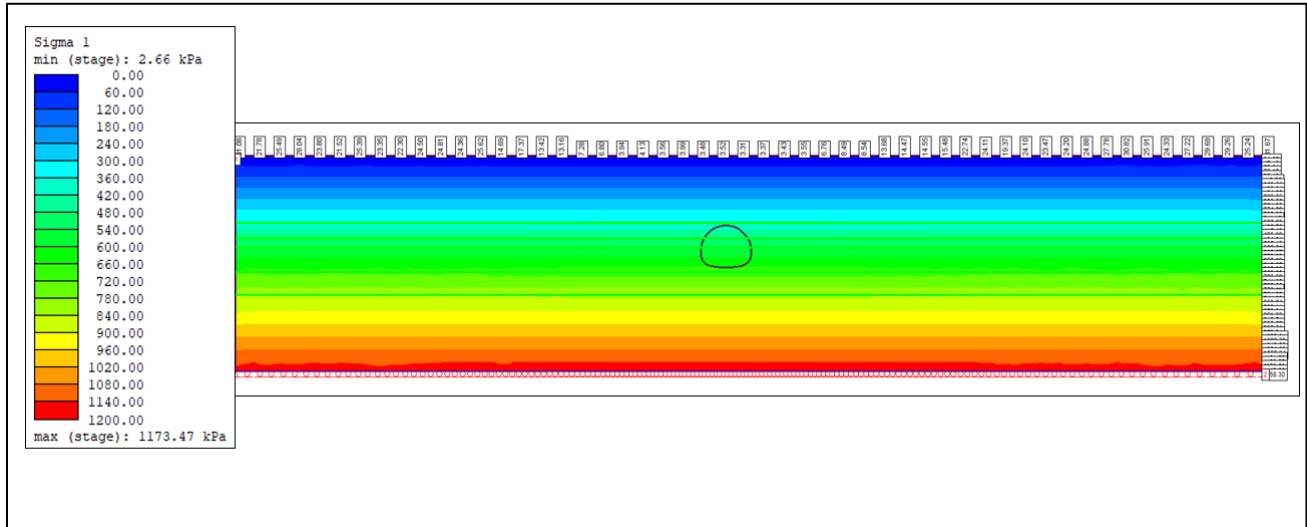


Figure 89 Initial in-situ state of stress

Since the k_0 was set to 1, the other initial state of stresses (σ_3) follows the same trend.

2- Stress state at the at the end of the excavation stage 3:

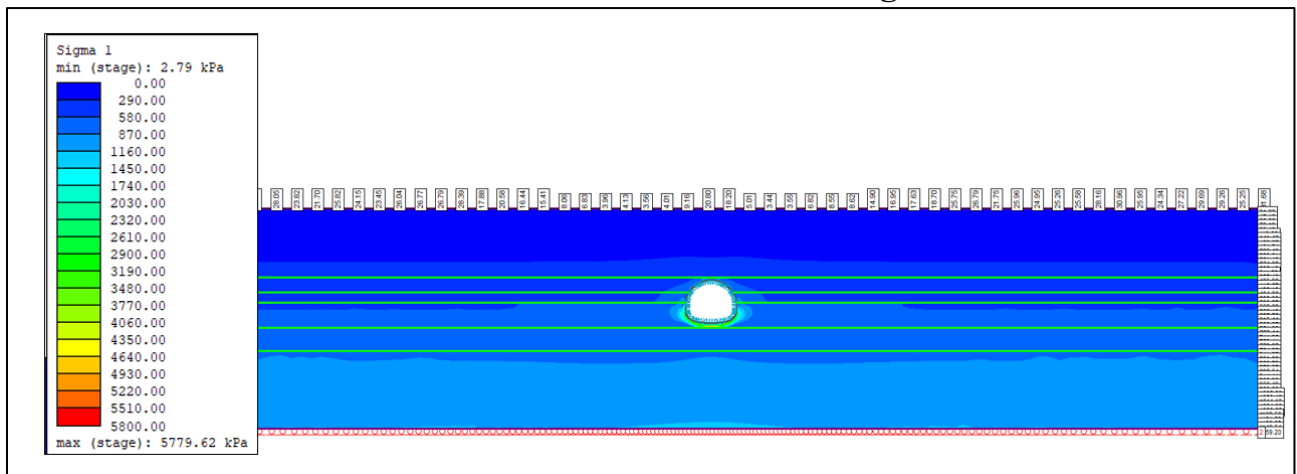


Figure 90 State of stress at the end of the excavation (stage 3)

3- Plastic zones at the end of the excavation stage 3:

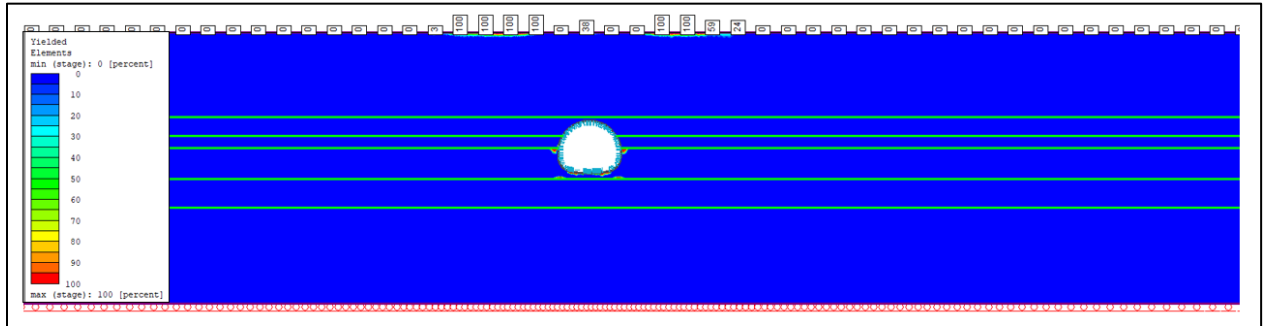


Figure 91 Plastic zones at the end of the excavation (stage 3)

4- Total displacement at the end of the excavation stage 3:

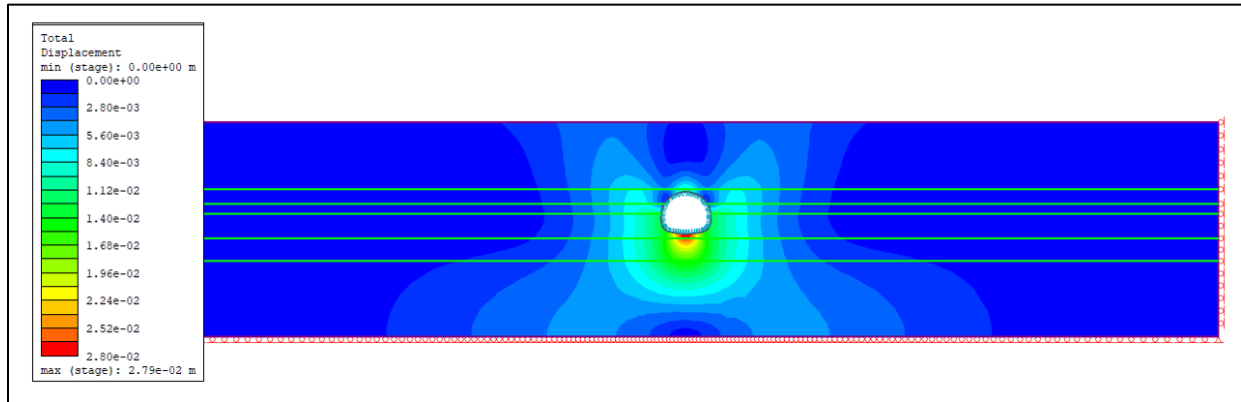


Figure 92 Total displacement at the end of the excavation (stage 3)

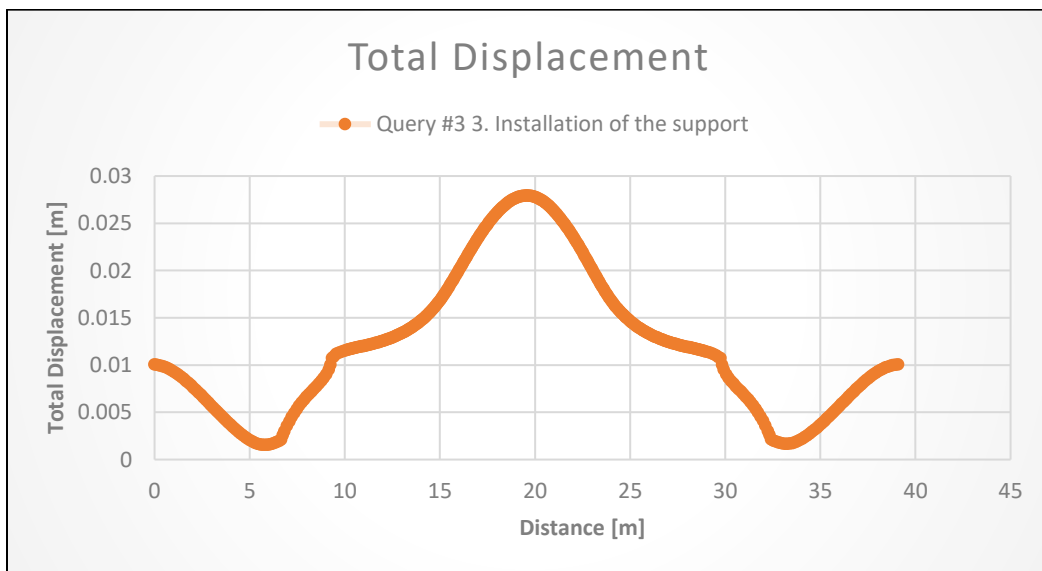


Figure 93 Total displacement vs the excavation boundary query distance (at stage 3).

It is noticeable that, the maximum total displacement is at the invert with a high value reach to 2.8 cm.

5- Surface settlement trough:

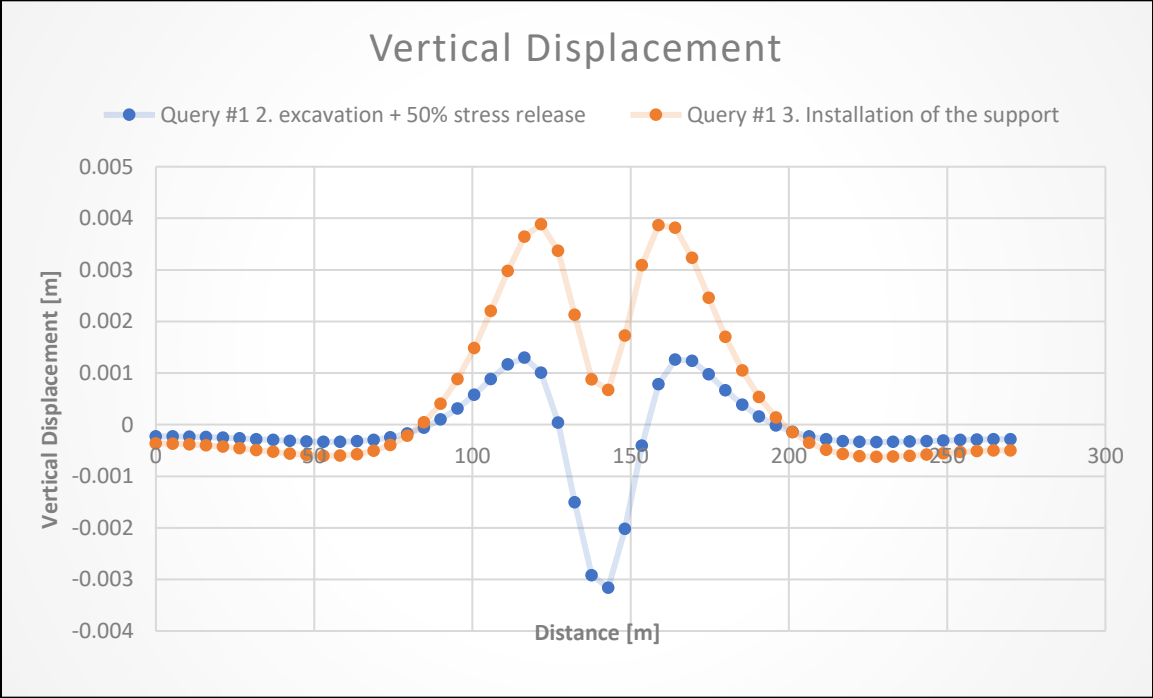


Figure 94 Vertical displacement Vs query distance at the surface

From figure (94), the model presents a 3mm lifting in the last stage. Indeed, the results of the vertical and total displacement are not acceptable. Therefore, it has been decided to run the model using different constitutive law that could better represent the loose soil's behaviour in such conditions of shallow underground construction. Therefore, it has been decided to use the Hardening Soil Model that was introduced in chapter 2 instead of Mohr Coulomb.

- **Hardening Soil Model**

This model was developed using the user-defined material model option in RS2 and RS3. The considered Harding soil model is based on (Schanz and Vermeer 1999) and also presented in the Plaxis manual “User’s manual of PLAXIS (2014)”.

All the parameters' definitions and the equations were introduced in chapter 2 in the section (2.5)

The hardening soil model parameters of the soil materials are presented in the tables below:

Sandy soil			
Unit Weight	γ	21	kN/m ³
Poisson ratio	ν	0.3	-
reference stiffness modulus at the reference pressure	E_{50}^{ref}	70000	kPa
The slope of the aforementioned curve at axial stress equal to the reference pressure	E_{oed}^{ref}	70000	kPa
elastic modulus in unloading and reloading	E_{ur}^{ref}	210000	kPa
Power m	m	0.5	-
coefficient of lateral pressure for normal consolidation	K_0^{nc}	0.455	-
failure ratio	R_f	0.9	-
Cohesion	C	5	kPa
Friction angle	φ	33	°
Reference Pressure	p_{ref}	100	kPa
mean effective stress limit	p_{limit}	10	kPa

Table 16 Hardening soil model parameters for the sandy soil

Fragment Pyroclastic rock			
Unit Weight	γ	21	kN/m ³
Poisson ratio	ν	0.3	-
reference stiffness modulus at the reference pressure	E_{50}^{ref}	120000	kPa
The slope of the aforementioned curve at axial stress equal to the reference pressure	E_{oed}^{ref}	120000	kPa
elastic modulus in unloading and reloading	E_{ur}^{ref}	360000	kPa
Power m	m	0.5	-
coefficient of lateral pressure for normal consolidation	K_0^{nc}	0.426	-
failure ratio	R_f	0.9	-
Cohesion	C	10	kPa
Friction angle	φ	35	°
Reference Pressure	p_{ref}	100	kPa
mean effective stress limit	p_{limit}	10	kPa

Table 17 Hardening soil model parameters for the fragment pyroclastic rock

Silty sand			
Unit Weight	γ	18	kN/m ³
Poisson ratio	ν	0.3	-
reference stiffness modulus at the reference pressure	E_{50}^{ref}	100000	kPa
The slope of the aforementioned curve at axial stress equal to the reference pressure	E_{oed}^{ref}	100000	kPa
elastic modulus in unloading and reloading	E_{ur}^{ref}	300000	kPa
Power m	m	0.5	-
coefficient of lateral pressure for normal consolidation	K_0^{nc}	0.546	-
failure ratio	R_f	0.9	-
Cohesion	C	20	kPa
Friction angle	ϕ	27	°
Reference Pressure	p_{ref}	100	kPa
mean effective stress limit	p_{limit}	10	kPa

Table 18 Hardening soil model parameters for the silty sand

The results in terms of the total displacement and the surface settlements trough are presented below:

1- Total displacement at the end of the excavation stage 3:

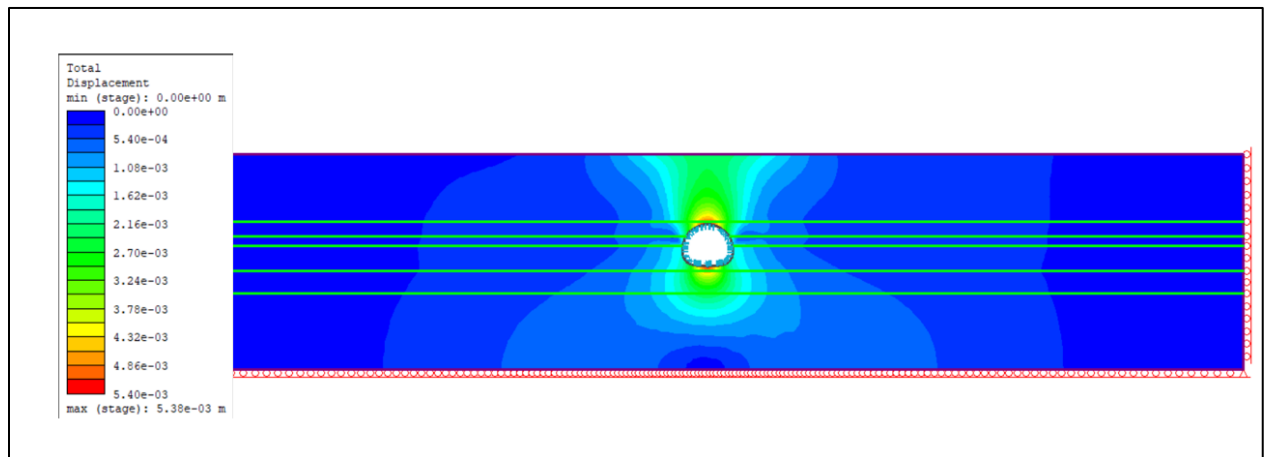


Figure 95 Total displacement at the end of the excavation

It is noticeable that the maximum total displacement is localised at the crown and the invert with a value equal to 5.4mm.

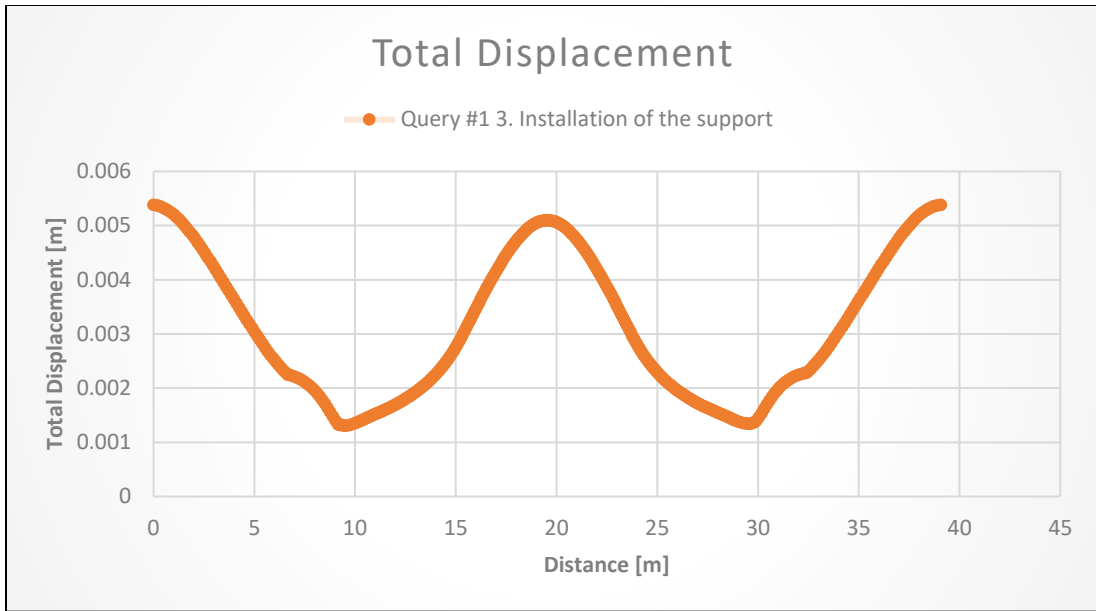


Figure 96 Total displacement vs the excavation boundary query distance (at stage 3)

2- Vertical displacement:

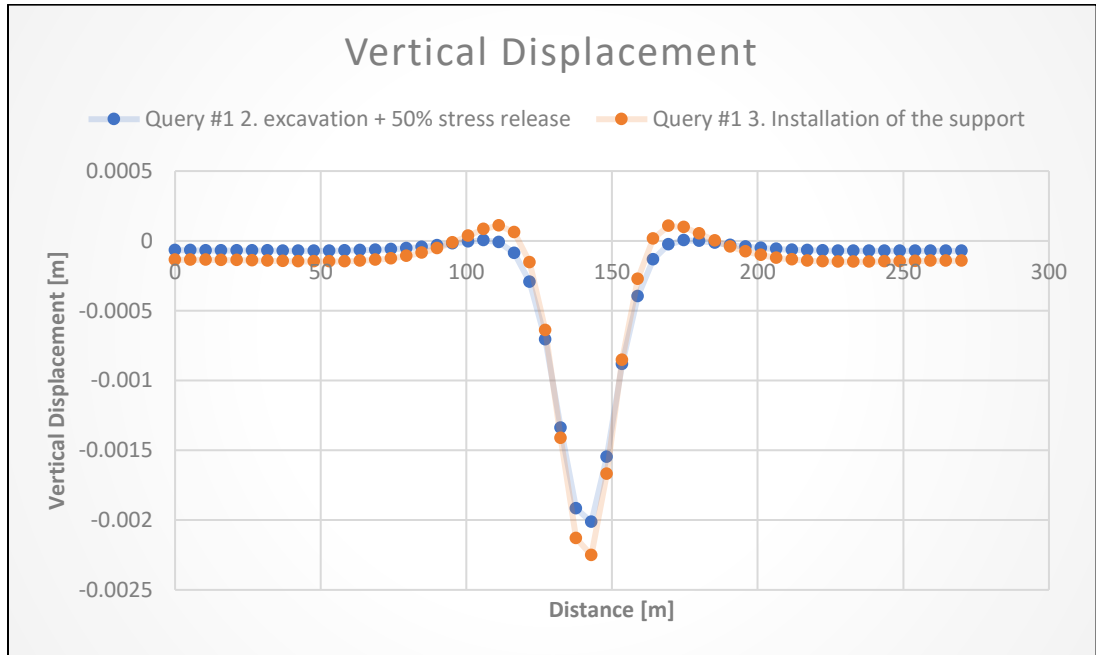


Figure 97 Vertical displacement Vs query distance at the surface

It can be clearly seen that the maximum surface settlement trough is equal to 2.5mm, and the shape of the curve represents well the expected Gaussian distribution curve.

- **Support verification:**

1- Axial force

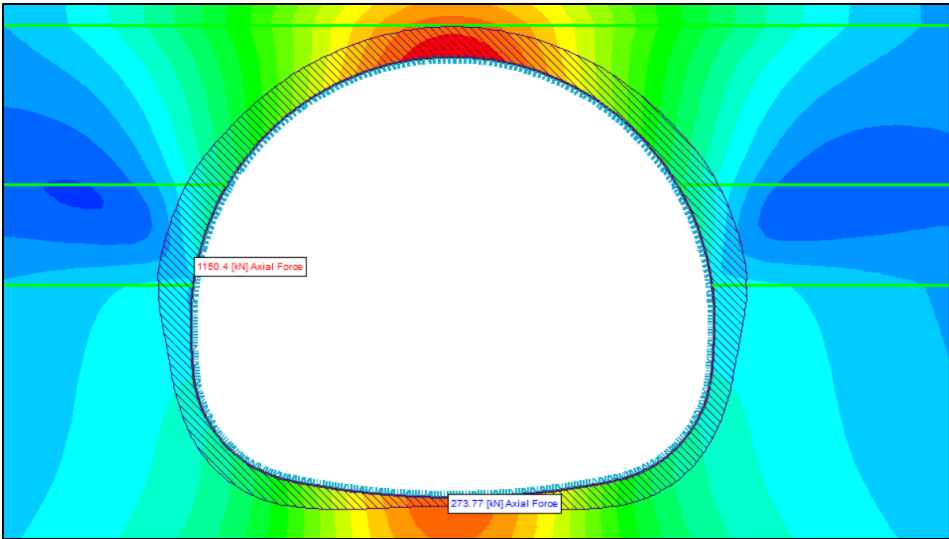


Figure 98 Axial force on the lining

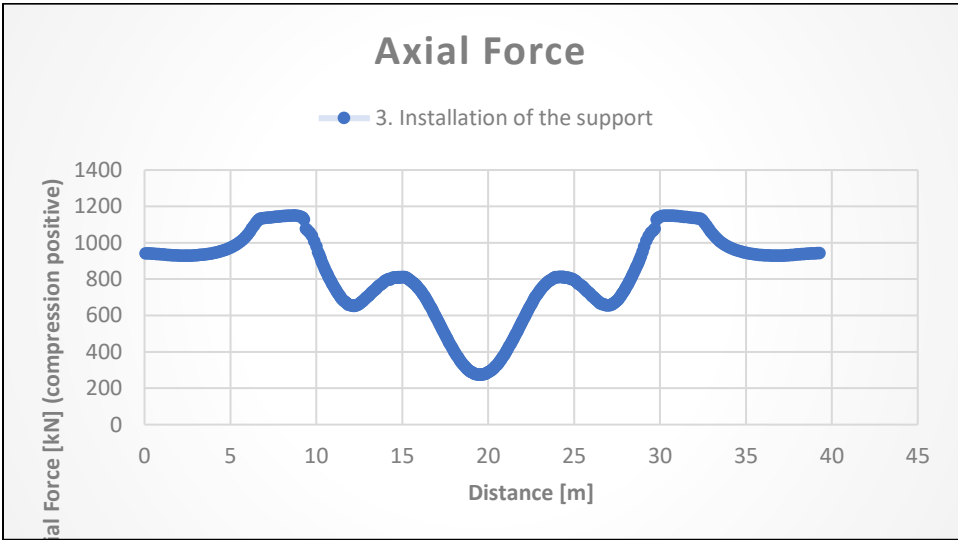


Figure 99 Axial force vs the lining boundary distance

The lining is under compression with maximum value at the spring line or the tunnel wall equal to 1550 KN.

2- Bending moment

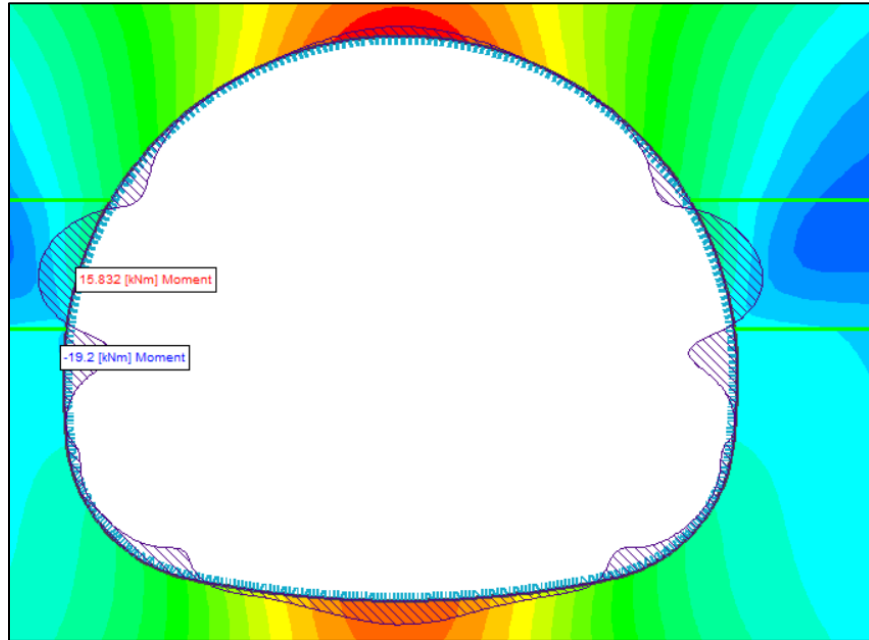


Figure 100 Bending moment on the lining



Figure 101 Bending moment vs the lining boundary distance

3- Shear force

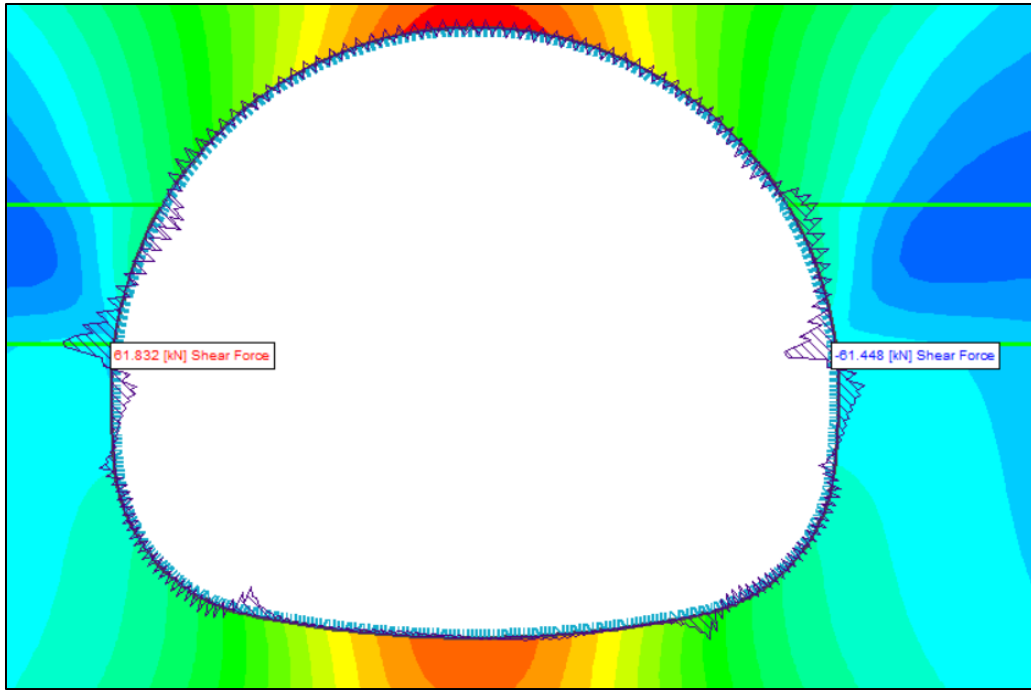


Figure 102 Shear force on the lining

4- Support capacity plot:

The values of the axial force and bending moment are introduced to the support capacity plot to verify the lining

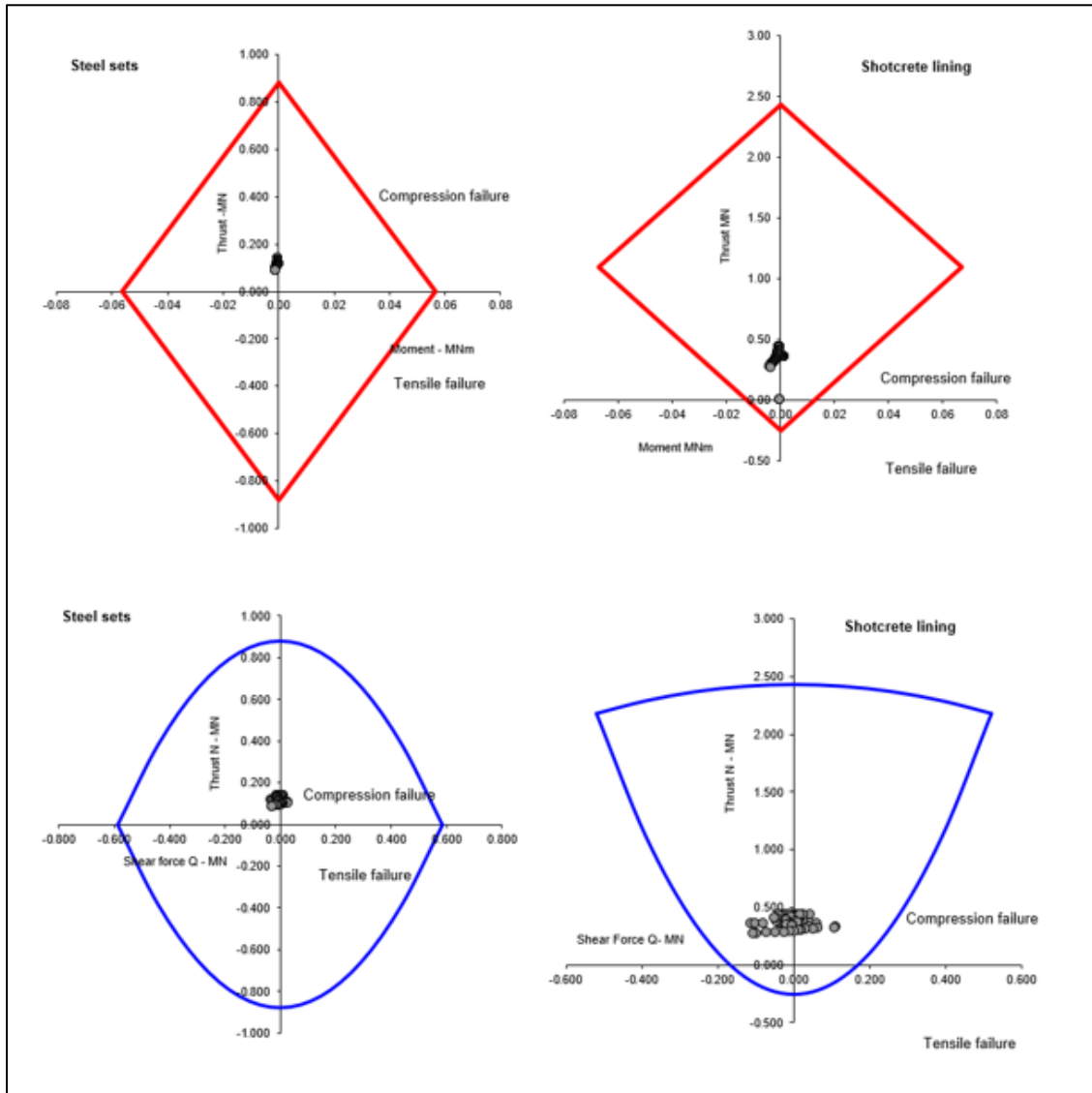


Figure 103 Support capacity plot

It can be clearly seen that all the points are within the domain. Therefore, the lining is verified. The same support system will be checked in the 3D model for the cross passages and the tunnel at the intersection.

6.2.3 Numerical model in 3D

In the following part, the full procedure for the numerical modelling in RS3 is presented.

❖ 6.2.3.1 Geometry

As mentioned in the section (5.2.1), the geometry was created in Rhino 7 as shown in figure (103)

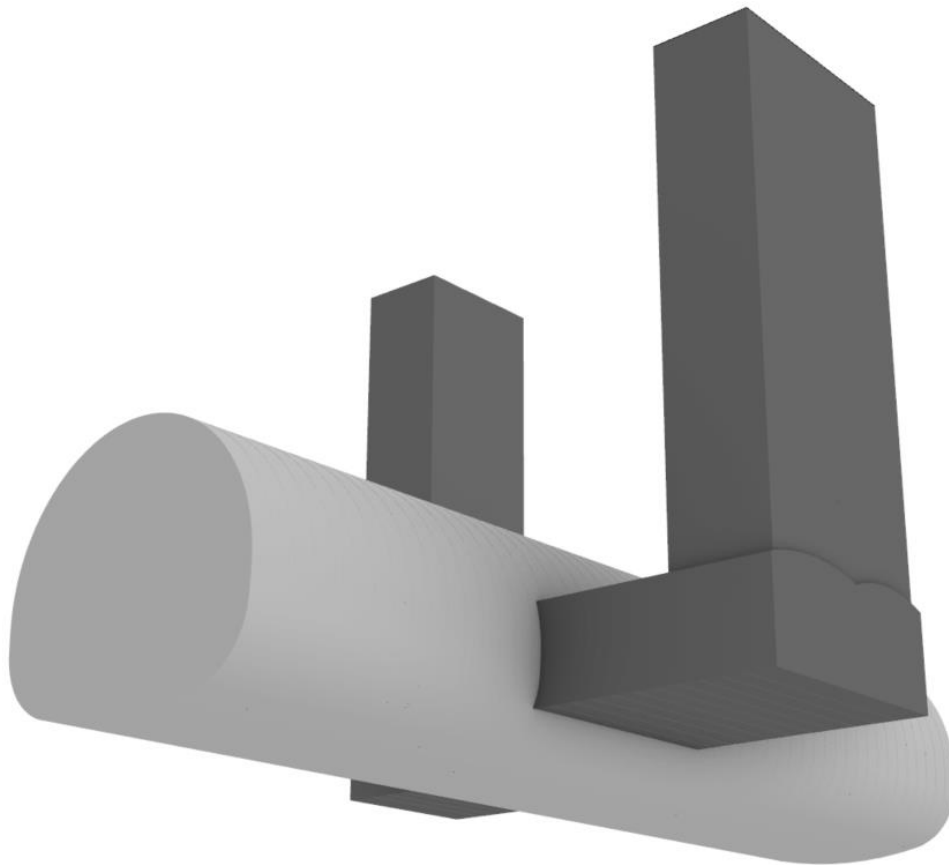


Figure 104 Creating of the 3D model in Rhino7 software

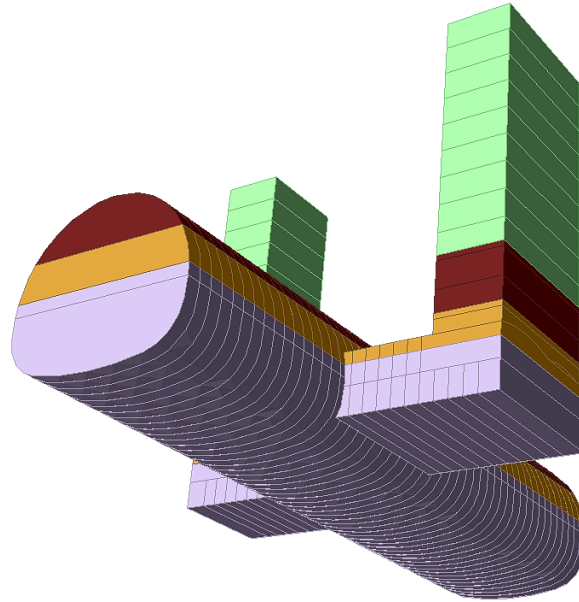


Figure 105 Imported geometry into the RS3

It's important to state that the length of the shafts and the cross passages are taken from the original documents of the project. About the considered longitudinal length of the metro tunnel, from the previous analysis in chapter 5, it has been realised that it could be reduced since the effect of the intersection on the longitudinal distance of the tunnel is affected within small range intersection area. The following figures demonstrate the intersection region:

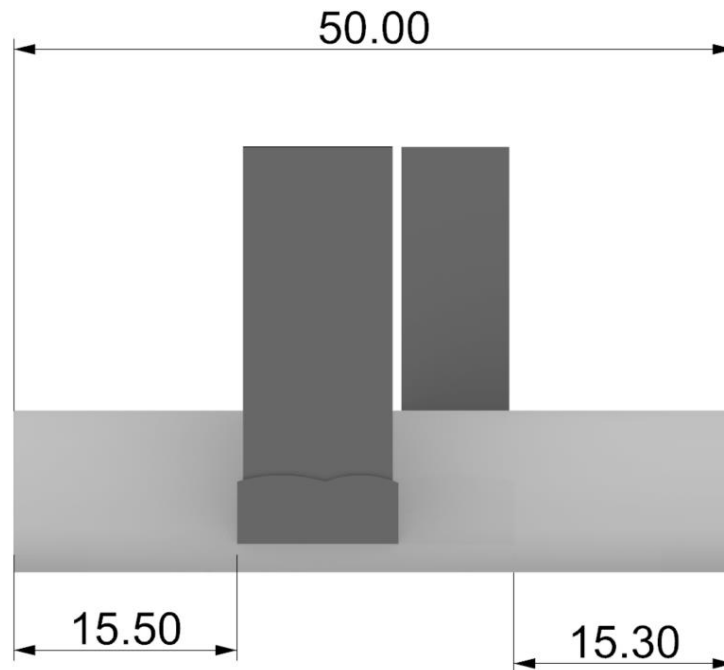


Figure 106 Longitudinal view of the intersection area

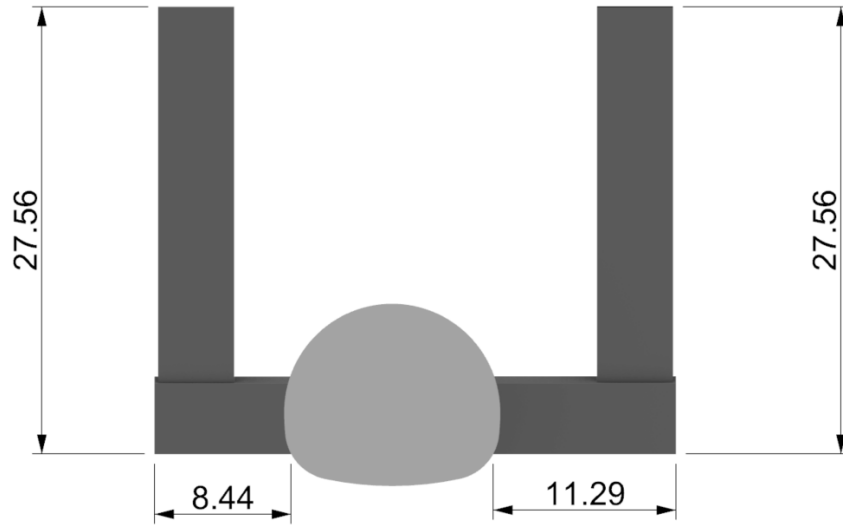


Figure 107 Transversal view of the intersection area

❖ 6.2.3.2 Geological model

Considering the size of the finite element model, it was decided to use an external box of (A = 270m, B = 270m, C = 56.61m)

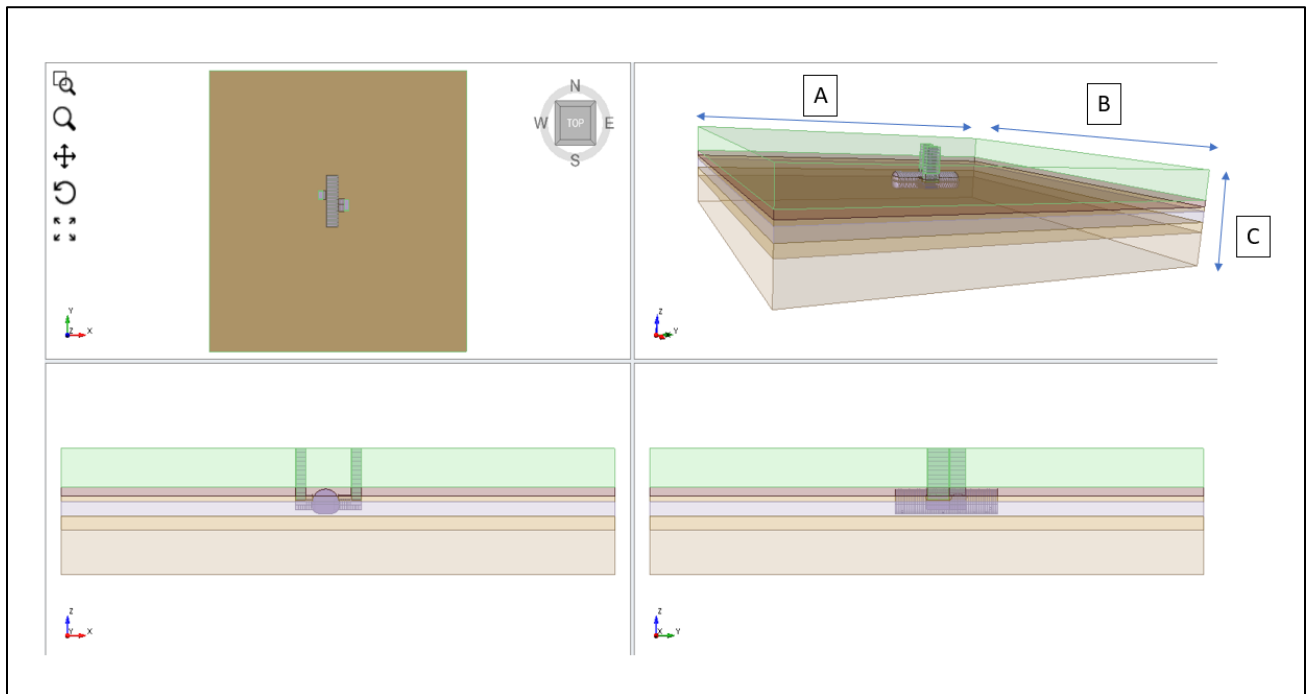


Figure 108 3D model external boundaries

❖ 6.2.3.3 Construction sequencing (staging)

The construction sequencing will be as follows:

- 1- Excavation of the metro tunnel.
- 2- Excavation of the cross passage from the metro tunnel (mucking of the excavated materials will be through the metro tunnel).
- 3- Finally, excavation of the vertical shafts from the surface and the mucking will be through pipes to the cross passage and then mucking will be from the metro tunnel.

Moreover, it is essential to describe the supporting structures that should be used in the considered section; as described before, the current section involves a presence of weak soils at the surface; therefore, for the stability of the vertical shaft's excavation, it has been decided to use micro piles (figure 109) with a diameter equal to 20cm. The micro piles are generally used when there are sensitive ground conditions.

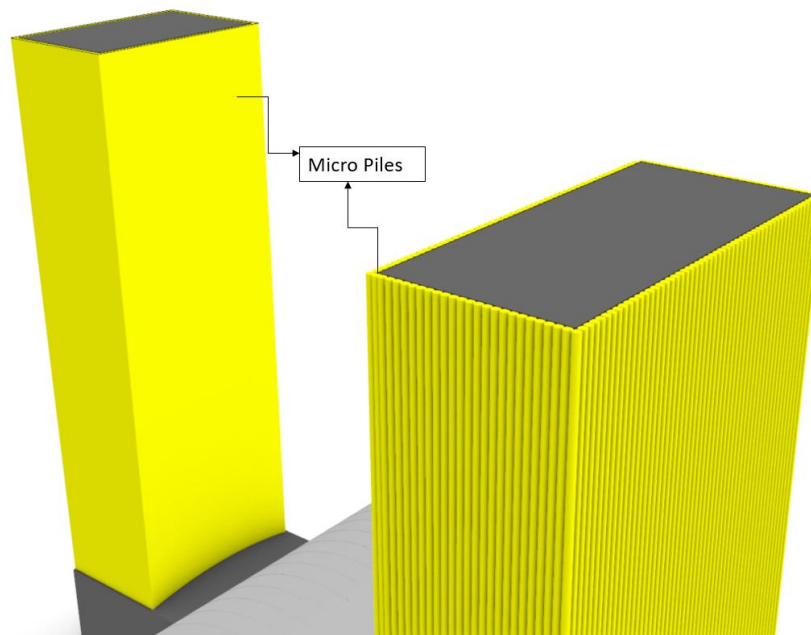


Figure 109 Micro piles overview

Regarding the simulation of the micro piles in the FEM models, two methods could be used. The first method is simulating the piles by structural elements that should be defined in the specific FEM software. For example, in RS3, micro piles could be

simulated using the “define piles” command; this method is useful when it is essential to evaluate the distribution of the averaged quantities such as bending moment, axial and shear force (N, M, T) on the piles. The second method is to model them within the 2D,3D continuum model by changing the surrounding material’s properties with an elastic material that characterised by particular deformability and strength parameters; this method is helpful for the detailed distribution of the stresses within the structural member. Since one of the interests of this thesis is to study the behaviour at the shaft\cross passage intersection and to evaluate the stress distribution and not a detailed design of the micro piles, the second method was used for the simulation of the micro piles by changing the material properties around the shaft within the diameter of the micro piles (20cm), the input data for the properties of the piles as follows:

Micro Piles			
Unit Weight	γ	24	kN/m ³
Elastic modulus	E	1.6	GPa
Poisson ratio	ν	0.2	
Cohesion	c	200	kPa
Friction angle	ϕ	35	°

Table 19 Micro piles properties

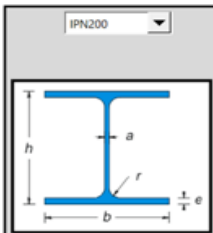
Concerning the stability of the metro tunnel and cross passage, the support system described in section (6.2.1) in the 2D analysis, which is steel sets and shotcrete, was used. The selected model for the (section 2) scenario is IPN200 + shotcrete 30cm; the parameters are as follows:

INPUT PRIMARY LINING

Element 1

RIBS (c)

IPN200



h_1	200	mm	Height of the ribs
b_1	90	mm	Width of flange
a_1	7.5	mm	Width of web
e_1	11.3	mm	Thickness of flange
r	7.5	mm	
A_1	0.00334	m ²	Area of rib
I_1	0.0000214	m ⁴	Moment of inerzia
E_1	210	GPa	Young modulus for steel

Geometrical characteristics of rib

S	1	m	Distance between ribs
n	2.00	N/m	Elements per meter

Element 2

SPRITZ (s)

h_2	300	mm	Thickness of spritz
b_2	1000	mm	Width
A_2	0.14666000	m ²	Area of spritz between 2 ribs
I_2	0.001104	m ⁴	Moment of inerzia
E_2	15	GPa	Young modulus of spritz

Figure 110 The primary lining input data

Therefore, the selected equivalent thickness t_{eq} & the equivalent elastic modulus E_{eq} that was applied to the standard liner in RS3 are:

E_{eq}	19.7	GPa
t_{eq}	0.3	m

Table 20 Primary lining input data

The construction process was simulated using step by step approach. A total of (168) stages were used for the simulation. In the staging process, the excavation was simulated by removing the selected materials, and the supporting structures were simulated by activating the structural elements. Moreover, in the model, the supporting systems were installed on a stage after excavating 1m advancement.

Therefore, the following model stages are adopted:

- 1- The first stage represents the original geostatic stress state or the initial conditions. So, in this stage, the information about the initial in situ state of stresses will be introduced.
- 2- Starting from stage 2, the top heading & bench excavation for the metro tunnel. The excavation length at each step in the construction was 1 m. Then after the excavation of the 1m was completed, the considered supporting structure was installed in a stage after.

Before starting to excavate the cross-passage type (a), the entire considered length of the metro tunnel (50 m) was excavated following the stages (2-108) of the model.

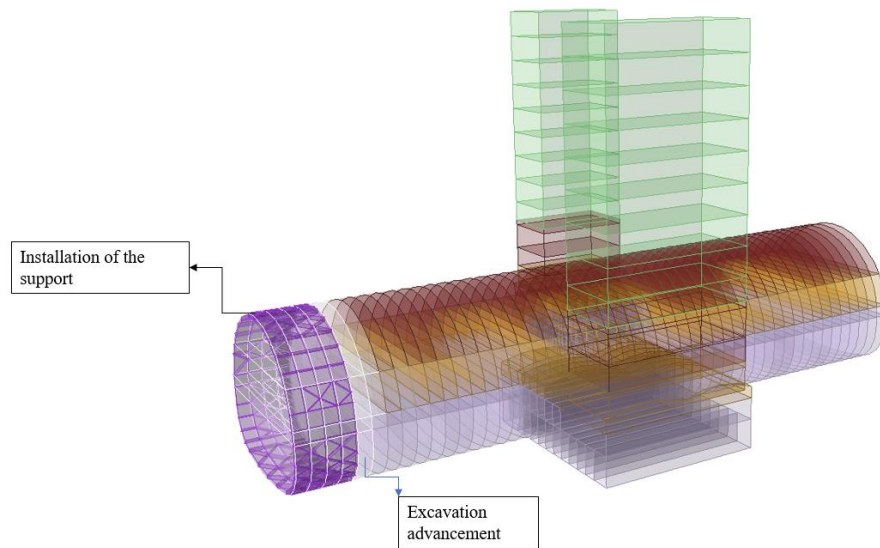


Figure 111 Example of the tunnel excavation

- 3- From stage 109, the excavation of the cross-passage type (a) from the tunnel was started. The excavation length at each step in the construction was 1 m. Then after the excavation of the 1m was completed, the considered supporting structure was installed in a stage after. Before beginning to excavate the vertical shaft type (a), the entire considered length of the cross passage (a) was excavated following the modelling stages (109-127).

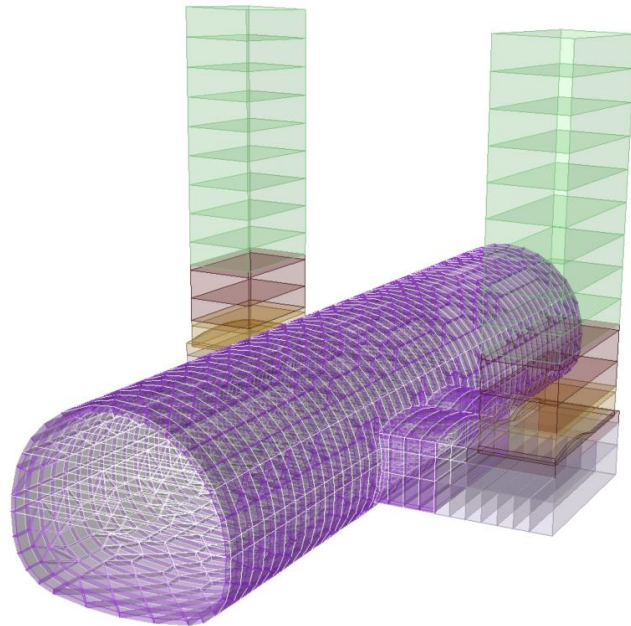


Figure 112 Example of the excavation of the cross passage type (a)

- 4- From the ground surface, the installation of micro piles at stage 128 for the stability of the vertical shaft (a) excavation, then the vertical shaft type (a) was excavated using the top-down full-face excavation method. The length of the excavation step was 2 m. After the excavation of the 2m was completed, the shotcrete was installed in a stage after. Before starting to excavate the cross passage type (b), the entire considered length of the shaft type (a) was excavated following the modelling stages (129-141).

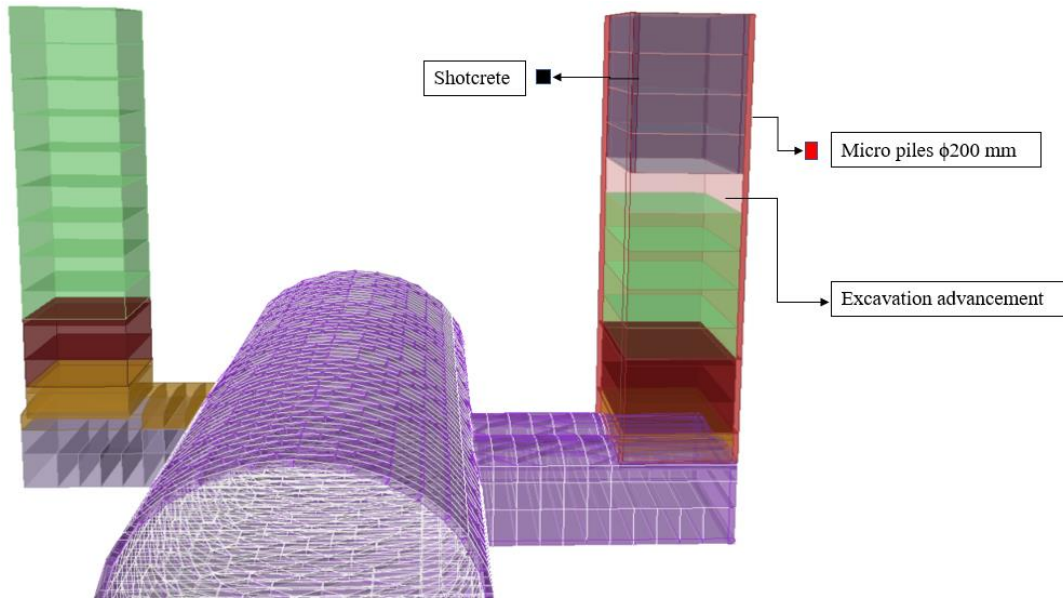


Figure 113 Example of the shaft (a) excavation

- 5- From stage 142, the excavation of the cross-passage type (b) from the tunnel has started. The excavation length at each step in the construction was 1 m. Then after the excavation of the 1m was completed, the considered supporting structure was installed in a stage after. Before beginning to excavate the vertical shaft type (b), the entire considered length of the cross passage (b) was excavated following the modelling stages (142-155).

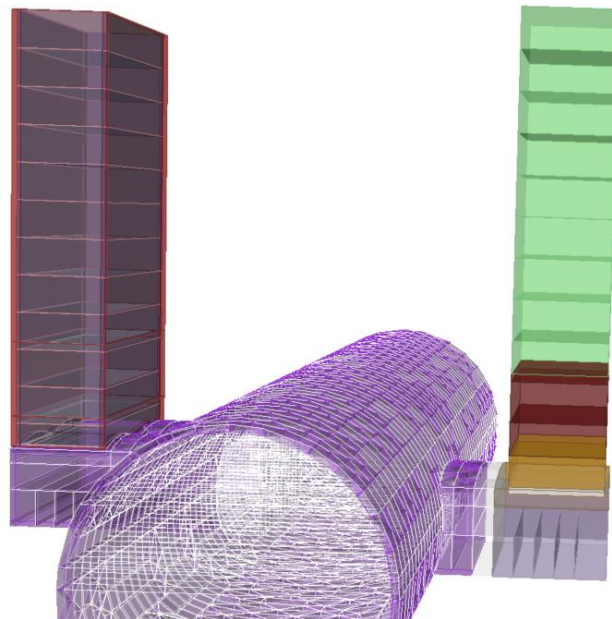


Figure 114 Example of the cross passage type (b) excavation

- 6- From the ground surface, the installation of micro piles at stage 156 for the stability of the vertical shaft (b) excavation, then the vertical shaft type (a) was excavated using the top-down full-face excavation method. The length of the excavation step was 2 m. After the excavation of the 2m was completed, the considered shotcrete was installed in a stage after. The entire considered length of the shaft type (b) was excavated following the modelling stages (156-168).

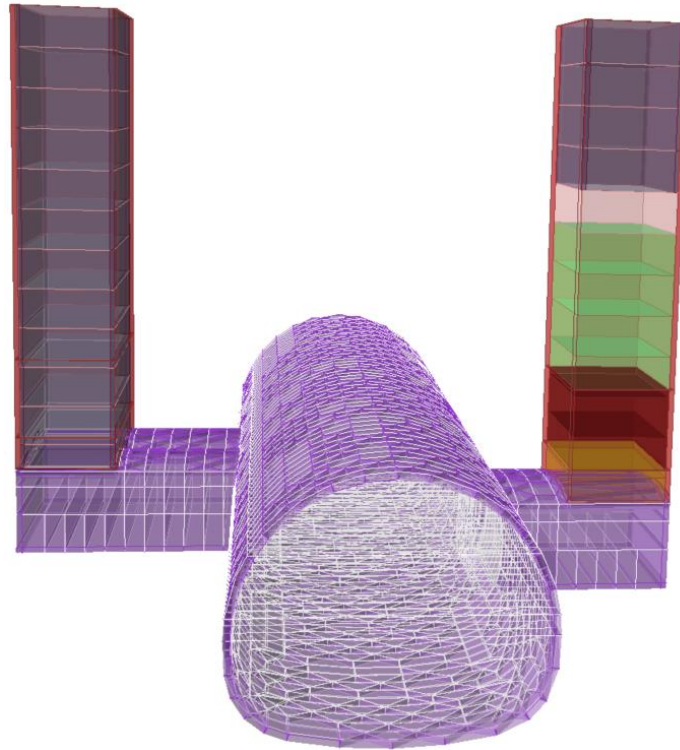


Figure 115 Example of the shafts (b) construction

6.2.4 Results of 3D analyses using RS3

To compare the 3D results with the 2D analysis results, the RS3 results are presented in stage (108), which is the end of the excavation of the metro tunnel.

❖ The initial state of stresses

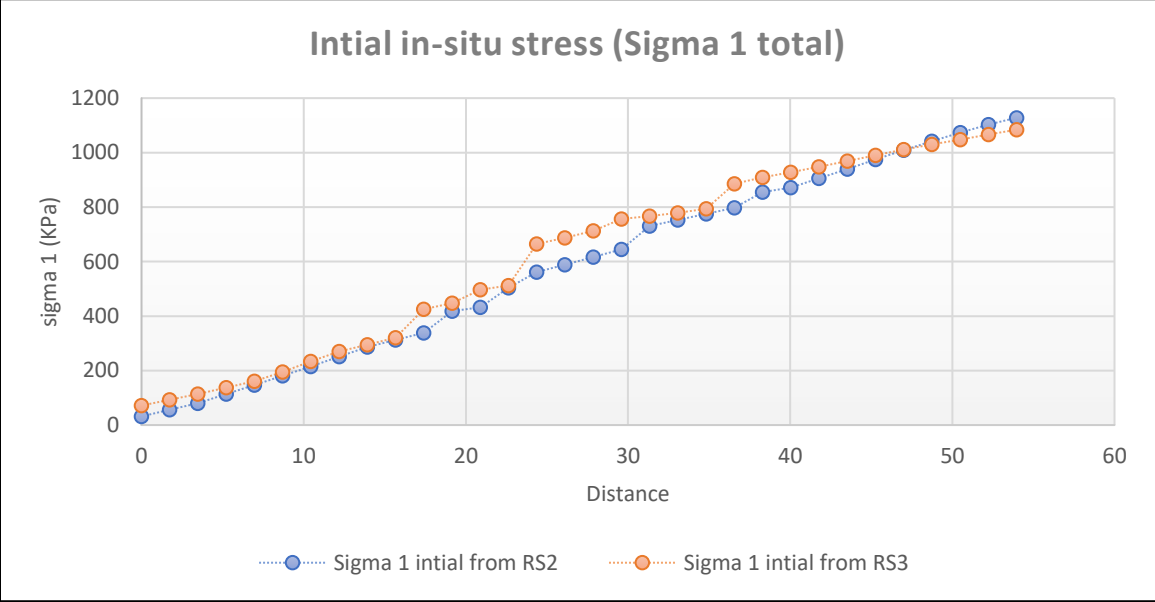


Figure 116 Initial state of stresses

Because of the application of the same conditions in the 2D and 3D, it is noticeable that the trend for the initial in-situ stress is the same in the 2 models.

❖ Stress state at the end of the excavation of the metro tunnel

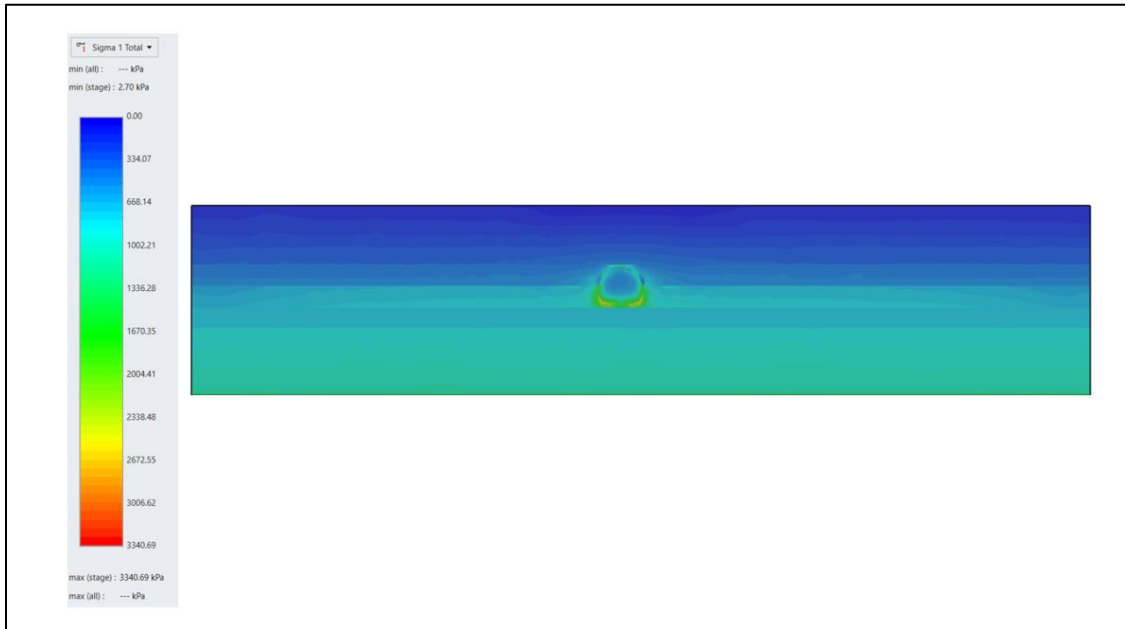


Figure 117 stress state RS3 results (stage 108)

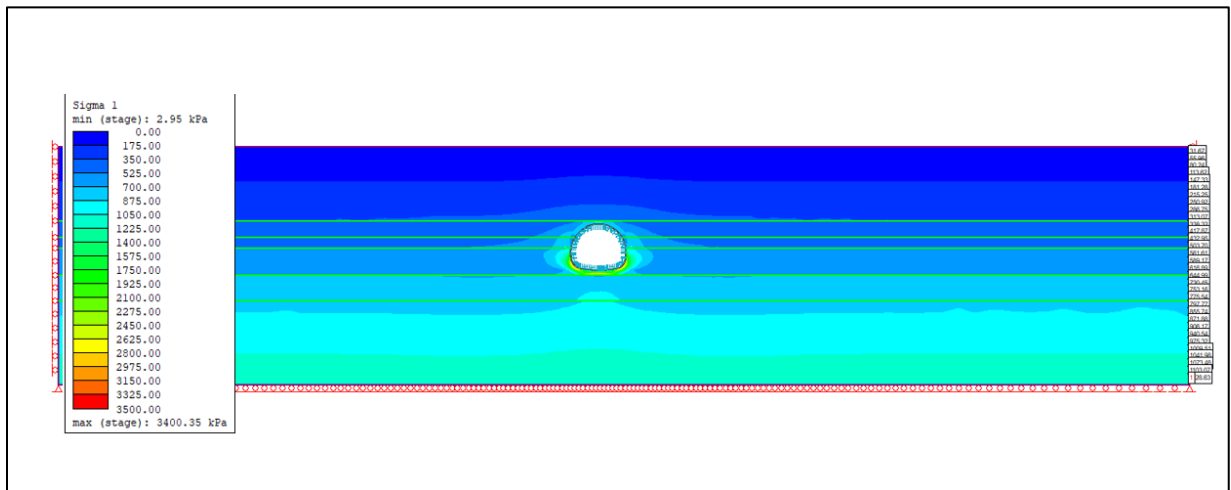


Figure 118 stress state RS2 (stage 3)

It can be clearly seen from the 3D & 2D analysis that the stress concentration at the end of the excavation of the tunnel is maximum at the invert of the tunnel.

❖ 6.2.4.3 Plastic zones at the end of the excavation of the metro tunnel

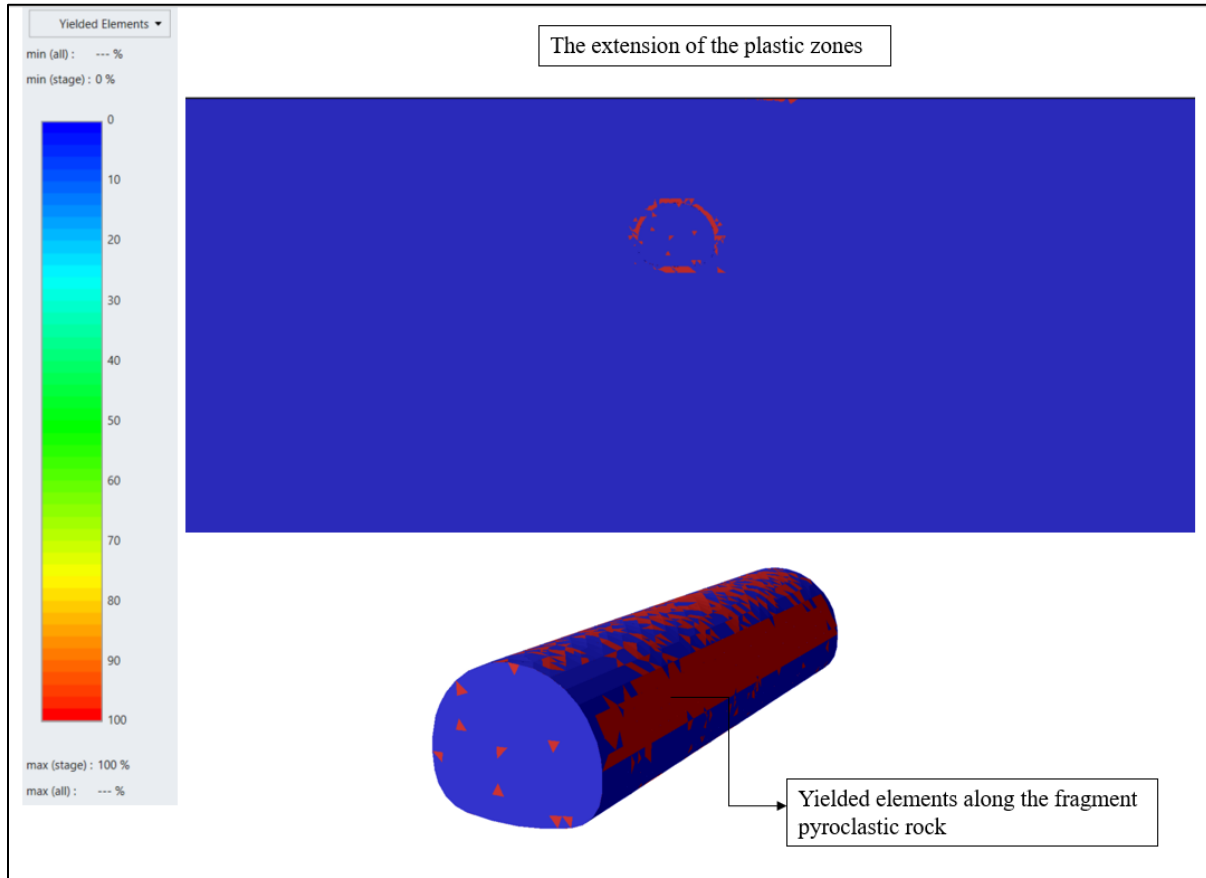


Figure 119 Plastic zones RS3 results (stage 108)

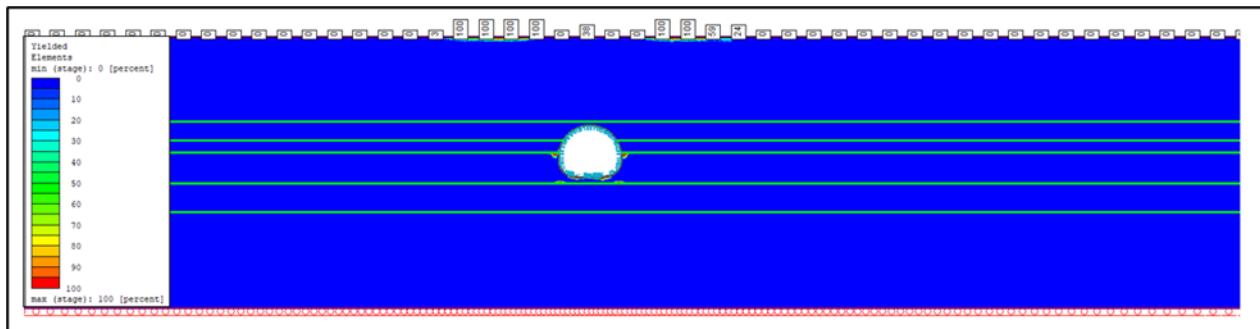


Figure 120 Plastic zones RS2 results (stage 3)

The development of the plastic zones in the 3D and 2D models are pretty close with a maximum extension of the yielded elements at the tunnel's walls, where the fragment pyroclastic layer crosses.

❖ **6.2.4.4 Total displacement at the end of the excavation**

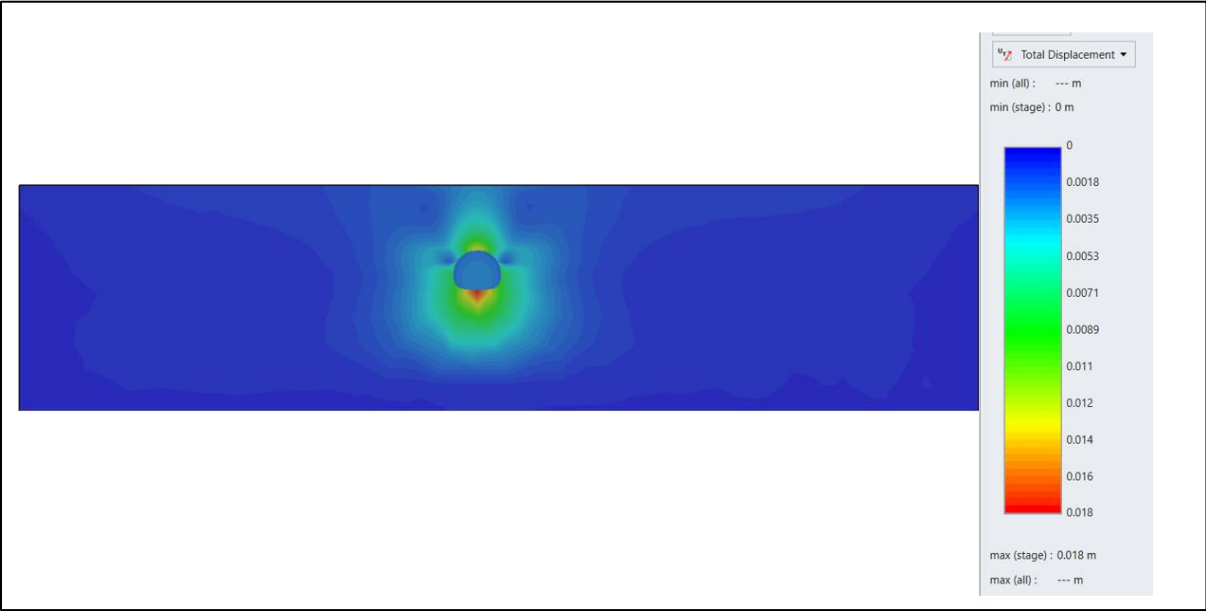


Figure 121 Total displacement RS3 results (stage 108)

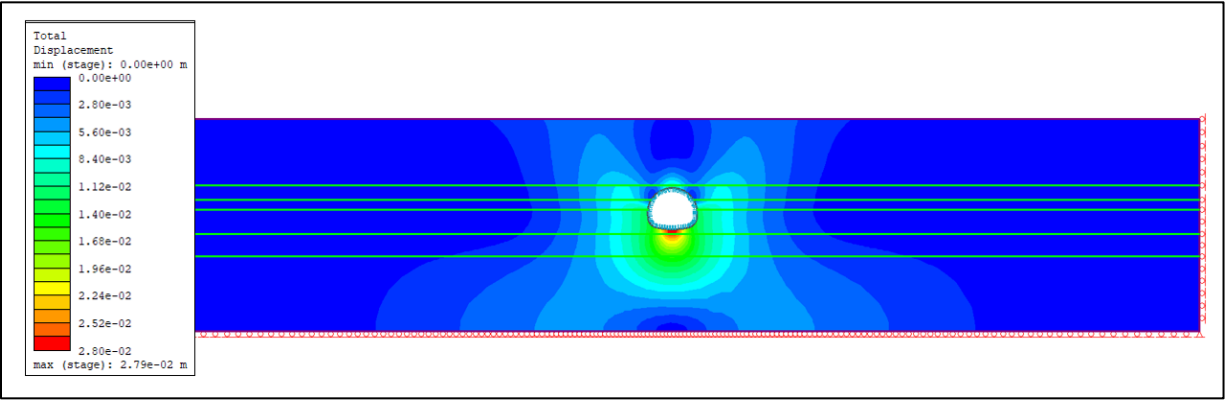


Figure 122 Total displacement RS2 results (stage 3)

As mentioned in the previous 2D analysis in section (6.2.2), using the Mohr coulomb criterion to represent the loose soil in this condition introduces high values at the invert of the tunnel.

❖ **6.2.4.5 Surface settlement trough**

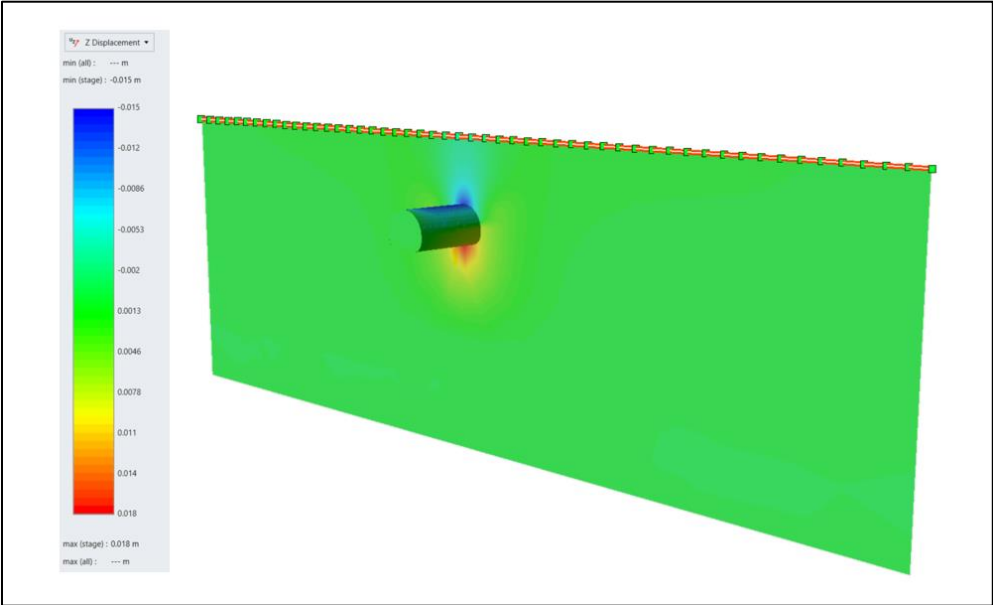


Figure 123 surface settlement trough at stage (108)

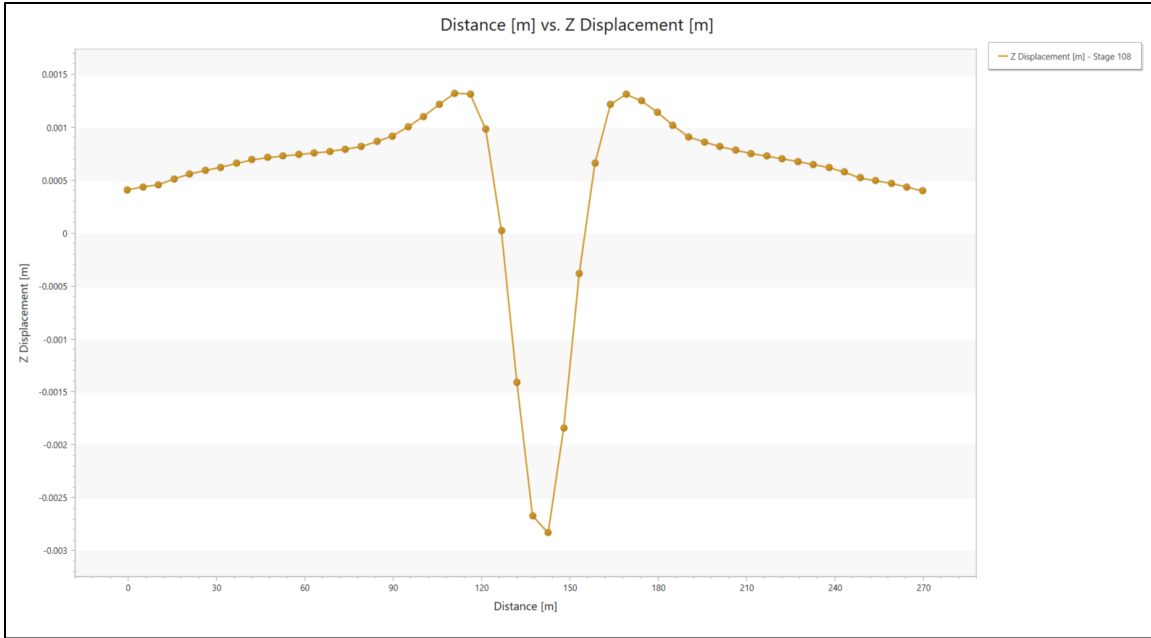


Figure 124 Z displacement VS query distance at the surface

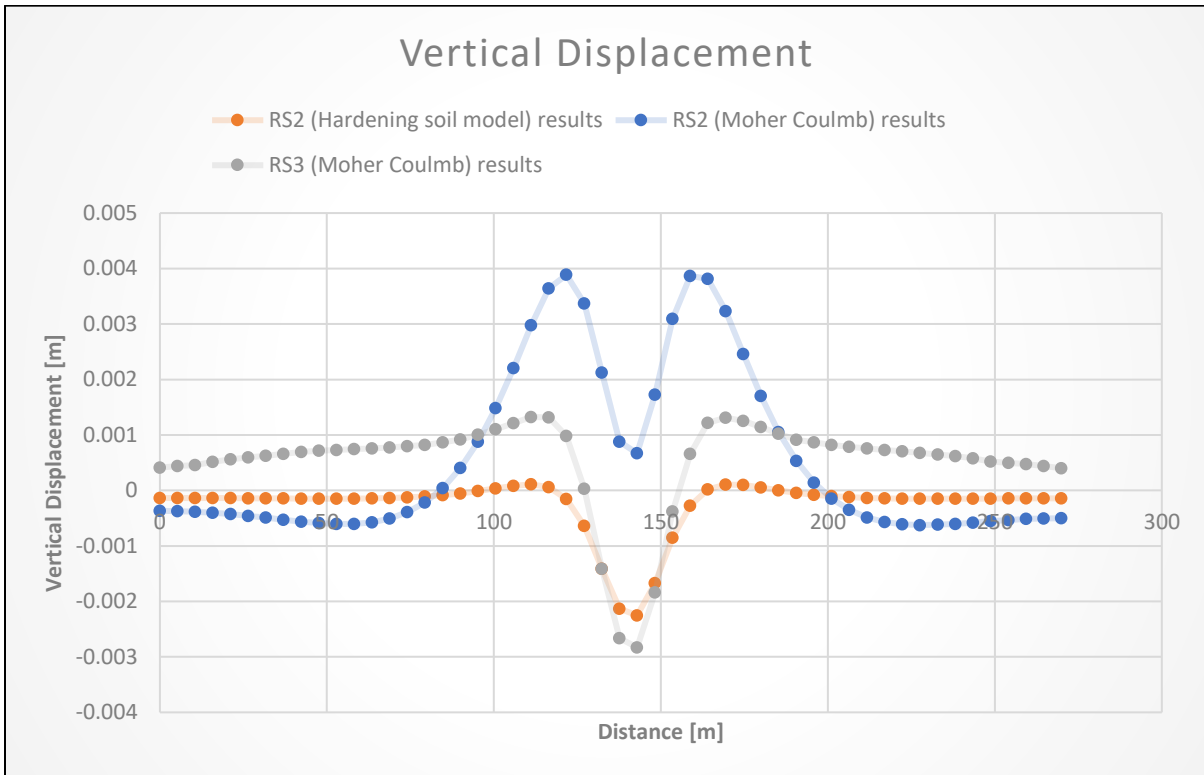


Figure 125 Surface settlement trough curve

From the 2D & the 3D analysis, it is noticeable that the results from the 2D (Hardening soil model) & the 3D are quite close, with a value equal to 3 mm, therefore are no concerns about the surface settlement due to the tunnel excavation.

❖ 6.2.4.6 Effect of the excavation of the cross passages and the shafts in section 2 related to the worst scenario:

In this part, the effect of the excavation of the cross passages & the vertical shafts are presented. The results are introduced for stage 168.

❖ 6.2.4.6.1 plastic zones at the end of the excavation (stage 168)

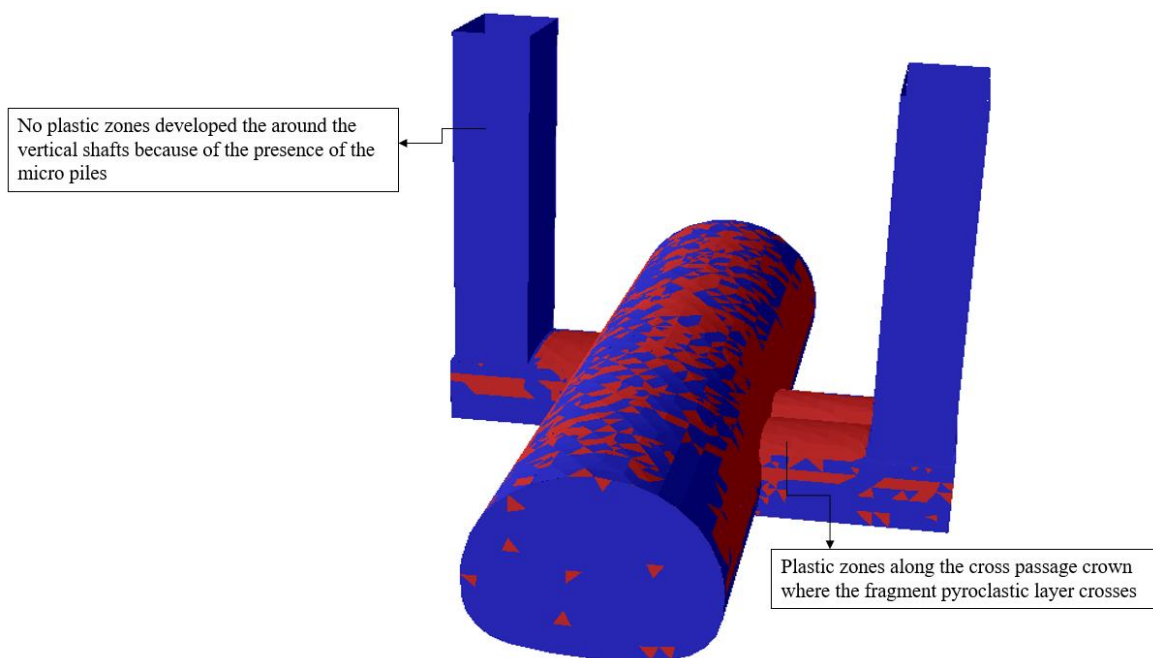


Figure 126 Yielded elements (stage 168)

It can be clearly seen that the intensive concentration of the yielded elements along the tunnel walls and the crown of the cross passages is due to the presence of the fragment pyroclastic rock. At the same time, no yielded elements developed in the contour of the vertical shafts due to the presence of the micro piles.

❖ 6.2.4.6.2 surface settlement trough:

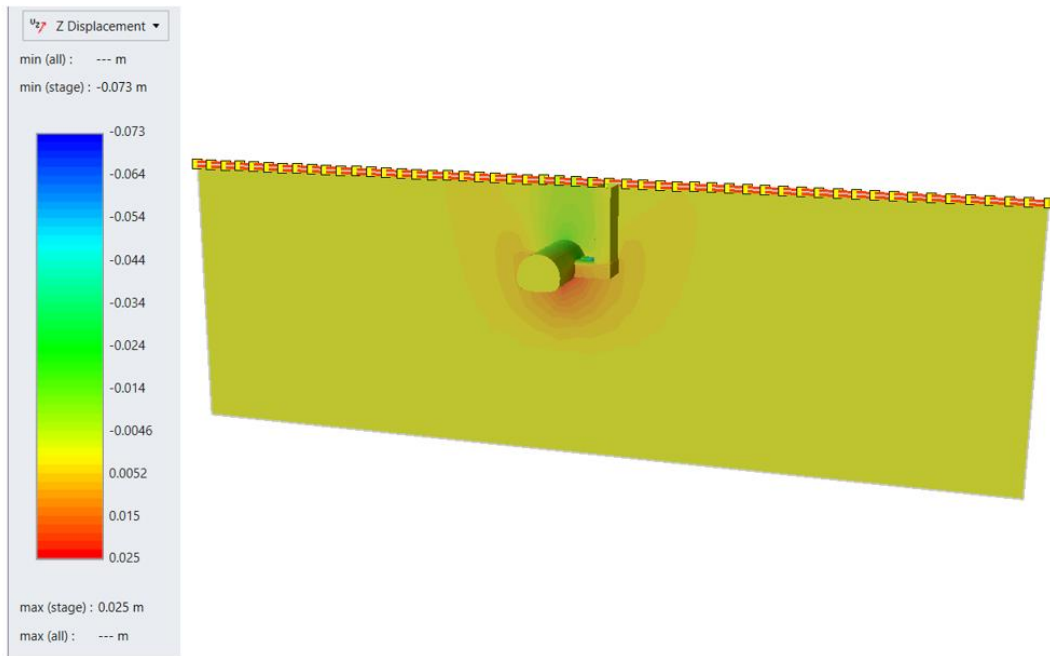


Figure 127 Surface settlement trough

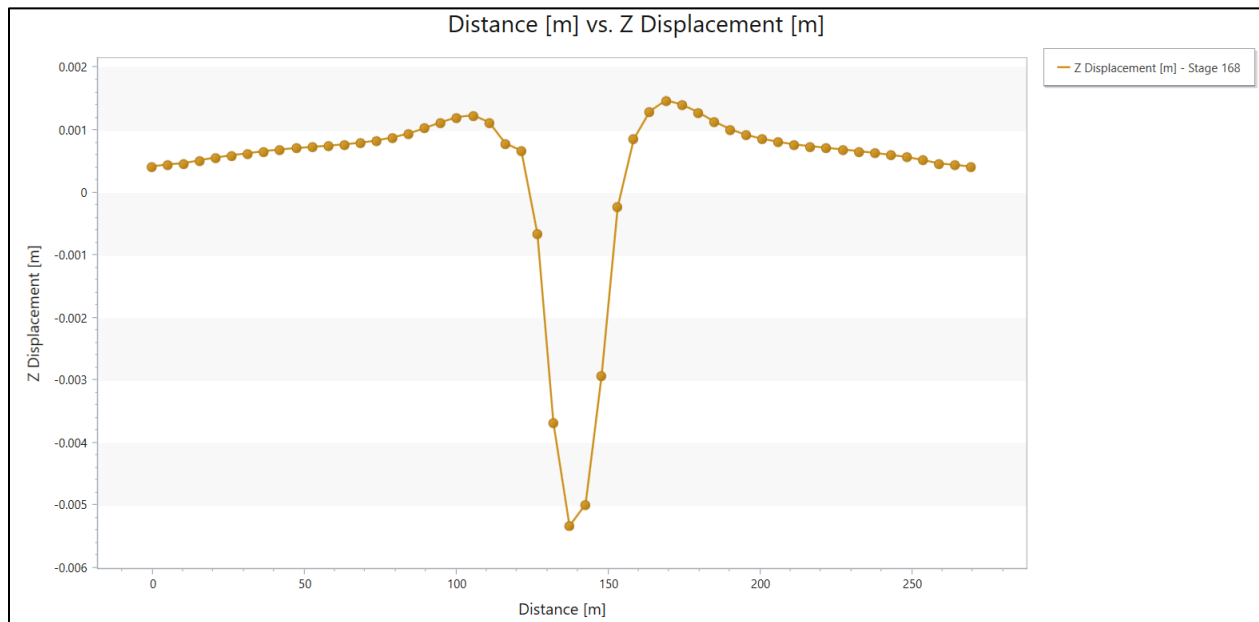


Figure 128 Query at the ground surface

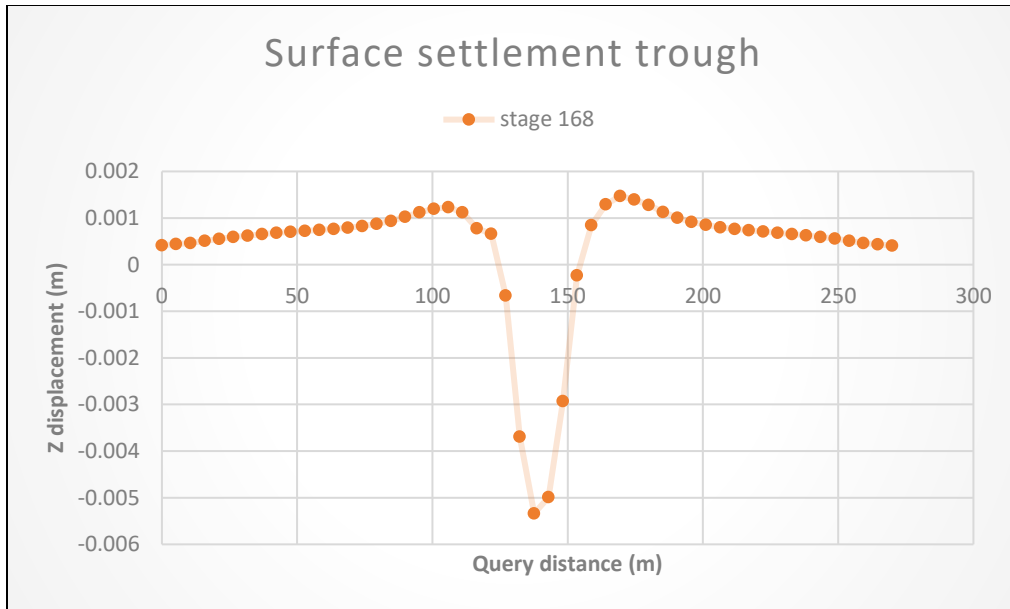


Figure 129 Z displacement vs query distance at the surface

According to the 3D analysis results, the maximum displacement at the surface due to the excavation of the shafts and the cross passage is increased to reach 5.5 mm (from 3mm to 5.5 mm).

❖ 6.2.4.6.3 Total displacement

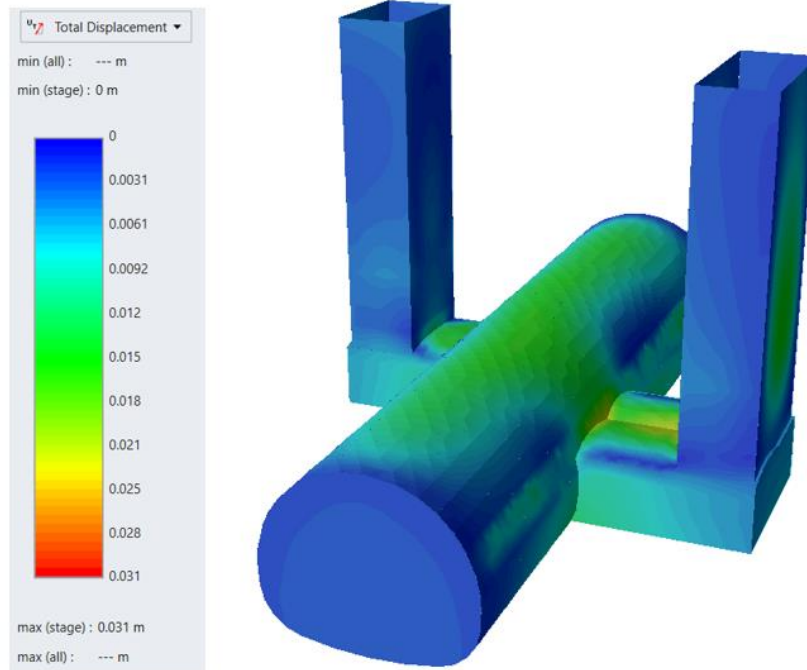


Figure 130 Total displacement (stage 168)

The maximum total displacement is localised at the invert of the tunnel and on the crown of the cross passage type (a) with a value that could reach 2cm.

❖ 6.2.4.7 Lining results:

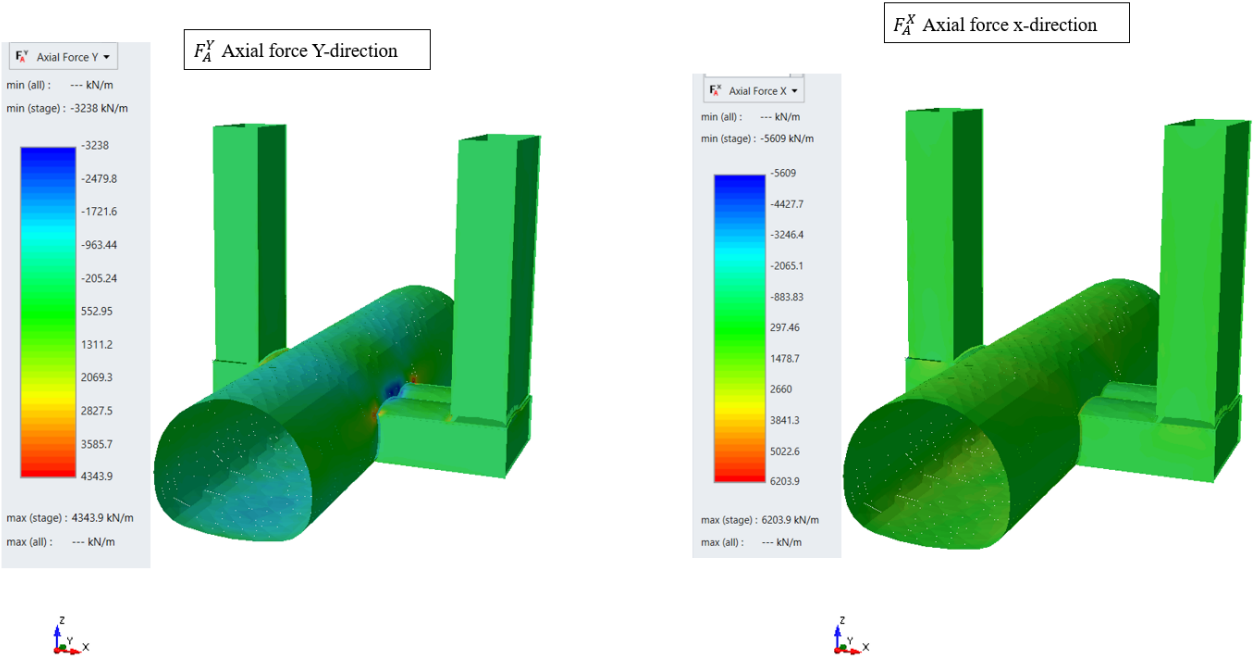


Figure 131 Axial forces (X & Y directions)

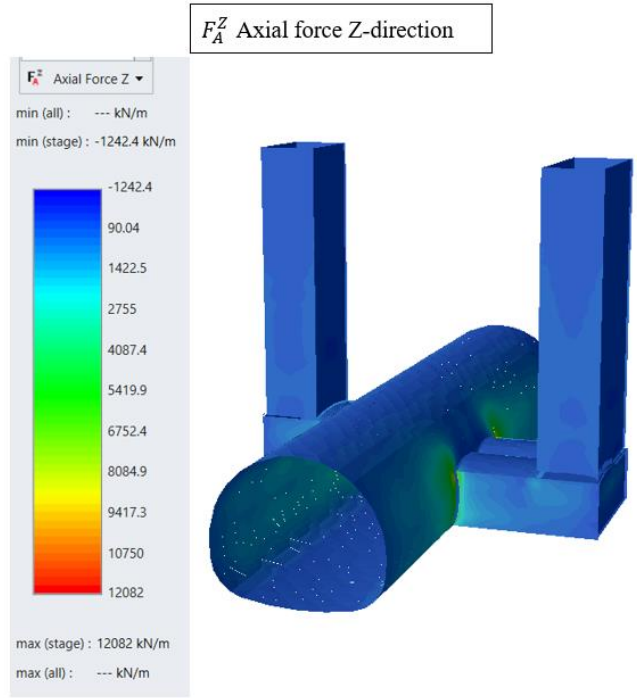


Figure 132 Axial force (Z- direction)

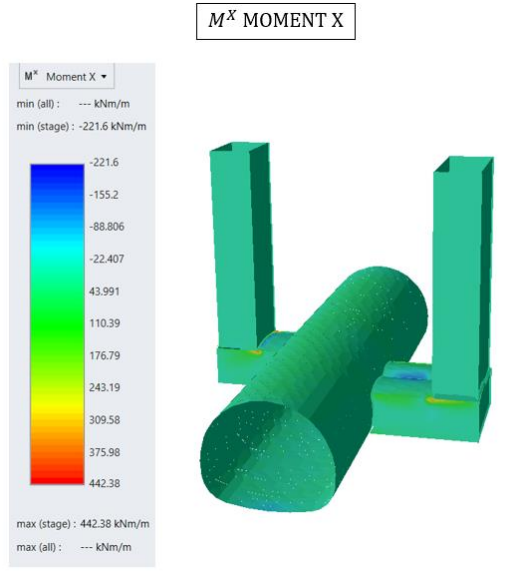
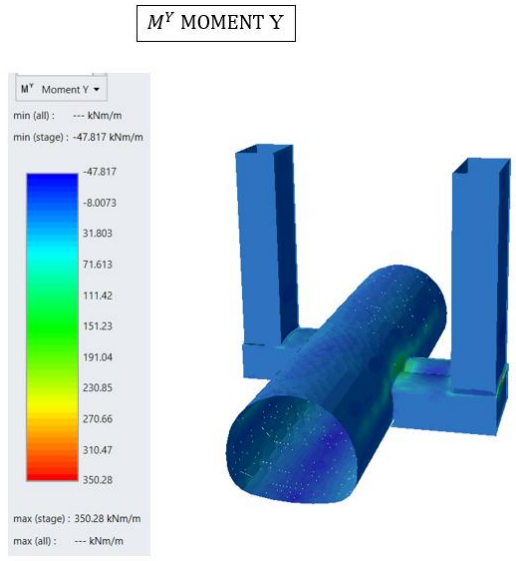


Figure 133 Bending moment (about X & Y axis)

M^Z MOMENT Z

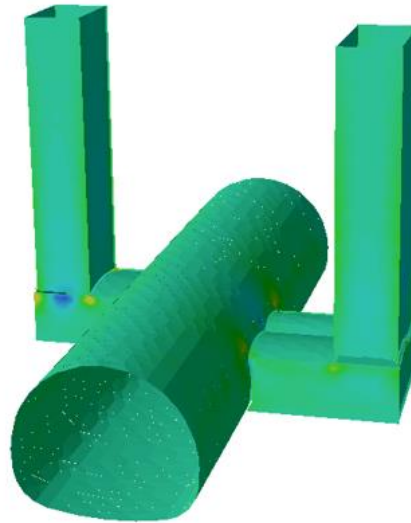
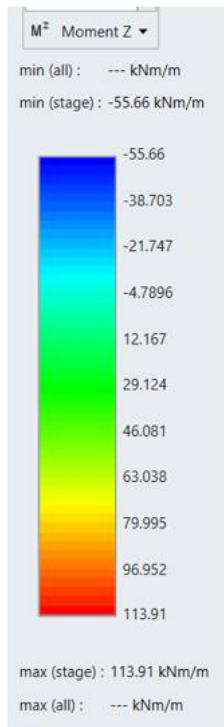


Figure 134 Bending moment about (Z-direction)

Note:

From the lining verification through the support capacity plot in the 2D analysis, and the 3D results related to the construction of the cross passage and the shafts, the mentioned support system is approved.

6.2.5 Detailing related to the worst scenario

This part introduces a representation of the detailing for the elements at the intersection region related to the worst scenario conditions. The detailing is presented only for the shaft (a) and cross passage (a) since the trend is the same for the shaft (b) & cross passage (b).

❖ **Intersection area overview (section for the intersection area)**

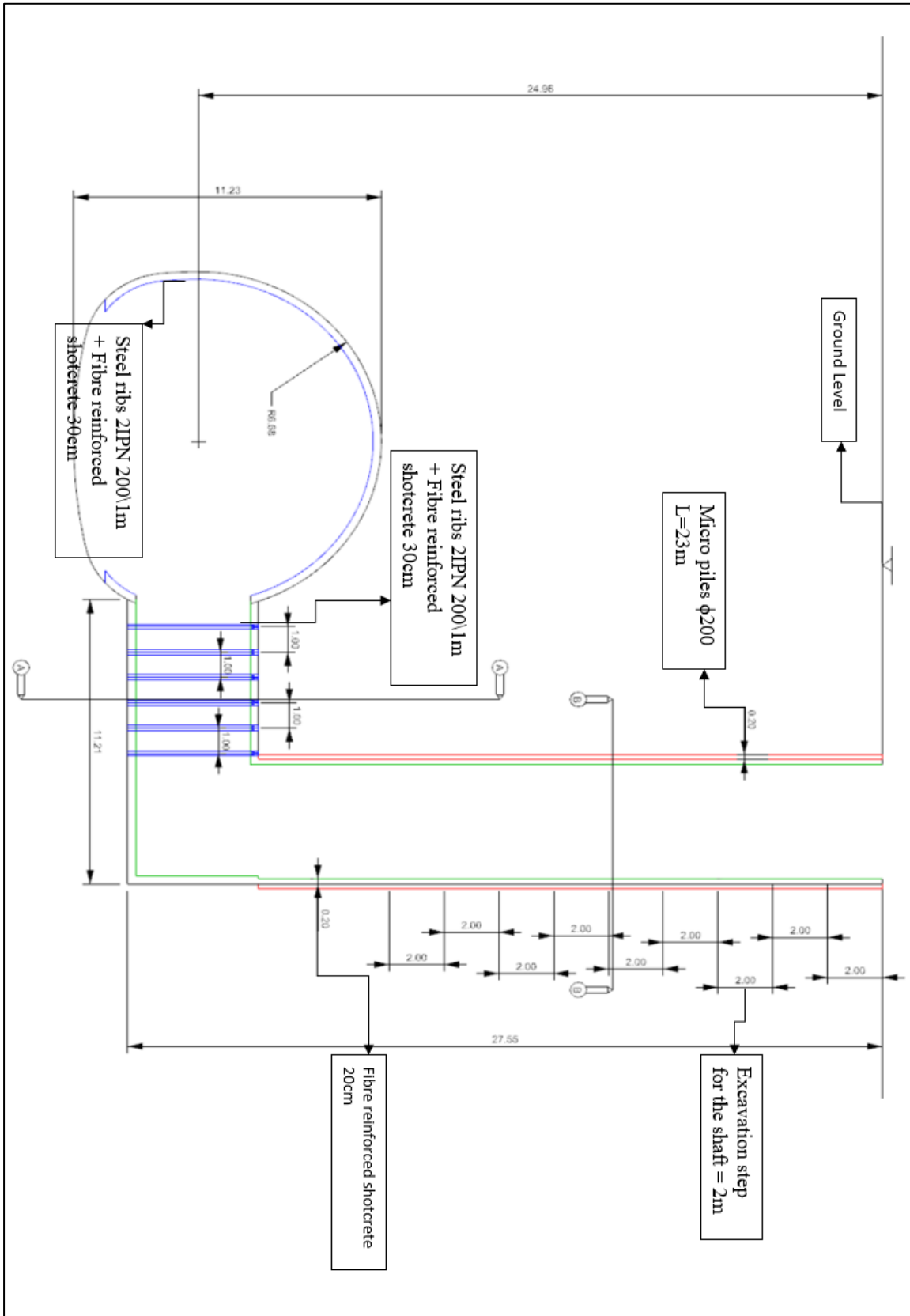


Figure 135 Intersection area overview with detailing

❖ **Section A-A (Cross passage cross-section)**

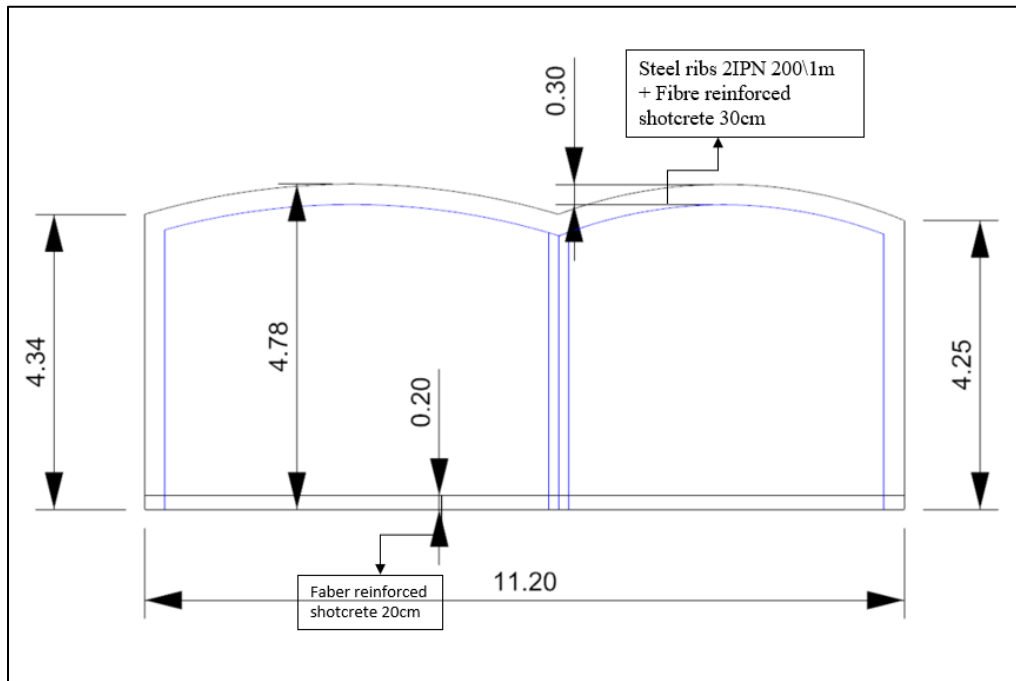


Figure 136 Section A-A (Cross passage cross-section)

❖ **6.2.5.3 Section B-B (Shaft cross-section)**

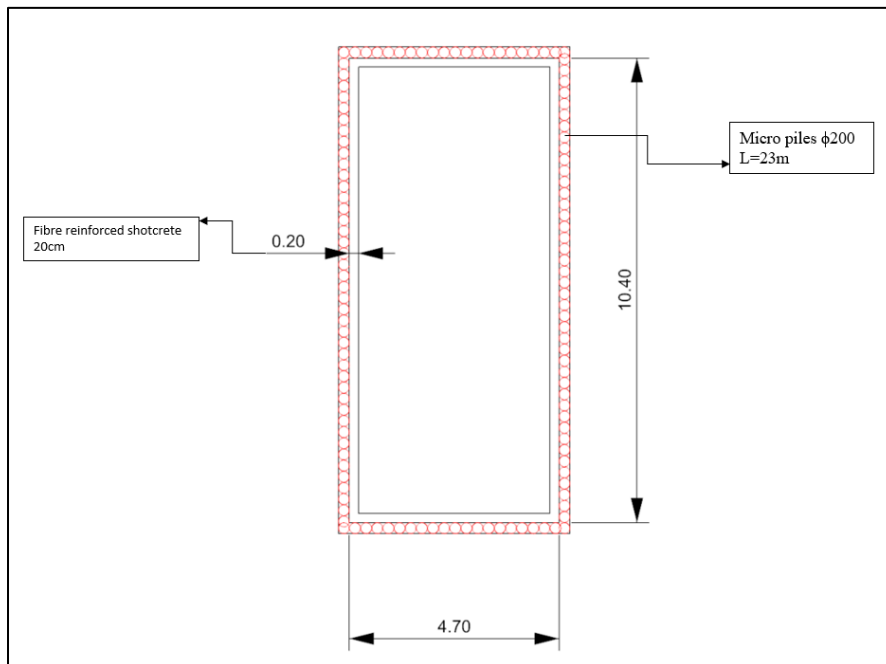


Figure 137 Section B-B (Shaft cross-section)

Chapter 7: Suggested models for the shafts & cross-passages

This chapter deals with a number of analyses carried out to investigate the optimum shape for the shafts & cross passages. The results provide a suggested shape which is demonstrated to lead to a more economical and sustainable solution.

3D FEM analyses are so repeated by considering a different transversal shape for the shafts. Therefore, RS3 is used to analyse the plastic zones of the surrounding rock, and the stress concentration and displacement distribution that could be expected during construction. Then the results are compared with the one established by the original model to demonstrate the influence in the case of using the suggested models instead of the original ones.

New analysis that refers to the favourable scenario conditions (section 1) since the conditions of the moderate rock mass help in a significant way to illustrate the effectiveness of the recommended model

In the following, the strategy used for selecting and creating the recommended models for the shafts & cross passages are reported.

7.1 Suggested model for the vertical shafts

Theoretically, shafts have in any geometric shape of the transversal section. However, the most common shapes are the circle, rectangle, square, and ellipse. The shape of the shaft is dependent on the use and ground conditions. Rectangular and square shafts are common in mines and generally are internal shafts, whereas the circular & ellipsoidal shafts are generally preferred for construction shafts, because they are much more robust and can be more efficiently supported. Indeed, shafts are recognised for their simple execution and reduced costs because the need to resort to a shoring system is significantly reduced by taking advantage of the arching effect. The circular or elliptical geometry is the main factor that allows taking advantage of this effect, making the construction of shafts more efficient.

Therefore, in this current project, it has been decided to recommend an elliptical shape instead of the rectangle one from the original documents of the project presented in chapter 3. It has been proven that using an elliptical shaft could reduce

in a significant way the need for the temporary and primary support, consequently having more economical conditions in the considered project.

For selecting the geometry of the elliptical shaft, it was necessary to ensure the functionality of the shaft to comprise a ventilation chamber and an emergency exit without a significant or any change in the architectural perspective or on the ground surface:

- **Effects of changing the geometry on the ground surface:**



Figure 138 Orthophoto for the shafts in section 1

The above orthophoto (138) for section 1 shows that changing and increasing the cross-sectional area of the shafts will not influence the ground surface in terms of the logistics aspects; all the other ventilation shafts have the same conditions.

- **Effect of changing the cross-section of the shaft on the shaft functionality:**

1- Shaft type (a)

As it has been illustrated in chapter 3, the shaft type (a) involves a ventilation chamber, and an emergency exits; the following figure (139) demonstrates that changing the shape and the area of the shaft cross-section to the recommended one respects its functionality as well.

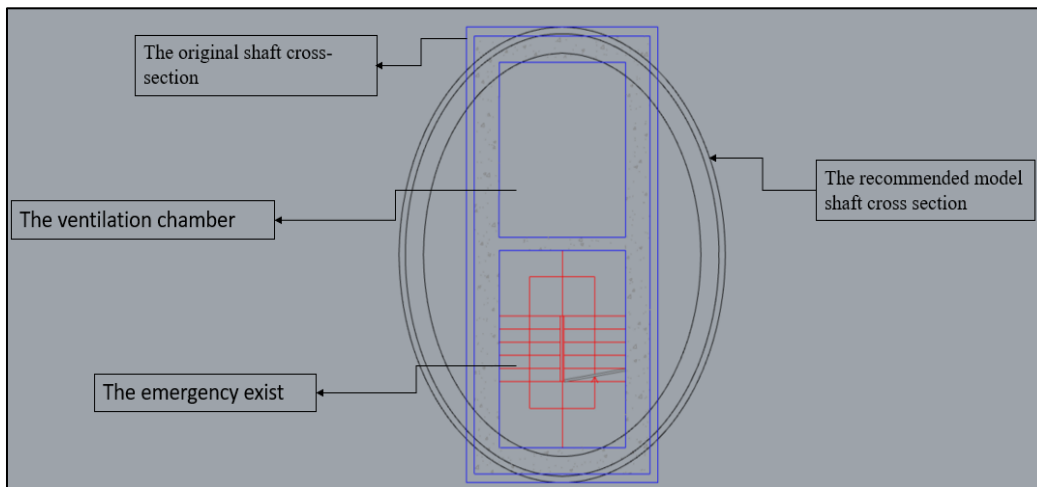


Figure 139 Original and recommended shaft cross-section type (a)

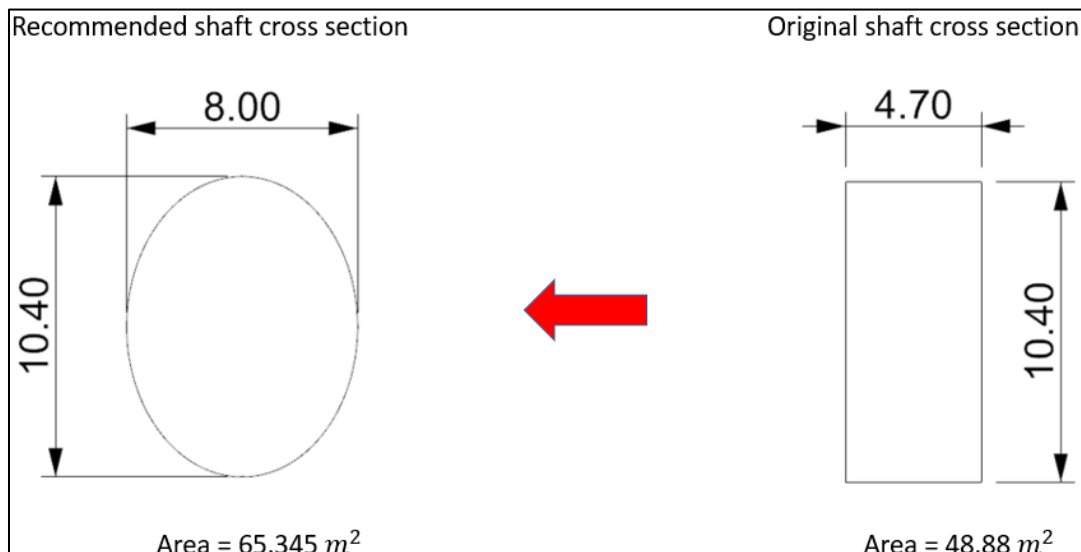


Figure 140 Original vs recommended shaft (a) model

2- Shaft type (b)

The shaft type (b) involves only an emergency exists; the following figure (141) demonstrates that changing the shape and the area of the shaft cross-section to the recommended one respects its functionality as well.

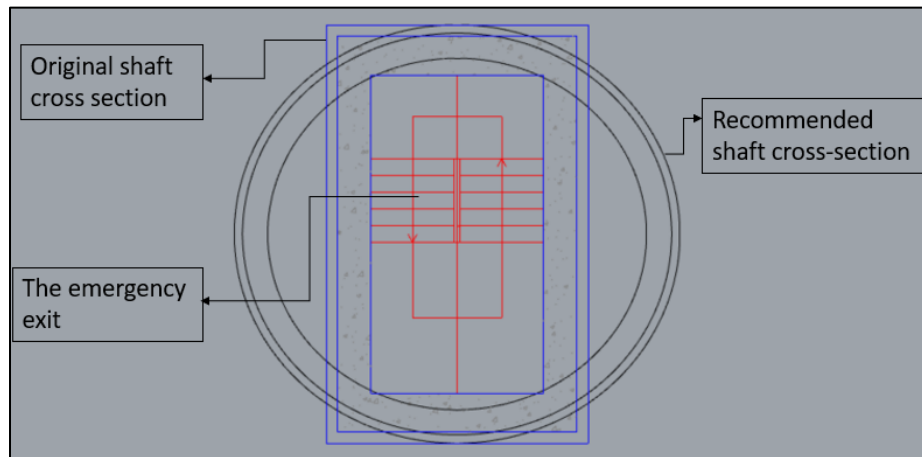


Figure 141 Original and recommended shaft cross-section type (b)

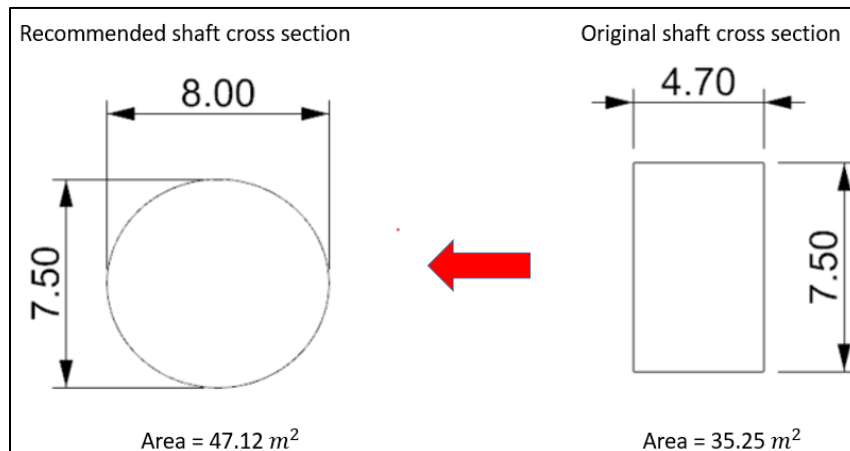


Figure 142 Original vs recommended shaft (b) model

7.2 Suggested model for the cross passages

Typically, cross passages are excavated following a horseshoe shape. Since excavation in rock is more stable, the cross-passage invert is cut off compared to a cross passage in soil. This project respects these conditions since the cross passage has a horseshoe shape. Still, the only concern is that the curvature of the crown of the cross-passage is very small “almost flat”, which leads to more concentration of the stresses on the crown and the sharp edges and corners. Furthermore, the small length of the cross passage between two intersection regions leads to high-stress concentration and significant extension of plastic zones and displacement distribution on the length of the cross passages, as obtained by the analysis of the original model in chapter five. Due to this, it has been found that increasing the crown's curvature reduces the concentration of the stresses, extension of the plastic zones and the radial displacement distribution along the length of the cross-passage in a significant way due to the arching effect.

Therefore, it has been decided to change the dimensions of the cross-passage to have better excavation conditions but considering that the functionality of the cross passages to comprise the ventilation chamber and the emergency exists is guaranteed.

- **Effect of changing the cross-section of the cross-passage on its functionality.**

1- Cross passage type (a):

As described in chapter three, part of the cross-Passage (a) will be for the ventilation chamber, and the other part to the emergency exits; figure (143) demonstrates that changing the shape and the area of the cross passage cross-section to the recommended one respects its functionality as well.

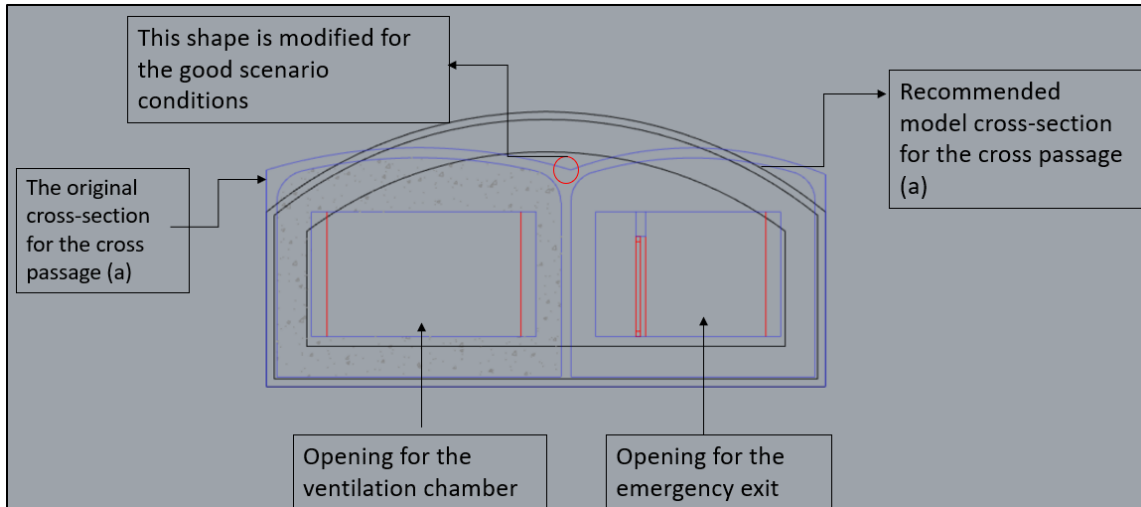


Figure 143 Original and recommended cross passage cross-section type (a)

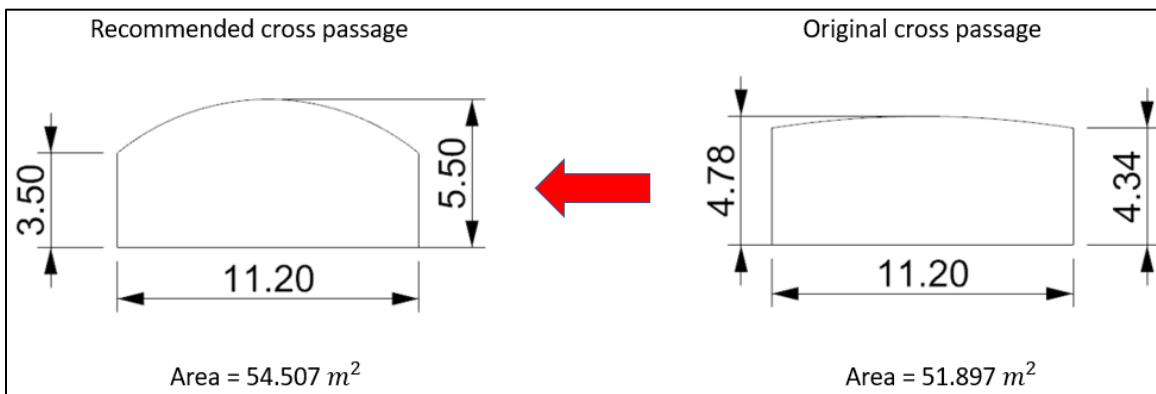


Figure 144 Original vs recommended cross passage (a) model

2- Cross passage (b)

As described in chapter three, the cross-Passage (b) involves only an emergency exists; figure (145) demonstrates that changing the shape and the area of the cross-section to the recommended one also respects its functionality.

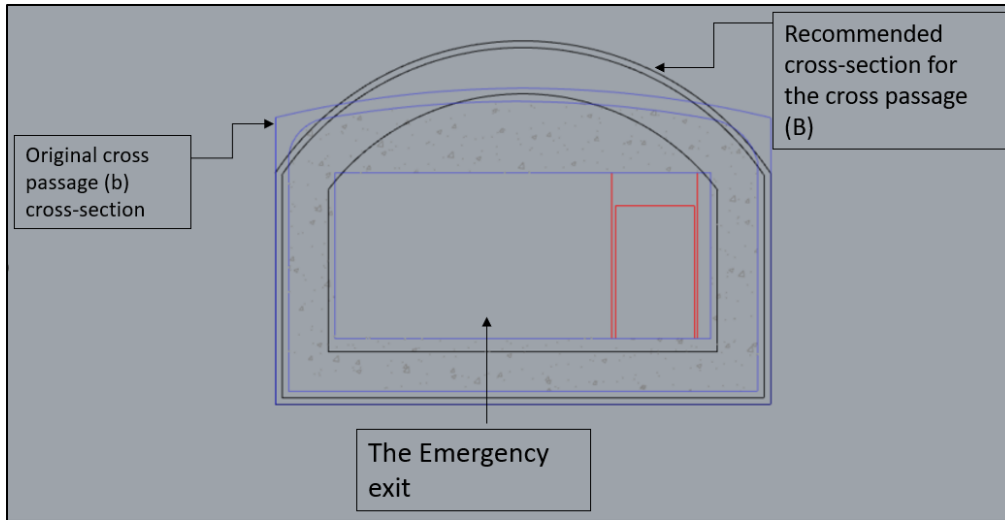


Figure 145 Original and recommended cross passage cross-section type (b)

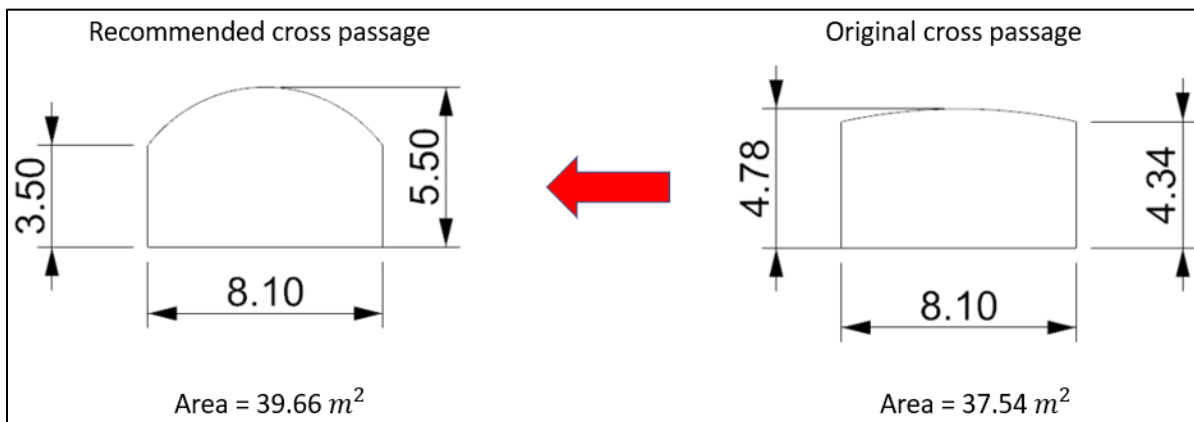


Figure 146 Original vs recommended cross passage (b) model

7.3 Analysis of the recommended model

The numerical modelling procedure regarding the geological model, material properties, constitutive laws, boundary conditions, the mesh setup & the initial field stress conditions is the same as the one introduced in chapter 5 section (5.2) for the original model. The only difference between the original model and the recommended one is the number of stages (the number of stages in the original model is 273 while for the recommended model is 283); this is due to the fact that the shape and the area of the shafts & cross passages are changed.

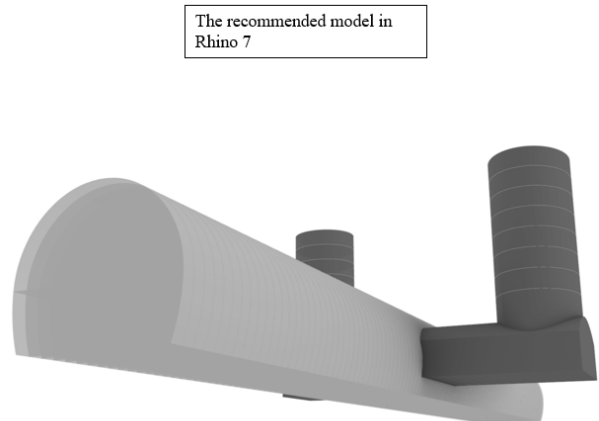
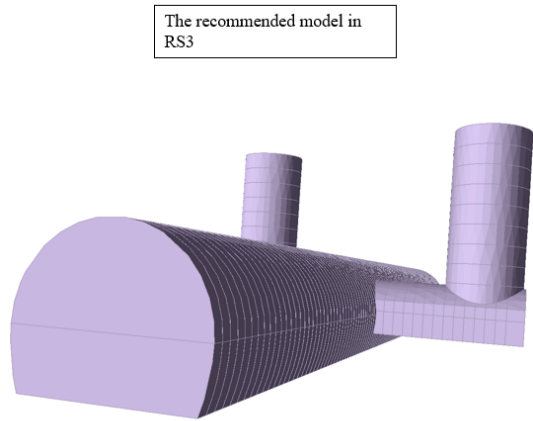


Figure 147 3D models in Rhino 7 & RS3

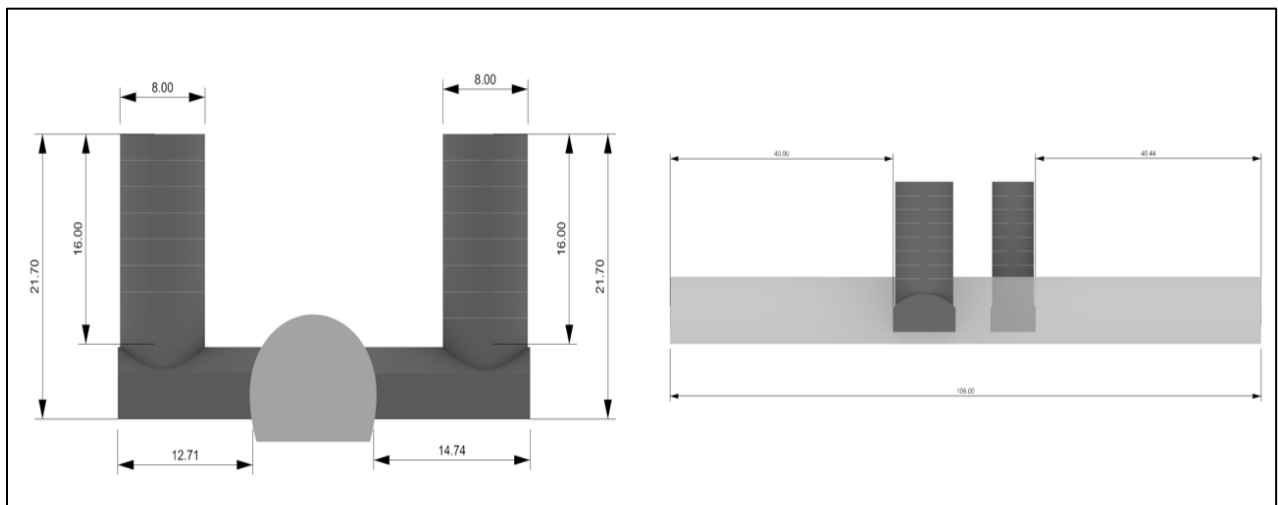


Figure 148 Transversal & longitudinal views for the intersection area

7.3.1 Staging (construction sequencing):

The construction sequencing is the same sequencing done with the original model:

- 1- The first stage is set for the geostatic or the initial condition.
- 2- Then starting from the second stage, the start of the top heading & bench excavation for the metro tunnel. The excavation length at each step in the construction was 1 m.

Before excavating the cross-passage type (a), the entire considered length of the metro tunnel (106 m) was excavated following the modelling stages (2-212).

- 3- From stage 213, the excavation of the cross-passage type (a) was started. The excavation length at each step in the construction was 1 m. Before beginning to excavate the vertical shaft type (a), the entire considered length of the cross passage (a) was excavated following the modelling stages (213-241).
- 4- From the ground surface, starting from stage 242 the excavation of the vertical shaft type (a) using the top-down full-face excavation method. The length of the excavation step was 2m can reach 3m in the mid of the length of the shaft. The entire length of the vertical shaft type (a) was excavated and the stages (242-250) in the model were used for this.
- 5- From stage 251, the excavation of the cross-passage type (b) from the tunnel was started. The excavation length at each step in the construction was 1 m. Before beginning to excavate the vertical shaft type (b), the entire considered length of the cross passage (b) was excavated following the modelling stages (251-274)

6- From the ground surface, starting from stage 275, the excavation of the vertical shaft type (b) using the top-down full-face excavation method. The length of the excavation step was 2m can reach 3m in the mid of the length of the shaft. The entire length of the vertical shaft type (b) was excavated and the stages (275-283) in the model were used for this.

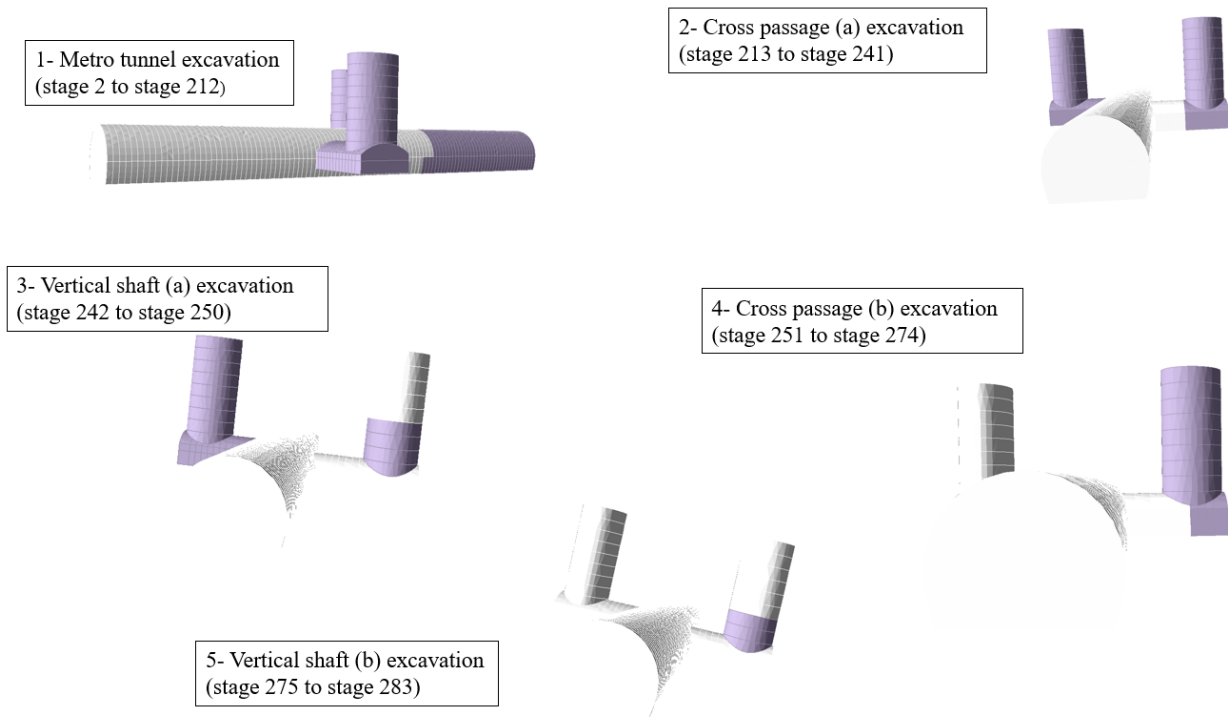


Figure 149 Model stages

7.4 Results

7.4.1 Initial state of stresses

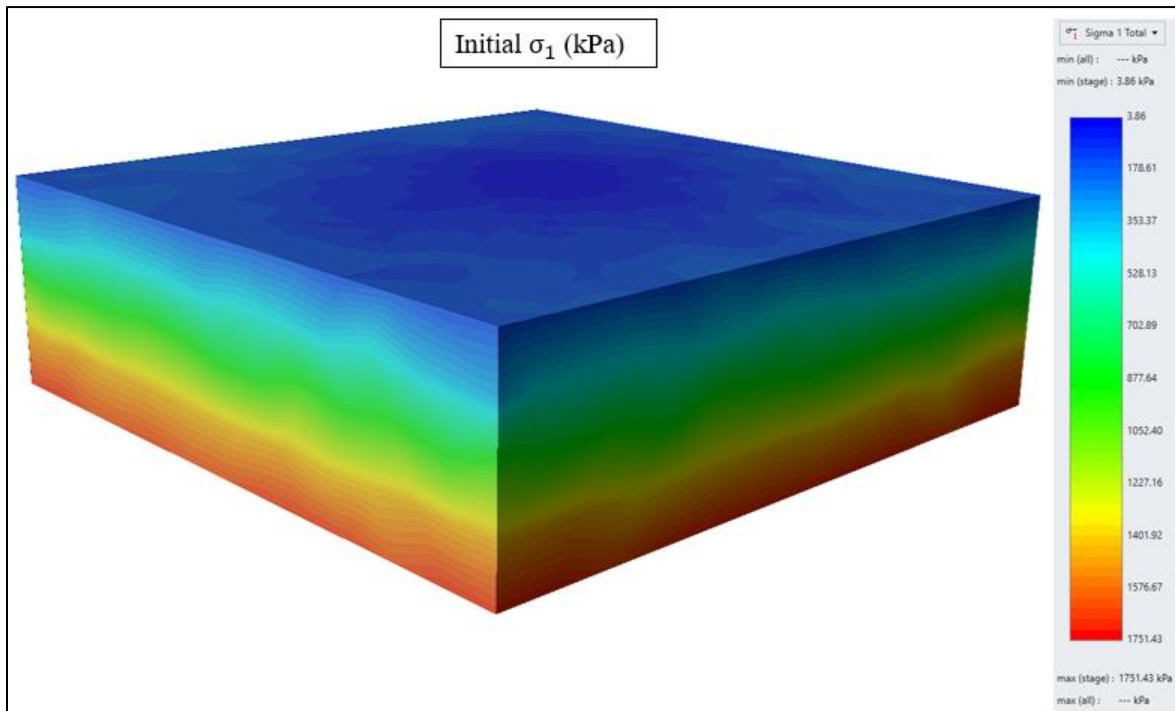


Figure 150 Initial in situ state of stress

Because of the application of the same conditions between the original & the recommended model, the trend of the initial in situ state of the stress is the same. Furthermore, since k_0 was set to 1, the other initial stress state follows the same previous trend. All the results of the stress state (σ_2 & σ_3) are attached to this thesis in the (Appendix) section.

7.4.2 state of stresses

During the construction of tunnel intersections, stress concentrations are a crucial matter of concern; one of the reasons to develop the recommended model is to reduce the stress concentration at the intersections, as well as at the shafts and the cross

passages crown. This section contains an illustration of the stress distribution at the end of the excavation (stage 283).

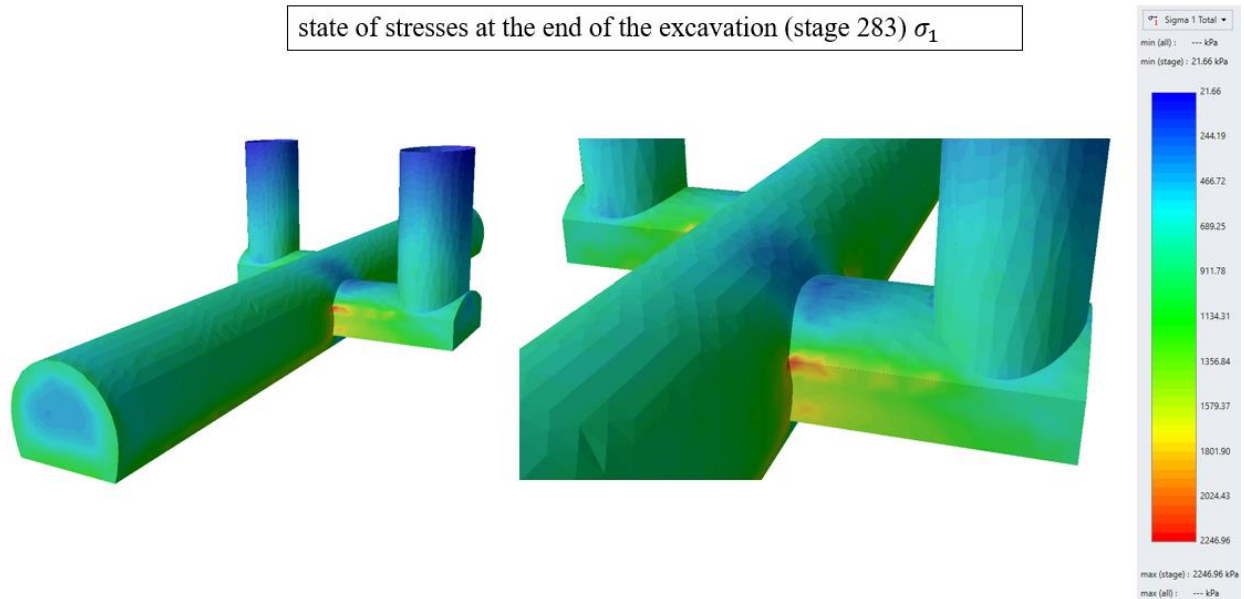
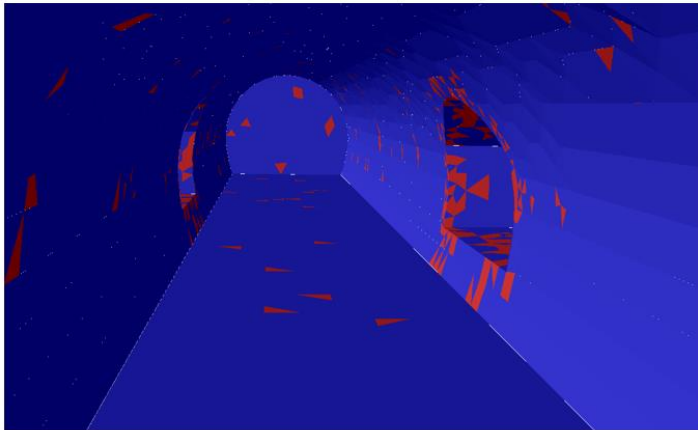


Figure 151 state of stress at the end of excavation (stage 283)

figure (151) shows the stress concentration at the cross passage\tunnel intersection. It is significantly lower than the one developed in the original model due to the more curvature at the crown of the cross-passage since the more circular excavation helped to control this phenomenon. Similarly, for the shaft\tunnel intersection, it can be clearly seen that there is a constant stress distribution at the intersection and close to it. In the original model, the rectangle shaft caused stress concentration along the shaft and the intersections.

7.4.3 Plastic zones

Plastic zones at the intersection of the tunnel\Cross passage from inside the tunnel



Top 3D view for the plastic zones

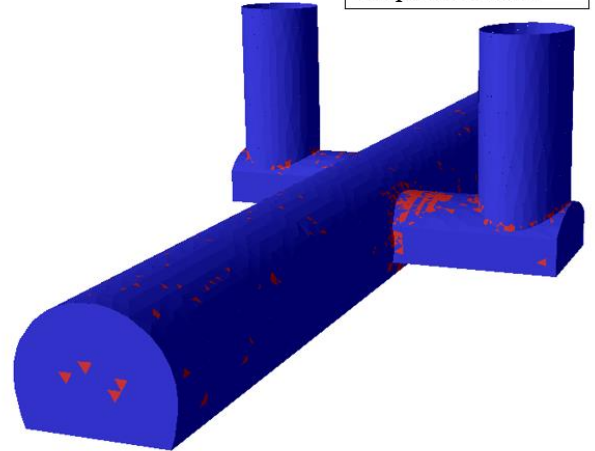
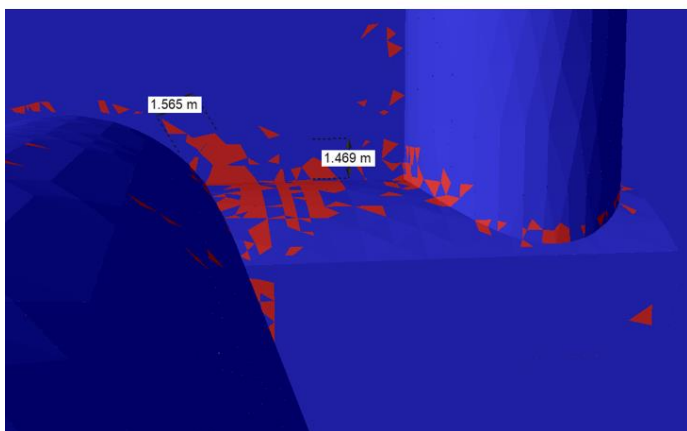


Figure 152 Plastic Zones overview

It can be clearly noticed the effect of the recommended shape regarding the development of the yielded elements, especially at the vertical shaft and at the intersection regions.

The extension of the plastic zone in the most critical area does not exceed 2m.



The Localisation of the yielded elements at the tunnel\cross passage intersection & cross passage\shaft intersection

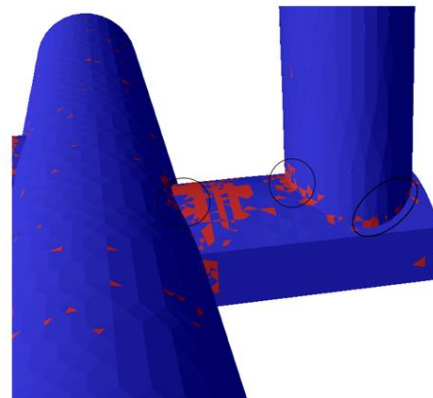


Figure 153 The extension of the yielded elements

The extension of the plastic zones is not exceeding 2m; this aspect was considered regarding the design of the length of the bolts pattern as primary support for the recommended model.

7.4.4 Transverse surface settlement trough

To introduce the effect of the excavation of the cross passages and shaft on the surface settlement, the results of the transverse surface settlement trough are shown at different stages.

1- At the end of the metro tunnel excavation (stage 212) (before the cross passage and shaft excavation)

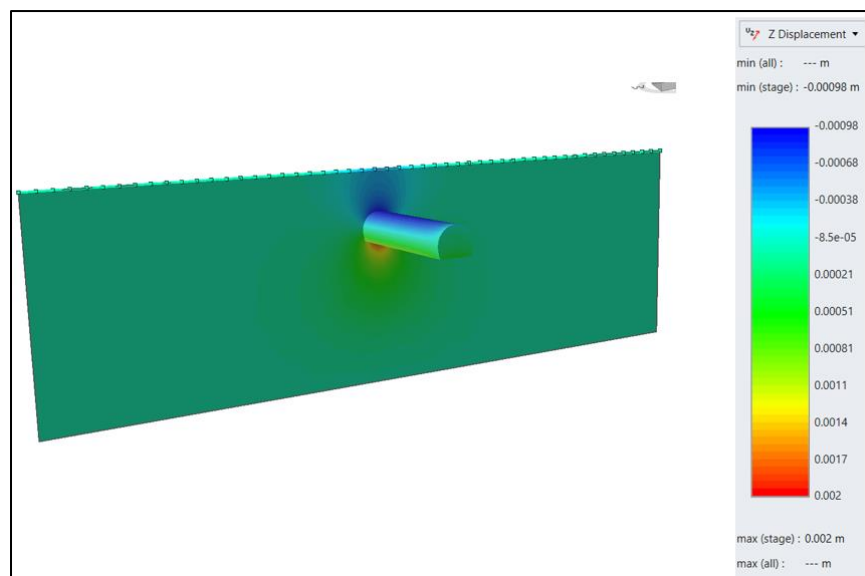


Figure 154 Transverse surface settlement trough

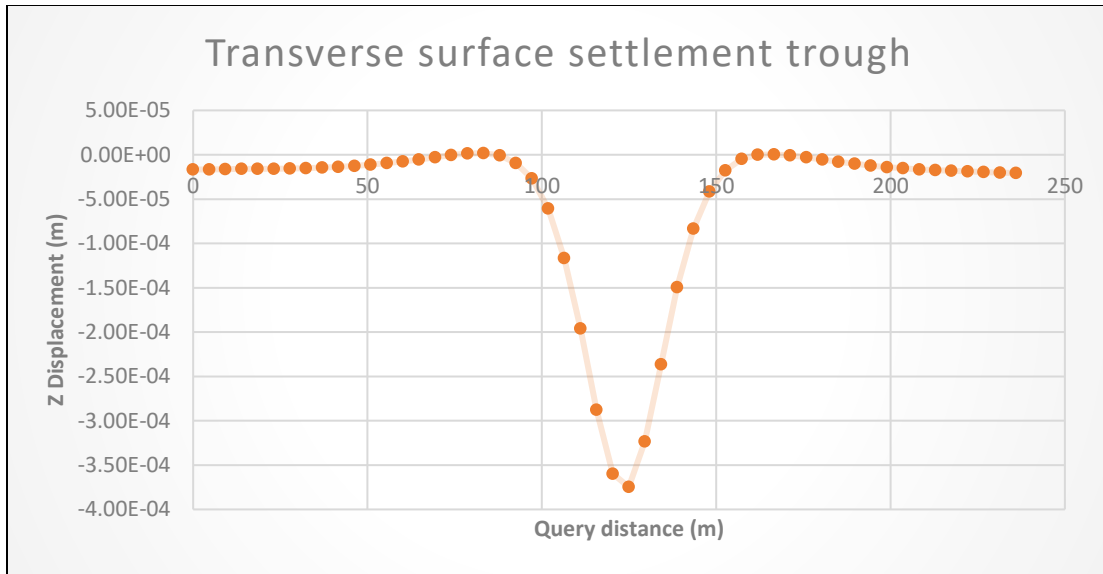


Figure 155 Displacement in Z-direction vs Query distance at the surface

From the above results, it can observe that the settlement at the surface is negligible (0.4mm), and it is the same results related to the original model.

**2- At the end of the excavation of the shafts & the cross passages
(considering section crossing between the cross passage (a) / shaft (a) &
cross passage (b) /shafts (b))**

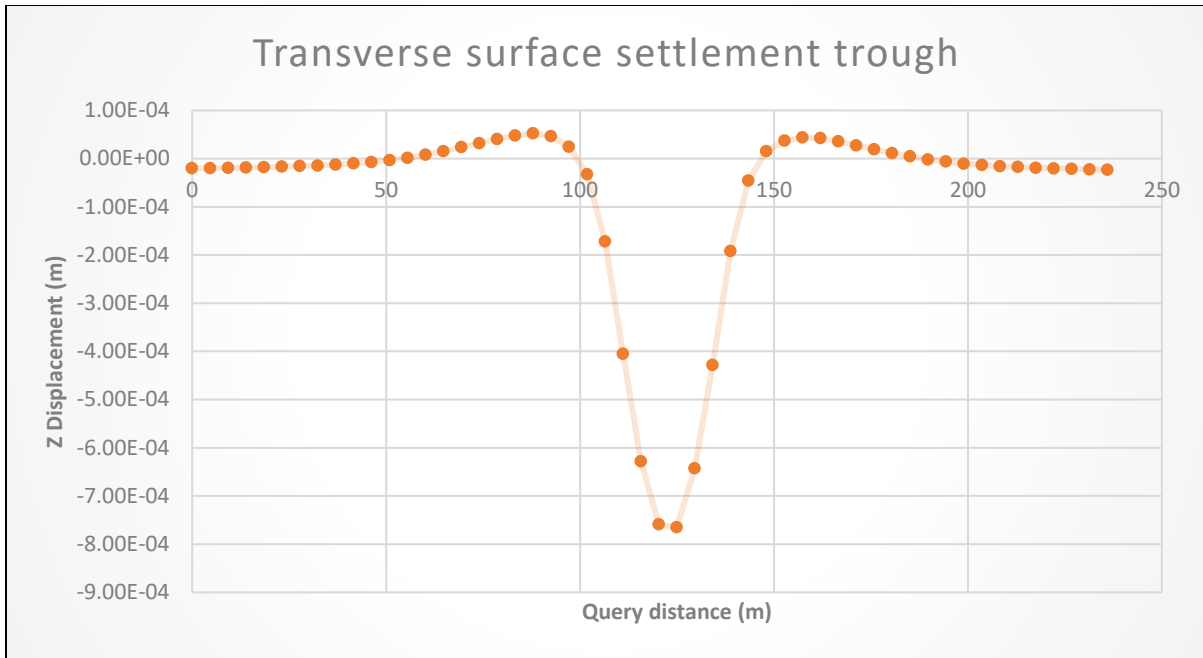


Figure 156 surface settlement at the end of excavation

Similarly, the results obtained from the original model, the maximum surface settlement could reach 0.9mm; therefore, as mentioned before, there is no concern about the surface settlement.

7.4.5 Total displacement

The total displacement due to the metro tunnel excavation is presented firstly at (stage 212), then, the effect of the cross-passage and the shafts are shown (stage 283).

1- At stage 212

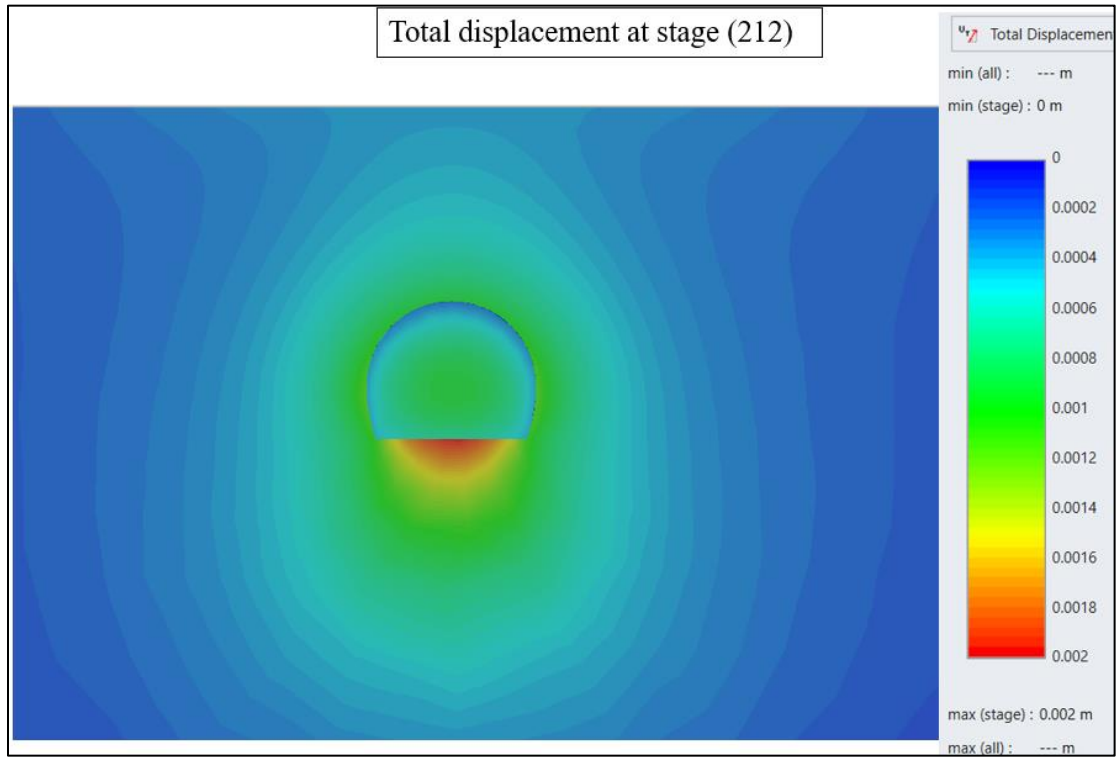


Figure 157 Total displacement 8stage (212)

The maximum total displacement is concentrated at the invert of the tunnel with a maximum value equal to 2 mm.

2- At the end of the excavation (stage 283)

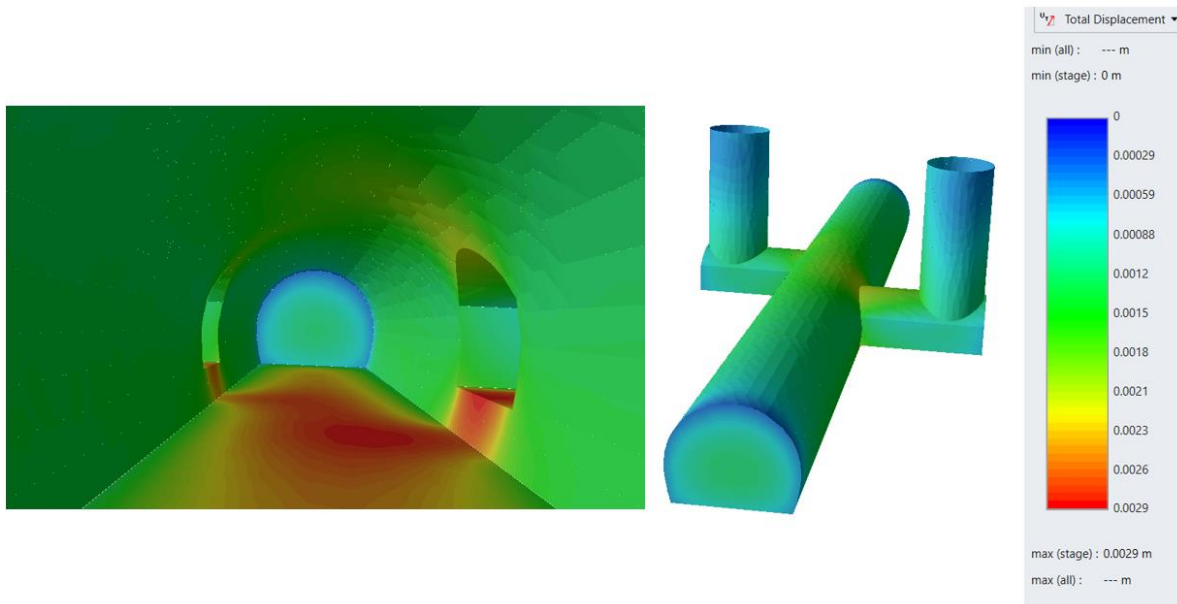


Figure 158 Total displacement stage 283

There is a significant effect of the recommended model regarding the distribution of the displacement at the intersections, as it can be clearly seen that the maximum values are localised only at the inverts of the tunnel and cross passages, where there is a trend of constant distribution along the shafts even at the intersection with the cross passage. The maximum values are pretty low considering the stratigraphy of the good Basalt, but the trend is lower in comparison with the original model.

3- At stage 283 considering 212 as reference stage:

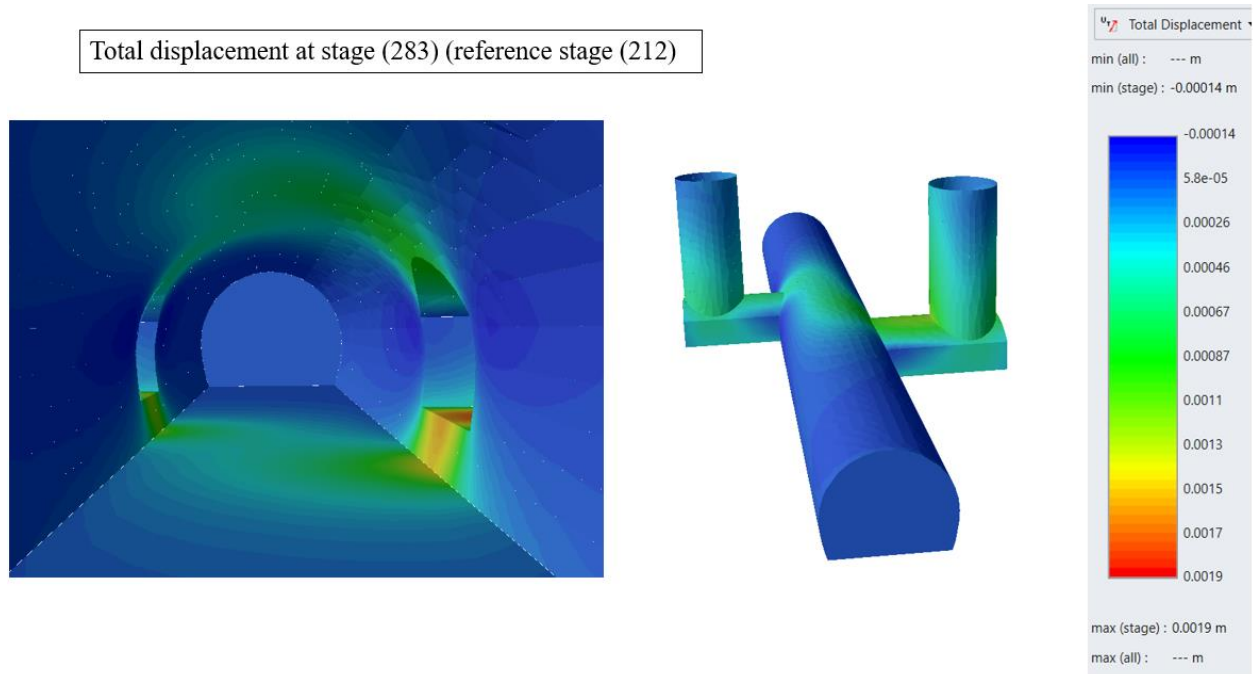


Figure 159 Total displacement (only the effect of the shafts & cross passages excavation)

The maximum total displacement is equal to 1.9 mm localised at the cross-passage (a) intersection with the metro tunnel and localised at the invert of the cross-passage length as well.

7.5 Design of the support for the structures for the recommended model

The primary support of the recommended model in the good scenario conditions, regarding the analysis without the support, depends on the extension of the plastic zones. The primary support that has been chosen is as follows.

1- For the cross passages & the tunnel at the intersection areas:

Bolts Fully Bonded	
Bolts diameter (mm)	25
Bolts modulus E (KPa)	3.50E+08
Tensile capacity (KN)	265
Residual tensile capacity (KN)	265
Length of the bolts pattern (m)	2.5
Spacing between the bolts (m)	1.5

Table 21 Bolts fully bonded properties for the tunnel & cross passages

Fibre-reinforced shotcrete	
Elastic modulus E (KPa)	1.50E+07
Poisson ratio (-)	0.2
Thickness (m)	0.1

Table 22 Fibre-reinforced shotcrete properties for the tunnel & cross passages

2- For the vertical shafts

Struts & shotcrete	
Young's Modulus (KPa)	1.5 E+07
Poisson's Ratio (-)	0.2
Thickness (m)	0.1

Table 23 Shotcrete Properties for the vertical shafts

7.5.1 Results

In this part, the results of the support system at the last stage are introduced.

❖ Bolts

Axial Force F_A :

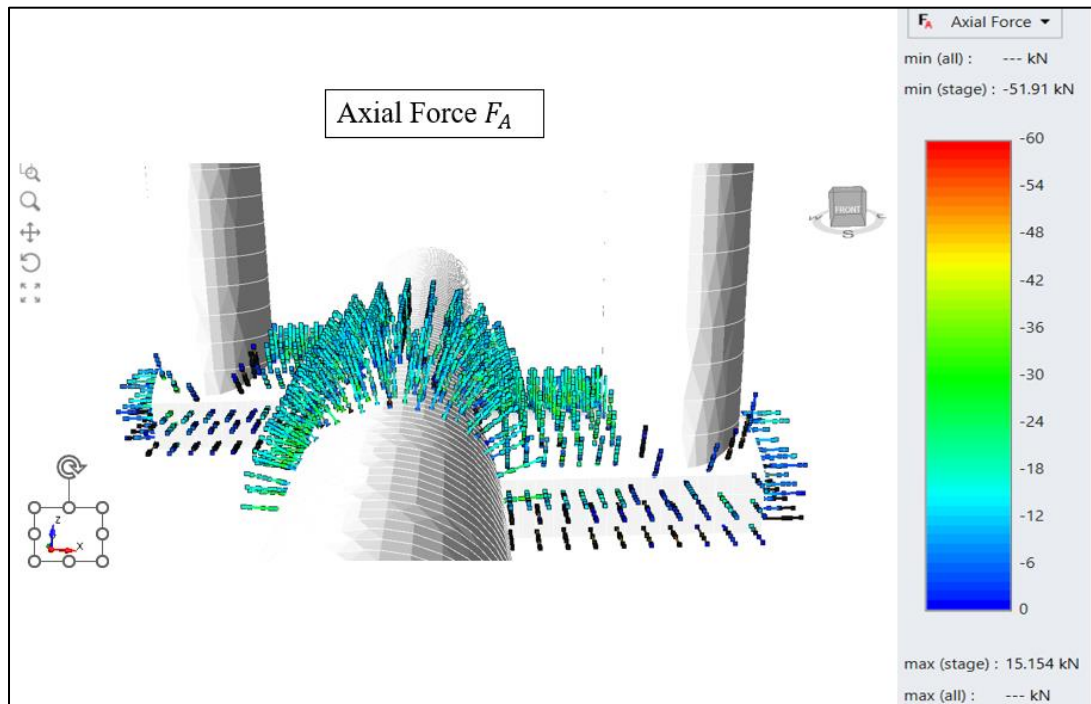


Figure 160 Axial Force F_A (bolts)

It can be clearly seen that the bolts are loaded with a maximum value of 50 kN, being the maximum values localised in the bolts near the intersections, and for the bolts far from the intersection; they are loaded by relatively low loads, and as mentioned before about the fully bonded bolts model, the stiffness of the grout and the strength and stiffness of the bolt/grout interface are taken into account. So, the failure mechanism of the bolt is by its tensile rupture, which is 265 kN. Therefore, the bolt pattern to support the cross-passage & the tunnel at the intersection areas in the good scenario conditions is accepted. The results of axial stresses are given in figure (161).

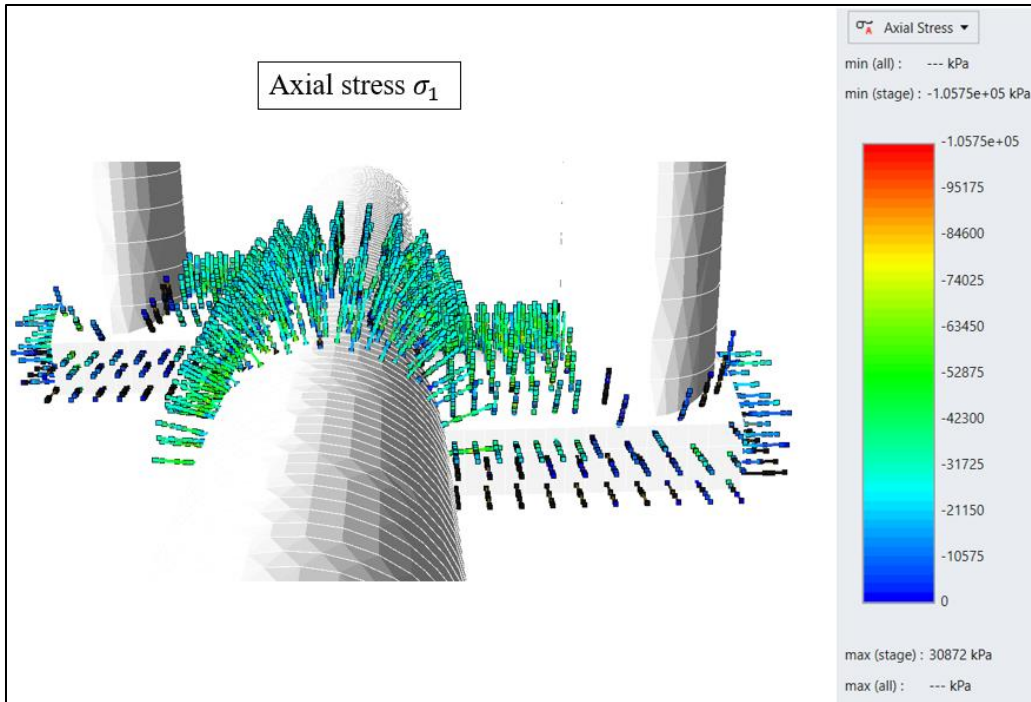


Figure 161 Axial stress (bolts)

❖ Results for the shotcrete on the shaft, cross passage & the tunnel:

- Displacement in X, Y & Z direction:

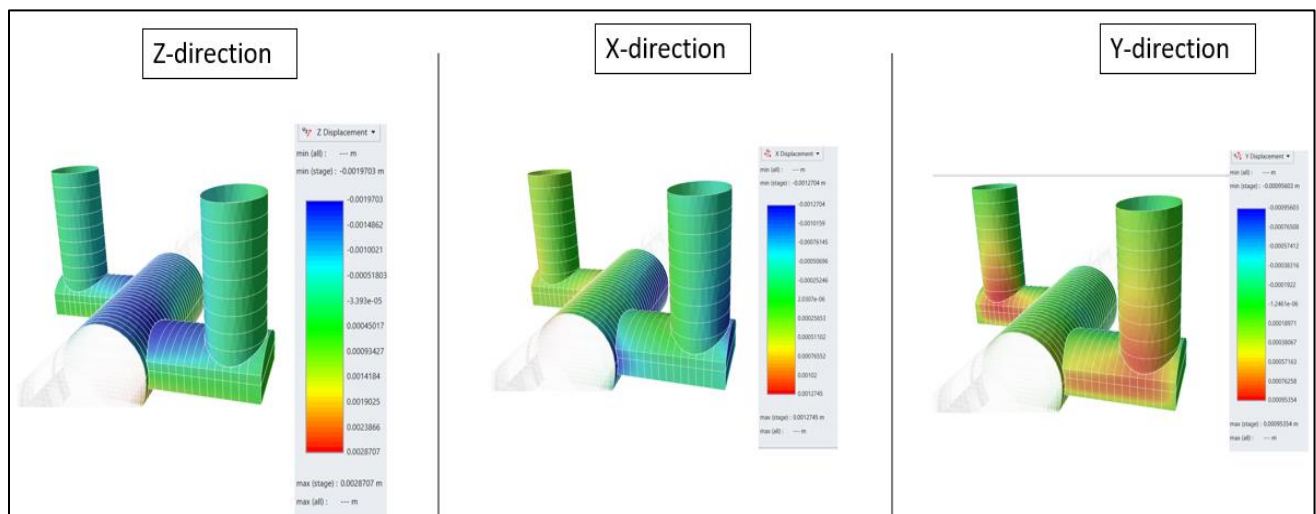


Figure 162 161 Displacement on (X, Y & Z)-directions for the shotcrete

The maximum displacement in X direction is equal to 1.27 mm on the shaft (a) and the tunnel, as shown in the in figure (162). In the Y direction the maximum value of 0.95mm on the shaft (a) &(b) and in the Z direction a value of 1.9 mm at the crown of the tunnel and the cross passages and 2.8mm at the invert of the tunnel and the cross passages are obtained. These results are acceptable, and the support system in good conditions is approved. All of the results are attached to this thesis in the appendixes.

Note:

It has been demonstrated that the recommended model is much more robust and can be supported more effectively. Indeed, this recommended model is distinguished for its ease of implementation and low costs thanks to the arch effect, the need for stabilising systems is considerably minimised in comparison with the original model. Furthermore, the analysis highlights that geometry is the most essential consideration in maximising this effect and making the structure more efficient.

❖ Visualization and Construction Sequencing

A visualisation of the final recommended 3D model has been performed to demonstrate the sequence of the work is logical and constructable in real life events. The method used is by using Building information modelling technology (BIM) which it has been adopted for the industry for the beneficial use of performing 3D visualised construction sequencing of projects at the early design stages, in this way defects could be recorded and fixed accordingly, in addition to the benefit of performing cost-benefit analysis of the available alternatives that could be used.

Starting from importing the 3D model from Rhino7 to Revit as shown in figure (163) using the “.3dm” format. Revit is a CAD and BIM program which allows design with elements of parametric modelling and drawing. Revit has been used as a platform to create simulation parameters that could be very helpful in automating the creation of simulation of construction. In Revit the tool of “project phases” has been used, phases are a great tool to filter elements by stages in a project. The phases defined in Revit software as illustrated in figure (164) respecting the construction sequencing staging that was described for the recommended model in section (7.3.1). Then the model was transferred to Navisworks using the Autodesk plugin in Revit.

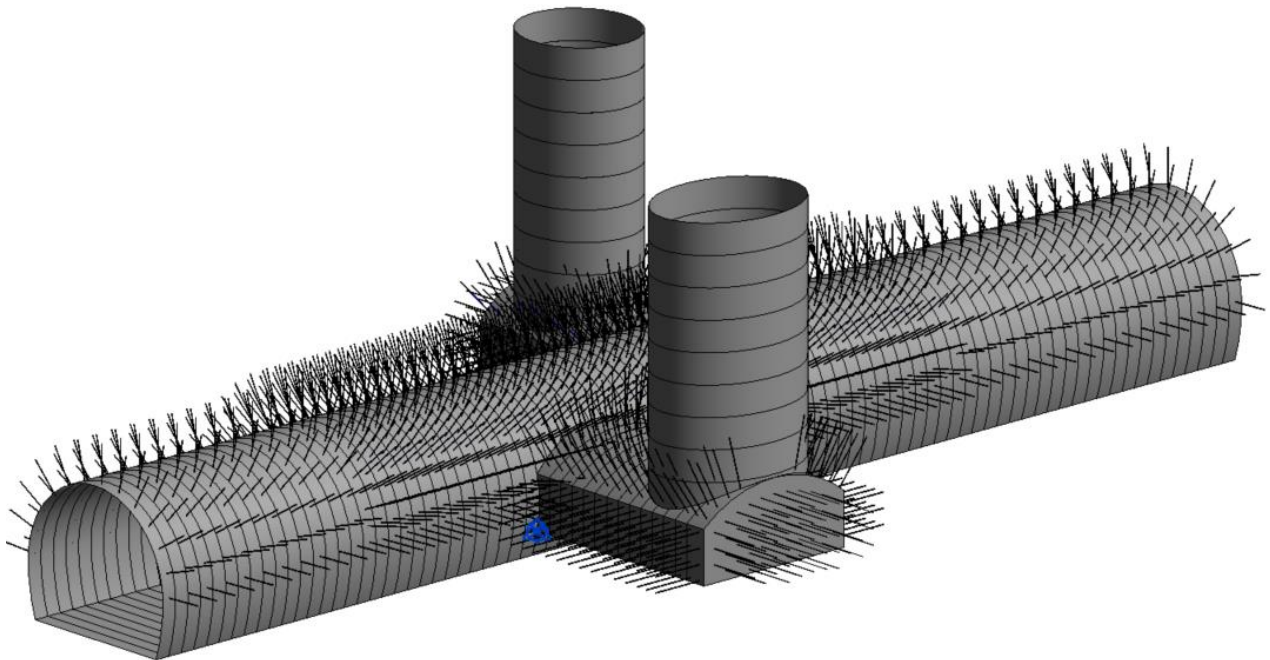


Figure 163 model in Revit

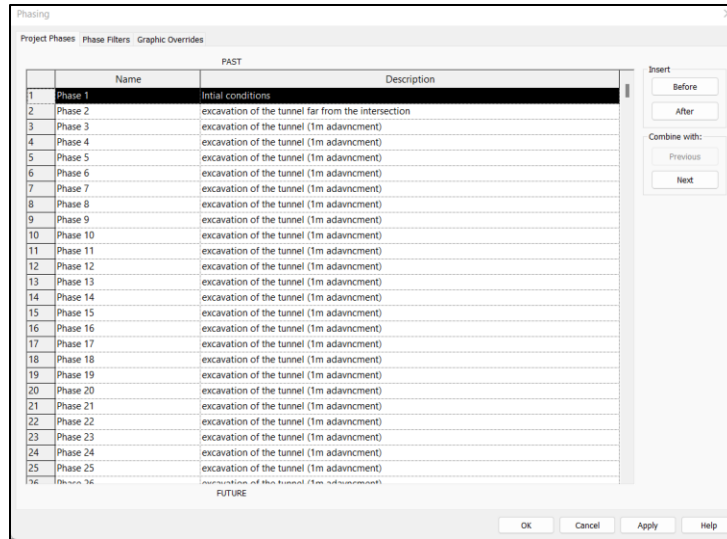


Figure 164 project phases in Revit

Moreover, Navisworks is a software responsible for creating a simulation of construction by allowing the users to open and combine 3D models, navigate around them in real-time and review the model using a set of tools including comments, redlining, viewpoint, and measurements. With the advantage of Autodesk integration, the project phases that were done in Revit were synchronised with the Navisworks; then, phases were connected to the imported Microsoft project file, which includes the same phases with assumed project scheduling. Eventually, by integrating the three components “Revit, Navisworks & MS project”, it was possible to visualise the construction sequencing of the project in Navisworks.

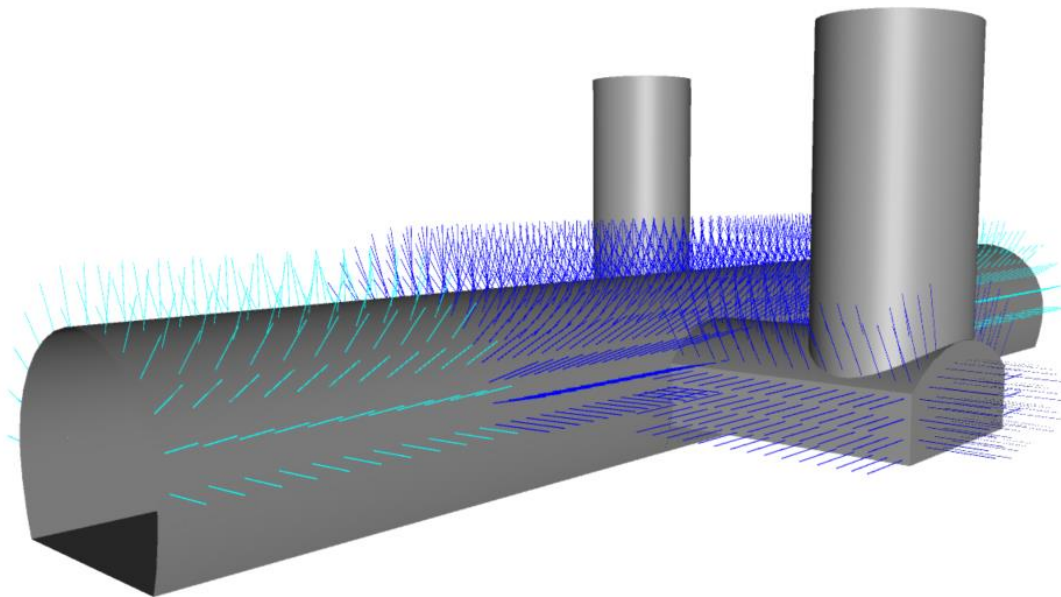


Figure 165 Model in Navisworks



Figure 166 Navisworks Simulation Video

Chapter 8: Conclusion and recommendations

This study was focused on the analysis of the intersection regions of a metro line tunnel that intersects with several ventilation\emergency shafts through cross passages. The following conclusions of the study may be drawn:

- 1- The metro line crosses different geological configurations; the favourable and the worst scenarios have been studied based on the geological conditions for the different intersection areas of the tunnel with cross passages & the shafts. The favourable scenario “section1” is related to the intersection positioned in a region where only a layer of shallow basalt is apparent. Whereas, for the worst scenario “section 2”, the intersection of the tunnel with the cross passage and the shaft is positioned in a region where a presence of a challenging geological formation characterised by the intersection of a thick layer of lava with a fragment pyroclastic rock and very fractured lava, moreover the presence of a loose sandy soil at the ground surface until depth close to the excavation boundaries makes this scenario particularly complex.
- 2- The problem in the intersection areas is a clearly three-dimensional. Therefore, the Finite-Element-Method (FEM) software RS3 (Rocscience,2022) was used to analyse the surface subsidence, the plastic zones of the surrounding rock mass, and the stress and displacement distribution induced by the construction at the intersection areas. Then, the suggested support systems were assessed and introduced.
- 3- The considered case study is in a preliminary design phase. Therefore, there are an absence of monitoring data and field measurements because the construction has not begun. Due to this reason, the analysis for a section of the metro tunnel near the intersection region was also done in 2D using RS2 software prior to starting the 3D analysis. The results of the 2D analysis (stress state, plastic zones, total displacement & the surface settlement trough) are compared to the 3D results at stage related to the end of the excavation of the metro tunnel and before the excavation of the cross passages and the shafts, to provide some validity and confidence for the 3D modelling results. The comparison between the 2D model & the 3D model showed that the results are quite close, which gives an indication of the validation of the all models.

- 4- For the good scenario “section (1)”, because of the presence of fair rock mass, the selected primary support for the stability of the metro tunnel and the cross passages are rock bolts with sprayed reinforced shotcrete. For the vertical shafts, the struts should be used as temporary support to stabilise the excavation with the sprayed reinforced shotcrete. Moreover, the excavation was first simulated in intrinsic conditions (without support) to examine the excavation stability and to indicate the extension of the plastic zones. The rock bolts' required length was chosen on the basis of the extension of the plastic zones. After designing the support system, the model was run again considering the mentioned support system, and then the verification of the support system was introduced.
- 5- For the worst scenario, the support system was selected in advance, and then its validity was introduced considering the 2D and 3D analysis results. The composite liner of steel sets and shotcrete for the stability of the tunnel and the cross passage was used. Moreover, the micro piles were suggested to stabilise the excavation of the shafts in addition to the shotcrete until the installation of the final lining. These choices turned out to be the best in terms of safety and costs for the stability of the considered underground structures at the intersections.
- 6- The designed support system must be applied to the whole length of the cross passages and the shafts. Whereas for the metro tunnel the designed support system is considered as heavier support at the intersection than the normal tunnel section “which a reduced support system could be used”, therefore the designed support system should be applied at least in a range equal to 1D of the metro tunnel from both sides from the centre of the tunnel\cross passage intersection.
- 7- From the analysis, it has been confirmed that the stress concentration and plastic zones around the boundaries of the intersections and their surroundings are incredibly significant to other areas. However, based on the analysis for both favourable and worst scenarios, it has been realised that there are no concerns about the settlement at the surface even after excavating the shafts and the cross passages. This aspect is due to the presence of the good rock (Lava and Basalt layers), which prevents the occurrence of a significant settlement at the surface.
- 8- Eventually, the considered project uses rectangular shafts and horseshoe-shaped cross passages with a slight curvature at the crown. This thesis

presented the possibility of using a recommended shapes for the shafts and the cross passages by using elliptical shafts and a more curved horseshoe shape for the cross passages, which helped to reduce the stress concentration and the total displacement at the excavation boundaries as well as decreases the disturbance in the surrounding strata. These recommended models are much more robust by utilising the arch effect; consequently, the need for stabilising systems is considerably minimised compared to the original model; therefore, the recommended models are anticipated to behave better, leading to a more economical solution for the project.

❖ **Based on the obtained results, the following recommendations could be drawn:**

- 1- Further investigation about the characteristics of discontinuities in a rock mass is fundamental for evaluating potential detachable blocks. A geo-structural survey devoted to a systematic and quantitative description of rock discontinuities is crucial to understanding the stability conditions of the Basalt in the considered project, by modelling the rock mass as a discontinuum.

In order to analyse the stability of rock blocks which could fail in the tunnel, the LEM (limit equilibrium method) could be used, implemented in a code like UNWedge (Rocscience); the program identifies wedges formed by the intersected joints and calculates the resulting factor of safety and required support pressure to achieve the design factor of safety (examples in Figures 1 and 2). Then is possible to compare the global factor of safety when assuming the medium equivalent continuum with those related to the discontinuum analysis. The global factor of safety could be obtained by performing a shear strength reduction (SSR) analysis using RS3. Indeed, in the preliminary design phase of the project, the only way to reduce the uncertainties and the design errors is by performing various analyses using different tools and methods, then comparing and interpreting the results, which lead eventually to the correct and best choices.

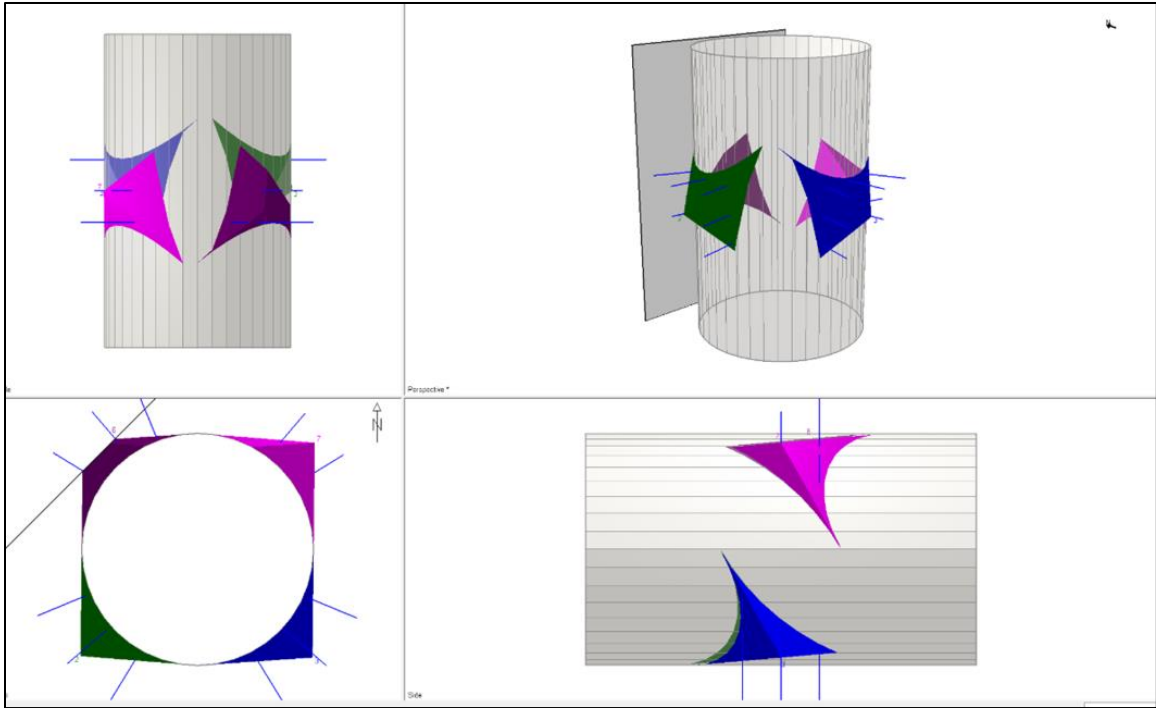


Figure 167 Example of the stability of wedges on a vertical shaft using UnWedge code (SF from LEM)

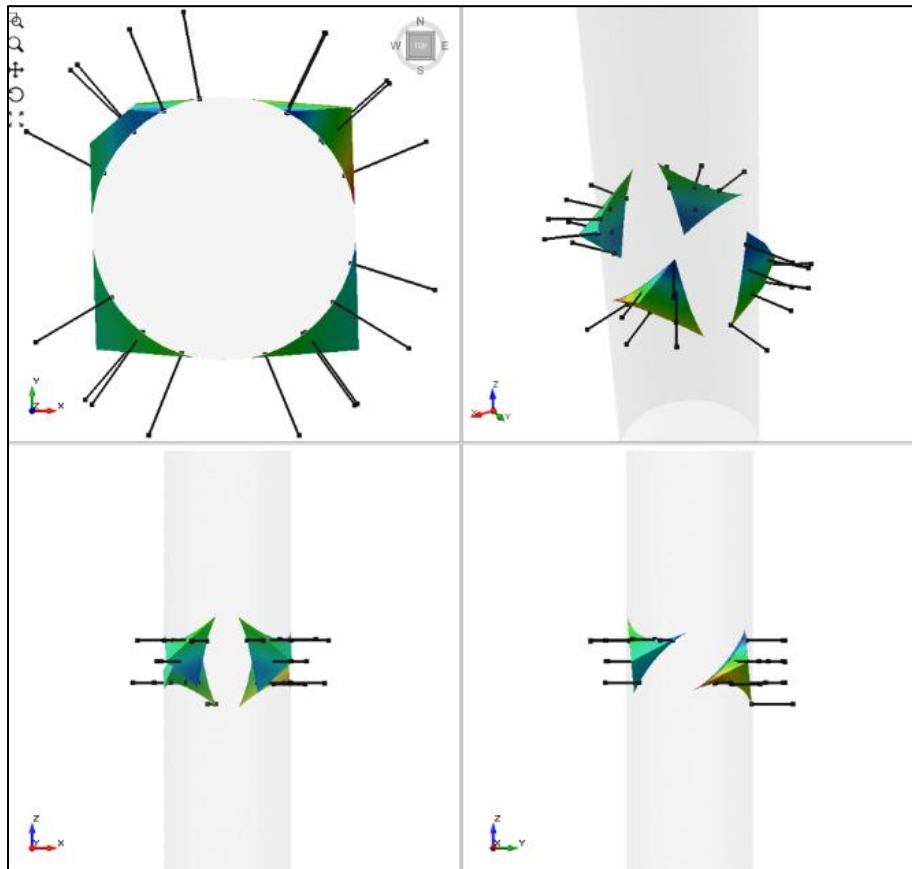


Figure 168 Example of the stability of wedges on a vertical shaft using RS3 software (SF from SSR method)

2- The results obtained from this thesis could be considered trigger values with an acceptable probability that the actual behaviour will be within these limits. Trigger values which are a synonym for “hazard warning levels” or “response levels”, are a common way in geotechnical engineering to show the actual behaviour of the structure in a comparison of what was predicted from pre-calculations. Therefore, a monitoring plan shall be devised to reveal whether the actual behaviour lies within the acceptable & predicted limits. The monitoring shall make this clear at a sufficiently early stage during the construction and with sufficiently short intervals to allow contingency actions to be undertaken successfully (the observational method). Furthermore, for the intersection areas, it is fundamental to introduce loads and pressure cells at the structural elements (rock bolts, steel sets, shotcrete) to evaluate the load and the pressure. Moreover, extensometers could be used to assess the relative displacement, especially for points near the intersection areas. As well as it is important to use radar technology or similar techniques to monitor the displacement at the ground surface, and the settlement of the building due to the underground construction work. The monitoring and field measurement data must be compared with the predicted behaviours, and the design must be reviewed if necessary.

3- Cost analysis could be performed for the recommended and the original models to demonstrate the difference in time and costs between the two models.

In this thesis, a model was developed in Navisworks software (Autodesk) to simulate the construction sequencing of the recommended model; this model could be improved to contain the accurate project scheduling and costs in terms of construction and support systems. This strong tool based on the building information modelling (BIM) could be used to do the cost analysis in addition to perform a comparison between recommended model and the original model using the visualization. These digital simulations could be introduced to the clients to easily and more clearly emphasise the priority of the recommended models for the shafts and cross passages on the original ones.

References

- [1] L. Zdravkovic, "Editorial: Tunnelling in the urban environment," *Geotechnique*, vol. 67, no. 9. ICE Publishing, p. 747, Jun. 01, 2017. doi: 10.1680/jgeot.2017.67.9.747.
- [2] G. Mollon, D. Dias, and A.-H. Soubra, "Face Stability Analysis of Circular Tunnels Driven by a Pressurized Shield," *Journal of Geotechnical and Geoenvironmental Engineering*, vol. 136, no. 1, pp. 215–229, Jan. 2010, doi: 10.1061/(asce)gt.1943-5606.0000194.
- [3] N. M. A. S. David Chapman, *Introduction to Tunnel Construction*. 2017.
- [4] P. Gary B. Hemphill PhD, "PRACTICAL TUNNEL CONSTRUCTION," 2013.
- [5] Z. Song, Q. Liu, Y. Zhang, X. Tian, and G. Zhou, "Analysis on the Influence of Shaft and Cross Passage Turn to the Main Line of Ingate under Different Construction Schemes," *Advances in Civil Engineering*, vol. 2021, 2021, doi: 10.1155/2021/6662489.
- [6] F. Y. Hsiao, C. L. Wang, and J. C. Chern, "Numerical simulation of rock deformation for support design in tunnel intersection area," *Tunnelling and Underground Space Technology*, vol. 24, no. 1, pp. 14–21, Jan. 2009, doi: 10.1016/j.tust.2008.01.003.
- [7] H. liang Liu, S. cai Li, L. ping Li, and Q. qing Zhang, "Study on deformation behavior at intersection of adit and major tunnel in railway," *KSCE Journal of Civil Engineering*, vol. 21, no. 6, pp. 2459–2466, Sep. 2017, doi: 10.1007/s12205-017-2128-y.
- [8] "User's manual of PLAXIS," 2014.
- [9] T. , P. A. V. and P. G. B. Schanz, "The hardening soil model: formulation and verification," 1999.
- [10] E. Hoekt and E. T. Brown~, "Practical Estimates of Rock Mass Strength," 1997.
- [11] G. Anagnostou and K. Kov~ri, "TUNNELS AND DEEP SPACE Face Stability Conditions with Earth-Pressure-Balanced Shields," 1996.
- [12] C. Carranza-Torres and M. Diederichs, "Mechanical analysis of circular liners with particular reference to composite supports. For example, liners consisting of shotcrete and steel sets," *Tunnelling and Underground Space Technology*, vol. 24, no. 5, pp. 506–532, Sep. 2009, doi: 10.1016/j.tust.2009.02.001.

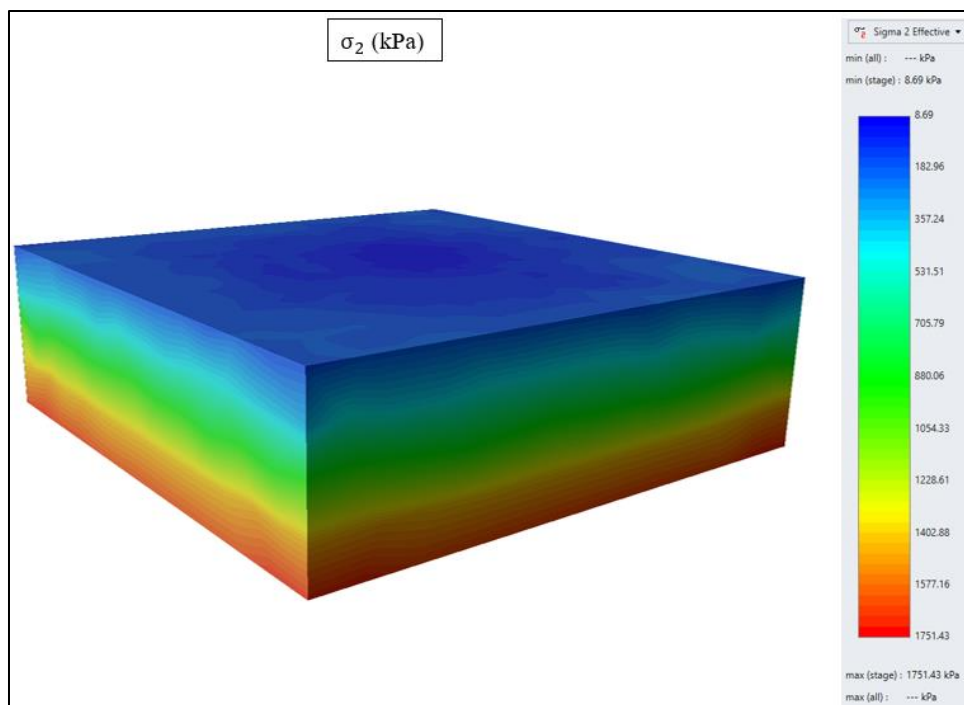
Appendix

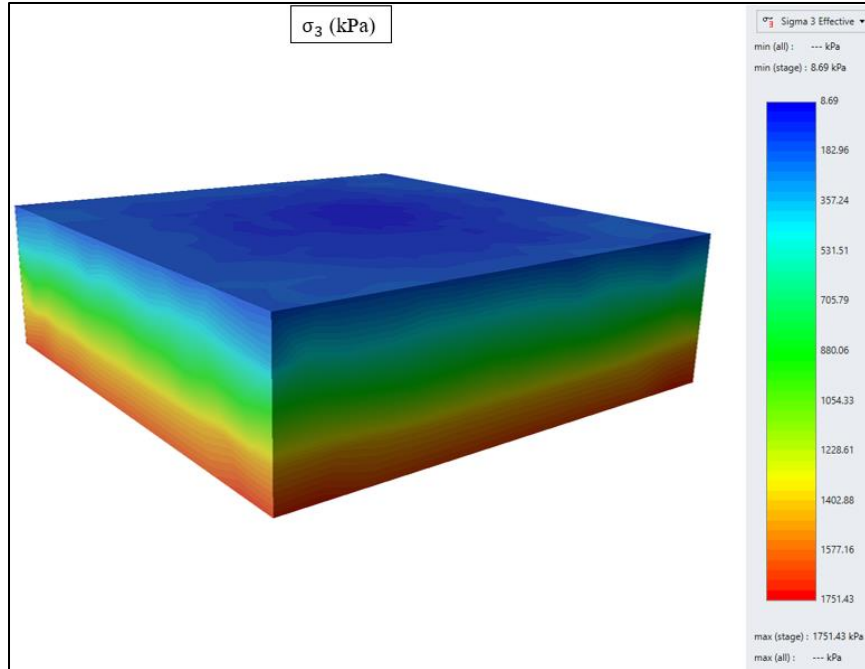
This section includes the results that were not presented in the analysis chapters (5, 6 and 7)

❖ Results related to the favourable scenario “section 1”

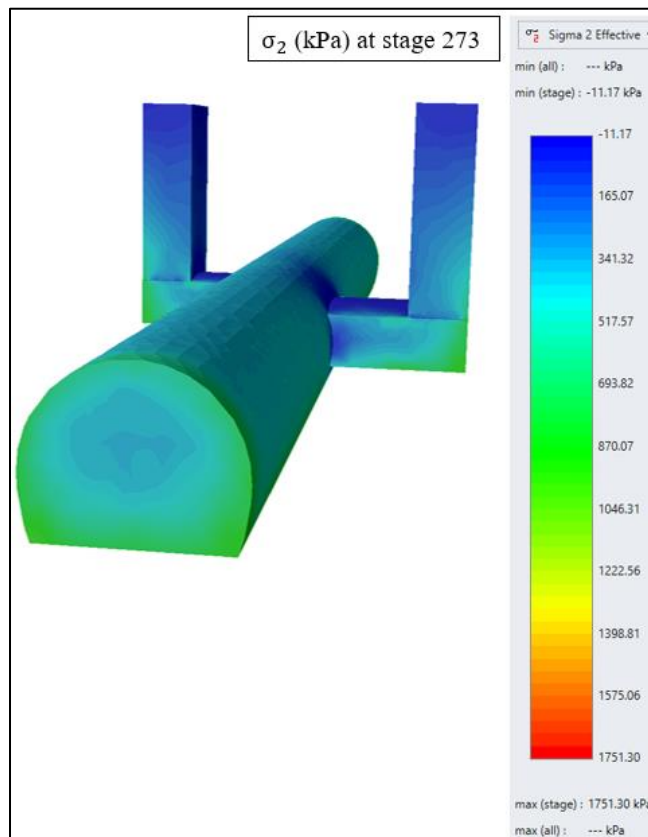
a) Original model

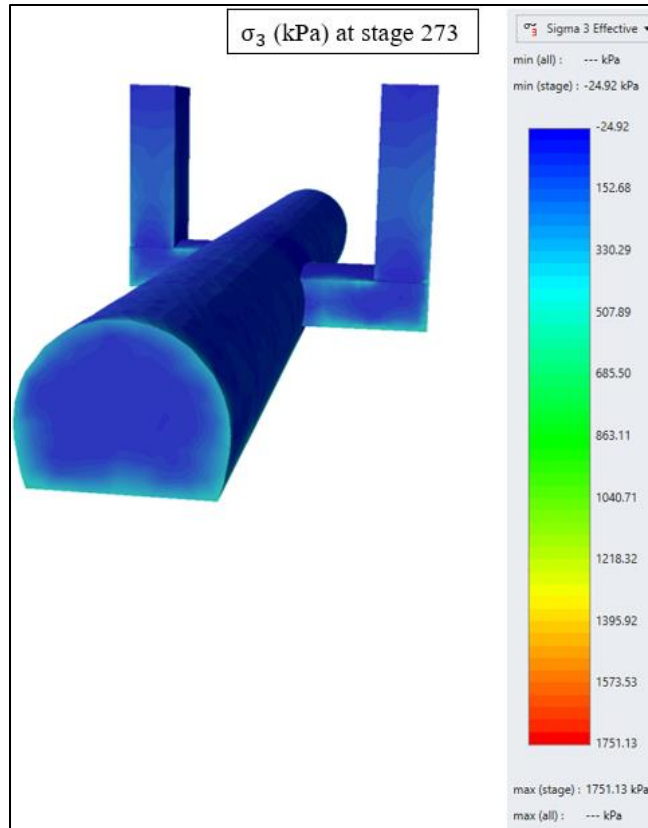
1- Initial stress state



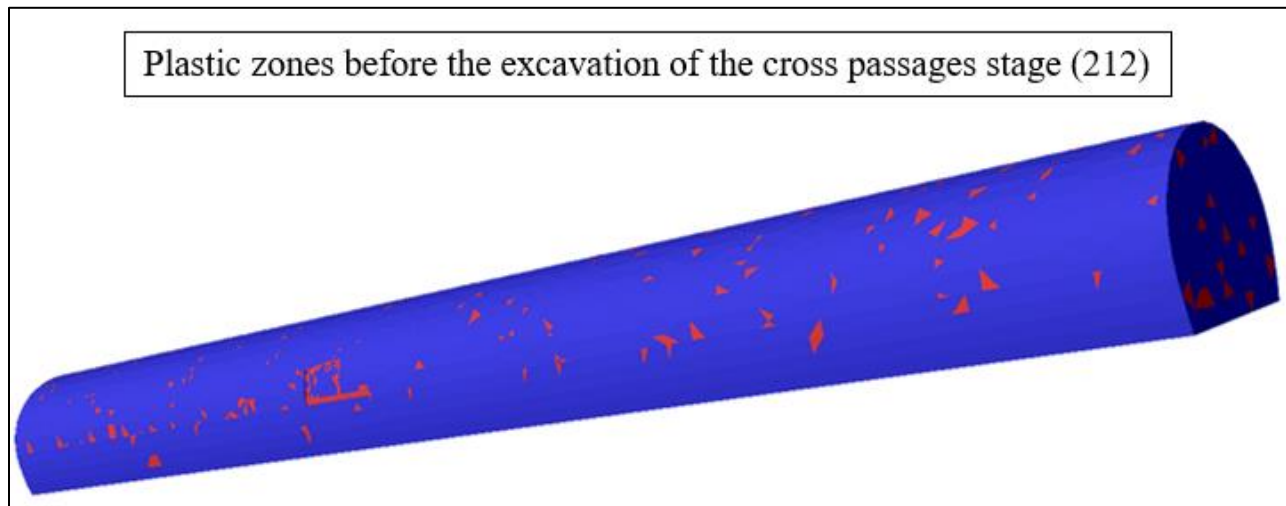


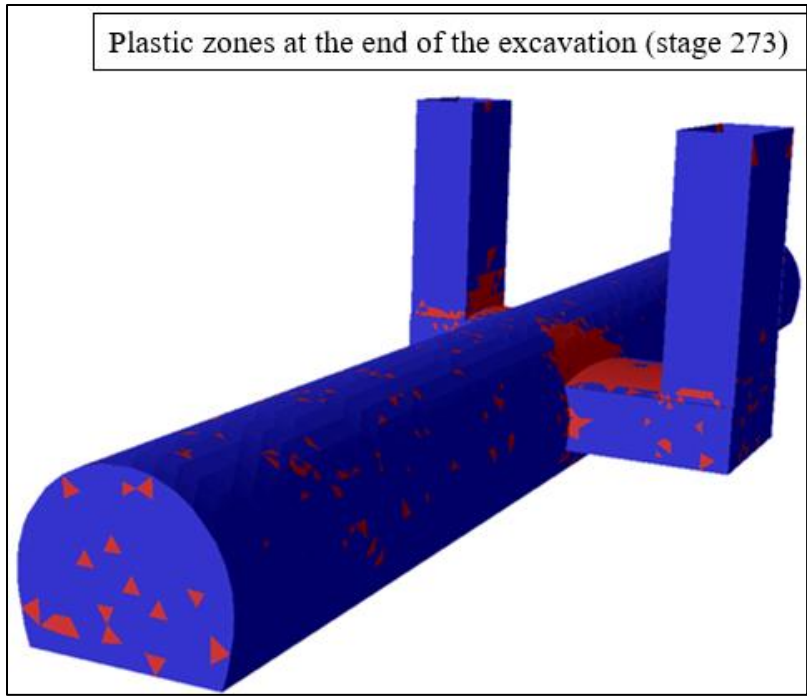
2- Stress state at the end of the excavation





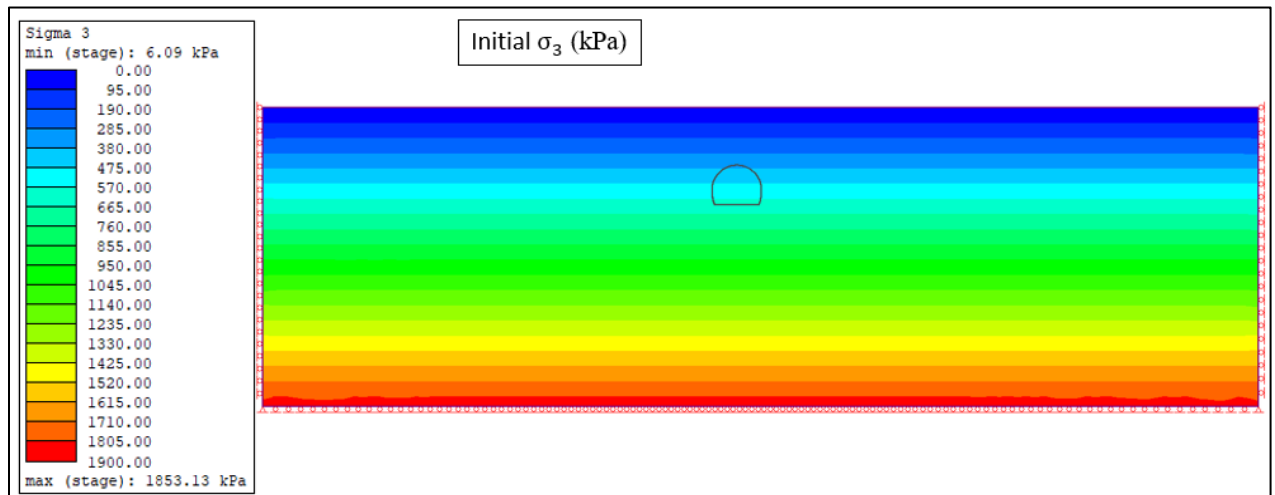
3- Plastic zones

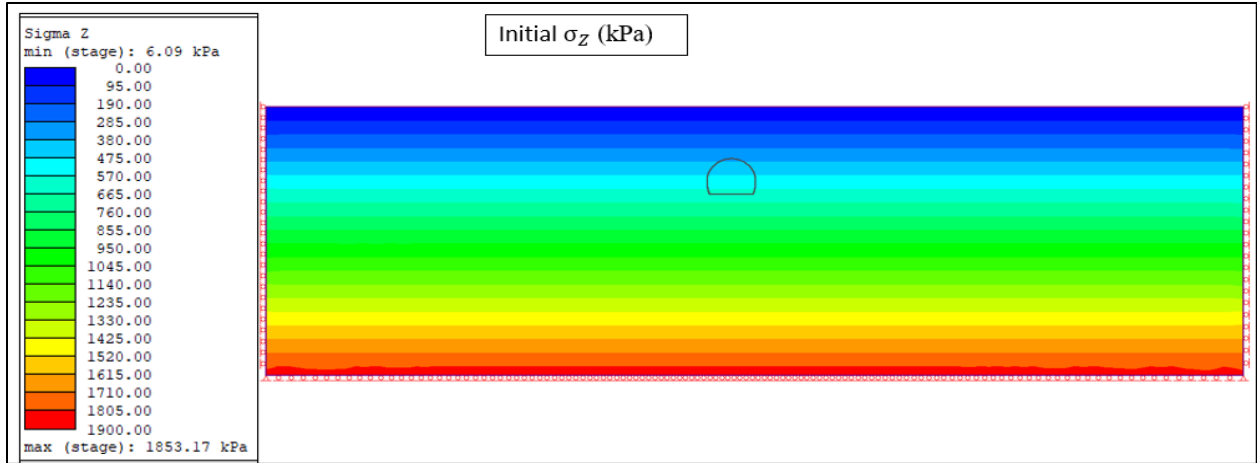




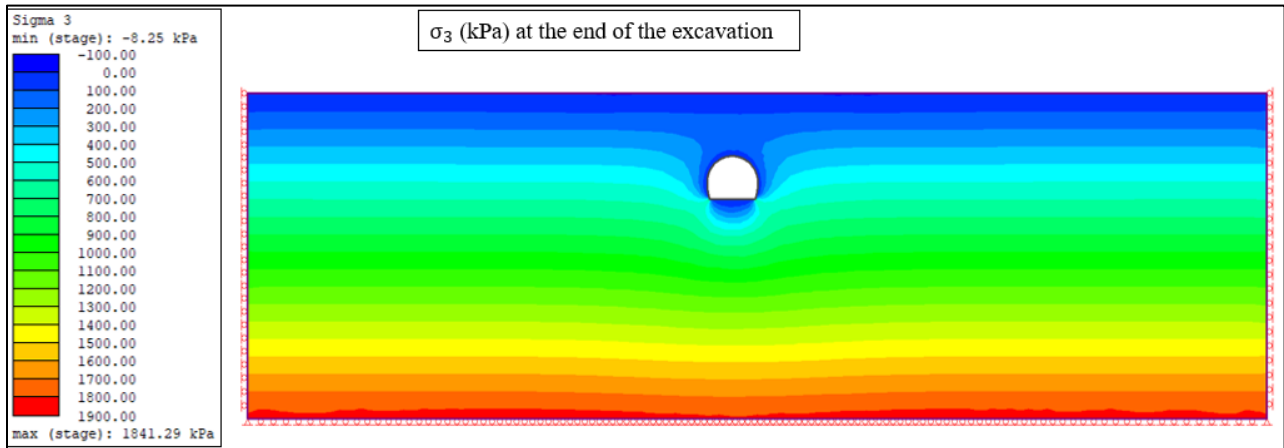
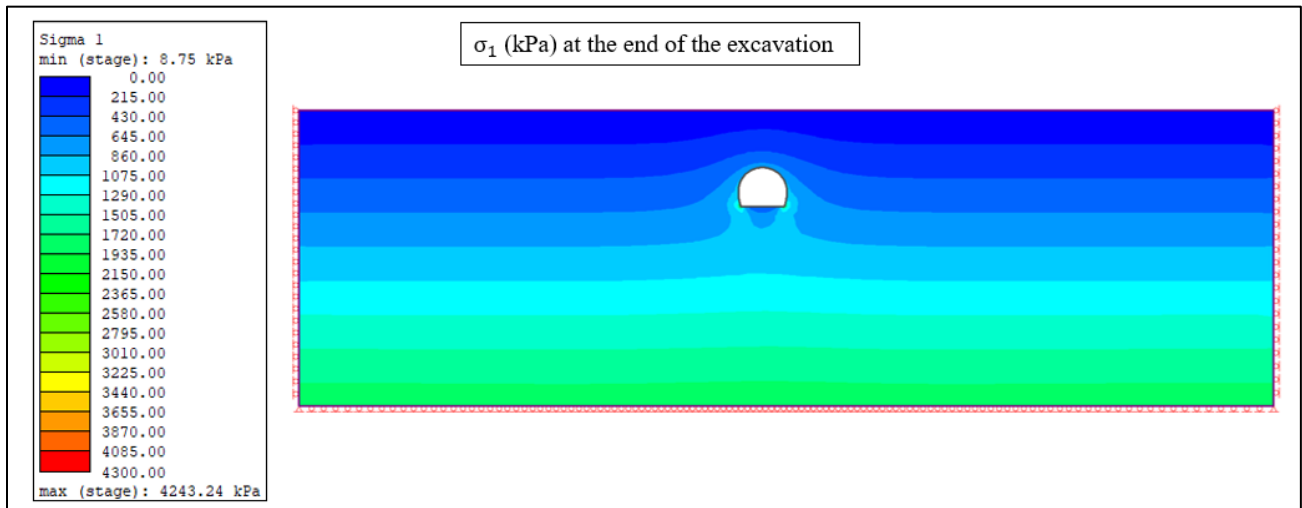
b) The 2D model for tunnel section near to the intersection

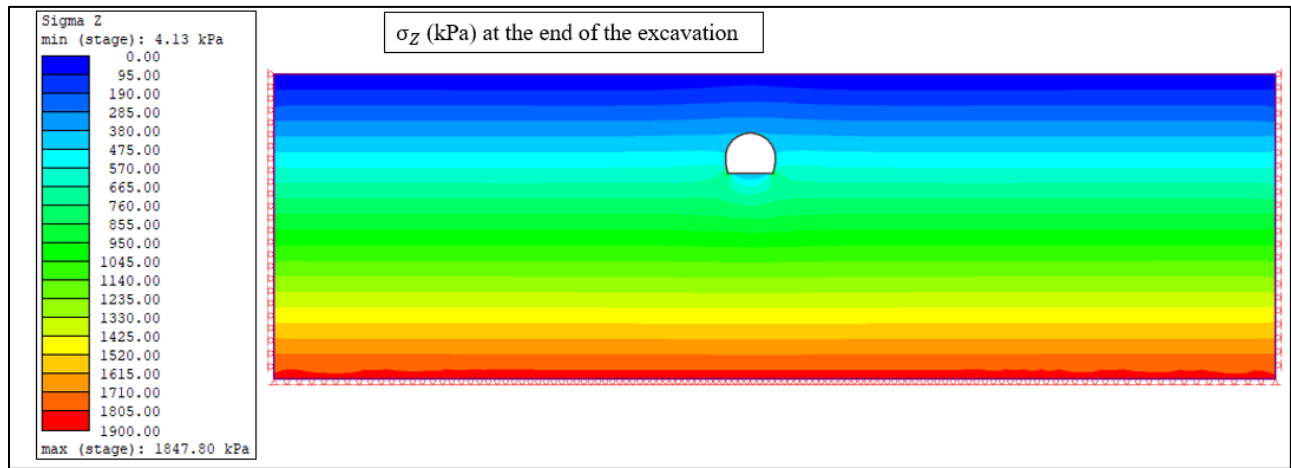
1- Initial stress state





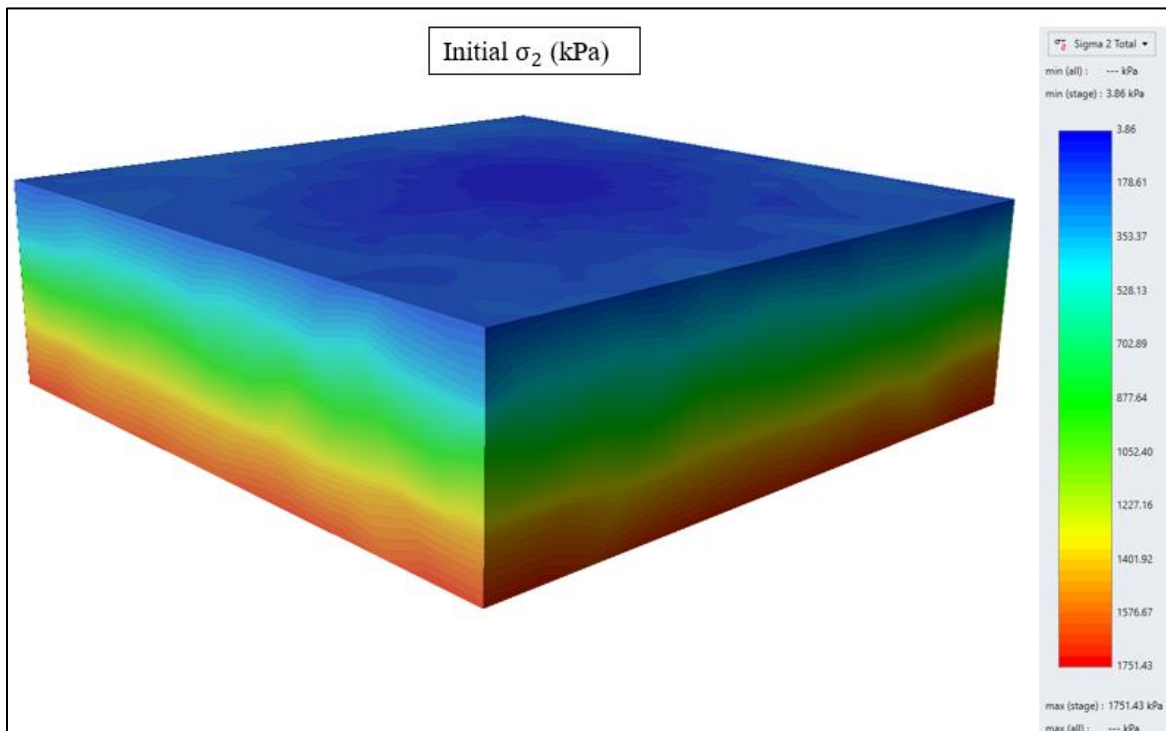
2- Stress state at the end of the excavation

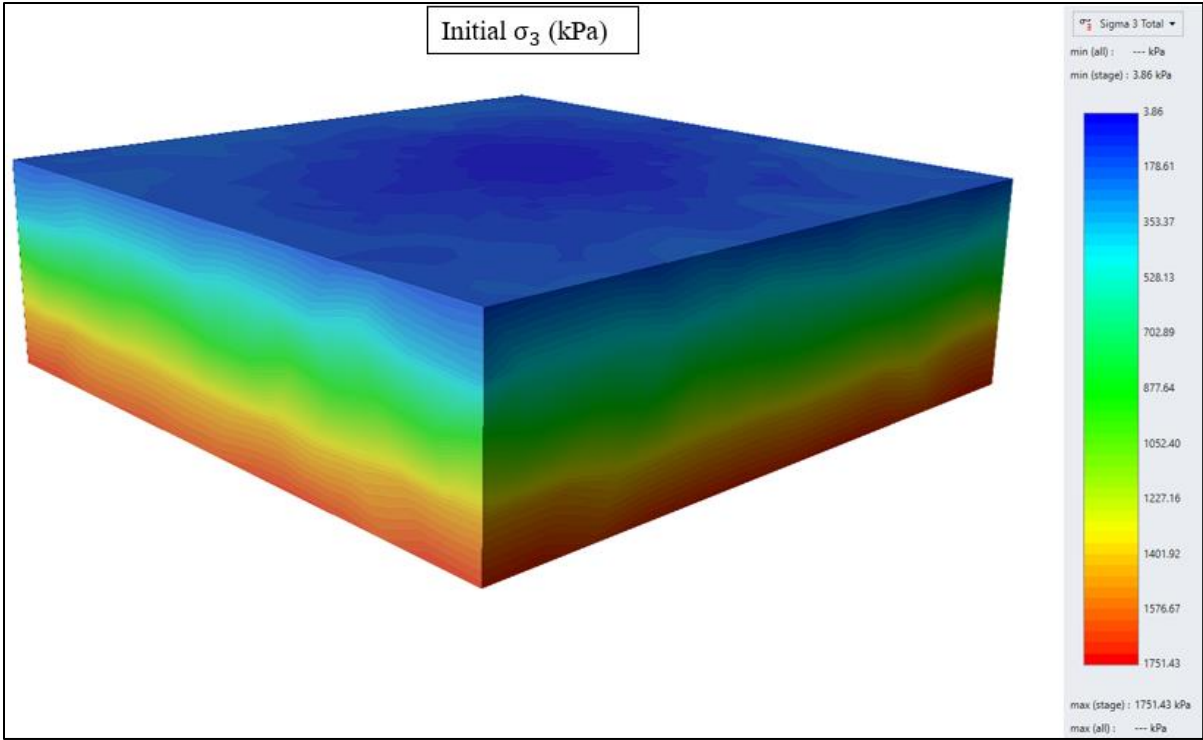




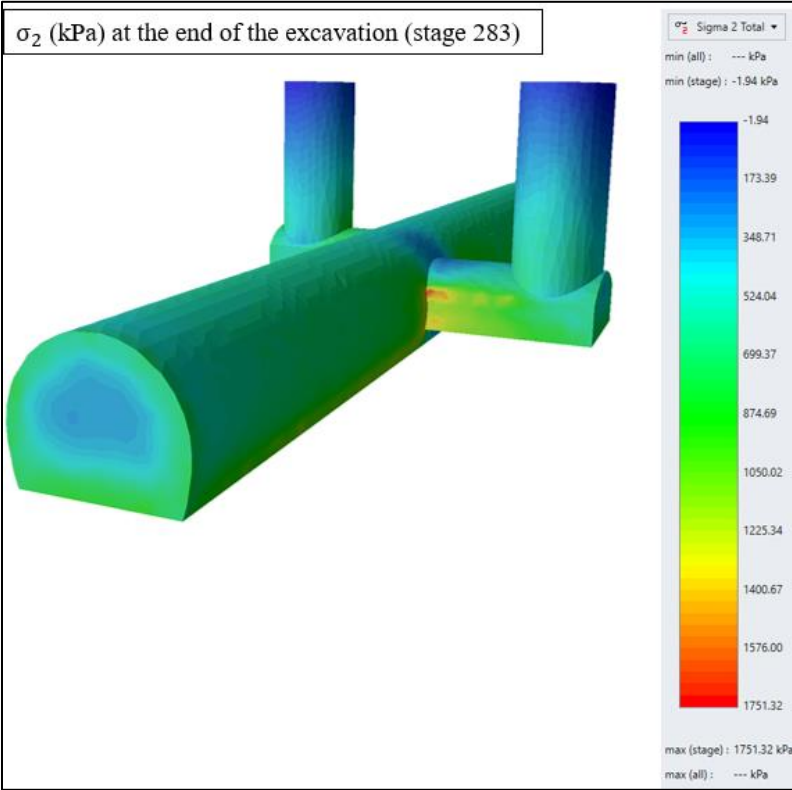
c) Recommended model

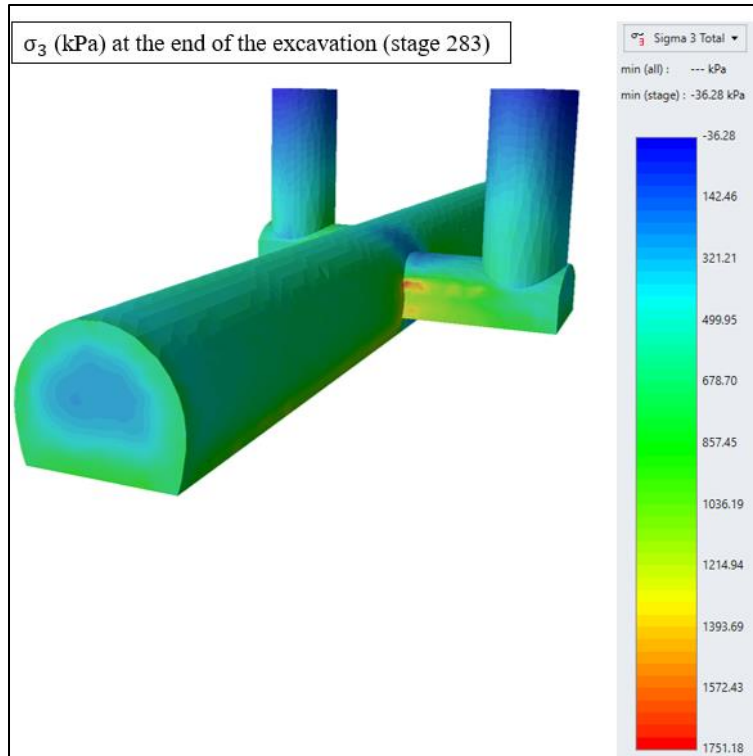
1- Initial stress state



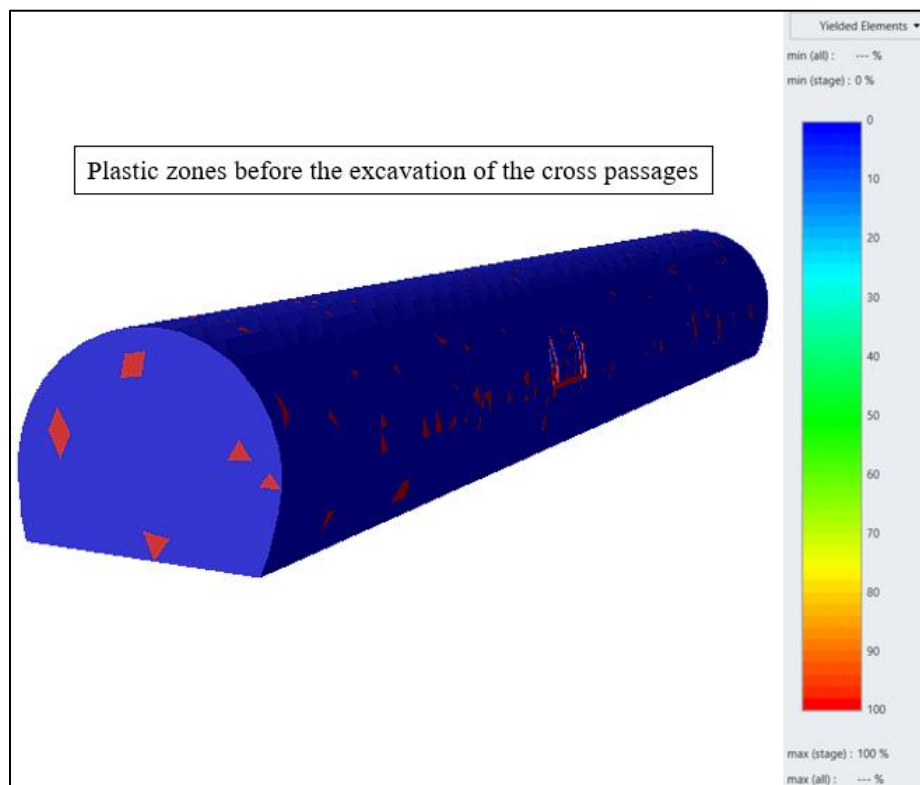


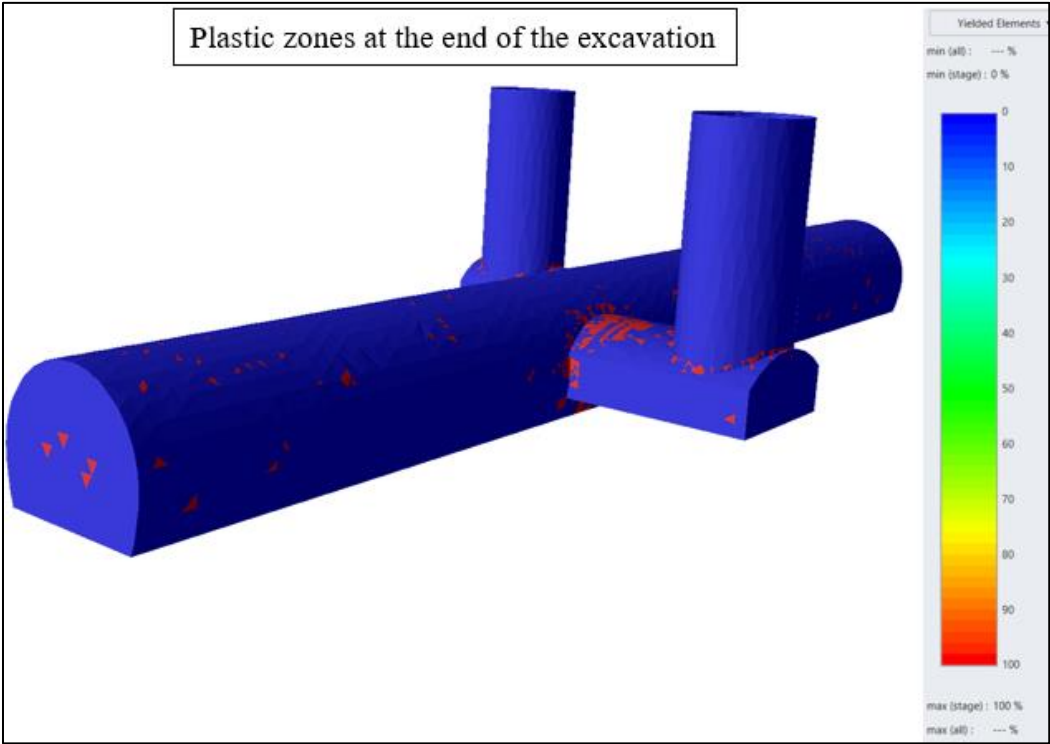
2- Stress state at the end of the excavation





3- Plastic zones

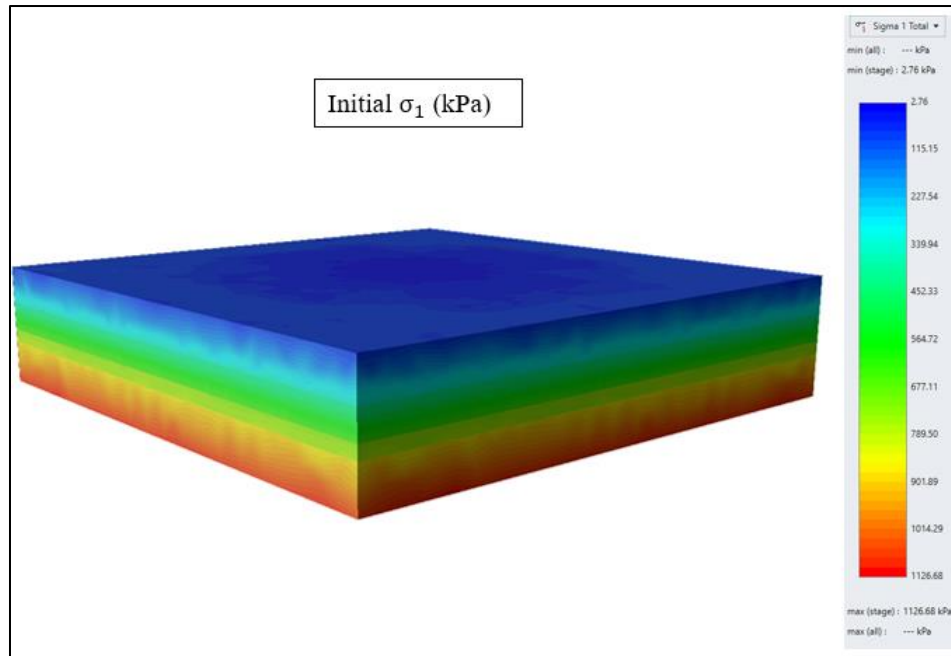


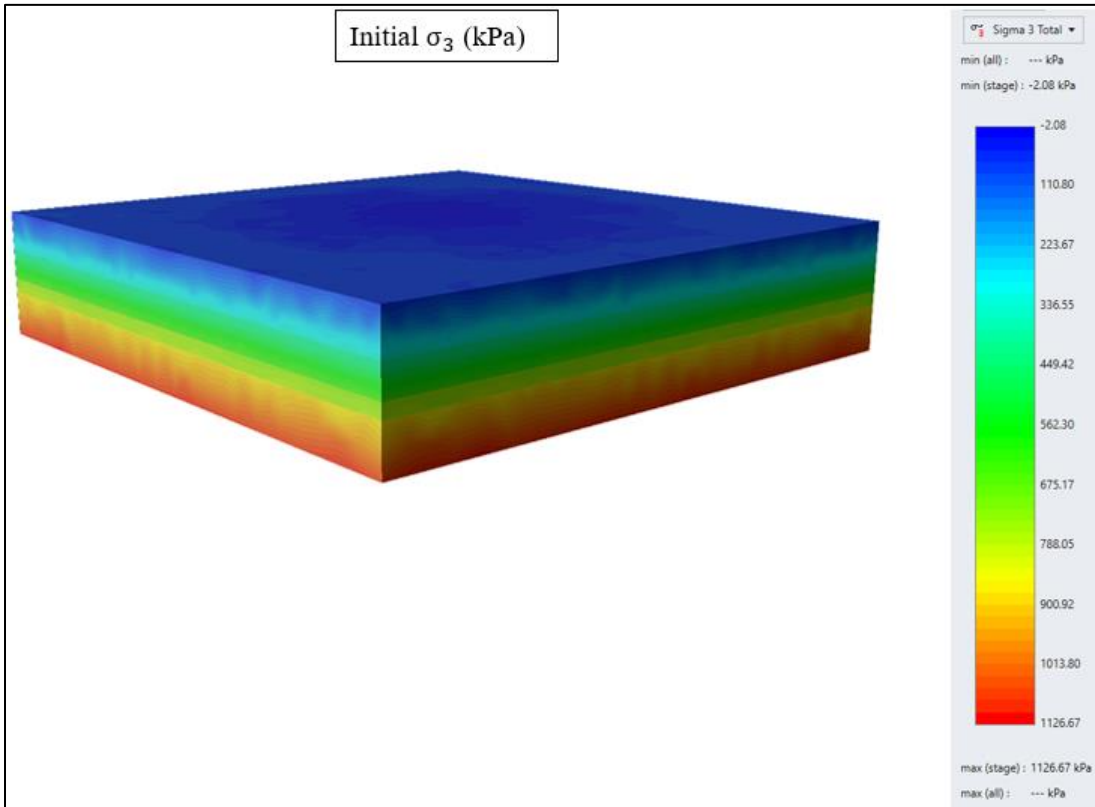
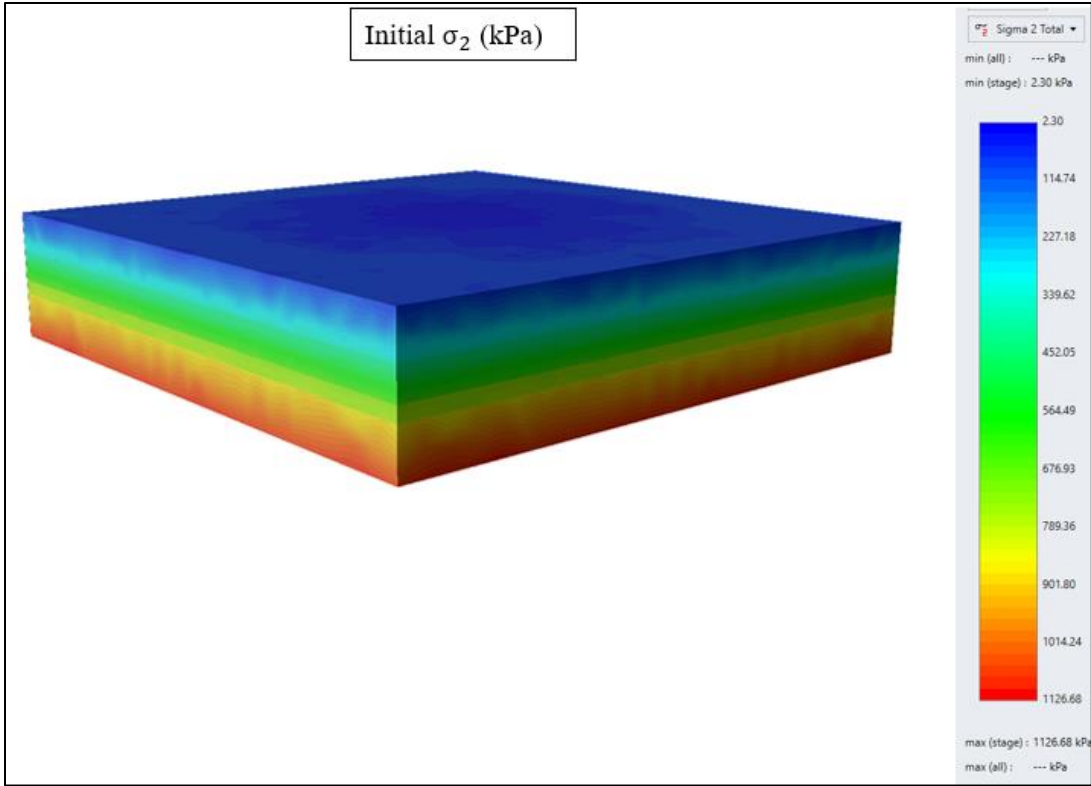


❖ Results related to the worst scenario “section 2”

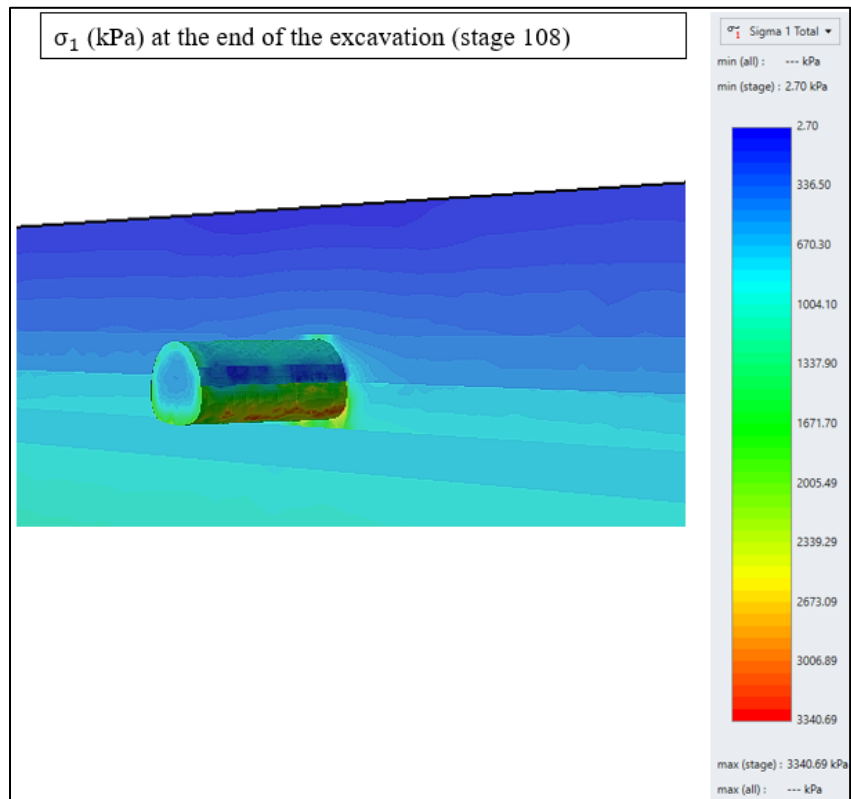
- 3D model

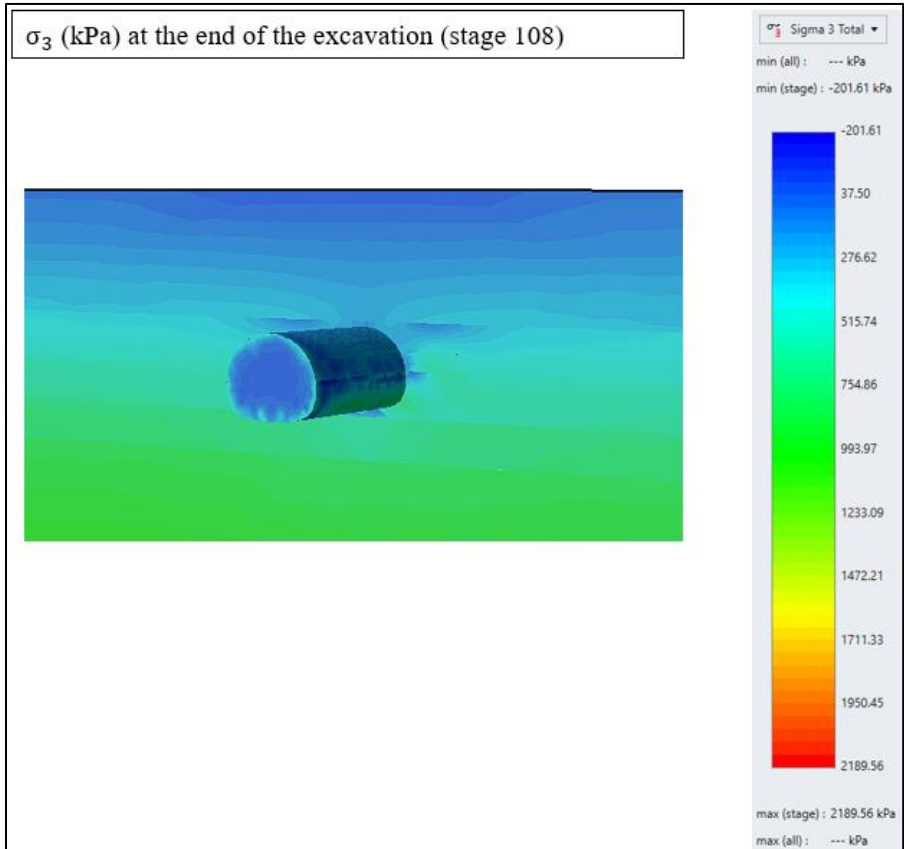
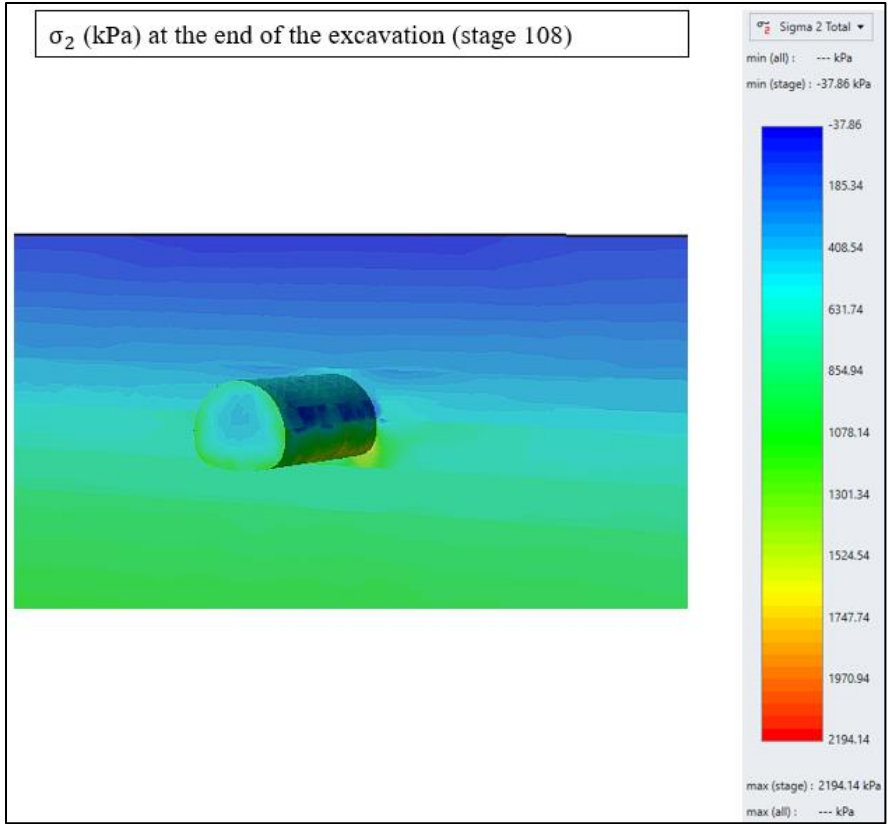
1- Initial stress state





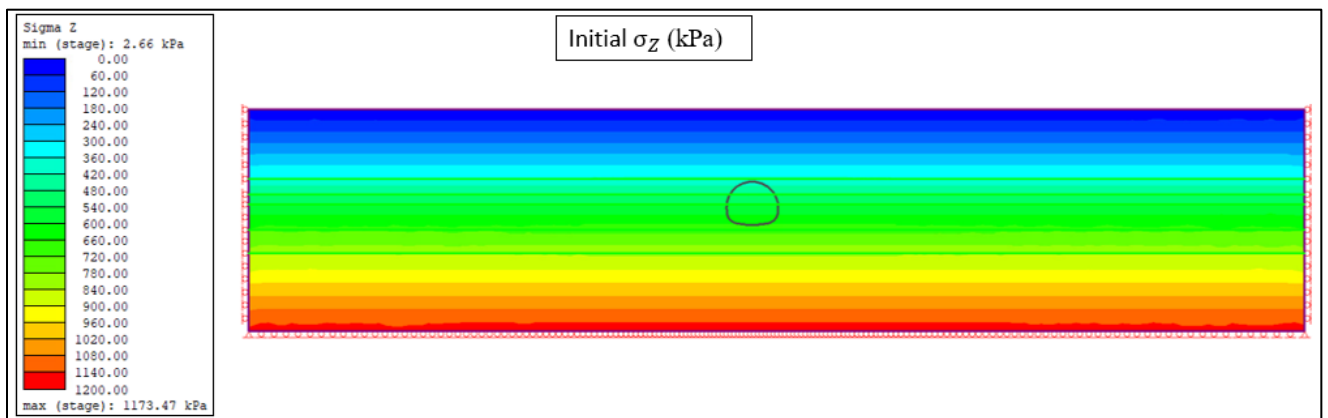
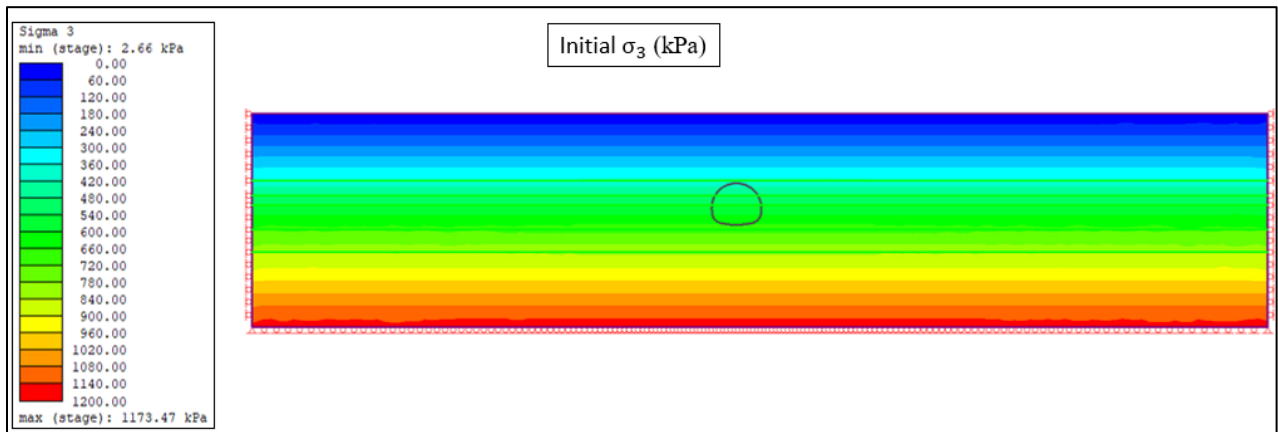
2- Stress state





- 2D model

1- Initial stress state



2- Stress state

